TOWARDS A REAL-TIME 24/7 STORM SURGE, INUNDATION AND 3-D BAROCLINIC CIRCULATION FORECASTING SYSTEM FOR THE STATE OF FLORIDA

By

VLADIMIR A. PARAMYGIN

A DISSERTATION PRESENTED TO THE GRADUATE SCHOOL
OF THE UNIVERSITY OF FLORIDA IN PARTIAL FULFILLMENT
OF THE REQUIREMENTS FOR THE DEGREE OF
DOCTOR OF PHILOSOPHY

UNIVERSITY OF FLORIDA

2009

© 2009 Vladimir A. Paramygin

ACKNOWLEDGMENTS

My most sincere thanks go to my wife, Natalia; my mother, Tatiana; and my sister, Janna for their love and support.

I wish to express my gratitude and sincere appreciation to my advisor and supervisory committee chairman Dr. Y. Peter Sheng. I would like to thank the members of my supervisory committee, Dr. Robert Dean, Dr. Renato Figueiredo, Dr. Kurt Gurley, and Dr. Kirk Hatfield.

I would also like to thank the sponsors for funding the University of Florida to conduct research. These sponsors include Florida Sea Grant (R/C-S-49, NA06OAR4170014), NOAA via Southeastern Universities Research Association (NA04NOS4730254), NOAA Integrated Ocean Observing System (NA07NOS4730211), and ONR via Southeastern Universities Research Association (N00014-04-1-0721).

Many thanks to Vadim Alymov, Justin Davis, Yangfeng Zhang, Bilge Tutak, Taeyun Kim, Andrew Lapetina, and Andrew Condon for their help and many fun moments.

TABLE OF CONTENTS

page

LIST OF TABLES

LIST OF FIGURES

Abstract of Dissertation Presented to the Graduate School
of the University of Florida in Partial Fulfillment of the
Requirements for the Degree of Doctor of Philosophy

TOWARDS A REAL-TIME 24/7 STORM SURGE, INUNDATION AND 3-D BAROCLINIC CIRCULATION FORECASTING SYSTEM FOR THE STATE OF FLORIDA

By

Vladimir A. Paramygin

December 2009

Chair: Y. Peter Sheng
Major: Coastal and Oceanographic Engineering

This work describes a prototype of a real-time forecasting system of storm surge, inundation, three-dimensional baroclinic circulation due to tropical storms for the state of Florida. The Storm Surge Modeling System (SSMS) features dynamic inclusion of wind, astronomic tides, various wave effects, rainfall and introduces land effects into the wind field to accurately predict storm wind over land where it dissipates rather quickly due to interaction with land features. SSMS uses coupled coastal models CH3D and SWAN with high resolution coastal grids for the southwest and the east coast of Florida. The system can use a variety of regional ocean models such as ADCIRC, HYCOM, and NCOM and WaveWatch III wave model which provide boundary conditions to the regional models.

SSMS uses a parametric wind model combined with land use data to adjust parametric wind field due to land exposure in the upwind direction to produce an accurate storm wind field. Parametric wind can also be blended with background wind fields such as NOGAPS and drive surge and wave models that are part of the SSMS.

The modeling system is verified using data during Hurricane Wilma (2005) - it successfully predicted inundation measured at almost 30 locations by the USGS. The modeling

system is also verified with data during Tropical Storm Fay (2008) - it predicted storm surge and salinity compared well with measured data. Inclusion of precipitation in the modeling systemhas been found to significantly improved the accuracy of simulated salinity. Inclusion of a watershed model into SSMS should increase the accuracy of salinity simulation even further.

The modeling system is very efficient and is able to produce 60-hour forecasts within the timeframe required by the NWS to be used for evacuation. The modeling system has an interactive front-end that can be used to effectively disseminate results to the users. The system could be used by state emergency and water resources managers to foresee flooding and flow conditions, by federal government agencies and private industry for flood mapping, by scientists for better understanding of surge and inundation processes and help planning of the field work.

CHAPTER 1
INTRODUCTION TO STORM SURGE AND INUNDATION FORECASTING

Introduction

Coastal regions have always been an attractive place to live. Today, by different estimates, 50-60% of the US population live in the coastal zone (Crossett et al., 2004) and the trend is that coastlines are getting more crowded every year. This is especially true for Florida – a state where no location is more than 80 miles away from either the Atlantic Ocean or the Gulf of Mexico, and more than 75% of Florida residents live in coastal counties (NOAA, 2004). Coastal communities in Florida have grown over 30% since 1990. Beach tourism is estimated to bring in about $40 billion (FDEP, 2006) and millions of tourists to Florida every year most of which stay at the coast.

Hurricanes are the most devastating hazards to impact the United States. They are also the costliest natural catastrophes, especially in the coastal regions with over 50% of the population living in coastal counties and that number rising each year. Hurricanes pose a major threat to coastal areas with strong winds, storm surge and flooding, Hurricane Katrina in 2005 is estimated to be the costliest natural disaster yet to strike the United States with estimated property damage of $81.2 billion in 2008 USD (Knabb et al., 2006). The state of Florida is one of the states that are historically among the states that are most vulnerable to hurricanes. Two out of three category 5 hurricanes to hit the United States made their landfall in Florida. Hurricane Wilma in 2005, for example, was the eighth hurricane to hit Florida in 15 months. However, an increased frequency of hurricane occurrence is not the only problem; research shows that hurricanes are becoming fiercer too. Emanuel (2005) concludes that the hurricanes have grown more powerful and destructive in the past three decades. Emanuel says that since the mid-1970s both the duration of storms and maximum wind speeds have increased by about 50%.

One of the main hazards associated with hurricanes is storm surge and inundation which is a great threat to life and property along the coast.

To mitigate hurricane damage several research programs have studied ways to “defuse” hurricanes in their developing stages, but none of them were successful. National Science and Technology Council's Joint Subcommittee on Ocean Science and Technology in their recent document *Charting the Course for Ocean Science* raises several priority topics for research during the next decade. The document outlines "Understanding and Capability to Forecast Ocean Processes" as one of the three key areas of science and technology that must be pursued. While currently there are no solutions to avoid hurricanes completely; more accurate and timely forecasts can help reduce the economic impact caused by hurricanes as well as help save people’s lives. Providing forecasts quicker gives more time to emergency managers to plan and execute evacuation procedures. Inaccuracies in forecasts are very costly, errors may lead to having areas unprepared for a hurricane to be affected by one, therefore, currently emergency managers issue warnings and execute evacuations in a much larger area than forecasted to account for possible errors in forecasts which costs billions of dollars.

For years the main damage from hurricanes has been attributed to the effects of wind and storm surge. However, in the past 5 years the term storm surge is usually mentioned along with the term inundation. Simulating inundation is a much more complex and involved process, not only it takes good skill in simulating the surge and waves, but in addition requires consideration of water/land/atmosphere interaction and various land-use types, including open land, tidal marshes, buildings, levees, and control structures. High-resolution topography and land-use data are required to correctly represent the various land cover types and their effects. Storm surge and inundation, however, is not the only challenge for the Florida coast where many other

phenomena and problems occur in the coastal zone and estuaries: red tide, rip currents, loss of wetlands and habitat, global climate change, global sea level rise (Florida Coastal and Ocean Coalition, 2008) and land use planning. All these problems pose great challenges not only to the science but to the management as well, hence accurate forecasting of circulation would be beneficial not only for scientific reason, but for purposes of better managing water resources in the state providing information that can be used as a guidance by managers.

Storm surge and inundation is the greatest cause for death and property damage during hurricanes, hence affecting the safety of coastal residents as well as habitability and security of their environment and property. Inundation also affects the navigation of waterways and accessibility of buildings, roads and railroads and can have a significant effect on hurricane evacuation.

What Is Storm Surge and Inundation?

Storm surge is an offshore rise of water associated with a low pressure weather system, typically a tropical cyclone. Interaction of a cyclone with the ocean surface forms a long gravity wave with a length scale similar to the size of the generating tropical cyclone. The wave can last from several hours to days depending on the cyclone size and speed of movement. In shallow water near the coast, bathymetry and reflections from the coast can significantly amplify that wave which becomes even more dangerous if the storm hits during high tide. During tropical storms, surge is perhaps the largest component that causes inundation – flooding of inland surface that is not normally submerged.

During storms at least six processes interact to create water level and inundation associated with it: gravitational tides, effect of pressure deficit in the eye of the storm, the direct effect of wind, the effect of the Earth's rotation (Coriolis effect), the effect of waves and finally the contribution of rainfall, rivers and run-off. During a hurricane the storm tide is the main

contributor to the inundation. Storm tide (Figure 1-1) consists of normal gravitational tide which is governed by the planetary motion and storm surge, which in turn consists of the wind surge and pressure surge (Figure 1-2). The Coriolis effect caused by the Earth's rotation can change the direction of the current which can bring the currents into more perpendicular contact and amplify the surge or lessen the surge by bending the current away from the coast.

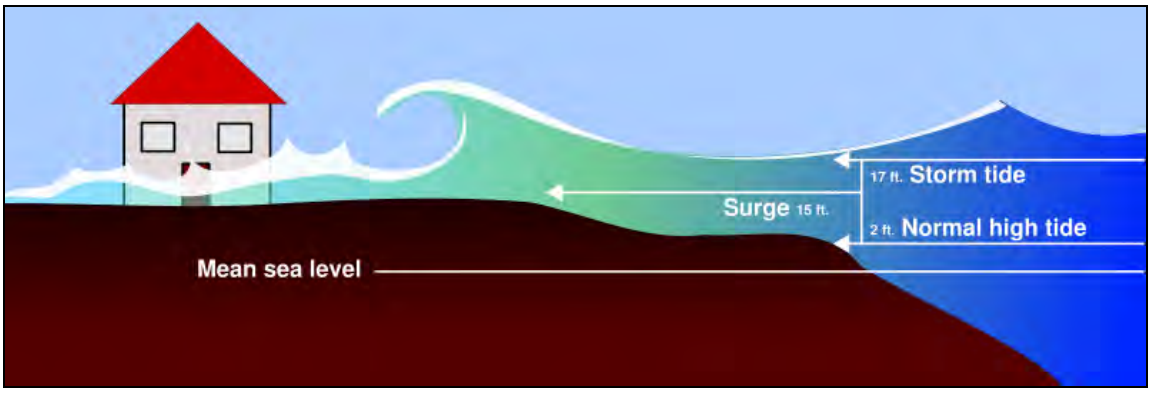

Figure 1-1. Storm tide and its components (WikiMedia Commons, 2009)

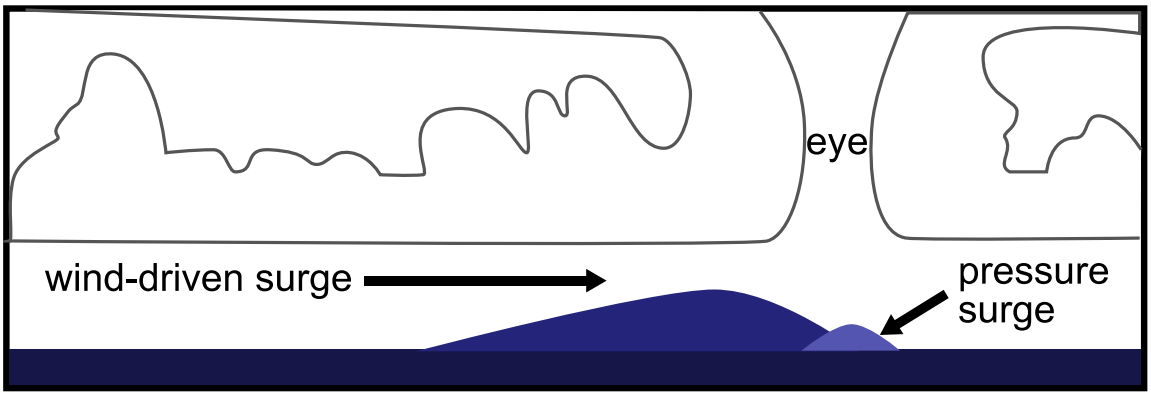

Figure 1-2. Components of storm surge (WikiMedia Commons, 2009)

The effect of waves, while directly powered by the wind, is distinct from a storm's wind-powered currents. Although these surface waves are responsible for very little water transport in open water, they may be responsible for significant transport near the shore. When waves are breaking on a line more or less parallel to the beach they carry considerable water shoreward. As they break, the water particles moving toward the shore have considerable momentum and may

run up a sloping beach to an elevation above the mean water line which may exceed twice the wave height before breaking (Granthem, 1953). Wave-induced currents interacting with surge currents can increase the momentum causing even higher setup.

Often tropical storms bring large amounts of rain with them, for example, tropical storm Fay (2008) never reached hurricane strength and did not create a big wind-driven surge. Yet, it dropped over 20 inches of rain in Brevard County on the east coast of Florida. Rainfall effect is predominantly observed in estuaries as watersheds drain water dumped by hurricane into the rivers which then overflow causing the flooding.

Forecasting of Storm Surge and Inundation

The state of Florida is the state most affected by tropical storms. Being open to the Atlantic on the east coast and to the Gulf of Mexico on the west coast, most of the state boundary is vulnerable to storm surge and inundation. Rather flat topography makes it even more vulnerable to high surges and inundation. While the hurricanes cannot be controlled, the vulnerability can be reduced through accurate forecasting to enable timely and efficient evacuation and preparedness. One of the solutions to the forecasting challenge could be a forecasting system consisting of a suite of state of the art numerical models using the latest scientific as well as technological advances. Such a forecasting system could be used for forecasting of an approaching hurricane as well as hindcasting of various scenarios including but not limited to storm surge and inundation problems.

Research of storm surge and inundation hindcasting and forecasting has a wide range of applications including generation of flood maps based on the historical data as well as forecasting storm surge and inundation in real-time and provide such information to emergency managers for evacuation management. Water resource managers can also find such data useful as it can provide information for manipulating control structures diverting the flow as necessary.

Results of high-resolution hindcasting based on historical storms can provide products to be used in flood mapping for insurance purposes and planning of land use. A forecasting system can also serve as a great tool for scientists, for example long term forecasting could provide insight into sea level rise and coastal upwelling and problems associated with it. Forecasting could also help researchers to plan the field work as forecasts could give information on possible locations of events of interest (such as storm surge and inundation, abnormal flow conditions, etc). Such information may help to set up the instruments accordingly to be able to capture such events.

Evacuation to save lives is the single most important task for emergency managers during an approaching storm. One of the challenges that the emergency managers are facing is determining the area that will be affected by the storm and planning the evacuation based on the area affected. However, to effectively help the emergency managers, forecasting needs to be very efficient and forecasts have to be produced very quickly, fast enough to allow the time for evacuation activities to be completed. Accurate forecasting of storm surge and inundation can also make the evacuation process more efficient by predicting the routes that are not affected by the storm and redirecting the traffic there, as well as minimizing evacuation in areas where inundation is not expected.

Developing a robust storm surge forecasting system is a challenging task. The system needs to meet many requirements: it needs to be available 24/7 and able to produce forecasts on demand, it needs to be completed within a minimum to allow 2-3 days for evacuation tasks to be completed, it has to have robust physics and represent a variety of processes that affect storm surge and inundation such as astronomical tides, waves, rainfall and runoff, etc. All these different requirement are described in details in the next section.

Forecasting System Requirements and Needs

Based on the information available from government agencies that perform storm forecasting, emergency as well as mitigation tasks, one can attempt to derive a set of desired features as well as requirements for a storm surge and inundation forecasting system.

Operational Modeling

The main requirement is the ability to run operationally in real-time with as little human intervention as possible. This is the most obvious and stringent requirement and comes from the fact that a forecast is an extremely time-sensitive product; therefore a forecasting system has to be ready and accessible at all times 24 hours a day, 7 days a week. A forecasting system has to be available when its results are needed. No matter how robust and accurate the forecasting system is – its results quickly become obsolete. The system has to be able to provide forecasts within a certain timeframe since the usefulness of the forecast is defined by when it is available. Different applications of forecast results require different timeframes, which can vary greatly from several hours to several days. However, recent personal communications with representatives of FEMA, NOAA and NWS have shown that the speed of forecast is a primary concern for any federal agency that makes use of forecast products. This work will be using the National Weather Service operational clearance times to define these timeframes, since these are readily available official timeframes that are based on, perhaps, the most important application of storm surge forecasts – evacuation. NWS operational clearance times will also be compared to NOAA NHC SLOSH warning goals to see whether or not current NHC surge forecasts satisfy these evacuation requirements.

Finally, verification of the forecasting system is very important. Currently, there is no set of procedures developed for model verification that would be agreed upon and used by the ocean modeling community. Different groups and entities use a variety of quality control methods and

procedures from visual observation of plots to RMS errors, correlations and others. However, there is an official set of verification procedures for real-time nowcast/forecast models developed by NOAA for models that are part of its PORTS (Physical Oceanographic Real-Time System) and these procedures (NOS, 1999, 2003) can be adopted for verification and skill assessment of a forecasting system.

Evacuation Clearance Times

The NWS operational clearance time for NWS is defined by the evacuation clearance time since safety of the people is the primary concern in storm operations. The NWS operational clearance times can be used to define the timeliness of forecasting system that is needed for emergency and evacuation managers. The managers need to have at least the amount of time listed in the Weather Service Operational Manual (WSOM, 2001, full table for the state of Florida is available in Appendix A) to proceed with the evacuation. Since any storm surge forecasting system requires wind and pressure as forcing it has to rely on one of the existing atmospheric storm forecasting systems to provide that forcing and the time required to produce that atmospheric forecast will have to be added to the time needed for the storm surge forecasting system to produce its products.

Weather Service Operational Manual (WSOM, 2001) shows the evacuation clearance times to be up to 44 hours for Category 3 hurricanes (Levy, Citrus and Hernando counties, Figure 1-3). The evacuation time for Dade county Category 3 is estimated to be 52 hours. Category 5 hurricane clearance times estimates are even higher for Dade county and are specified as 71-81 hours, which, however is an exceptional value compared to number for other counties which are significantly lower and with the next highest value being 50 hours, therefore, a clearance time of 52 hours, which would satisfy clearance times for all counties up to Category

3 and all counties with an exception of Dade up to Category 5, will be used as a reference value required for timeliness of forecasts.

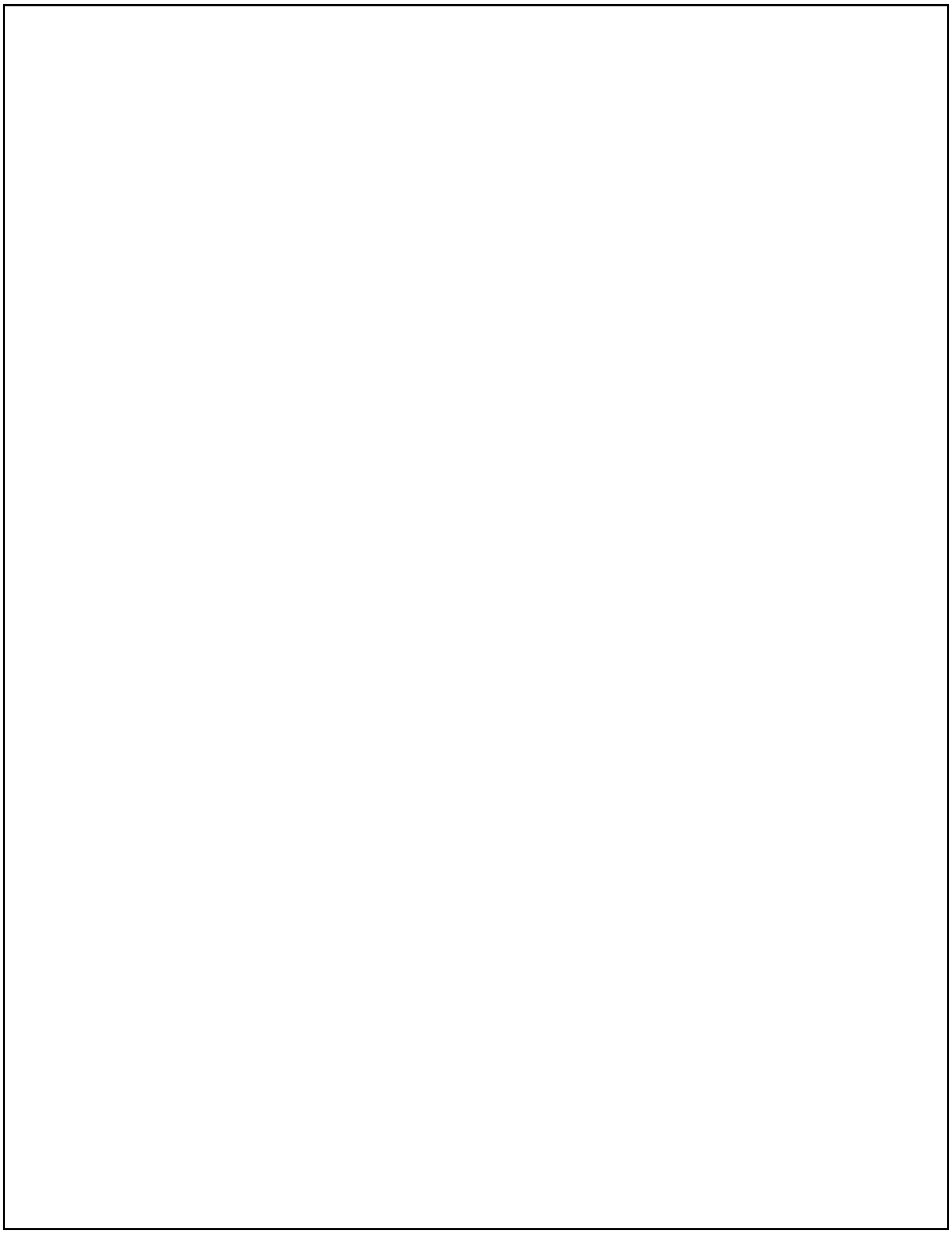

Figure 1-3. Map of Florida counties

Model Verification and Skill Assessment

NOS procedures for developing and implementing operational nowcast and forecast system for PORTS (NOS, 1999) dedicated to model evaluation discusses the policies and

procedures for the evaluation of nowcast and forecast models for navigation. These procedures are designed for operational models that forecast navigability and therefore are very stringent and involved. Due to the time constraints and limited man-power and due to differences in available data measurements for navigable areas and areas affected by hurricanes, these procedures will be adopted with certain modifications that are explained below.

The procedures primarily focus on water levels and currents and suggest various model simulation scenarios for different phases (tide only, test nowcast, test forecast, semi-operational nowcast and semi-operational forecast) evaluation criteria for water levels and currents. Verification and skill assessment within this work will focus on semi-operational nowcast/forecast criteria to attempt to come as close to an operational system as possible within the time frame allowed for this work.

NOS procedures list the following relevant variables: the magnitude of water level at all times and locations (for under-keel clearance), the times and amplitudes of high and low water at docking/anchorage sites, the speed and direction of the currents at all times and locations but especially at channel junctions (for maneuvering) and the start and end times of slack water before flood to ebb at all locations. The focus of this work is different from the focus for the NOS procedures therefore the list of relevant variables will be modified to 1) the magnitude of water level at all times at locations and 2) the speed and direction of currents all times at locations where measured data is available.

Skill assessment variables include series mean, root mean square error, standard deviation, central frequency, positive outlier frequency, negative outlier frequency, maximum duration of negative outliers, worst case outlier frequency, and principal current direction. Many of these statistics have associated acceptance criteria. These variables and the acceptance criteria are

defined and discussed in detail in Appendix B. Some of the statistics require comparisons of water level variable not only to the measured data but also to the computed astronomical tides. All NOAA water level observation stations have astronomical tides data available, however, not all data used in this work have this information available, and therefore, some statistics will only be available for NOS stations.

Results and Products

Results produced by any nowcasting or forecasting modeling system are interpreted by humans and decisions made based on the results. The system should be able to provide results in a form that can be used by different users from emergency managers to planners. The data has to be readily available and at the same time secured to prevent unauthorized access. Forecast data is sensitive to interpretation and it should only be accessed by those qualified to interpret such data, therefore it is essential for the forecasting system to be able to effectively limit access to the products and data.

Data standards and compliance

Recently there have been many efforts in the ocean science community to unify and standardize the data including model output. There are two commonly accepted data file formats in the ocean science community: GRIB and NetCDF. GRIB (GRid In Binary) is an accepted file format in the meteorological community, its rather complicated for implementation. NetCDF (Network Common Data Form) is a set of software libraries and machine-independent data format that support the creation, access, and sharing of array-oriented scientific data. It is used by many scientists; it was designed and is supported by Unidata. However, NetCDF is a generic file format that is not tailored in any way to the ocean sciences needs. Although it does have a capability to be further standardized to suit the needs of the ocean sciences community as it allows carrying metadata along with the data. A convention is needed that would standardize and

define the minimum requirements for metadata such as specification of units, directions and types of variables. All the metadata needs to be specified in a standard way such that any system that supports the convention would be able to process the data. COARDS (Conventions for the standardization of NetCDF Files) was one of the earlier noteworthy efforts, sponsored by the Cooperative Ocean/Atmosphere Research Data Service, a NOAA/university cooperative for the sharing and distribution of global atmospheric and oceanographic research data sets. This initiative ended in 1997, but the COARDS conventions were then extended and generalized by NetCDF Climate and Forecast (CF) Metadata Conventions (Eaton et al., 2009), which is an ongoing effort that involves many organizations such as NOAA, UCAR, USGS, UK Met Office and others and includes conventions for climate data including forecasts. The conventions are designed to promote the processing and sharing of NetCDF files and are increasingly gaining acceptance and have been adopted by a number of projects and groups as a primary standard.

Dissemination and accessibility of results, communicating results to the public

Communicating results to the public is a big problem as well. Many studies show that public understanding of information on hurricane forecasts in various forms is still very low. It can be especially dangerous when the public attempts to make evacuation decisions based on own reasoning and that's why direct access of the public to forecast data might be undesirable. Proper security measures, and user authentication should be employed. It is desirable to separate users by level of access providing access to appropriate data by different users.

New products and methods are needed for communicating forecast information to the public. Storm surge maps are currently used when trying to communicate the results of potential surge to the public. However, interpreting such information can be a challenging task. Most people do not know at what elevation their property is located and what an "X-feet surge" would mean for them. Inundation maps should eventually replace surge maps as they give a better

understanding of how much actual flooding is to be expected in any given area. A collaborative effort (Bright et al., 2008) by the NOAA/NWS at Charleston, South Carolina and the College of Charleston, Charleston, South Carolina has resulted in a number of sociological studies on improving ways to communicate storm surge forecasts and associated risks to the public. One of the suggested methods was development of a website where visual aids would be supplied that could help the public understand the level of flooding that could be expected. It was suggested that every area or neighborhood could have a location that most residents are familiar with (such as a local school) or a shopping center and that level of flooding would be displayed in reference to such a landmark (Figure 1-4). In order to employ such a method of communicating the results major upgrades of current NHC capabilities would be required. SLOSH model resolution is significantly coarser than needed (in order to reasonably resolve features such as raised roads, railroads, etc at least 30-50 meters horizontal resolution is needed) for such products to exist and SLOSH only calculates surge, while inundation levels are required for this type of products.

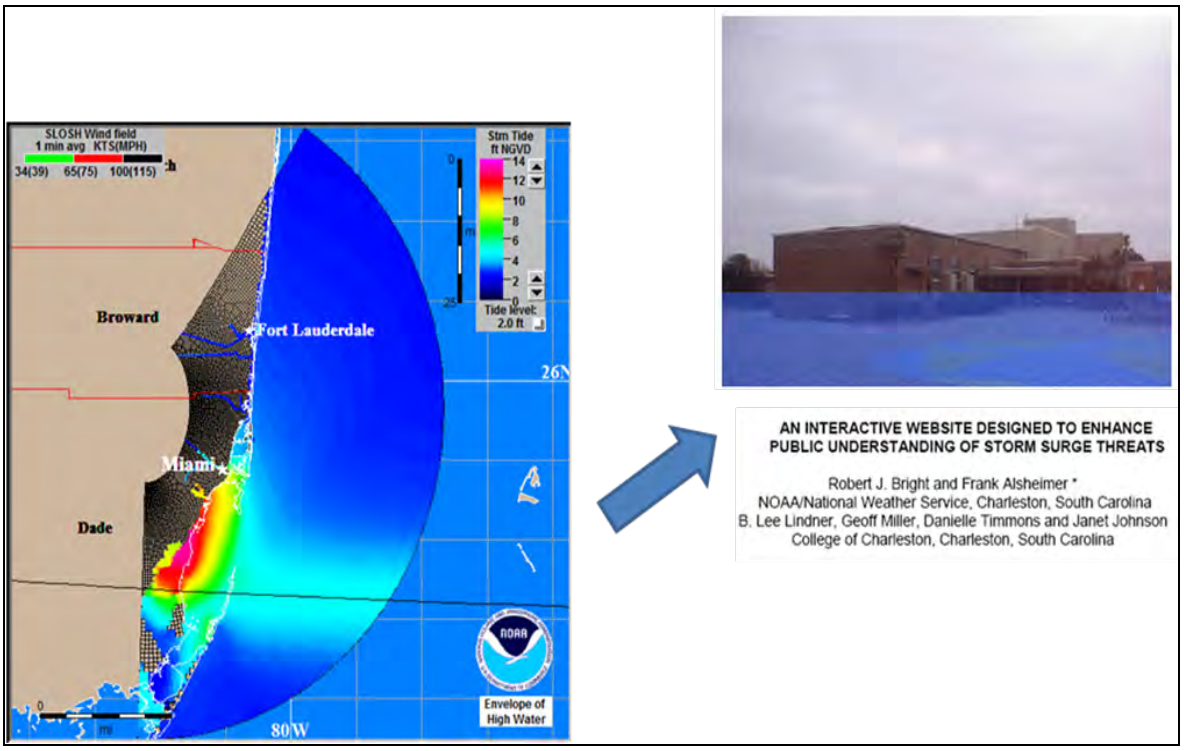

Figure 1-4. Enhancing methods to report storm surge forecasts to the public

A new forecasting system should leverage upon what currently exists and improve the weak points of current systems while attempting not to sacrifice the desirable properties of what is currently available. For example the currently used SLOSH system is extremely efficient and it is essential to create the forecasting system that would be efficient as well. It would be almost impossible to create the system that is as efficient as SLOSH while adding significantly more robust physics, but interests of users of such systems such as emergency and water resource managers should be taken into account by the SLOSH modeling team to keep the system useful and up to date.

Development of such a system requires reviewing the current state of the art models to re-use and leverage models and technologies that currently exist, combine them and improve the weaker points that need to be improved.

Overview of Modern Wind, Surge and Wave Models

Currently there are many models that can be used to simulate wind, water levels, waves and currents. All these models have their own strengths and weaknesses and generally can be used in a rather narrow range of applications due to their focus and limitations. This section will attempt to overview some of the widely known models either standalone or those that are currently used in different forecasting systems and address the advantages and disadvantages for each one of these models that can be used to evaluate their suitability to be included in the system that would satisfy the needs and requirements defined in this work.

Review of Wind Models and Assimilation Systems

Wind and pressure fields are the primary forcing factors in storm surge and inundation simulations, therefore it is extremely important to have the best possible wind and pressure forecasts to be able to produce a quality storm surge forecast. There are a number of models that can be currently used to provide atmospheric forcing for storm surge simulations. Table 1-1 gives a brief description of some wind models that can provide atmospheric forcing to drive a storm surge and inundation model and can be used for forecasting. There are two types of models described in the table: synthetic parametric models that are rather simple and more complex atmospheric models such as GFDL and WRF. Parametric wind models are designed for storms only, they require a few parameters and allow one to generate a wind and pressure field at a certain vertical level that attempts to reproduce the structure of a storm, such models can produce wind fields for one storm in a matter of seconds. Atmospheric models use much more robust physics at the core, however they require significant amounts of data and computational resources to produce required wind and pressure fields.

For this study the parametric wind model by Xie et al. (2006) was selected as the main model, however, all other options were tested. Sensitivity tests of wind fields will be presented in the following chapters.

Table 1-1. Atmospheric/wind models overview

Model	Features and Description	Comments
GFDL (Geophysical Fluid Dynamics Laboratory) hurricane model	Three-dimensional atmospheric model. Multiply nested movable mesh system. Model initial condition is defined through a method of vortex replacement, generates a realistic hurricane vortex by a scheme of controlled spin-up.	Adopted by US National Weather Service as an operational hurricane prediction model in 1995. Kurihara, Tuleya and Bender, 1998
WRF (Weather Research and Forecasting) model	Fully compressible, Euler non-hydrostatic with run-time hydrostatic option. Conservative for scalar variables.	Flexible, portable, massively parallel and efficient code. Highly modular, offers numerous physics options and is suitable for use in a broad spectrum of applications. Janjic et al., 2004, Skamarock et al., 2005
Synthetic wind model of the wind and pressure profiles in hurricanes	Synthetic model of the radial profiles of sea level pressure and winds in a hurricane. Equations contain two parameters that can be estimated empirically or determined climatologically. $P = P_c + (P_n - P_c)\exp(-A/r^B)$ - pressure at sea level and the wind speed is defined as: $V = C_r\left[AB(P_n - P_c)\exp(-A/r^B)/\rho r^B + r^2 f^2/4\right]^{1/2} - rf/2$ Where A and B are the empirical parameters, r is the radial distance, p_n is the ambient pressure, p_c is the central pressure, ρ is the air density, f is the Coriolis parameter and C_r is a coefficient that is used to convert geostrophic wind speed to a 10-meter wind speed and is generally set in the range 0.85-0.95.	Most of the required parameters for the model are forecasted by NHC and others. Does not consider effects of interaction with land. Can be used as a basis and improved by combining with other models. Holland, 1980

Table 1-1. Continued

Empirical model for predicting the decay of hurricane winds after landfall	Simple two-parameter exponential decay model. The wind speed is a function of wind speed at landfall and the time since landfall. Can be adjusted for fast and slow inland moving storms. $V(t) = V_b + (RV_0 - V_b)e^{-\alpha t} - m\left[\ln\left(\frac{D}{D_0}\right)\right] + b$, where t-time after landfall, $V(t)$ is the wind speed, V_0-wind speed at landfall, α-decay constant, D-distance from shoreline, D_0-distance from shoreline where the shoreline has affects wind, V_b-background wind speed, m, b and R are selected empirically based on a fit to existing storm data	This model could be combined with other parametric wind models that do not account for decay after the landfall. Combined with the Holland (1980) it can provide more accurate estimates of wind once the storm makes its landfall. Kaplan, DeMaria, 1995; 2000
Real-Time Hurricane Surface Wind Forecasting Model	Based on Holland (1980) model this model incorporates asymmetry using NOAA NHC hurricane forecast guidance for prognostic modeling and assimilating NDBC real-time buoy data in the model's initial field. The equations are based on Holland (1980) but introduce dependency on angle θ which allows accounting for NHC predictions of wind radii by quadrants. $R_{\max}(\theta) = P_1\theta^{n-1} + P_2\theta^{n-2} + \cdots + P_{n-1}\theta + P_n$ $P(r,\theta) = P_c + (P_n - P_c)e^{-\left[R_{\max}(\theta)/r\right]^B}$ $V = \left[\frac{B}{\rho_a}\left(\frac{R_{\max}(\theta)}{r}\right)^B (P_n - P_c)e^{-\left[R_{\max}(\theta)/r\right]^B} + \left(\frac{rf}{2}\right)^2\right]^{1/2} - \frac{rf}{2}$ $B_0 = \frac{V_{\max}^2 \rho_a e}{P_n - P_c}$	NOAA NHC forecast advisories provide radii for wind speed contours at four quadrants. This information is used to construct an asymmetric wind and pressure field that is based on NHC official forecasts. Xie et al., 2006

Storm Surge Models

A number of circulation models were reviewed in order to select models to be included in a storm surge forecasting system. The main criteria were robustness of the model – the preferred model would have multiple successful applications including those in Florida and efficiency – in order to satisfy the NWS evacuation time criteria the model needs to be very efficient and be able to run simulations in a rather short amount of time.

ADCIRC

The ADCIRC (Advanced CIRCulation) model developed by Luettich and Westerlink (1992) solves equations of fluid motion based on hydrostatic pressure and Boussinesq approximations discretized in space using the finite element method on a non-orthogonal unstructured grid. It can be run either as a 2-D depth integrated or a 3-D model and can use both Cartesian and spherical coordinate system. The water surface elevation is obtained from a solution of a depth-integrated continuity equation. To avoid oscillations that are associated with a primitive Galerkin finite-element formulation of this equation ADCIRC uses the Generalized Wave Continuity Equation (GWCE) formulation (Luettich and Westerlink, 2004). The velocity is solved from either the 2-D depth integrated equations or 3-D momentum equations for 2-D and 3-D models respectively. In a 2-D case the equations are solved using a lumped mass matrix and explicit formulation. Earlier versions of the model use a non-conservative, approximate integration of the momentum equation before it is substituted into the GWCE, while the later versions benefit from mass conservation due to vertically-integrated momentum equations in the conservative form in the GWCE.

ADCIRC features include flooding and drying, overflow and throughflow barriers, bridge piers and wave radiation stress terms that can be used to introduce the effects of wave on circulation. ADCIRC can be forced with elevation boundary conditions, normal flow boundary

conditions, surface stress boundary conditions, tidal potential and the earth load or self attraction tide. ADCIRC code has been parallelized using MPI parallelization techniques typically with better than 90% efficiency.

ADCIRC has been used in many applications, including the recent Interagency Performance Evaluation Task Force (IPET, 2008) study to simulate hurricane Katrina in the Gulf of Mexico, and has been verified using a variety of problems including storm surge, unstructured grid allows to fit the shoreline well and to implement varying grid resolution. The 3-D version of ADCIRC is under development and its application has been mostly limited to a few idealized cases. The explicit formulation of non-linear terms, however, imposes quite stringent stability conditions (especially in the presence of structures such as piers in the grid) on the model and fine resolution models do require significant computational resources due to time step limitations. The use of mean sea level datum in most of ADCIRC grids can adversely affect the ability to calculate inundation due to storm induced surge since the topography data generally exists in NGVD/NAVD and establishing mean sea level over land can be problematic.

CH3D

CH3D (Curvilinear Hydrodynamics in 3D) is a hydrodynamic model originally developed by Sheng (1986, 1990). The model can simulate 2-D and 3-D barotropic and baroclinic driven circulation by tide, wind and density gradients. CH3D uses boundary-fitted non-orthogonal curvilinear grid in the horizontal direction and terrain following sigma grid in the vertical direction. As such, the model is capable of accurate representation of complex shoreline and geometries in coastal regions. It uses a robust turbulence closure model to represent vertical turbulent mixing (Sheng and Vilaret, 1989) and a Smagorinsky type model for horizontal turbulent mixing. Numerical solution of CH3D model satisfies conservation.

One of the advantages of the CH3D model is non-orthogonality of the grid that allows for the use of automated grid generation techniques, such as elliptic grid generation method developed by Thompson (Thompson et al., 1985). Also, an exclusive use of NAVD88 datum in all CH3D grids to represent bathymetry and topography is a very useful feature for computing inundation.

CH3D has been applied to various water bodies in Florida such as Biscayne Bay, Florida Bay, Indian River Lagoon, Lake Okeechobee, Sarasota Bay, St. Johns River, Tampa Bay and the U.S., such as Chesapeake Bay and the Gulf of Mexico. CH3D has been coupled to models of wave, sediment transport, water quality, light attenuation, and sea grass dynamics to produce CH3D-IMS (Sheng et al., 2003, Sheng and Kim, 2009), an Integrated Modeling System for simulating the response of estuarine and coastal ecosystem to anthropogenic (e.g. increased nutrient loading) and natural (e.g. sea level rise) changes.

More recently, CH3D has been coupled to models of wind and wave to produce CH3D-SSMS (hereafter referred to as SSMS), an integrated Storm Surge Modeling System (Sheng et al., 2006). CH3D supports flooding and drying and has been coupled to a wave model (SWAN and REF-DIF) by including wave radiation stress terms into the momentum equations. Numerical solution of the CH3D model satisfies conservation. In the past few years SSMS has been used extensively to simulate storm surge and inundation due to various tropical storms (Alymov, 2005, Zhang, 2007) including Hurricanes Charley (2004), Dennis (2005), Isabel (2003), Frances (2004), Ivan (2004), Jeanne (2004) and Katrina (2005).

The CH3D model has been parallelized using both shared memory (OpenMP) and distributed memory (MPI) approaches which makes it very efficient.

In the present study the SSMS will be significantly enhanced in several aspects. One major goal is to combine the 3-D baroclinic feature and flooding and drying functionality of the CH3D model. The wind modeling component of the SSMS will be enhanced to enable the SSMS to use a combination of wind sources. In addition, the preliminary SSMS will be made into a semi-operational nowcasting/forecasting system of storm surge, inundation as well as 3-D baroclinic circulation Its performance will be tailored to satisfy the needs of an operational forecasting system which then will be validated using new data that has become available recently. Specifically, the ability of SSMS to simulate inundation will be validated using the extensive USGS data collected during Hurricane Wilma (2005).

ELCIRC

ELCIRC is an unstructured-grid model designed for the simulation of 3D baroclinic circulation across river-to-ocean scales, one of the later applications of the model is hindcasting the 3D baroclinic circulation in the Columbia River (Zhang et al., 2004, Baptista et al., 2005). It uses a semi-implicit finite-volume/finite-difference Eulerian-Lagrangian algorithm to solve the shallow water equations developed on horizontally Cartesian, non-orthogonal unstructured and vertically unstretched z-coordinates. ELCIRC uses a low-order numerical algorithm, which however is conservative (local and therefore global mass conservation is guaranteed), stable and computationally efficient. The barotropic pressure gradient in the momentum equation and the flux term in the continuity equation are treated semi-implicitly, the vertical viscosity term and the bottom boundary condition for the momentum equation are fully implicit, while the rest of the terms are explicit. It should also be noted that in the limit of only one vertical layer the formulation of ELCIRC and its solution automatically reduce to the 2D depth-integrated version.

The model includes terms for tidal potential and atmospheric pressure gradients and provides mechanisms for air-water exchanges. Flooding and drying processes are also

represented by the model. ELCIRC uses multiple two-and-a-half equation turbulent closure schemes as well as a zero-equation model. In all approaches vertical mixing similarity for heat and salt is assumed.

One of the major advantages of ELCIRC is the use of an orthogonal unstructured grid that allows it to use large computational domains with sparse resolutions in some regions and fine resolutions in other regions where it's important, such as shallow water regions and regions located near boundaries. Another advantage is that it avoids the usual Courant number constraints by incorporating advection in total derivatives and solving the resulting equations in an Eulerian-Lagrangian context. An important part of this approach is the ability to accurately backtrack characteristic lines starting from known location at the time step n+1. Backtracking process is one of the most time-consuming parts of obtaining the solution therefore as a compromise between the speed and accuracy the backtracking in ELCIRC is using linear interpolation at the feet of characteristic lines for both momentum and scalar-transport equations. The defining advantage of linear interpolation is the positivity of solutions; however, the disadvantage of this type of interpolation is that it introduces significant numerical diffusion in the solution. Also, even though an orthogonality requirement on the computational grid can be relaxed, the accuracy of solutions suffers from it. While a second-order accuracy can be achieved with uniform orthogonal grids only first-order accuracy is attainable with non-uniform orthogonal grids. In addition to that, for non-orthogonal grids another source of error is introduced due to the fact that the line that connects the two element centroids isn't orthogonal to their common side.

FVCOM

FVCOM is a prognostic, unstructured-grid, finite-volume, free-surface, 3-D primitive equation coastal ocean circulation model developed by the joint efforts of University of

Massachusetts-Dartmouth and Woods Hole Oceanographic Institution (Chen et al., 2006). FVCOM has been applied to numerous US coastal areas (Gulf of Maine, Nantucket Sound, Massachusetts Bay, South Atlantic Bight), estuaries (Satilla River, Ogeechee River, etc) and lakes (Lake Superior, Lake Michigan) with the later applications to the East China Sea (Chen et al., 2008). The model consists of momentum, continuity, temperature, salinity and density equations and is closed physically and mathematically using turbulence closure sub-models. The model allows for a variety of ways to force the model including tides, river discharge, atmospheric forcing and ocean surface to air exchange.

The model uses a non-orthogonal unstructured triangular mesh in horizontal direction and a terrain-following grid in a vertical direction. The model can use Cartesian or spherical coordinate system for basin and global applications. FVCOM is solved numerically by a second-order accurate discrete flux calculation in the integral form of the governing equations over an unstructured triangular grid. This approach combines the grid flexibility of the finite-element methods with numerical efficiency of the finite-difference methods. Finite-volume approach guarantees both local and therefore global conservation. The equations are solved using mode splitting into an external 2D mode and internal 3D mode and the time step of the model is subject to the CFL (Courant-Friedrichs-Levy) stability criterion in which the time step of the internal mode is restricted by the phase speed of internal gravity waves.

Currently FVCOM features include: a mass conservative flooding and drying process, a General Ocean Turbulent Ocean (GOTM) sub-model (Burchard and Baumert, 1995) that provides an optional vertical turbulent closure scheme, a water quality model for simulating dissolved oxygen and other environmental indicators, various data assimilation methods (4-D nudging and reduced/ensemble Kalman filters), a fully non-linear ice model, a 3-D sediment

transport model, which is based on USGS national sediment transport model, and a biological model. A non-hydrostatic version of FVCOM is currently a work in progress.

FVCOM is a model with some attractive features such as conservation, which naturally comes in finite-volume models, but the CFL condition can make simulations on fine grids too computationally expensive.

HYCOM

HYCOM (HYbrid Coordinate Ocean Model) is a primitive equation ocean general circulation model (Halliwell et al., 1998; 2000, Bleck, 2002) that uses a hybrid vertical coordinate grid (Bleck and Benjamin, 1993). It is a result of joint efforts between the University of Miami, the Los Alamos National Laboratory, and the Naval Research Laboratory.

The hybrid vertical coordinates in HYCOM remain isopycnic in the open stratified ocean and smoothly transition to z-coordinates in the weakly-stratified upper-ocean mixed layer to the terrain-following sigma coordinate in shallow water regions and back to level coordinates in very shallow water. One of the important HYCOM features is the capability to select among several different vertical mixing schemes for both the surface mixed layer and the comparatively weak interior diapycnal mixing. The model is fully parallelized for efficiency.

HYCOM has been designed to work as a global/regional scale model therefore its schemes, parameterizations and boundary conditions are targeted towards that and assume relatively low resolution computational domain, which makes model useful as a large-scale model in a nesting set that would provide boundary conditions to a finer-scale model, which would resolve coastal and estuarine features necessary to accurately predict storm surge and inundation.

DHI MIKE

MIKE 21 and MIKE3 are the modeling packages developed by DHI (Danish Hydraulic Institute) for 2D/3D surface flow, waves, sediment transport, morphology and environmental processes that can be used for inland, coastal and offshore modeling. MIKE 21 solves the vertically integrated equations for the conservation of continuity and momentum on a rectangular, non-orthogonal unstructured or a Cartesian grid. It includes the effects of precipitation, evaporation, river discharge, etc. The impact of hydraulic structures such as bridge piers, piles and weirs on the flow conditions can also be included. Water quality modules simulate the fate and transport of conservative or linearly decaying constituents, eutrophication processes including nutrient cycling, phytoplankton, zooplankton, and benthic vegetation growth, processes affecting dissolved oxygen, exchange of metals between the bed sediments and the water column, and sediment transport/deposition/erosion. The model also supports flooding and drying. MIKE 21 can be used with a wave module which can introduce effects of waves on currents which is done through wave radiation stress terms in the momentum equation.

MIKE 3 is a three-dimensional model which is similar in features to MIKE 21. MIKE 3 simulates unsteady flow, taking into account density variations, bathymetry and external forces, such as winds, tidal elevations, currents, etc. MIKE 3 is based on the numerical solution of the three-dimensional incompressible Reynolds averaged Navier-Stokes equations with the Boussinesq assumptions and can use either hydrostatic with a generalized sigma coordinate transformation or non-hydrostatic pressure with a z-level coordinate formulation. A variety of turbulent closures can be used: constant eddy viscosity, Smagorinsky subgrid scale model, k model, $k-\varepsilon$ model or a mixed Smagorinsky / $k-\varepsilon$ model. Particle tracking is included in the model as well.

MIKE 21 and MIKE 3 are modeling packages with a variety of features for different applications, however, the fact that these are proprietary codes and their cost can make them less attractive for many researchers.

NCOM

NCOM (Navy Coastal Ocean Model) is a baroclinic, hydrostatic, Boussinesq, free-surface ocean model (Barron et al., 2005). NCOM is being used for hindcasting and forecasting by the NRL (Naval Research Laboratory) in the following regions: global, Indian Ocean region, Mediterranean, Pacific region, Atlantic region and the Arctic region.

The vertical grid of NCOM consists of sigma-coordinates for the upper layers with z-levels below a specified depth. This flexibility allows terrain following sigma coordinates in the upper ocean for better resolution and topographic fidelity in shelf regions where flow is most sensitive to its representation and z coordinates for deeper regions to provide high near-surface vertical resolution in the open ocean. In the horizontal direction the model uses an orthogonal structured curvilinear grid. NCOM uses a Smagorinsky horizontal mixing and the Mellor-Yamada Level 2.5 turbulence model (Mellor and Yamada, 1982) for vertical mixing and uses mode-splitting to solve the equations.

For its simulations the NCOM model is forced with the wind, pressure and thermal variables from the Fleet Numerical Meteorology and Oceanography Center (FNMOC) Navy Operational Global Atmospheric Prediction System (NOGAPS).

The use of a hybrid z-sigma grid in NCOM makes it very attractive for large scale (global or regional) simulations since it alleviates weaknesses related to either sigma or z grid models by resolving shelf bathymetry and providing good resolution near the free surface while avoiding problems with pressure gradient terms in the deep water that z-grid models usually provide by simple calculation of pressure gradient terms and avoiding truncation errors that can be

encountered when calculating these terms along steeply sloping bottom. However, the orthogonality requirement for the horizontal grid makes grid generation in the coastal zone a challenging task.

POM

The Princeton Ocean Model (POM) is an ocean model that is able to simulate a wide-range of problems, such as circulation and mixing processes in rivers, estuaries, shelf and slope, lakes, semi-enclosed seas and open and global ocean (Blumberg, Mellor, 1987, Mellor, 2003) with the later applications including the effect of Hurricane Wilma on the loop current warming (Oey et al., 2006) and baroclinic tidal flows and inundation processes in Cook Inlet, Alaska (Oey et al., 2007). POM uses an orthogonal curvilinear coordinate system in horizontal directions and an "Arakawa C" differencing scheme. In vertical direction it is a sigma-coordinate, free surface ocean model with flooding and drying capability. POM uses explicit time differencing in horizontal and implicit in vertical, which allows it to use fine vertical resolution in surface and bottom boundary layers. The model has a split time step with two-dimensional external and three-dimensional internal mode and it is a subject to the CFL computational stability condition. POM implements complete thermodynamics as well as it has an embedded wave model as well as embedded second moment turbulence closure sub-model to provide vertical mixing coefficients. The model facilitates the inclusion of river discharges, precipitation and evaporation; it implements three types of boundary conditions: inflow, elevation and radiation boundary condition.

POM is currently used in a number of forecasting systems such as PROFS – Princeton Regional Ocean Forecasting System, Coastal Survey Development Laboratory Forecasting System (NOAA/NOS), COFS - U.S. East Coast Coastal Ocean Forecast System (run by NCEP – National Centers for Environmental Prediction) and others. While having a formidable list of

features and capabilities POM is a structured grid model, which makes it harder to create grids with refined areas, especially with the orthogonality requirement posing additional restrictions and also it is subject to CFL condition.

SLOSH

Sea, Lake and Overland Surges from Hurricanes (SLOSH) is a 2-D linear barotropic model developed by Chester Jelesnianski (Jelesnianski et al., 1992). The model is used to estimate storm surge heights and winds resulting from historical, hypothetical and predicted hurricanes by taking into account storm central pressure, size, forward speed and track. The model uses a curvilinear, polar coordinate grid scheme, implements flooding, overtopping of barriers such as levees and dunes, channel flows and flow through barrier cuts. It does not include the effects of tides (which are generally accounted for as a single value in a form of added sea level). SLOSH is extremely efficient and most simulations can be done within a few minutes.

SLOSH is officially adopted by the National Hurricane Center for forecasting of storm surge and is used by the NOAA National Weather Service and the US Army Corps of Engineers to create flood maps representing the Maximum of the Maximum (MOM) storm surge composite of hypothetical storms. SLOSH model grids cover the entire United States coastline; model grids include local shoreline, bathymetry, topography as well as various features such as bridges and roads. Existing SLOSH grids are referenced to the National Geodetic Vertical Datum (NGVD) due to its temporal invariance. However, SLOSH grids are fairly small and even though they do overlap, sometimes it is hard to choose a domain to be used for storm surge simulation because the affected area is larger than any of the available grids and boundary effects on the computed results could be significant no matter what grid is selected. According to the NHC, the SLOSH model is generally accurate within plus or minus 20% (NHC SLOSH).

One of the biggest advantages of SLOSH is the execution speed, a 5-day simulation can be run in under 1 minute on a single CPU PC, however, the lack of dynamic effect of tides (tides are included as a fixed offset from the mean sea level), waves, low resolution of computational grids, their limited coverage, and an synthetic wind model (although it takes into account two types of wind – ocean and lake, with lake winds having reduced values) that drives the surge and a fixed wind drag coefficient can have a negative effect on the accuracy of predictions. The SLOSH model has a graphical user interface developed for it that can be useful for post-processing and analysis of simulated data.

Surge Model Summary and Selection

Table 1-2 contains a summary of features of the models described above that are of importance for storm surge and inundation simulations. The important processes include tides, river discharges, rain, and ability to include river discharges as boundary conditions.

Table 1-2. Summary of surge model features

Model	Dim.	Coord. System	Grid Horizontal	Grid Vert.	Cons.	Waves effects	Wind	Rain / Evap.	River Discharge	Tides
ADCIRC	2D/ 3D	Cartesian/ spherical	unstructured non-orthogonal	z	yes	yes	any	no	yes	yes
CH3D	2D/ 3D	curvilinear / spherical	structured non-orthogonal	σ	yes	yes	any	yes	yes	yes
ELCIRC	2D/ 3D	Cartesian	unstructured orthogonal	z	yes	yes	any	yes	yes	yes
FVCOM	2D/ 3D	Cartesian / spherical	unstructured non-orthogonal	σ	yes	yes	any	yes	yes	yes
HYCOM	3D	Cartesian	structured	hybrid	yes	no	any	yes	no	no
MIKE	2D/ 3D	Cartesian / curvilinear	structured / unstructured non-orthogonal	σ	yes	yes	any	yes	yes	yes
NCOM		curvilinear	structured orthogonal	σ-z	yes	no	NOGAPS	yes	no	no
POM	2D/ 3D	curvilinear	structured orthogonal	σ	yes	yes	any	yes	yes	yes
SLOSH	2D	curvilinear polar	structured orthogonal	n/a	??	no	synthetic (ocean / lake)	no	no	fixed offset

Based on the model features, and their advantages and disadvantages two models were selected to be included in the SSMS and another two models were picked as external sources of boundary conditions. The CH3D model was selected as the coastal model for the SSMS as it is a robust model that has been under development for over two decades and has been validated with various data in different areas of the US coastal zone. It uses a curvilinear non-orthogonal grid and therefore is very suitable to fit complex coastal lines. The ADCIRC model has been selected to be part of the SSMS suite and represent a regional scale 2-D model as it is also a well-validated model for the storm surge applications. The ADCIRC model is used to provide the surge boundary conditions to the CH3D model to run the SSMS with 2-D scenarios. The 3-D baroclinic scenarios, however, require salinity conditions at the open boundary of the CH3D model which ADCIRC can't provide. For this purpose two models HYCOM and NCOM were selected as these models produce forecasts on global grids as well as a number of regional grids around the globe on a regular basis and the results of these forecasts can be used to create boundary conditions for 3-D simulations of the CH3D model.

Wave Models

Waves are another important feature that can have a dramatic effect on storm surge and inundation, it is not uncommon to see 3-5 meter or larger waves hitting the shore during a large storm. Interaction of waves with surge can be rather complex, not only waves interact with currents in deep water; they can also affect the air-sea interaction at the water surface. Younger waves are rougher and allow wind to induce larger stress on water surface. Waves can create rather significant setup producing large surge and inundation.

Therefore a wave model is needed to be coupled with a circulation model for more accurate representation of surge and inundation. Just as with circulation models – a number of wave models were reviewed in order to select a model that would best fit the task.

COULWAVE

COULWAVE (Cornell University Long and Intermediate Wave Modeling Package) is a model developed for wave generation, evolution, and interaction with depth-integrated, dispersive wave equations (Lynett, Liu, 2004a, 2004b). It uses a multi-layer approach to wave modeling, deriving a separate velocity profile for each layer matched at the interfaces.

The governing equations employed in this model allow for the evolution of fully nonlinear (wave amplitude to water depth ratio $= O(1)$) and dispersive waves over variable bathymetry, in addition the generation of waves by movement of the sea floor can be examined. The general fully nonlinear model can be truncated to include either only weakly nonlinear effects, or model a non-dispersive wave system. A deep water accuracy limit of the model $L_s / h_c > 3.5$ is used in the model. Two types of boundary conditions are used in COULWAVE – the reflective or no flux boundary condition and radiation boundary condition (for this type of condition a sponge layer is utilized). The numerical model uses a predictor-corrector scheme for marching forward in time and finite differences for spatial derivatives. The model is formally accurate to Δt^4 in time and Δx^4 in space. The corrector segment of the procedure is implicit in time and uses an iterative algorithm to arrive at a solution.

The main feature of the COULWAVE code is its ability to simulate large domain with 10's of millions grid points and is well suited for simulations of landslide tsunami generation and propagation, nearshore tsunami evolution and inundation and nearshore wind wave modeling.

DELFT WAVES

Delft-WAVES is a numerical wave modeling system for coasts, harbors, structures and ships developed by Delft University of Technology. It consists of the following components: a spectral wave model SWAN, the mild slope equation model PHAROS for short wave and long wave propagation in harbor regions, and the time-domain Bousinessq model TRITON for applications in

coastal and harbor regions; a SKYLLA module can be used to analyze wave motion on coastal structures. All four modules of this system can be coupled to be able to handle a variety of coastal wave applications with each component adding unique features into the system.

SWAN (Simuating WAves Nearshore) is a third generation phase-averaged wave model for the simulating of waves in waters of deep, intermediate and finite depth and can also be used as a wave hindcast model.

PHAROS (Program for HARbor Oscillations) is a numerical wave model for the simulation of wave agitation and wave resonance in harbor basins. It is based on the mild-slope equation, which governs linear wave propagation over a mildly sloping bathymetry with no restrictions to water depth. PHAROS can represent the following processes: diffraction, refraction due to depth variations and refraction due to ambient currents. It includes the effects of dissipation by wave breaking and bottom friction, partial reflection from complex seawalls, beaches, etc and partial transmission due to overtopping or permeability.

TRITON is a Boussinesq wave model for computing wave dynamics in detail by simulating intra-wave properties such as individual wave height transformations, wave skewness and wave asymmetry, and drift velocities for arbitrary bathymetries. Processes represented by TRITON include: dispersion, diffraction, refraction, shoaling, nonlinear wave-wave interactions, wave breaking and run-up, reflections at structures, wave absorption at boundaries. TRITON numerical method guarantees conservation of mass and momentum.

SKYLLA is a viscous flow model designed to model wave motion on coastal structures. It solves the Navier-Stokes equations. A so-called cut-cell method is used to implement the boundary conditions at arbitrarily shaped structures. A Volume-of-Fluid technique that can handle a highly-irregular interface that may develop between water and air is used to simulate the motion of the free surface.

STWAVE

STWAVE (STeady State spectral WAVE) is a half-or full- plane model for nearshore wind wave growth and propagation. STWAVE (Resio, 1987, 1988a, 1988b) is a phase-averaged spectral, finite-difference model based on the wave action balance equation. The model is formulated on a Cartesian grid, operates in a local cross-shore, alongshore coordinate system; nesting can be used to implement variable grid resolution, nested models are coupled by saving the spectrum of the coarse model simulation and using it as a boundary condition for a fine grid. Lateral boundary conditions can be specified as water or land, with land blocking wave propagation from land directions, with water boundary conditions allowing the waves to propagate in and out of the domain.

STWAVE simulates depth-induced wave refraction and shoaling, current-induced refraction and shoaling, depth- and steepness-induced wave breaking, diffraction, parametric wave growth because of wind input, and wave-wave interaction and white capping mechanism for energy dissipation and redistribution in a growing wave field. It also includes calculation of radiation stresses and identification of regions of active wave breaking. Model assumptions include: mild bottom slope and negligible wave reflection, spatially homogeneous offshore wave conditions, steady-state waves, currents, and winds, linear refraction and shoaling, depth-uniform current, the bottom friction is neglected. Currently work is being done on extending STWAVE from a half-plane to a full-plane model, which includes propagation and generation from all directions. STWAVE has a graphical user interface developed for it as part of SMS (Surface Modeling System, software developed by Aquaveo).

The advantages of STWAVE is a relatively fast execution time and a solid set of simulated processes, however, the steady state assumption negatively affects the usefulness of this model for storm surge simulations, which is especially relevant for fast moving storms when the wave field becomes very dynamic.

SWAN

SWAN (Simulating WAves Nearshore) while a part of the Delft-WAVES modeling system is a very capable wave model that can be used as a standalone model as it can handle a variety of problems (Booji et al., 1999, Ris et al., 1999, SWAN Team, 2009).

SWAN is a third-generation phase-averaged wave model that can be applied to the nearshore wave modeling. The model uses Cartesian coordinate system and can use a variety of computational grid arrangements including non-orthogonal regular, curvilinear and unstructured triangular grids. SWAN accounts for wave propagation in time and space, shoaling, refraction due to currents and depth, frequency shifting due to currents and dynamic depth, wave generation by wind, energy dissipation by bottom friction, depth-induced breaking and transmission through and reflection from obstacles (full or partial reflection can be considered).

SWAN represents waves using a two-dimensional wave action density energy spectrum and the evolution of the spectrum is described by the spectral action balance equation in which a local rate of change of action density in time is related to the propagation of action in geographical space, shifting of relative frequency due to currents and depths, depth-induced and current-induced refraction all balance by the source term in terms of energy density representing the effects of energy generation, energy dissipation and nonlinear wave-wave interactions. Generation of waves due to wind in SWAN is described as a sum of linear and exponential growth. The dissipation of wave energy consists of whitecapping, bottom friction and depth-induced wave breaking. In deep water the evolution of the spectrum is dominated by the wave-wave quadruplet interactions which transfer wave energy from the peak of the spectrum. In very shallow water, triad wave-wave interactions transfer energy from lower to higher frequencies where the energy is dissipated by whitecapping.

SWAN is currently used as part of several wave forecasting efforts, such as a sub-regional scale wave forecasting system developed by the Naval Research Laboratory (NRL) for the National

Weather Services Coastal Storms Program (Rogers et al., 2006). SWAN has a set of features so that it can be used as a standalone model for nearshore wave modeling, however, its efficiency can become an issue in applications where sufficiently large computational grids have to be applied.

WAM

WAM is the global ocean Wave prediction Model (WAMDIG, 1988) and is a third generation wave model that describes the evolution of a two-dimensional ocean wave spectrum without ad hoc assumptions regarding the spectral shape by integrating the basic transport equation. The model uses a spherical latitude-longitude grid. The model is formulated with a deep water assumption and then the deep-water transport equation is extended to shallow water by adding additional source functions representing loss of energy due to bottom friction and percolation and appropriate assumptions are added to other terms of the transport equation. The source functions that are prescribed explicitly are the wind input, nonlinear transport and white-capping dissipation. Bottom dissipation source function and refraction terms are included in the finite-depth version of WAM. The bottom friction term for finite-depth is based on the JONSWAP study (Hasselmann et al., 1973).

Verification has been carried out in three areas where National Oceanic and Atmospheric Administration (NOAA) moored buoys are available on the Global Telecommunications System (GTS).

WaveWatch III

WaveWatch III (Tolman, 1999, 2002) is a third generation wave model developed at NOAA/NCEP following the WAM model (WAMDIG, 1988, Komen et al., 1994). It is a further development of WaveWatch I (Delft University of Technology) and WaveWatch II (NASA, Goddard Space Flight Center), which, however, is significantly different from its predecessors in all aspects of the numerical modeling.

WaveWatch III solves the spectral action density balance equation for wave number direction spectra. The assumptions used in this equation are that the water depth and current as well as the wave field itself vary on time and space scales that are much larger than the variation of scales of a single wave. In addition the parameterizations of physical processes in the model do not address conditions in which the waves are strongly depth-limited. These assumptions imply that the model can be used on large spatial scales (1-10km grid resolution) outside the surf zone.

WaveWatch III can use either a Cartesian or a regularly spaced longitude-latitude grid. Wave energy spectra are discretized using a constant directional increment covering all directions and a spatially varying wave number grid (an invariant logarithmic intrinsic frequency grid). The model can use either a first order accuracy or a third order accuracy numerical scheme for wave propagation. The source terms in the model are integrated in time using a dynamically adjusted time stepping algorithm, which concentrates computational efforts in conditions with rapid spectral changes.

The governing equations of WaveWatch III include refraction and straining of the wave field due to temporal and spatial variations of the mean water depth and of the mean current, such as tides and surges. The implemented physical processes are wave growth and decay due to wind, nonlinear resonant interactions, dissipation (whitecapping) and bottom friction. All the nonlinear processes are implemented as source terms, since wave propagation is considered to be linear. The model includes several alleviation methods for the garden sprinkler effect, includes sub-grid representation of unresolved islands and the options for choosing between the two source term packages: one is based on cycles 1 through 3 of the WAM model and the other is based on Tolman and Chalikov (1996). WaveWatch III also supports data assimilation and includes dynamically updated ice coverage. WaveWatch supports parallelism using both OpenMP and MPI.

The limitations in WaveWatch III physics prohibit it from being used in the coastal zone, but it serves its purpose well as a regional wave model and is being operationally run by NOAA/NCEP

(both hindcast and a 120-hr forecast) as has a record of producing good results during tropical storm evens when compared to the measured data.

Wave Model Summary and Selection

Based on the review of wave models, which are summarized in Table 1-3, two models were selected for the development of the storm surge forecasting system. Delft Waves is omitted from the table as it is suite of commercial codes and would be prohibitively expensive. SWAN and WaveWatch III models were selected for simulation of waves. SWAN is a robust model that has been coupled to CH3D before and can use the same grid as CH3D model which makes coupling the two models easier and makes it more accurate compared to models that use different model grids and require interpolation when exchanging information. SWAN is a coastal model and requires the open boundary conditions and that's why the WaveWatch III was selected to provide those to the SWAN model. WaveWatch III is being run by NOAA and results are made available to the public and can be used to drive the SWAN model. This method has been successfully employed previously when running coupled CH3D/SWAN simulations.

Table 1-3. Overview of wave model features

Wave model	Scale	Horizontal grid	Dimension	Type
COULWAVE	coastal	structured	2D multi-layer	Bousinessq
STWAVE	coastal	structured Cartesian	2D	spectral
SWAN	coastal	unstructured / structured curvilinear	2D	spectral
WAM	global	structured	2D	spectral
WaveWatchIII	regional / global	Unstructured / structured curvilinear	2D	spectral

A Few Selected Storm Surge, Inundation and Waves Forecasting Systems

Currently there are many forecasting systems that differ in operations, area of coverage, targeted processes and capabilities. A short review of several systems that are used or can potentially be used for storm surge and inundations forecasting is presented here.

NCFS

NCFS (North Carolina Forecast System) is a real-time, event-triggered storm surge forecasting system for the state of North Carolina (Mattocks and Forbes, 2008). It uses a high-resolution, two-dimensional depth-integrated version of the ADCIRC model with winds from a synthetic asymmetric gradient wind vortex. Tidal harmonic constituents are prescribed at the open water boundaries and applied as tidal potentials in the interior of the ocean model domain. The winds are modulated using directional surface roughness based on the types of land cover encountered upwind.

NECOFS

NECOFS (Northeast Coastal Ocean Forecast System) is a system that targets similar goals as the proposed system and focuses on the Northeastern part of the United States. It is currently based on WRF, MM5 and FVCOM and is able to produce 3-days's forecast of surface winds, air pressure, water level and currents with intent to add simulation of surface wave, sediment transport, biological models as well as local inundation models. However, some components of the system are still under development.

RTFS of Winds

Real Time Forecasting System of Winds, Waves and Surge in Tropical Cyclones (Graber et al., 2009) - the system focuses on the forecasting of surge and waves for tropical cyclones. The system is forced by WINDGEN winds and uses WAM and ADCIRC at its core. The system is based on 2-D models and hence is limited to accurate simulation of water levels.

RTOFS

RTOFS (Spindler et al., 2006) – based on a HYCOM provides nowcasts and forecasts of sea levels, currents and salinity. The emphasis of the system is on the coastal ocean, Loop Current and the Gulf Stream regions. Due to its coverage resolution of the model domain varies around 5 kilometers which is not sufficient for the near shore and estuarine areas.

SLOSH

SLOSH is a computerized two-dimensional linear barotropic model, run by the National Hurricane Center to estimate storm surge heights and winds resulting from historical, hypothetical, or predicted hurricanes by taking into account:

- pressure deficit
- size
- forward speed
- track
- winds

The model does not take into account such processes as:

- evaporation and precipitation
- river flow
- wind-driven waves
- currents
- heat exchange
- tides are not included dynamically into the model
- coarse grid resolution
- 3D and baroclinic processes

SLOSH in being run operationally in an event-driven (storm driven) manner by the NHC.

SSMS

SSMS (Sheng et al., 2006, 2008) is an integrated storm surge modeling system that was designed to simulate storm surge in coastal regions. It is based on CH3D and SWAN model for the coastal zone and uses regional models ADCIRC and WaveWatch III to the coastal models. SSMS has been used to simulate hurricane-induced storm surge, wave, and coastal inundation in high-resolution coastal regions during several hurricanes (2003-2005) such as Hurricane Ivan (2004),

Hurricane Frances (2004), Hurricane Charley (2004), Hurricane Dennis (2005). SSMS is able to use a variety of wind fields including internal synthetic models (ANA), GFDL, H*Wind, WNA (WaveWatch III wind), etc.

Enhancing CH3D-SSMS

Table 1-4 contains a summary of existing forecasting systems. A review of these systems shows that SSMS, which already includes coastal and regional scale circulation and wave models, supports a variety of winds and has multiple grids developed for the state of Florida, has a good potential to be enhanced and expanded to a semi-operational forecasting system for the state of Florida.

Table 1-4. Summary of forecasting systems

Forecasting System	Surge Model	Wave Model	Wind	Assimilation	Operational	Region	
						Coastal	Basin
CH3D-SSMS	CH3D / ADCIRC	SWAN / WWIII	ANA, GFDL, H*Wind, WNA, etc	no	no	Multiple grids in Florida and the GOM	Florida and GOM
NCFS	ADCIRC	none	synthetic asymmetric	no	no	North Carolina	North Carolina coast
NECOFS	FVCOM	SWAN	WRF/MM5	yes	no	North-East US coastal region	North-East US coastal region
RTFS of Winds	ADCIRC	WAM	WindGEN	yes	yes	GOM	North Atlantic and GOM
RTOFS	HYCOM	none	GDAS/GFS	yes	yes	n/a	Atlantic
SLOSH	SLOSH	None	synthetic (ocean / lake)	no	yes	multiple grids cover the entire US coastline	n/a

This work will improve the SSMS everaging upon the existing framework and set of models by improving the physics of the SSMS, improving its performance and reliability to create a semi-operational hindcast and forecast system, which could serve as a prototype for an operational system and to validate the newly created system with the data from recent storms since 2005. An option to perform forecasts of baroclinic flow will be added, which will require adding coupling to other regional scale models in addition to ADCIRC in order to obtain vertically varying salinity profiles at the open boundaries. Two main scenarios will be studied using the proposed SSMS: *Full3D* – featuring 3D version of CH3D with wetting and drying and baroclinic circulation, SWAN for waves and, optionally, HYCOM or NCOM model to provide the salinity open boundary condition to CH3D and *Fast2D*, which would use a 2D version of CH3D which is significantly more efficient than the 3D model and requires less data to run simulations and can be run in a smaller amount of time. The *Fast2D* scenario would aim to run within the shortest amount of time possible to satisfy the time requirements needed for emergency managers for evacuation and *Full3D* will strive to produce the best forecast possible at the expense of time. The two scenarios will then be compared to determine the gains and trade-offs associated with each scenario.

The proposed system will be used to attempt to answer the following questions:

- Can hurricane winds and pressures be adequately represented by a parametric model for the purpose of storm surge and inundation forecasting?
- Does inclusion of land exposure and “background” wind increase the accuracy of storm surge and inundation predictions?
- Is dynamic coupling of surge, tides and waves important for accurate predictions of storm surge and inundation?
- Is inclusion of rainfall and runoff important for accurate prediction of surge, inundation and salinity?
- Can the proposed system provide timely warnings for Florida coastal counties?
- What model scenarios (combination of models, model features and data) are feasible to provide timely warning for Florida coastal counties?

- How long does it take to provide the most accurate forecast (*Full3D*) possible? Is it practical? Does it meet the NWS evacuation times? How that can be improved in the future?

- How important is model resolution when simulating inundation?

- Can the *Full3D* model scenario using NCOM or HYCOM models predict baroclinic circulation in the coastal zone with reasonable accuracy?

- Can the proposed system timely and accurately predict measured storm surge, inundation and salinity during the storms since 2005, such as hurricane Wilma (2005) and tropical storm Fay (2008)?

Goals and Objectives

The goals of this study are as follows:

I) Improve the physics of the SSMS
II) Improve the performance of SSMS to create a semi-operational forecast system
III) Validate SSMS with the new data since 2005

In order to reach the goals above, the following objectives are set for research:

1. Add a Wind Modeling System (WMS) to the SSMS which would allow for flexible processing of various wind fields and

    a. would be able to produce wind field input for any model included in SSMS at any temporal and spatial resolution automatically handling the interpolation in space and time;

    b. would contain a synthetic wind model by Xie et al (2006) to improve wind field representations for simulations using the parametric model;

    c. would have an ability to blend wind fields for the purpose of combining wind fields with coarse resolution that cover large area with those with fine resolution which only cover small areas and insufficient to cover the model domain;

    d. would support data assimilation;

    e. would support land-induced wind dissipation.

2. Enhance the SSMS by coupling the 3D wetting and drying version of CH3D to NCOM and HYCOM models and by doing so enabling the CH3D to simulate baroclinic flow and salinity transport.

3. Enhance the performance of the SSMS by

    a. Parallelization of the main loops of CH3D code that supports wetting and drying using OpenMP technique to enhance performance on multi-CPU systems;

b. Design job submission / scheduling software that would take into account the parallel nature of the SSMS where one or more models such as CH3D, SWAN and ADCIRC could be running at the same time each being able to run in parallel;

c. Add the ability to use a variety of computational resources distributed geographically;

d. Full automation of data collection, run setup and scheduling, post-processing and publishing of results to create a semi-operational system that can function without human intervention for a prolonged period of time.

4. Validate the SSMS using the new data since 2005 from hurricane Wilma (2005) and tropical storm Fay (2008).

Reaching these goals and objectives would produce a functional real time semi-operational forecasting system prototype for the state of Florida that could be used for practical purposes such as providing information to emergency and water resource managers and/or future research.

CHAPTER 2
DEVELOPMENT OF SSMS

This chapter will describe the development of the Storm Surge Modeling System (SSMS) as a computational system. SSMS consists of multiple computer models for simulating circulation, waves and winds. It also makes use of a variety of measured data, guidance, advisories, as well as output of computer models, such as GFDL, HYCOM, NCOM, NOGAPS, WRF, and WaveWatch III provided by different organizations via different methods. The physical processes that are represented in the system, their importance and effects will be discussed followed by the technical implementation of the system including the computing facilities, data collection, scheduling, running simulations and dissemination of results.

SSMS Models and Processes

Simulating surge and inundation is an involved process that consists of many components such as flooding and drying, wind induced surge and waves, tides, river flows and rainfall and all these processes need to be adequately represented by the modeling system.

SSMS Model Coupling

The SSMS core consists of two tightly coupled coastal models - CH3D and SWAN (Figure 2-1). The models are coupled by including wave radiation stress terms based on the SWAN calculations into the CH3D model and by passing the water level and currents from CH3D to SWAN. The two models use the same computational grid, but run at different time step intervals. CH3D model typically runs at 1-minute time step and SWAN runs at 5-minute time step. SWAN running on the same grid as CH3D takes 5-10 times longer to complete one time step than it takes for CH3D to complete its time step. Given the difference in time step length the two models run at approximately the same pace and neither model is significantly delayed by the execution of the other model. The models exchange information at every SWAN time step. CH3D passes updated water level and currents and SWAN passes the radiation stress terms to the CH3D model. Both models use

the same bathymetry and wind input which ensures consistency. Since CH3D-SWAN both use relatively structured grids it becomes computationally expensive to cover large areas; therefore larger scale models are used to provide boundary conditions to each model. WaveWatch III is used as a provider of wave boundary conditions for SWAN, while there is a choice of options for CH3D open boundary conditions depending on the simulation scenario. The options for CH3D are to use ADCIRC, HYCOM and NCOM models results. ADCIRC is the preferred option for 2D forecasts since ADCIRC is a 2D model and it provides surge at the CH3D open boundary. ADCIRC is being run locally using the same wind source as used for CH3D simulation. For 3D simulations and simulations with salinity the SSMS uses HYCOM or NCOM results at the CH3D open boundary conditions. Outputs of these models consist of water level and salinity. Vertically varying salinity is used at the open boundary of the CH3D to drive the model simulation.

Flooding and Drying

A flooding and drying version of the CH3D model is used in the SSMS. Flooding and drying is implemented in CH3D as follows: a grid cell is considered dry if water level in it falls below a predefined tolerance depth (generally tolerance depth is defined as 1-5 cm depending on horizontal grid size to ensure stability). A dry cell then becomes wet if any neighboring cell can provide sufficient flux into the dry cell in question to fill it to the predefined tolerance.

Wind

Wind is the most important and dominant contributor to the storm surge and inundation as it is the wind that drives the flow inland, creates waves and causes significant damage to life and property. Correct representation of the wind field is a vital part of the storm surge modeling. Since surface drag is a quadratic function of the wind speed even small errors in wind field can create significant differences in surge. Forecasting winds in a storm is also a very involved process and is not covered in this work. However, significant efforts were dedicated to use the existing forecast models and products to their fullest potential, whether these are global scale atmospheric models or

simplified analytical solutions for wind fields in a storm. A Wind Modeling System (WMS) was developed to provide a seamless interface between existing wind products such as HRD H*Wind, GFDL model output, WRF model output, etc and the SSMS. Generally atmospheric models and measurements provide data at different time intervals, using a variety of spatial representations and all these datasets have different characteristics. However, circulation and wave models are designed to only ingest one type of data. All the models that are part of the SSMS use winds at 10 meters elevation and pressure at mean sea level. The parameterization of wind stress (surface drag) is such that it is desirable to use 10-min average winds. The purpose of the WMS is to manipulate various datasets to make them usable by the models that are included in the SSMS. WMS addresses the following issues:

- extraction of winds at 10-meters elevation and pressure at mean sea level from all supported datasets
- conversion of winds to 10-min average equivalent
- data assimilation and blending (smoothly combining two or more data sets for example including a high resolution hurricane wind snapshot that covers only limited area of the model domain onto a lower resolution snapshot that covers the entire model domain and provides background wind) of different datasets
- lagrangian interpolation of wind fields - generally model wind fields are provided at 3- to 6-hour intervals, surge and wave models use linear temporal interpolation between data snapshots, which alters the structure of the storm especially for fast moving storms. The WMS uses advanced algorithms to detect storm centers at each data snapshot and uses interpolation in time that takes into consideration the translation of the storm
- over land and open water winds, once storm makes a landfall it dissipates rather quickly due to higher roughness over the land compared to the open ocean. The WMS takes this factor into consideration. It uses land cover data to compute land roughness data and can apply it to various sources of wind as required. This is very important step to be able to correctly represent the surge on the side of the storm where wind blows from the land to the open ocean

Tides

Tides can make an important contribution to the total surge and inundation. Currently none of the forecasting systems that were reviewed include tides dynamically. Given that tidal range at Florida coast reaches 4-5 feet, it can make a significant contribution. Some forecasting systems

include tides as an offset that is added to the storm surge or inundation, which is not an accurate solution. Slower moving storms may spend six hours or more making landfall, which can cover the entire range of a semi-diurnal tide and then the resulting surge is very dependent on timing of the tide.

The SSMS includes tides dynamically into simulations. Tides are incorporated into the open boundary conditions of the CH3D domain by linearly adding tidal components to the surface elevation. The tidal contribution to the open boundary is calculated based on the tidal constituents. The SSMS uses the following methodology to define tidal constituents at the open boundary:

1. a set of stations from the NOAA CO-OPS (Center for Operational Oceanographic Products and Services) is selected. CO-OPS provides a list of 37 tidal constituents at several hundred locations at the United States coast (Figure 2-2)
2. a set of significant constituents for the domain is selected - a constituent is included into the boundary condition if its amplitude is larger than 1 cm at any of the stations selected in step 1
3. the open boundary constituents are extrapolated based on the data at selected stations
4. CH3D simulation is performed (usually a 30-day simulation), results of the model are output at the location of stations and harmonic analysis is done to compute constituents of the model output at these location
5. the open boundary conditions are adjusted depending on the results of the harmonic analysis at step 4, constituent amplitudes are increased/decreased and phase is adjusted depending on the lag at the stations
6. steps 4 and 5 are repeated until desired accuracy at the output stations is reached

This procedure allows arriving at a set of harmonic tidal constituents that is universal for the domain. These constituents can be used for all simulations within the same domain when appropriate phase lag depending on simulation start time taken into the account.

Surge

In certain cases a domain size can become a reason for inaccuracies of model simulations. CH3D/SWAN domains generally extend 30-50 miles offshore and cover 150-200 miles alongshore. However for a large storm the offshore extents of such a domain may be insufficient. In order to address this problem, the SSMS uses regional scale models that provide surge boundary conditions

at the open boundary of the coastal domain. This allows model to account for surge accumulated outside of the coastal domain. The SSMS has an ability to use the data from three different large scale models: ADCIRC, HYCOM and NCOM. ADCIRC model is part of the SSMS model suite and runs in real-time along with CH3D and SWAN providing the open boundary conditions. HYCOM and NCOM results are obtained from external sources and can also be used to define the open boundary conditions of the coastal domain. As mentioned previously, the surge from the regional model is added to the tides generated based on the harmonic constituents to form the final water level at the open boundary of the CH3D domain.

Waves

The waves are introduced into the CH3D model by the means of radiation stress. The radiation stress terms are incorporated into CH3D equations (details are presented in Appendix D). A wave model SWAN is coupled to CH3D via these terms. CH3D model provides water level and currents to the SWAN model and SWAN provides the variables that are required to calculate the radiation stresses for the CH3D model. SSMS uses vertically uniform formulation of radiation stress everywhere except for the top layers which fall above the wave trough. Below the wave trough, Stokes drift is assumed to be zero and the formulation based on Longuet-Higgins and Stewart (1964) is used. Above the wave trough an additional contribution to the radiation stress term is calculated which represents surface roller (Haas and Svendsen, 2000) and accounts for Stokes drift.

Currently a vertically varying formulation of radiation stress is being considered for CH3D/SWAN coupling based on a recent work by Mellor (2008).

River Flow

CH3D model allows for flow boundary conditions and river flows and runoff are added to CH3D model domains whenever possible. SSMS uses river forecasts provided by the National Weather Service's Advanced Hydrologic Prediction Service (AHPS). Locations of AHPS forecasts and observations are shown on Figure 2-3. Unfortunately such data is very sparse and there is still

room for improvement. Coupling with watershed models would be a sound solution and it is being considered for future development of the SSMS.

When using the AHPS data the SSMS attempts to use all available data. Locations that provide observed data only are used as well as locations that provide both observations and forecasts. The latest observed or forecasted value is extended until the end on the duration of the simulation. Thus if a 48-hr forecast is available for rivers but a 72-hr forecast is being simulated by the SSMS all times between 48-hr and 72-hr forecasts will be forced by the same value and that value is equal to the value at 48 hr forecast time.

Salinity

Salinity transport is implemented in CH3D and therefore can be simulated by the SSMS. SSMS relies on HYCOM or NCOM to provide salinity values at the open offshore boundaries of the domain by interpolating HYCOM/NCOM vertical transect located at the CH3D open boundary to the CH3D boundary cells. Water that is brought in by rivers through flow boundary conditions as well as precipitation is assumed to be fresh.

Precipitation and Evaporation

Precipitation and evaporation terms are included in the CH3D model equations and are used whenever possible. HYCOM provides forecasts of precipitation and evaporation. These data are incorporated into HYCOM/CH3D coupling and the water flux provided by HYCOM is input into the CH3D model as fresh water flux from the surface. It will be shown later that these data can be very important in predicting salinity as storms usually bring heavy rains which in turn can significantly decrease the salinity. The National Weather Service Southeast River Forecast Center also provides forecasts of precipitation for the state of Florida that can be fed into the SSMS.

SSMS Operational Cycle

SSMS modeling cycles are similar to the NOAA and NHC cycles. There are two possible scenarios for SSMS forecasts to be run: 24/7 regular interval forecasts, these are typically done at 6-

hour intervals since they depend on the data that is supplied at 6-hour intervals; the other option is running event-triggered simulations (triggered by tropical storm advisories that are issued by the National Hurricane Center). In either case the SSMS attempts to run simulations in a continuous manner. Every forecasting cycle (Figure 2-4) is preceded by a hindcast cycle unless this is the first simulation in the series or when the data stream used for model input has been interrupted for any reason and it is impossible to fill the gap between the previous simulation in the series and the current one.

Datum

Datum is a very important topic when it comes to computing inundation since topographical datasets in the United States are generally referenced to the NAVD88 datum and the MSL (Mean Sea Level) datum used by many models and systems is inappropriate due to the fact that it is not defined for dry land. Computing the amount of flood when referenced to the NAVD88 datum is simple and transparent and therefore it is a datum of choice for the CH3D model and the SSMS system. All CH3D and therefore SWAN grids are referenced to that datum. Unfortunately some of the data used for comparisons, bathymetric data as well as the output of larger scale models are provided in a variety of other datums such as Mean Sea Level (MSL), MLLW (Mean Low Low Water), etc. In order to resolve these conflicts and bring all the data to the common datum the SSMS uses a conversion method.

The only available dataset that can help in relating different datums such as MSL and MLLW to the NAVD88 is the datum information provided by the NOAA Tides and Currents (Figure 2-5). The datums are based on the 1983-2001 Epoch and are provided at many locations throughout the Florida coastline. VDATUM project by NOAA that targets integrating the elevation data for the continental US provides a multitude of data on the west coast of the US, but the data for Florida is limited to the western part of the Florida panhandle and a small area in the Tampa Bay region (Figure 2-6).

The SSMS uses NOAA Tides and Currents stations to convert data between the datums. The difference between the datums in question at any given location is interpolated using a linear inverse distance method based on the available NOAA stations that contain the data for both datums in question and are located in proximity (20 miles) to the point where datum shift is being calculated. The calculated difference is then applied to convert elevation data from one datum to another.

SSMS: Implementation

The Storm Surge Modeling System is a software suite which includes models such as CH3D, SWAN and ADCIRC, service programs which automate various processes such as coupling between model codes, collecting, archiving and cataloging of data and model results, data pre-processing and setting up model simulations, post-processing the results and display in an interactive form on the SSMS website. These softwares use a variety of technologies and programming languages. Some of the most important properties of the SSMS are full automation, compliance with standards and efficient use of available computational resources.

The SSMS consists of four distinct modules (Figure 2-7): Data Acquisition Module, Wind Processing Module, Core Module and Publishing Module. All modules are independent and are connected via the central archive and catalog.

The Data Acquisition module is responsible for data collection and consists of software that monitors (polls) the data providers for new datasets and obtains the data as it becomes available. Monitors for a variety of datasets are available such as: NOAA NHC advisories, ATCF forecast products, GFDL model winds, WRF model winds, WaveWatch III model output, HYCOM model output and NCOM model output, etc. All the data is downloaded as soon as it becomes available, processed, archived and cataloged. Based on data availability, the SSMS triggers the start of forecast cycles. Two types of forecast cycles exist: 24/7 scenario, which consists of 4 forecasts per day at 6-hour intervals. These simulations follow the NOAA cycles and are based on wind products that are available at 6-hour intervals. The second type of forecasts is triggered by NHC advisories.

Whenever NHC issues a new advisory it becomes a potential trigger (depending on the location of the storm and its forecasted path) for a forecast. This type of forecast follows storm events and has a priority in simulations over the 24/7 scenario. Data availability is the basis for initiating a new forecast cycle; a complete data set such as source wind, the waves at the open boundary, the surge at the open boundary, the flow rates at rives should be available (waves, surge, river flows can be optional depending on the model scenario) from the archive for the forecast cycle to be initiated. The data is pulled from the archive by the Wind Processing Module and all necessary wind input files are generated for all the simulations that are scheduled to run within that cycle. Completion of this process triggers the start of the cycle at the Core Module which is responsible for setting up the boundary conditions for all the models involved in the cycle, scheduling and submitting the simulation to one of the available computational resources.

Model Coupling

Model coupling in SSMS is implemented by providing input and output files standard for each model. CH3D is modified to write water level and currents in SWAN input format every N time steps and SWAN outputs variables required to calculate wave radiation stresses for CH3D in ASCII format.

Both coastal models CH3D and SWAN are dependent on open boundary conditions from larger scale models such as ADCIRC (HYCOM, NCOM) and WaveWatch III.

CH3D boundary conditions can be provided by ADCIRC, HYCOM or NCOM models. HYCOM and NCOM boundary conditions are required for 3D simulations with salinity transport since only these two models are able to provide vertically varying salinity profile at the open boundary of CH3D model. One of the three models provides a surge component of the CH3D open boundary which is then combined with tidal constituents.

ADCIRC model output consists of ASCII files, HYCOM and NCOM are obtained in NetCDF format. WaveWatch III model results are provided in GRIB format. The SSMS is able to process either one of the aforementioned file formats converting them as necessary.

The SSMS uses a three-point inverse distance interpolation method to interpolate water level values from the large-scale model to the CH3D model boundary. Since the grids of all three models are fixed, the interpolation scheme is pre-computed - each boundary cell of CH3D model is associated with three cells of the large scale model domain, whether ADCIRC, HYCOM or NCOM and an appropriate coefficient based on the distance to that cell is assigned to each of the three cells. Salinity boundary condition is setup in a similar manner but vertical interpolation is added to specify a vertical profile of salinity at each of the CH3D boundary cells. The ADCIRC model usually runs at the same time-step as CH3D and models exchange information at every time step. HYCOM and NCOM data are provided at 6-hour intervals and temporal interpolation is applied between the snapshots internally by the CH3D model.

WaveWatch III data is provided in GRIB format in a form of spatial snapshots at 6-hour intervals. The open boundary conditions for SWAN are handled similarly to those of the CH3D model water level boundary conditions, since these data are two-dimensional. Also in the same manner linear temporal interpolation is applied between the times at which the snapshots are provided.

Data Standards

Standardization is another important issue for any system that integrates a variety of data and attempts to provide results that are intended for use by others. Results should be provided in a form that follows existing standards. Potential users can be encouraged to take advantage of the product if it comes in a form that makes it easy to use. The file format of choice for all the SSMS output is NetCDF which makes the results platform independent and easily accessible as a multitude of NetCDF compliant software exists for processing and plotting of the data. However, additional

products can be generated based on the needs of the system and its users. The SSMS supports GIS shape files which is readily supported by a variety of GIS software, including the MapServer which is located at the heart of the SSMS interactive web-based user interface. Google's KML (Keyhole Markup Language) is also supported by the SSMS which can generate model output in KML format that can be displayed using Google Earth software. All of the archived data is stored in NetCDF format as it is much more compact. Shape files and KML files are generated on demand and are stored in a short-term cache so that they are readily available for plotting on a website or download.

NetCDF files use Climate and Forecast (CF) Metadata Conventions (Eaton et al., 2009) for variable naming and standardization of the metadata. Output data generally consists of hourly snapshots of the following variables: water level, currents (2-D averaged currents and 3-D if applicable), salinity (if applicable), significant wave height, significant wave period and direction (if applicable), snapshots of maximum water level, inundation and maximum wave height over the period of the forecast. Time-series of wind speed, wind direction, water level and currents at 1-minute intervals at selected stations (stations are based on locations of the available measured data).

Data Acquisition

The SSMS acquires a variety of data such as winds, waves and surges from large scale models from different sources using different methods. The Data Acquisition Module of the SSMS supports the following transports: FTP, HTTP, LDM, SCP, and SFTP. A dataset can be obtained via any of the methods above. The module contains monitors that use different methods to query for new data from connecting and listing FTP folders looking for new files to parsing RSS feeds looking for updated NHC advisories. OPeNDAP is also supported although only one of the datasets (NCOM) is provided using it.

All acquired data is placed in a designated place in the archive and catalog entries are added as appropriate to indicate arrival of the new data as well as its location in the archive.

Archive and Catalog

The SSMS archive consists of a disk space on a file server which is accessed by the SSMS via NFS. The catalog consists of a MySQL 5.x database running under Linux CentOS. The catalog database is designed to hold locations of various files from input data to output products produced by the SSMS. The database also holds various information about forecast cycles (which simulations have been done, which are running and which are scheduled to run) as well as locations of measurement stations, information about SSMS domains, etc. Most of the SSMS internals are written in Perl and use DBD to access MySQL database. The web components use PHP/MySQL to access the database.

Running Simulations

The Core SSMS Module has functionality to prepare and run model simulations. Once all the input data required for a given cycle is available and processed, the Core Module prepares the simulations. This includes automatically creating input files for all models, combining the input files and model codes in a temporary directory, and adding the simulation to the queue to be submitted for computation. The queue is polled by the scheduler component of the Core Module and it makes decisions about submitting jobs from the queue based on the information about priorities of each simulation and availability of resources. The scheduler then submits simulations, monitors them for completion, brings the results back from computational resources back to the archive and passes them to the post-processing components of the Publishing Module, which runs appropriate post-processing procedures to generate the final products which are then displayed on the interactive SSMS website.

The SSMS attempts to take advantage of all computational resources available to it and make runs in the most efficient manner to produce forecast in the shortest amount of time possible. Therefore parallelization plays an important role in SSMS's functionality as the most critical and time consuming components of the SSMS are parallelized.

Virtual grid and grid appliance

Virtualization is another technology that SSMS attempts to take full advantage of (Davis et al., 2006). Not only SSMS components are packaged as virtual machines that can be run on VMware hosts but one of the resource pools that SSMS uses for computations consists entirely of resources that are based on virtual machines. SSMS uses a pool of computational resources that are run using virtualization technology. Particularly it uses a cluster of virtual machines based on a virtual grid appliance (Grid Appliance Team, 2009). The Grid Appliance is a self-configuring virtual machine appliance that is used to create pools of computer resources. These resources can be connected via local area networks or across a wide-area network that can be used to execute computationally intensive jobs efficiently. Grid Appliances are connected to each other through a peer-to-peer virtual network called IPOP (IP over P2P). Grid Appliances are self-configuring and upon start-up they automatically join a Condor-based pool of resources and become readily available to execute jobs. Such networks are very flexible and easily expandable due to simplicity of deployment of new resources.

Parallelization

The SSMS takes advantage of parallelization whenever possible to increase performance of the system and to be able to produce forecasts faster than it is possible to do with serial simulations. All of the most important components of the SSMS are parallelized. CH3D, SWAN, ADCIRC and all the critical components of the WMS are able to take advantage of multiple processors. This can become even more important as computational grids become more refined and require more and more computational resources. All components currently use shared memory parallelization approach - OpenMP, while CH3D also supports MPI (Message Passing Interface).

The scheduling of simulations is done in such a way that even if each model uses only a single CPU, the scheduler attempts to submit simulations to resources that have at least as many CPUs available as there are models running as part of the simulation. For example if only two models

CH3D and SWAN are being run, then the scheduler attempts to find a resource with at least two CPUs if ADCIRC is added to the simulation, then a minimum of three CPUs is requested to run the simulation.

Job management / scheduling

The SSMS relies on Condor for job management, but uses its own approach to scheduling by assigning priorities to each simulation. Since SSMS can be used for forecasting as well as hindcasting and research, the forecasting tasks receive the highest priority.

SSMS is a fully automated system designed to be able to operate without human intervention. Based on the latest accessible information about approaching storms and their tracks and landfall locations, it schedules forecasting simulations. Domains that are potentially affected by the storm are included into the list of simulations to be run. Currently the SSMS uses a simple criterion: if a storm passes anywhere within 100 miles of the domain then the domain is included into the forecasting cycle. Domains are then prioritized based on the proximity of the storm and the final list of simulations is formed.

SSMS supports several job submission mechanisms: direct (via SSH), PBS and Condor. It can submit jobs, query them and retrieve the results using either one of these methods. Available resource pools can be one of those types. Every resource pool has a range of priorities assigned to it and jobs are then submitted to the appropriate resource pool. Jobs with higher priorities can still be assigned to the pool with lower priority range if submission to resource pools with higher priority failed.

Currently SSMS uses three resource pools – a) a set of machines with direct (SSH) access to them, these resources are local and are located on the same network as the main SSMS server, they have a capacity (CPU and memory) to run simulations on any of the SSMS domains within required (benchmarked) time; b) virtual grid, which is based on Condor and has the second highest priority rank, this resource pool is designed as a backup for forecasting simulations as well as

research/hindcast simulations that are performed on as needed basis and c) University of Florida High-Performance Computing Center cluster (UF HPC) which uses PBS for job submissions, UF HPC is actively used by different research groups within the university and therefore jobs may take an unpredictably long amount of time to run. This resource pool is generally used for routine hindcasting simulations.

Submitted jobs are periodically polled for their status which can be monitored using the SSMS job monitoring page. Finished jobs are transferred back to the SSMS main server where they get archived and go through a post-processing step. Post-processed data is then stored in the archive and catalogued and at this point it becomes accessible from the interactive web interface.

GIS Frontend & Web Interface

The SSMS has an interactive GIS-based web interface that allows a user to access post-processed data in the archive by using the catalog. The web interface is located at http://ch3d-ssms.coastal.ufl.edu. It uses authentication to overcome potential legal issues of making storm surge and inundation data freely available to the public as it is research data that does not pass QA/QC prior to being published on the web.

The web interface is based on Javascript for interactivity and uses PHP with MySQL to access the catalog and the archive. MapServer – the UMN product (MapServer Team, 2009) is used as a GIS of choice as it's a powerful, flexible and an open source solution that is being actively developed and well supported by its developers. The MapServer runs as Web Map Service (WMS) and Web Feature Service (WFS) providing on demand maps and features (such as measurements stations, etc) based on the data in the archive.

OpenLayers (OpenLayers, 2009) provides the technology to allow interactivity in mapping as well as extra features such as ability to overlay a variety of maps that are based on a multitude of standards such as WMS and WFS as well as proprietary services such as Google Maps and Yahoo Maps for the maps being displayed to the user.

Virtualization is used for the web server as the entire operating system (CentOS Linux) with an Apache web server and all of the supporting technology such as MapServer, OpenLayers is packaged into a VMware-based virtual machine, which allows for easy migration, backup and restoring in the event of a hardware failure.

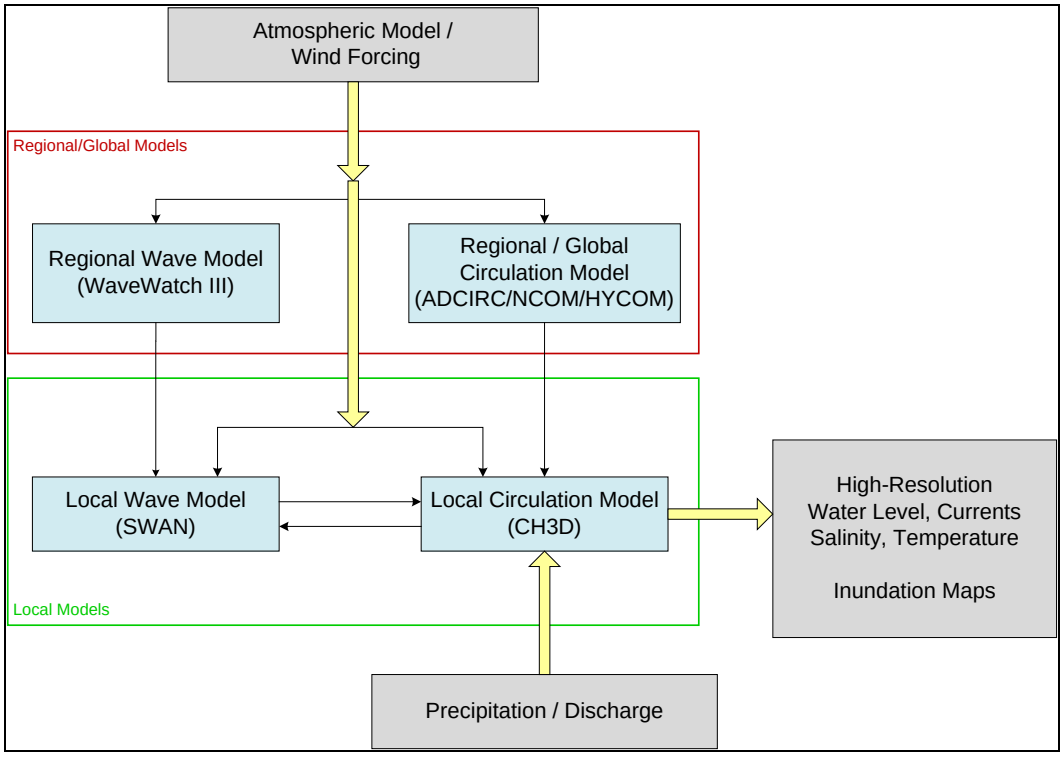

Figure 2-1. SSMS Model Coupling Diagram

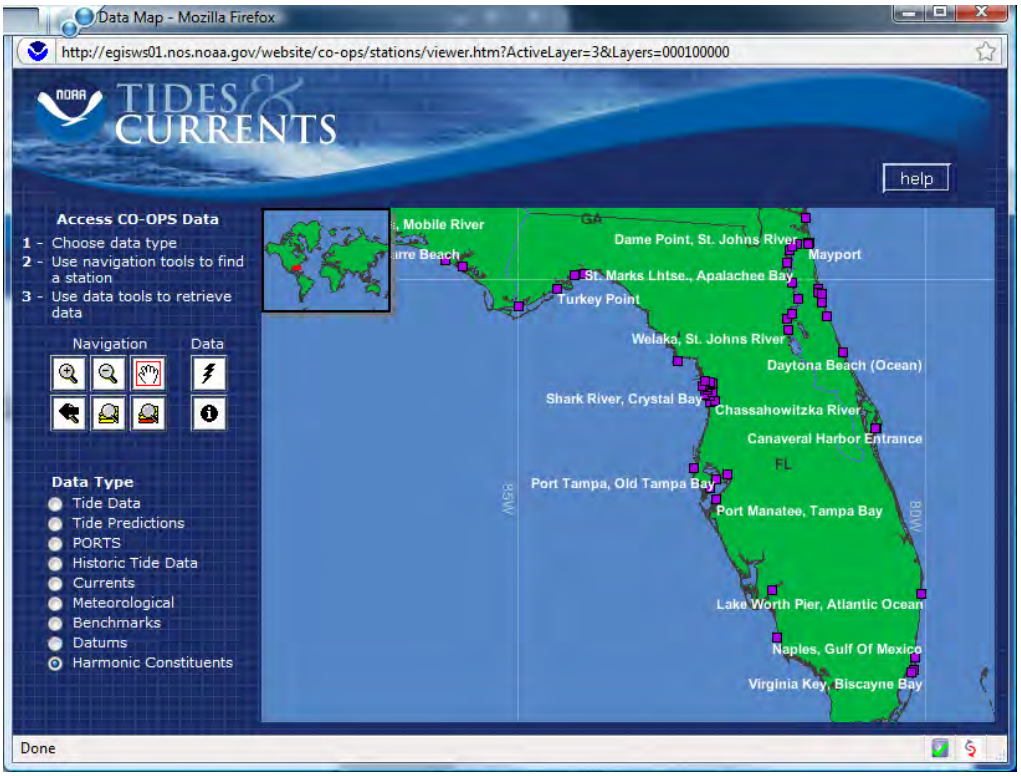

Figure 2-2. NOAA CO-OPS interactive data map of harmonic tidal constituents stations

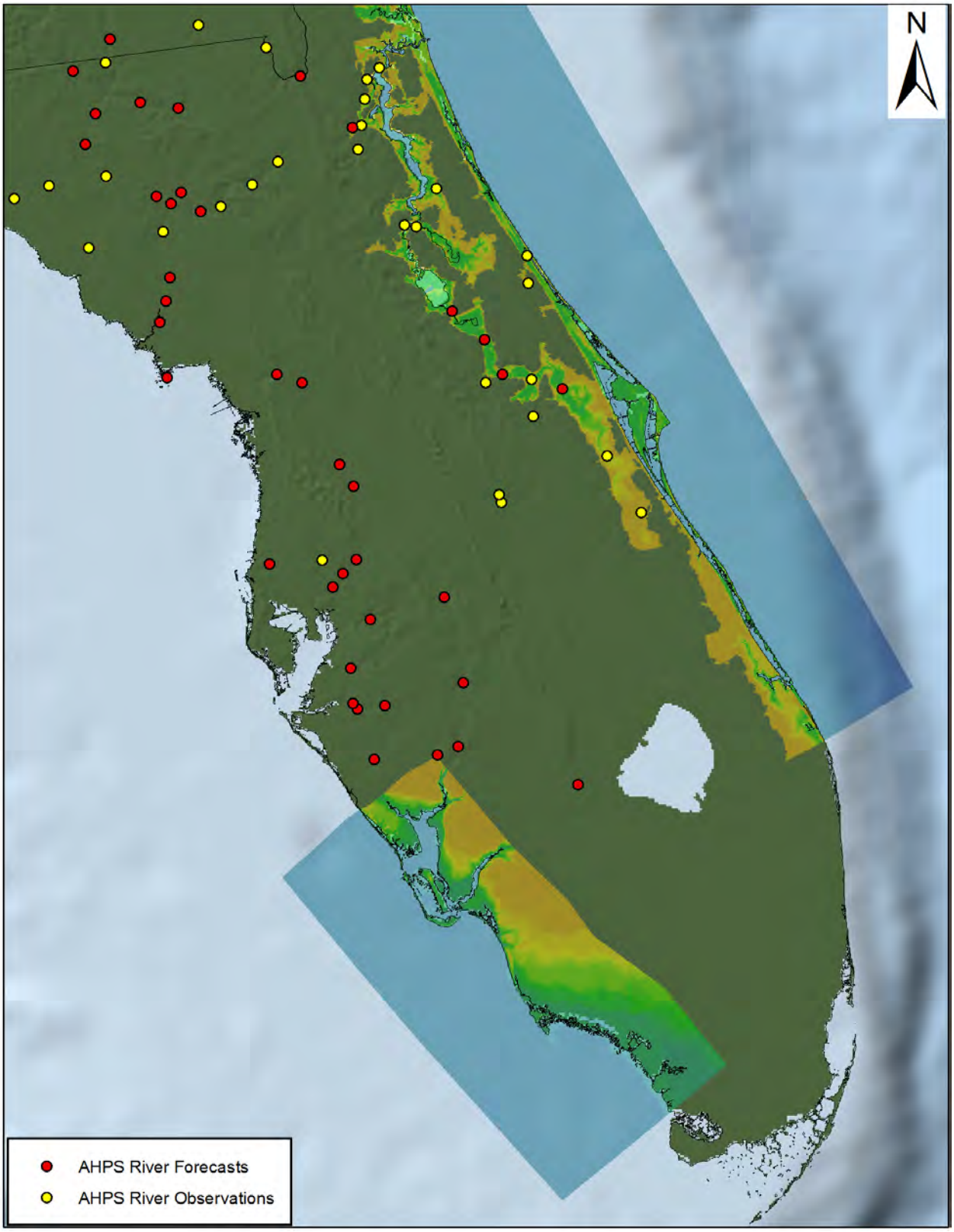

Figure 2-3. Locations of river forecasts provided by the National Weather Service Southeast River Forecast Center

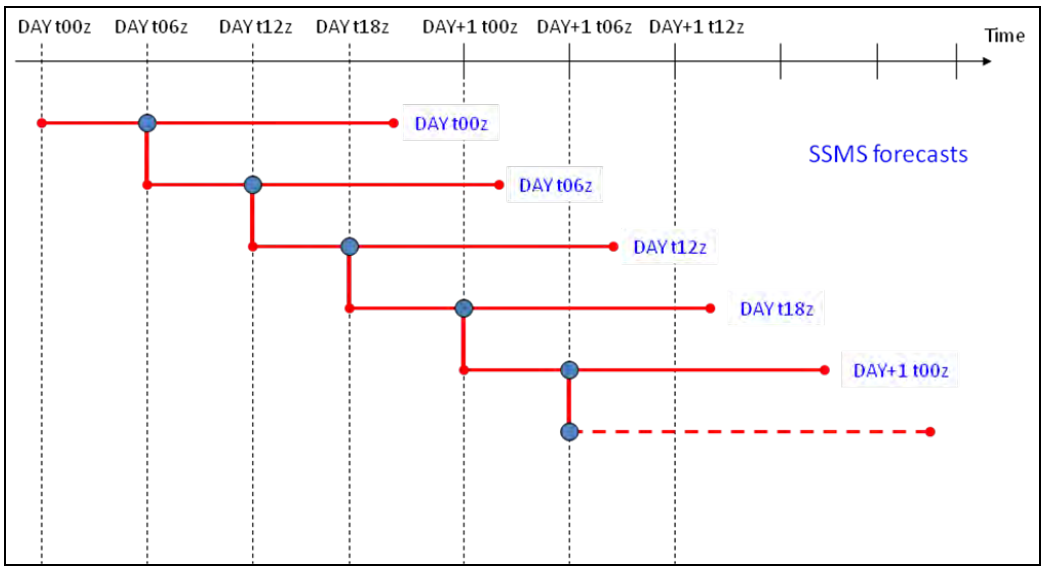

Figure 2-4. SSMS forecasting cycles

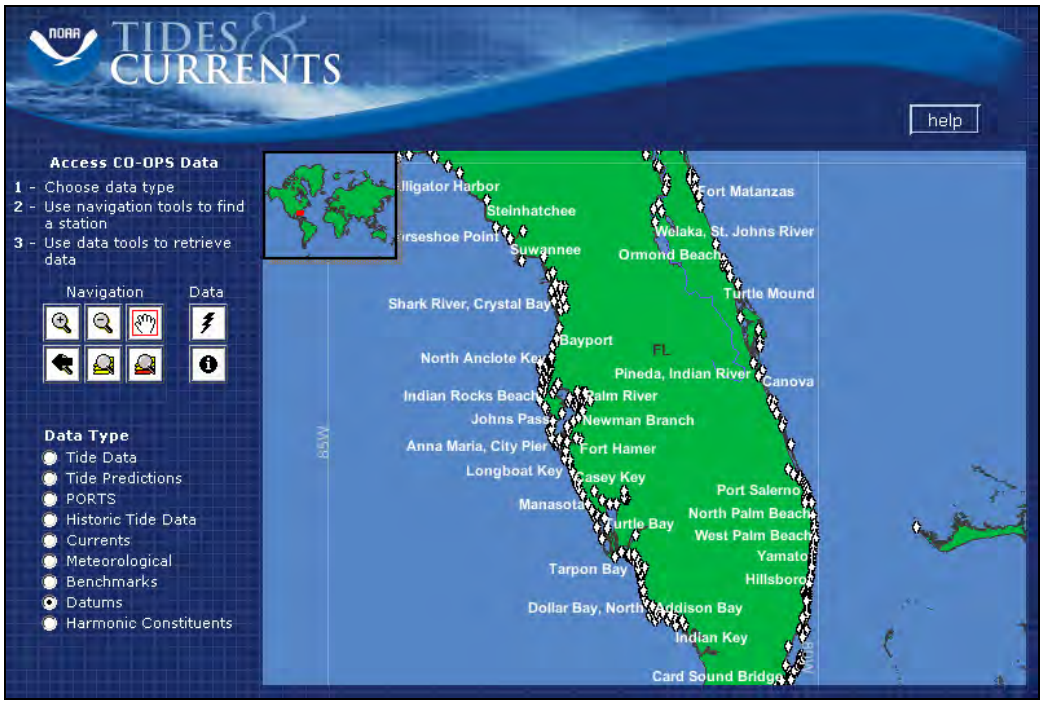

Figure 2-5. NOAA Tides and Currents datum product locations

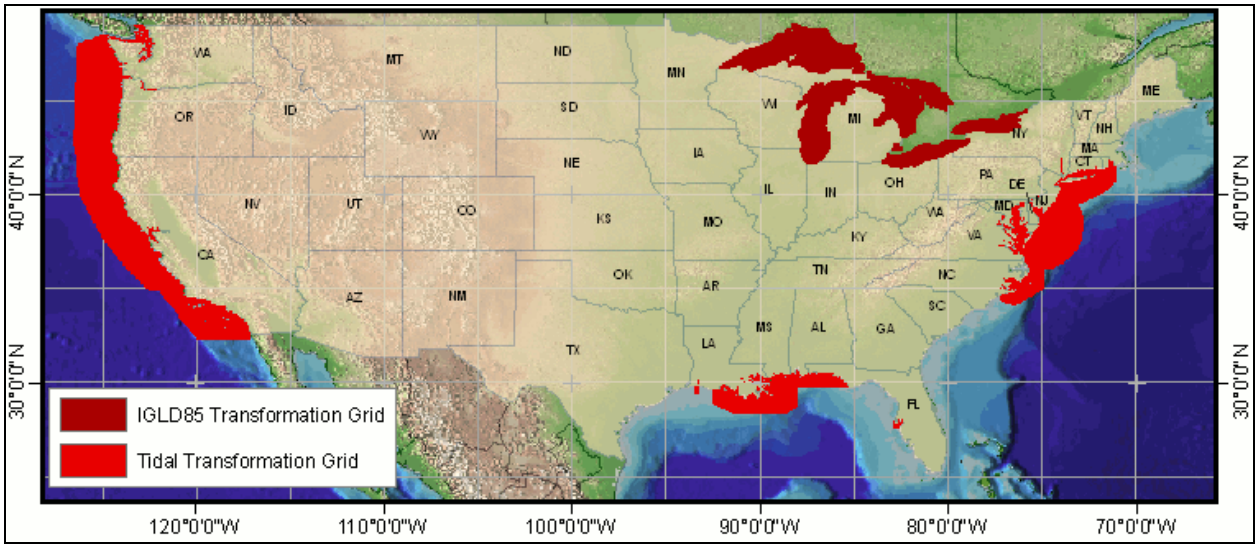

Figure 2-6. NOAA VDATUM project coverage

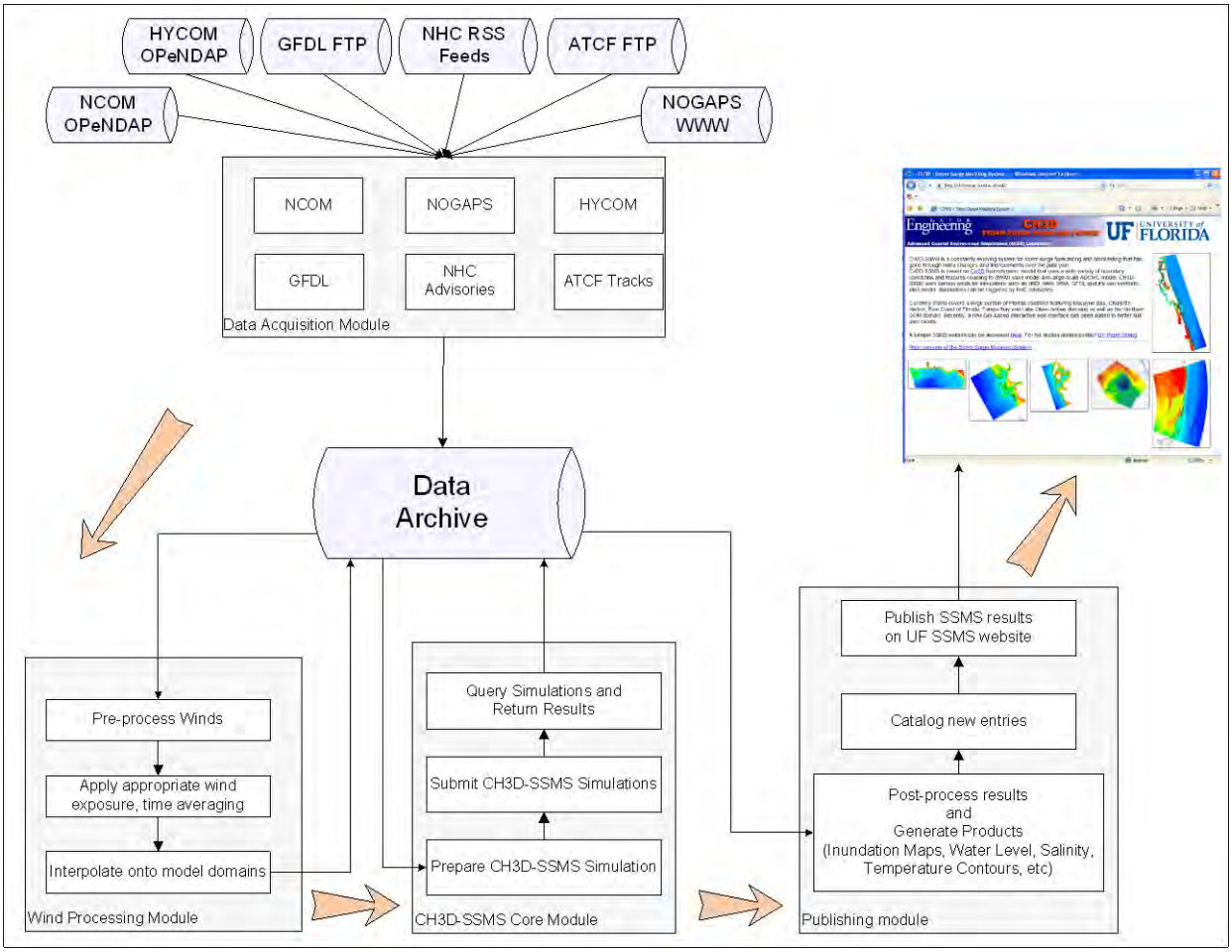

Figure 2-7. SSMS data flow diagram

CHAPTER 3
DEVELOPMENT OF WMS

Overview

Any storm surge model is highly dependent on quality wind and pressure data to drive the surge. Wind is the most significant forcing in a storm surge simulation as it is a major contributor to the generation of the storm surge and waves. There are many atmospheric models that differ in coverage, resolution, representation of physics and more, the data that comes from these different models is provided by different methods and in different formats, which makes it hard to be used for storm surge modeling. WMS (Wind Modeling System) is an attempt to standardize these datasets and make them readily available in a convenient and uniform fashion. It aims to provide capabilities to obtain and manipulate various available datasets, whether analysis or forecasts, in a seamless fashion to supply wind and pressure fields to a storm surge modeling system.

In addition to existing complex atmospheric models, WMS features a few synthetic parametric hurricane models that allow one to quickly obtain wind and pressure fields at the expense of simpler physics. These parametric models are not as sophisticated as the full atmospheric models, however the SSMS only requires forecasts of wind speeds at 10-meters elevation and pressure at the mean sea level and the parametric models often provide a reasonable estimate of these and they do it in a fraction of time it takes to obtain results of models such as GFDL, WRF, etc. The downside of parametric wind models is the limited domain that is affected by the winds. Often atmospheric processes create fairly strong winds in the area of hurricane landfall long before the hurricane arrives which can affect the surge and synthetic wind models only predict wind in a limited radius from the center of the storm and do not represent the “background” wind – the wind that is not associated with the hurricane vortex but is rather created by local weather conditions.

Another significant downside of parametric models is their ignorance of underlying terrain. Hurricane winds change significantly with roughness of the terrain over which they travel. Open

ocean winds are significantly stronger compared to winds over land, additionally heavy forestation and other types of rough terrain can weaken the hurricane even further. However, the parametric models always assume an open ocean wind exposure everywhere in the domain which leads to overestimated winds on the side of the hurricane where they blow from land to the ocean. The WMS features wind adjustments due to land exposure by creating maps of land roughness derived from land cover datasets and using these roughness data to adjust wind speed depending on the direction of the fetch.

The WMS allows a user to combine (blend) two datasets together. This can be useful to combine for example a low resolution background wind from a model like NOGAPS or NAM, etc with a high-resolution H*Wind or synthetic wind model of hurricane winds which have limited coverage. In this case one can obtain a wind field that has both a well resolved hurricane structure and the background wind features that may also affect the surge. Time-averaging and data assimilation can also be dealt with. The WMS allows a user to assign time-averaging properties for each dataset and the time-averaging properties for the output and all datasets would be adjusted to represent the same time-averaging period. Data assimilation option is also available which allows user to specify point locations and time-series of data associated with those locations the system then assimilates data provided by these time-series into the wind field.

The WMS is capable of handling input and output datasets in a variety of formats such as GRIB, NetCDF (with CF compliance), ESRI shapefile, Google KML files, native input formats for ADCIRC, CH3D and SWAN models, native output formats for H*Wind and GFDL, TecPlot and plain text.

Figure 3-1 shows an overall workflow of WMS in forecasting mode. The main wind field is generated using one of the synthetic parametric models and is then blended with the optional background wind fields (such as NOGAPS). Once blended the land-induced wind dissipation is applied and the final wind field is interpolated onto SSMS model grids.

Data Sources

A number of existing atmospheric models provide their results and these wind fields and pressure data can be obtained and used to force a circulation model. The WMS provides capabilities to automatically obtain such data using one of the supported transport methods, convert the data as needed and provide it to the models that are part of the storm surge modeling system using required format.

Various datasets are provided via different methods and WMS needs to be able to access them in a seamless manner. The system can use various data transport methods to obtain data depending on the dataset that is being accessed. Data access procedures are completely transparent to the user and data transport methods are chosen automatically based on the type of data being accessed. The following transport methods are currently supported by the WMS:

- http
- ftp
- LDM
- OPeNDAP
- local disk
- local network via NFS or Samba

Currently the WMS supports multiple sources of wind and pressure fields. Table 3-1 provides descriptions for each wind source along with its access mechanism. In addition to external sources WMS implements three synthetic parametric models for surface wind and pressure during tropical storms. Synthetic models allow wind and pressure fields to be obtained quickly and to calculate these fields at model resolution which is generally significantly finer than any available wind and pressure data. In addition to external sources WMS has three built-in synthetic wind models that can be used to generate wind fields based on a set of parameters.

Table 3-1. Sources of wind and pressure data supported by the WMS

Wind Model	Details	Access Method	References
GFDL (Geophysical Fluid Dynamics Laboratory) hurricane	Three-dimensional atmospheric model. Multiply nested movable mesh system. Model initial condition is defined through a method of vortex replacement, generates a realistic hurricane vortex by a scheme of controlled spin-up. Adopted by US National Weather Service as an operational hurricane prediction model in 1995. Files are provided in a GRIB format.	FTP / HTTP from NOMADS (National Operational Model Archive & Distribution System)	Kurihara, Tuleya and Bender, 1998 Kurihara, Bender, Tuleya, 1995
GFS	Global Data Assimilation System is based on a three-dimensional atmospheric model that uses sigma coordinate Lorenz grid in vertical direction. It employs primitive equations with vorticity, divergence, logarithm of surface pressure, specific humidity virtual temperature, and cloud condensate as dependent variables.	FTP / HTTP	Kanamitsu, 1989, Kanamitsu et al., 1991, Kalnay et al., 1990.
H*Wind	Produced by a Hurricane Research Division (HRD). Analysis wind that combines satellite data, hunter airplanes and over land and over sea measurements from a variety of sources. Files are provided as zipped ASCII text.	Local disk/network	Powell et al., 1998
NOGAPS (Navy Operational Global Atmospheric Prediction System)	Global forecast model that is spectral in the horizontal and energy-conserving finite difference (sigma-coordinate) in the vertical. The variables used in dynamic formulations are vorticity and divergence, virtual potential temperature, specific humidity, surface pressure and ground wetness. Files are provided in GRIB format.	FTP / HTTP / LDM	NOGAPS, 2009

Table 3-1. Continued

WRF (Weather Research and Forecasting)	Fully compressible, Euler non-hydrostatic with run-time hydrostatic option. Conservative for scalar variables. Flexible, portable, massively parallel and efficient code. Highly modular, offers numerous physics options and is suitable for use in a broad spectrum of applications. Files are provided in a GRIB format. NAM (North American Mesoscale) is also based on a WRF model.	FTP	Skamarock et al., 2005 Janjic et al., 2004
Synthetic wind model of the wind and pressure profiles in hurricanes	Synthetic model of the radial profiles of sea level pressure and winds in a hurricane. Equations contain two parameters that can be estimated empirically or determined climatologically. Most of the required parameters for the model are forecasted by NHC and others. Does not consider effects of interaction with land. Can be used as a basis and improved by combining with other models.	internal	Holland, 1980
Synthetic wind model of the wind and pressure profiles in hurricanes	Synthetic parametric model similar to Holland's, but eliminates the maximum velocity parameter used in the Holland, 1980 model and derives it from the pressure deficit and the radius to maximum wind.	internal	Wilson, 1960
Synthetic, parametric Holland-based model that	Synthetic, parametric model that is based on Holland, 1980, but makes use of the parameters forecasted by the NHC that are issued in form of advisories. Instead of using the radius to maximum wind to define the size of the storm it uses wind radiis, such as radii of 34kt winds, 50kt winds and 64kt winds which are forecasted by the NHC.	Internal	Xie et al., 2006

Synthetic Wind Models

Three parametric synthetic wind models are supported by WMS: Wilson (1960), Holland (1980) and Xie (2006). The model by Wilson is referred to as ANA and the model by Xie is referred to as ANA2. Both of these models are parametric and use information that is contained in National Hurricane Center forecast advisories. ANA wind model is based on storm track, central pressure deficit and radius to maximum wind. The ANA2 wind model is more complex and takes advantage of NHC wind radii forecasts. NHC forecasts wind radii by quadrants of 34 kt, 50 kt, and 64 kt winds. The usage of these forecasts allow ANA2 model to reproduce more of the storm complexity and asymmetry compared to ANA model which uses single value of radius to maximum wind.

Synthetic Wind Model (ANA)

Wilson (1960) derived a parametric idealized model for a tropical storm in the northern hemisphere with circular isobars and streamlines, under such conditions the horizontal wind vector may be takes anti-clockwise and tangential to a circular streamline at any point in the storm. The storm is considered to move forward at a uniform velocity. The cyclostrophic wind is represented as follows:

$$U_c = \sqrt{\frac{\Delta p}{\rho}\frac{R}{r}e^{-\frac{R}{r}}}, \tag{3-1}$$

where Δp - pressure deficit, ρ - air density, R - radius to maximum wind and r is the distance from the center of the storm.

Synthetic Wind Model (ANA2)

The ANA2 wind model takes a similar approach to Wilson (1960) and Holland (1980), but extends it and makes use of additional parameters: wind radii of 34 kt, 50 kt and 64 kt winds. These parameters are forecasted by the NHC, four values for each speed are forecasted representing the radii at NW (southwest), NE (northeast), SE (southeast) and SW (southwest) quadrants.

$$P(r) = P_c + (P_n - P_c)e^{-(R_{\max}/r)^B} \tag{3-2}$$

and the tangential wind field is given by the pressure field via cyclostrophic balance,

$$V(r) = \left[\frac{B}{\rho_a}\left(\frac{R_{\max}}{r}\right)^B (P_n - P_c)e^{-(R_{\max}/r)^B} + \left(\frac{rf}{2}\right)^2\right]^{1/2} - \frac{rf}{2} \tag{3-3}$$

where $P(r)$ is the surface pressure at a distance of r from the hurricane center, P_n - ambient surface pressure, $P(r)$ - hurricane central surface pressure, $R_{\max}$ - radius of maximum wind (RMW), B - hurricane-shape parameter, f - Coriolis parameter, and $V(r)$ - velocity at a distance r from the hurricane center. For hurricanes at low latitudes, the terms associated with the Coriolis parameter, f, can be neglected.

$$R_{\max}(\theta) = P_1\theta^{n-1} + P_2\theta^{n-2} + \cdots + P_{n-1}\theta + P_n \tag{3-4}$$

$$P(r,\theta) = P_c + (P_n - P_c)e^{-\left[R_{\max}(\theta)/r\right]^B} \tag{3-4}$$

$$B_0 = \frac{V_{\max}^2 \rho_a e}{P_n - P_c} \tag{3-5}$$

where $V_{\max}$ is hurricane maximum wind speed, and $e = 2.7183$. Then, the NHC forecast guidance is used to curve fit the polynomial (3-4) to obtain $R_{\max}$ as a function of θ. Note that in Eq. (3-3), when values of $V(r)$ and r are given, $R_{\max}$ has two solutions in each of the four quadrants.

Numerically, WMS uses Lambert's function to obtain the value of $R_{\max}$ and LAPACK library (LAPACK, 2009).

Lagrangian Interpolation

"Lagrangian" interpolation is another method that is essential to storm wind analysis. Generally circulation models using simple linear temporal interpolation of wind between times. This method produces big errors in storm surge simulations (Figure 3-2 shows that linear temporal

interpolation between snapshots does not preserve the structure of the storm) and needs to be improved. Parametric wind models included in WMS are fast and can be used to quickly generate wind fields at any time step. However, some winds are provided in a form of snapshots, for example NOGAPS. WMS uses interpolation method that recognizes the fact the storm is moving in time and improves upon the simple linear interpolation which in this case is inadequate.

The Lagrangian interpolation method first shifts wind snapshots in space (Figure 3-3) so that the storm center of both input snapshots is located at the storm center predicted by the storm track at the time. To interpolate variable $P(t, X, Y)$ from snapshots $P_1 = P(t = T_1, X, Y)$ and $P_2 = P(t = T_2, X, Y)$ WMS uses the following steps:

1. Calculate shift distances for each of the snapshots: $\Delta x = X_{i,j} - \overline{X}_t$, $\Delta y = Y_{i,j} - \overline{Y}_t$, where $\left(\overline{X_t}, \overline{Y_t}\right)$ is the position of the storm at time t.
2. Shift grids of both snapshots P_1 and P_2 by $(\Delta x, \Delta y)$, accordingly. Now the center of hurricane on both snapshots should be in the location $(\overline{X}_t, \overline{Y}_t)$
3. Interpolation between the snapshots using linear temporal interpolation:

$$P(t, x, y) = (1 - \theta)\,\overline{P_1}(x, y) + \theta\,\overline{P_2}(x, y), \tag{3-6}$$

where $\theta(t) = \dfrac{t - T_1}{T_2 - T_1}$

Time Averaging

WMS supports a variety of wind fields and different datasets often use different averaging time. For example, HRD H*Wind data consists of 1-min sustained wind, NOAA data are 6-min sustained wind, etc. The difference in wind speed can be significant between different time averaging periods. Hurricane Research Division quotes 11-14% difference between 1-minute and 10-minute sustained winds and recommends on their FAQ web page (HRD, 2006) to use 1.12 factor to convert 10-minute sustained wind to 1-minute sustained wind.

WMS has a capability to adjust wind speeds using a gust factor relationship in a form proposed by Masters (2004):

$$GF(t, z_0) = \alpha_1(t) + k\left[\alpha_1(t)\right]\left[\beta(z_0)\right]^{1/2}\left[\ln(10 / z_0)\right]^{-1} \quad (3\text{-}7)$$

where $\alpha_1, \alpha_2, \beta$ curves are determined based on the best fit to empirical data.

Data Assimilation

WMS supports data assimilation. Time-series of wind and pressure data can be used for data assimilation. Implemented method follows Cressman (1959) with some modifications. The assimilation is done as follows:

N - number of assimilation data series (stations)

a_i, w_i - model wind direction and speed

a_i^m, w_i^m - measured wind direction and speed

$e_i^w = \dfrac{w_i}{w_i^m}$ - error for wind speed and

$e_i^a = \dfrac{a_i}{a_i^m}$ - error for wind direction

Then correction factors can be developed for model wind within a predefined radius (r_i) of one of the measurement stations:

$$E^w = \frac{\sum_{i=1}^{N} e_i^w W_i}{\sum_{i=1}^{N} W_i} \text{ - correction factor for wind speed} \quad (3\text{-}8)$$

$$E^a = \frac{\sum_{i=1}^{N} e_i^a W_i}{\sum_{i=1}^{N} W_i} \text{ - correction factor for wind direction} \quad (3\text{-}9)$$

where

$$W_i = \begin{cases} \dfrac{R^2 - r_i^2}{R^2 + r_i^2} & when\ r_i < R \\ 0 & when\ r_i > R \end{cases}, \tag{3-10}$$

r_i - distance from station i to location of model value

R - radius of influence (arbitrary predefined value, in WMS is usually set to 3 miles)

This assimilation method allows modifications to be done to any wind that is supported by the WMS. However, when ANA2 model is used to generate a wind field a different method can be used for data assimilation, which is more natural for the ANA2 model and provides smoother wind fields. An extra level of optimization of the initial wind field cab be performed using analysis wind data. The optimal values of the parameters B and P_i, $i = 1..5$ in the equations (3-1) and (3-2) for the initial wind field are those that minimize the following root-mean-square (RMS) error function:

$$\sqrt{\sum_{n=1}^{N} \left[V\left(B, P_{1-5}\right) - V_{measured} \right]^2} \tag{3-11}$$

Data Standards and Supported Winds

The WMS supports a variety of data types and it can use wind data from any supported data as an input and provide output in format native to any of the models that are used as part of the SSMS: ADCIRC, CH3D and SWAN. The WMS supports NetCDF as a universal and portable data format for output as well as GIS compatible shapefiles and Google's KML file format, these files are used as part of the SSMS interactive website where wind fields and pressures can be visualized. Table 3-2 lists types of wind supported by the WMS and characteristics for each type of wind such as vertical level at which data is provided, frequency of forecasts, length of forecast cycle, etc.

Table 3-2. Wind model data overview

Wind Data Set	Source	Type* (BGD/ HUR/ CMB)	Spatial Resolu-tion	Vert. Level	Cycles	Cycle Length/ Snapshot Frequency	Mean Sea Level Pressure	Analysis/ Forecast	Assimi-lated	Wind Over Land
NAM	NCEP	BGR	12 km	10 m	00, 06, 12, 18	84 hrs 6 hrs	yes	FCAST	no	yes
NDAS**	NCEP	BGR	12 km	10 m	00, 06, 12, 18	6 hrs 6 hrs	yes	ANL	yes	yes
GFDL	NCEP	HUR	Varies	35 m	00, 06, 12, 18	126 hrs 6 hrs	yes	FCAST	no	yes
GDAS***	NCEP	HUR	Varies	35 m	00, 06, 12, 18	6 hrs 6hrs	yes	ANL	yes	yes
HRD	NOAA	HUR	6 km	10 m	-	varies	no	ANL	no	no
WNA	NCEP	CMB	28 km	10 m	00, 06, 12, 18	120 hrs 6 hrs	no	ANL+ FCAST	yes	no
ANA	Wilson (1960)	HUR	any	10 m	-	-	yes	-	no	yes
ANA2	Xie (2006)	HUR	any	10 m	-	-	yes	-	no	yes
NOGAPS	NRL	HUR/ BGR	12 km	10 m	00, 06, 12, 18	6 hrs	yes	ANL+FCAST	yes	yes
WRF	NCEP	BGR	4 km	10 m	00, 06, 12, 18	36/84 hrs 3 hrs	yes	ANL+ FCAST	yes	yes

*BGD/HUR/CMB – Background, Hurricane, Combined;

**NDAS – NAM Data Assimilation System;

***GDAS – GFDL Data Assimilation System.

Land Cover and Land Exposure

One of the drawbacks of various wind fields, which is especially valid for synthetic parametric wind models included into the WMS is the lack of land effects on wind. Storm winds generated by these models consider uniform bottom roughness as if storm is always located over water. Land can significantly reduce wind speed due to higher roughness. IPET (2008) developed a method to include effects surface roughness due to various land cover on the wind field. A slightly modified version of this method is used in the WMS.

Inclusion of land effects is implemented by developing wind reduction coefficients for every point in the domain and adjusting the wind speed using these coefficients. The coefficients are pre-computed once for the entire domain and reused.

Powell (1998) suggested the following equations for adjusting the wind speed to different types of exposure:

$$\frac{u_{*s}}{u_*} = \left(\frac{z_{0s}}{z_0} \right)^{0.0706} \tag{3-12}$$

u_{*s} - standardized friction velocity

u_* - friction velocity

z_{0s} - standardized surface roughness

z_0 - surface roughness

Powell also suggests the values for open terrain exposure to be $z_0 = 0.03$ and open marine exposure to be $z_0 = 0.07 - 0.015$.

Equation (3-12) then can be written a form of a wind reduction coefficient due to land exposure:

$$f_{r-directional} = \left(\frac{z_{0_{marine}}}{z_{0_{land-directional}}} \right)^{0.0706} \tag{3-13}$$

IPET (2008) suggested that the roughness values are calculated as follows:

$$z_{0_{land-directional}} = \frac{\sum_{i=0}^{n} w(i) z_{0_{land}}(i)}{\sum_{i=0}^{n} w(i)}, \text{ where} \tag{3-14}$$

$$w(i) = \frac{1}{\sqrt{2\pi\sigma}} e^{\left(-\frac{d(i)^2}{2\sigma^2} \right)} \text{ and} \tag{3-15}$$

$\sigma = 3km$ - determines importance of closes points, $d(i) <= 10km$, and

$$z_{0_{marine}} = \frac{\alpha_c C_d W_{10}^2}{g}. \tag{3-16}$$

Hence σ and $d(i)$ determine the length of fetch that is used to calculate land roughness. Masters (2004) suggested that the length of required fetch for the equilibrium profile to adapt to upwind roughness can be calculated using the following formula

$$F \approx 2z_0 \left(\frac{10z}{z_0} \left[\ln \frac{10z}{z_0} - 1 \right] + 1 \right) \tag{3-17}$$

This formula is used to calculate σ in equation (3-15) in WMS.

WMS divides all possible upwind directions (360 degrees) into sectors (36 sectors, 10 degrees each with centers of sectors at 0 degrees, 10 degrees, 20 degrees, etc) and a directional wind reduction coefficient is computer for each upwind direction. Since calculation of wind reduction coefficients is computationally intensive, all directional coefficients are precomputed, stored in a file and can be reused by the WMS.

The USGS National Land Cover Dataset (USGS, 2001) is used to develop a map of roughness values $z_{0_{land}}$ over the state of Florida. Figure 3-4 shows the NLCD (2001) land cover map for Florida and Figure 3-5 shows a classification legend explaining each type of land use on the map. Table 3-3 shows $z_{0_{land}}$ factors for all NLCD classes in the classification. Table 3-1 was derived based on the data in IPET (2008).

Table 3-3. $z_{0_{land}}$ factors for NLCD classifications

NLCD Class	Description	z_0
11	Open Water	0.001
12	Ice / Snow	0.012
21	Developed, Low Intensity	0.330
22	Developed, Medium Intensity	0.390
23	Developed, High Intensity	0.500
31	Barred Land	0.090
41	Deciduous Forest	0.650
42	Evergreen Forest	0.720
43	Mixed Forest	0.710
51	Dwarf Scrub	0.120
52	Shrub / Scrub	0.120
71	Grassland / Herbaceous	0.040
72	Sedge / Herbaceous	0.040
74	Moss	0.040
81	Pasture Hay	0.060
82	Cultivated Crops	0.060
90	Woody Wetlands	0.550
95	Emergent Herbaceous Wetlands	0.110

The NLCD (2001) products include land cover, impervious surface and canopy density products and are generated from a standardized set of data layers mosaicked by mapping zone. Typical zonal layers include multi-season Landsat 5 and Landsat 7 satellite imagery centered on a nominal collection year of 2001 and Digital Elevation Model based derivatives at 30 meters spatial resolution.

Wind Blending

Wind blending is implemented in WMS and allows blending two different wind fields into one. The method is designed to blend synthetic parametric wind fields with other analysis or forecast winds. One of the drawbacks of synthetic wind models is that the wind outside a certain radius (size of the storm) is zero. While in reality fairly strong "background" winds usually start appearing long before the storm makes its landfall and often last for some time after it passes the area. Wind blending allows producing a wind field that resolves a storm well and at the same includes the effects of a background wind. Since parametric winds have a well defined radius where the wind speed goes to zero and wind speed is known to decrease as we increase the distance from the center of the storm. It is possible to track a decreasing curve of wind speed along the until wind speed of the main (synthetic wind field) becomes equal to the wind speed of the background wind field then all values at distances larger than that are replaced by the values of the background wind.

Parallelization and Performance

WMS optimization is achieved by parallelizing its main loops using OMP method. Given the naturally parallel nature of most functions within WMS, it is nearly 100% parallelizable and efficiency increase can be seen by running WMS using multiple processors. In serial mode WMS can produce a wind field for all SSMS models (ADCIRC, CH3D and SWAN) in less than 5 minutes using a benchmark system (Intel Core2 3.0 Ghz CPU with DDR2-800 RAM). Using four processors reduces that time to approximately one minute.

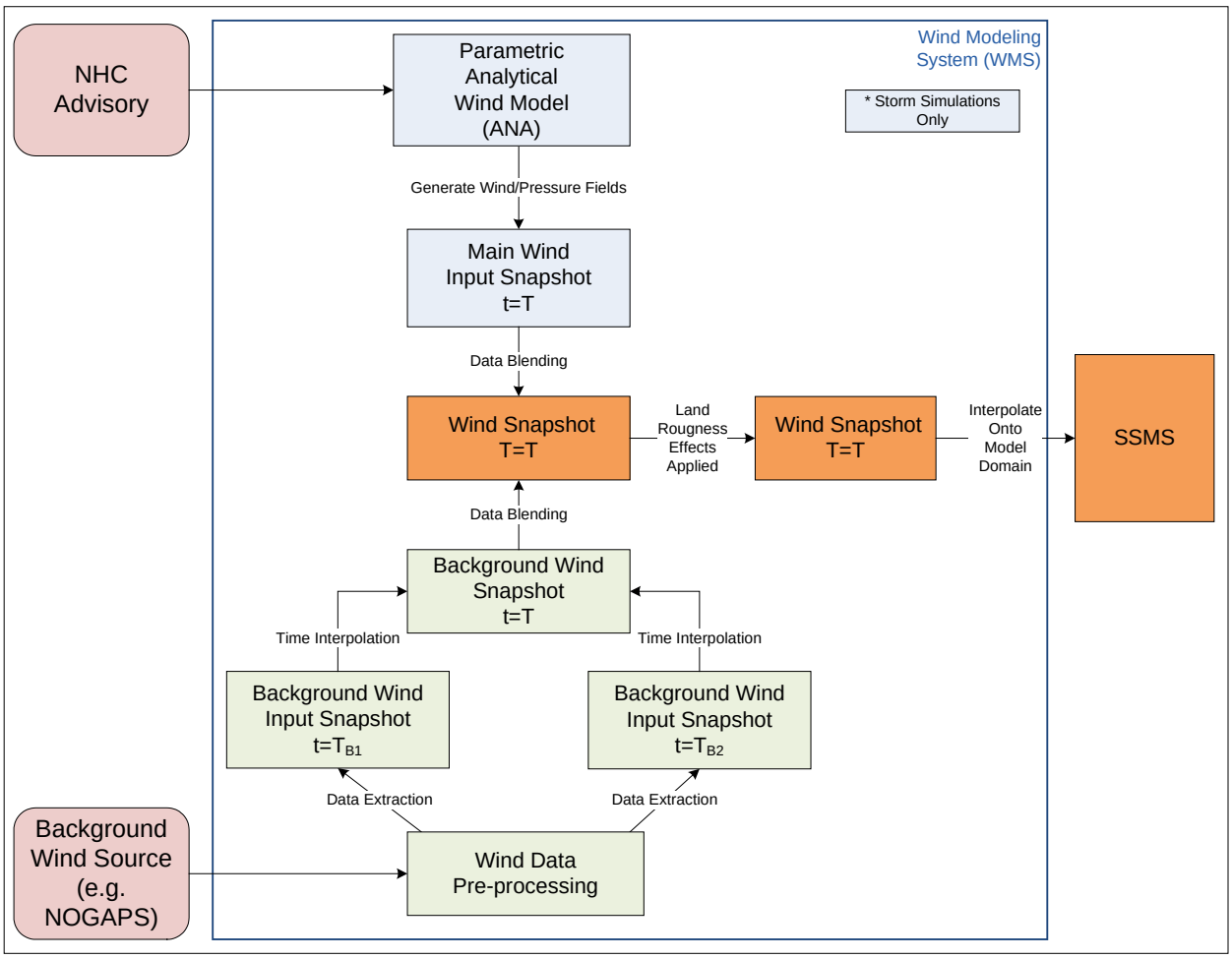

Figure 3-1. WMS flow diagram

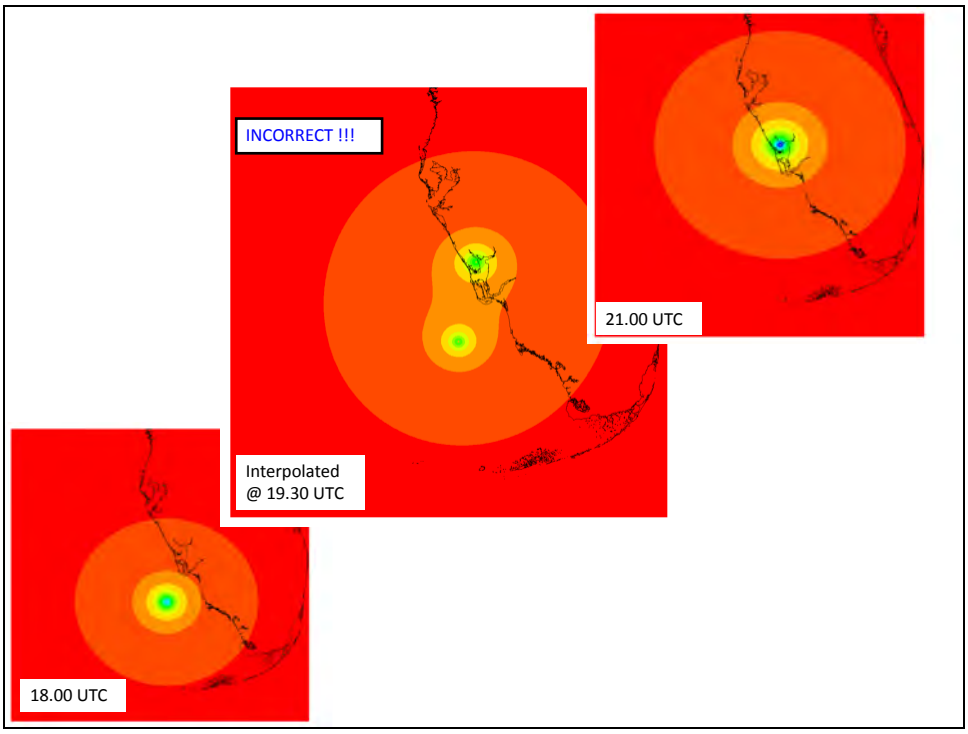

Figure 3-2. Result of linear temporal interpolation at 19:30UTC between pressure snapshots at 18:00 and 21:00UTC.

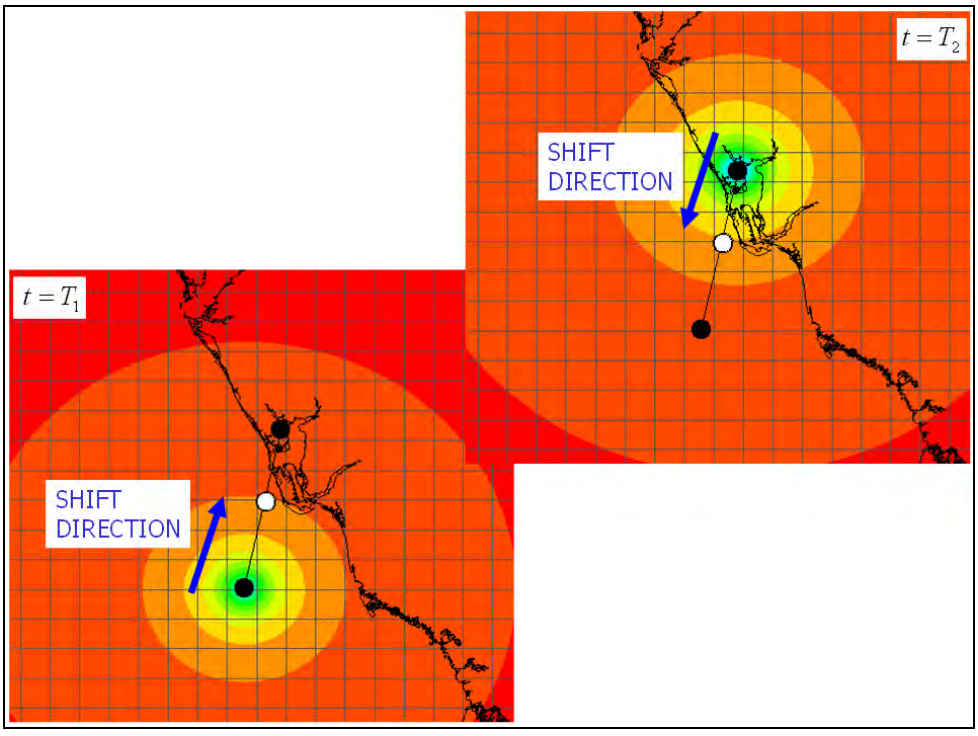

Figure 3-3. Shifting input snapshots using Lagrangian interpolation

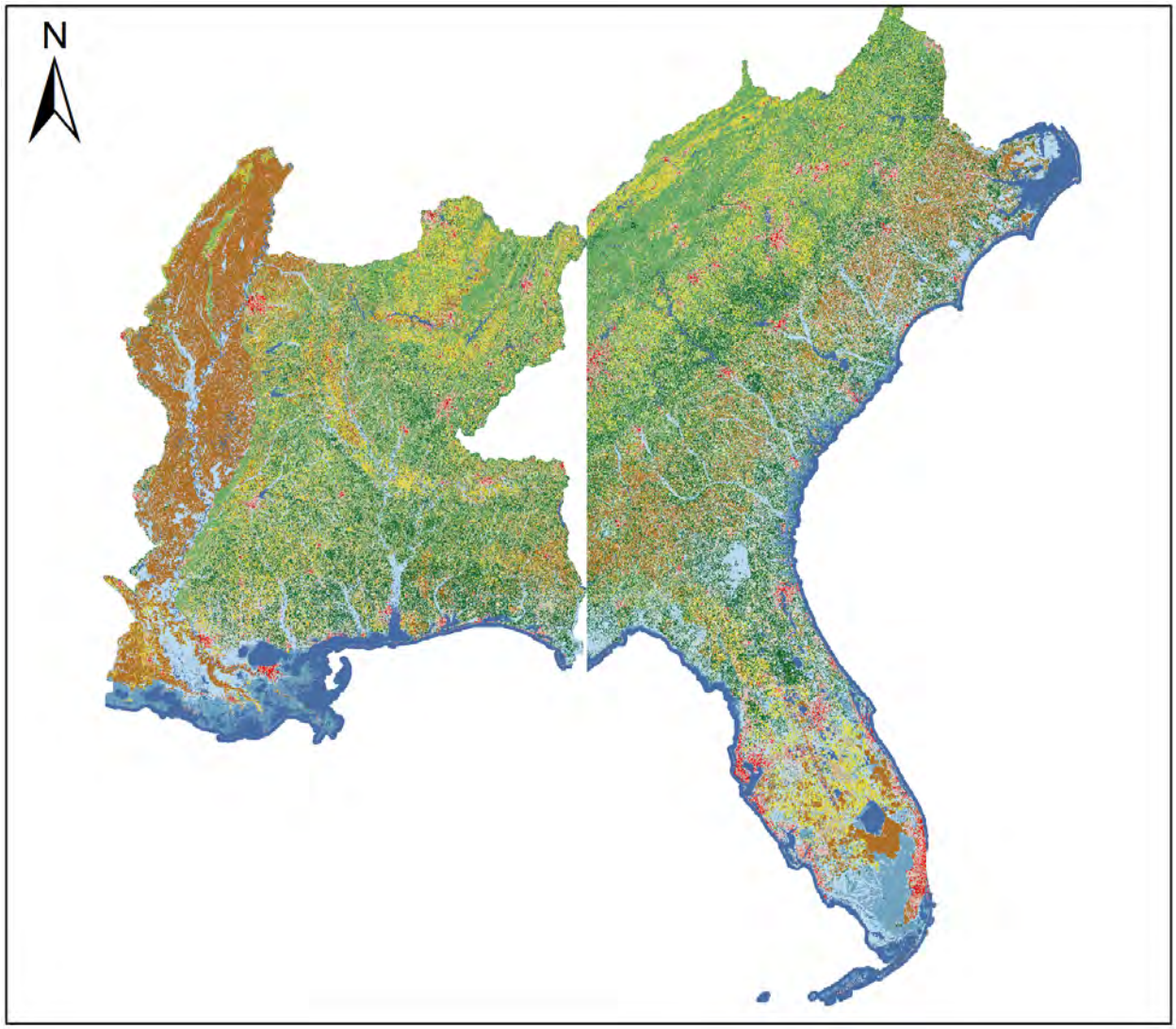

Figure 3-4. National Land Cover Dataset (2001) land use data

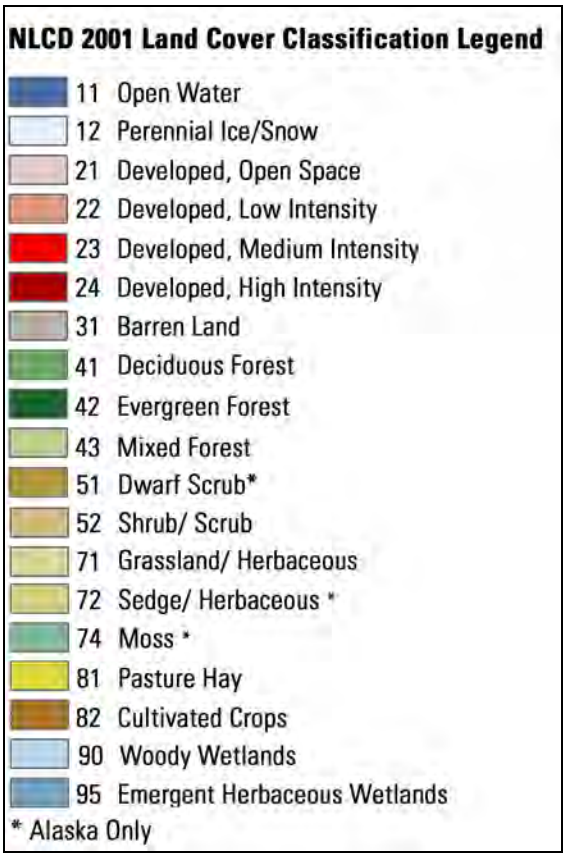

Figure 3-5. National Land Cover Dataset classification system legend (image courtesy of National Land Cover Institute)

CHAPTER 4
FORECASTING USING SSMS

SSMS is a flexible system, it contains a number of different models that can be combined to perform various tasks from quick two-dimensional storm surge forecasts to long term hindcast of baroclinic circulation and salinity transport. This chapter will describe in details SSMS setup that is used for this work.

Currently, SSMS includes two coastal models - CH3D and SWAN and one regional model - ADCIRC that can be run to produce open boundary conditions to CH3D model. In additions, the CH3D model has been coupled to NCOM and HYCOM regional circulation models that provide open boundary conditions to CH3D model and a regional wave model WaveWatch III that provides wave boundary conditions for SWAN. These three models are not part of the SSMS set of models, but are being run operationally externally by various groups and results of these models are obtained over the Internet and are used to run SSMS.

SSMS Models and Domains

Two coastal models CH3D and SWAN, which are tightly coupled as described in Chapter 2 are being run on the same model grid. Both models support curvilinear grids in horizontal direction and using the same grid for both models makes coupling the two models easier.

CH3D

CH3D model has a multitude of grids developed for it, Figure 4-1 shows some of the grids, which cover the entire Florida coast. Two CH3D grids were selected for this work: one that covers most of the east coast for Florida (EC) and one that covers most of the southwest coast of Florida (SW).

East coast of Florida grid (EC)

The EC CH3D grid, shown in Figure 4-2, covers approximately 280 miles of the east coast of Florida from Ponce Inlet to St. Johns River inlet. It extends 35 miles offshore and about 40 miles inland covering the St. Johns River and the Indian River Lagoon. The grid is 256 by 1201 cells. The minimum cell size is 42 meters and the average cell size is 250 meters. The bathymetry of the grid comes primarily from GEODAS (NGDC GEOphysical DAta System, GEODAS, 2009). The St. Johns River bathymetry was obtained directly from the St. Johns River Water Management District. Grid topography is based on the National Elevation Dataset (USGS NED, 2009) data and has 1/3 arc second spatial resolution. All data is adjusted to the NAVD88 datum.

For computational efficiency all grid cells with elevation over 10 meters NAVD88 are disabled since it's highly unlikely for water level to reach 10 meter level in a typical simulation. CH3D has been verified to be stable on the EC under a variety of conditions at 60-second time step. 2D and 3D (with 6 vertical layers) CH3D models take approximately 16 and 88 minutes wall time per day of simulation on a benchmark system using one CPU (or one CPU core). Therefore a typical 5-day simulation takes 80 minutes for a 2D model and 440 minutes for a 3D model to complete. The benchmark system is an Intel Core2 3.0Ghz CPU with DDR2-800 RAM. An EC grid simulation requires approximately 700MB (1300MB for 3D) of RAM to run.

Southwest coast of Florida grid (SW)

The SW CH3D grid, shown in Figure 4-3, covers approximately 150 miles of the southwest coast of Florida spanning from . It extends 40 miles offshore and about 25 miles inland. The grid is 313 by 645 cells. The minimum cells size is 36 meters and the average cell size is 180 meters

The bathymetry of the grid comes primarily from GEODAS (GEODAS, 2009). Grid topography is based on the NED (USGS NED, 2009) data and has 1/3 arc second spatial resolution. All data is adjusted to NAVD88 datum.

For computational efficiency all grid cells with elevation over 10 meters NAVD88 are disabled. CH3D has been verified to be stable on the EC under a variety of conditions at 60-second time step on a benchmark system. CH3D model takes approximately 9 minutes wall time clock per day of simulation for a 2D version of CH3D and 52 minutes for a 3D version of CH3D. Therefore a typical 5-day simulation takes 45 minutes for 2D and 260 for 3D version of CH3D to complete. A SW grid simulation requires approximately 400 MB (780MB for 3D) of RAM to run.

ADCIRC

ADCIRC is one of the regional models used in SSMS to force the CH3D model at the open boundary. The grid used for ADCIRC simulations is a modified EC2001e grid, which is used in ADCIRC tidal database (Mukai et al., 2001, Figure 4-4) and covers the Western North Atlantic, Caribbean and Gulf of Mexico. The modifications include a slight refinement in the area of Florida Keys and the addition of Charlotte Harbor to the grid. The grid consists of 254,750 nodes and has 1-2 km resolution near the coast and maximum 25 km resolution (Mukai et al., 2001). The ADCIRC model runs in 2D mode, it is forced by wind only, and it provides water level which is interpolated to the open boundary of CH3D model using 3-point inverse distance interpolation. Coupled simulations with ADCIRC, CH3D and SWAN models always use the same wind field generated using the WMS. The ADCIRC and CH3D models in SSMS always run synchronized and exchange information in real time with ADCIRC passing information to CH3D every CH3D time step. Since ADCIRC uses MSL as a datum, the CH3D boundary conditions are adjusted to NAVD88 as specified in Appendix C. The ADCIRC model has been

verified to be stable on EC2001e under variety of conditions at 5-second time step. It takes approximately 16 minutes wall clock time per day of simulation on a benchmark system. Therefore a typical 5-day simulation takes 80 minutes to complete. An EC2001e grid simulation requires 180MB of RAM to run.

HYCOM

HYCOM is another model that is used to provide open boundary conditions for CH3D model. SSMS uses RTOFS (Real-Time Ocean Forecast System) Atlantic basin forecasts. RTOFS is being run daily and produces a 24 hour assimilation nowcast and a 120 hour forecast. The data is provided in a form of GRIB files and is obtained from NOAA NCEP (RTOFS, 2009).

The following variables are being obtained: ssh (sea surface elevation), emnp (evaporation/precipitation), and salinity, which allows to specify water level and salinity at CH3D open boundary and precipitation over CH3D domain. HYCOM results are provided on a 1/12th degree horizontal grid (Figure 4-5) with the following vertical layers: 0.0, 10.0, 20.0, 30.0, 50.0, 75.0, 100.0, 125.0, 150.0, 200.0, and 300.0 to 5,500.0 at 100.0 intervals. The SW CH3D grid open boundary varies from 25 to 35 meters depth and the EC grid varies from 30 to 800 meters and HYCOM data is interpolated horizontally from HYCOM grid to CH3D grid using 3-point inverse distance interpolation and linearly in vertical direction from HYCOM to CH3D vertical layers.

NCOM

NCOM model can also be used to force the CH3D model at the open boundary. The NCOM model output in NetCDF format is obtained by SSMS via OPeNDAP from servers at the Naval Research Lab (NRL). NCOM IASNFS (Intra-Americas Sea Ocean Nowcast/Forecast System) provides nowcasts and up to 72 hour forecasts once daily. The variables obtained are surface elevation and salinity (at 41 vertical layers) which are then interpolated to CH3D open

boundary. NCOM model is driven by NOGAPS (Navy Operational Global Atmospheric Prediction System Model wind. NOGAPS wind data is also obtained from GODAE (Global Ocean Data Assimilation Experiment, NRL, 2008). IASNFS covers the Caribbean Sea, the Gulf of Mexico and the Straits of Florida with 1/24th degree horizontal resolution and 41 vertical layers (Figures 4-6 and 4-7).

WaveWatch III

WaveWatch III model is used to provide boundary conditions for SWAN simulations. NOAA NCEP (National Centers for Environmental Predictions) provides WaveWatch III results 4 times a day (at 00, 06, 12, and 18UTC cycles). Each cycle contains a nowcast and a 180-hr forecast. Significant wave height, period and wave direction are obtained by SSMS and are used to set up SWAN boundary conditions. WaveWatch III Western North Atlantic (WNA) grid has a 1/4th degree horizontal resolution (Figure 4-8).

Accuracy and Speed

Forecasting efforts usually face a problem of accuracy versus speed. Generally, the amount of time required to produce a forecast grows with increasing accuracy of a prediction. At the same time - the longer it takes to produce a forecast the less time we have to take advantage of it. For example, if it takes two day to produce a three-day forecast then we can only take advantage of the last day of a forecast, which is generally the least accurate. Chapter 1 cites NWS operational clearance times that are used to determine the amount of time required for evacuation. According to the Weather Service Operational Manual (NOAA-NWS WSOM, 2001) the evacuation clearance times to be up to 44 hours for Category 3 hurricanes (Levy, Citrus and Hernando counties) with exception of Dade county, which requires 52 hours. The maximum evacuation clearance times for a Category 5 hurricane is 50 hours except for Dade county which is exceptionally high at 81 hours. It should also be noted that it is generally considered that the

prediction of a storm track and intensity is best up to 2 days and it becomes increasingly less accurate after. However, a 48-hour forecast is insufficient to meet any of the aforementioned clearance times, therefore a 2.5-day (60-hour) forecast is considered. If SSMS can produce a 60-hour forecast in less than 8 hours then an emergency manager would be able to use the information for timely evacuation. Therefore all the actions required to produce a forecast including obtaining necessary data, data processing, model simulations, post-processing, archival and publishing the results should be completed in less than 8 hours.

Obtaining Data

Different model configurations require different initialization and forcing data to be obtained. The most basic and crucial information is the track file, which is obtained from the Automated Tropical Cyclone Forecast (ATCF) system. The data is based on NHC advisories and is usually available within 10-20 minutes from the time when an official advisory is released by the NHC. SSMS downloads ATCF data via FTP protocol from ftp://ftp.nhc.noaa.gov/atcf/.

WMS, described in the previous chapter, is responsible for generation of wind fields in the SSMS. WMS supports a variety of wind models which can be used to force circulation and wave models. There are parametric synthetic wind models: ANA and ANA2 (which require ATCF track to produce a wind and pressure field) that are generated locally by the WMS and there are wind models results of which are obtained by SSMS via the Internet, such as GFDL, HWRF, etc. Table 4-1 lists typical times that are required to obtain each wind field, which includes downloading data, running models (in case of synthetic wind models) and post-processing the data to obtain wind fields in a format required by models (ADCIRC, CH3D and SWAN). These times were established by averaging the times over two months in 2008 that were needed to obtain these wind fields using WMS.

Table 4-1. Typical times required to obtain various wind fields supported by SSMS

Model Name	Acronym	Time	Forecast length (hours)
Synthetic parametric model (Wilson, 1960)	ANA	20 minutes	120
Synthetic parametric model (Xie et al., 2006)	ANA2	20 minutes	120
Geophysical Fluid Dynamics Laboratory Model	GFDL	12 hours	120
Navy Operational Global Atmospheric Prediction System	NOGAPS	4 hours	144
Weather Research and Forecasting Model	WRF	10 hours	126

The amount of time required for blended products is the maximum of required times for individual winds that are blended, so if ANA wind is blended with NOGAPS wind then the time required to obtain the blended field is 4 hours. However, it is possible to expedite the production of blended wind fields; this can be done by using a forecast of a background wind, which is less dynamic, from a previous cycle. In that case a blended NOGAPS / ANA wind product can be obtained within 20 minutes from the start of the cycle.

SSMS also depends on other external sources of data such as WaveWatch III, HYCOM, and NCOM models. Boundary conditions for SSMS coastal models: CH3D and SWAN are derived from these models. Table 4-2 shows typical time required to obtain data for each of these three models, frequency of forecasts and length of forecast.

Table 4-2. Typical times required to obtain various wind fields supported by SSMS

Model Name	Time to obtain	Forecast frequency	Forecast length (hours)
WaveWatch III	06:00	4 times / day	120
HYCOM	14:00	once daily	120
NCOM	22:00	4 times / day	72

Nowcasts and Forecasts

All NOAA NCEP models follow the same cycles: 00:00, 06:00, 12:00 and 18:00UTC for models that run 4 times daily, 00:00 and 12:00UTC for models that run twice daily and 00:00UTC for models that run once a day, in the same manner the NHC issues tropical storm advisories four times a day. The SSMS follows similar setup: SSMS cycles follow the cycles of models that they depend on. For example, Full3D-HYCOM scenario only runs once daily because this scenario depends on HYCOM model forecasts which are produced once a day.

A typical SSMS cycle consists of a nowcast and a forecast. Nowcasts form a continuous simulation (Figure 4-9), each following nowcast is initialized using the data from the last time step of the previous nowcast. A forecast is initialized with the data from the current nowcast. For example, for a 4 times daily scenario and 00:00UTC cycle, first a nowcast simulation is initialized at 18:00 using the data from the previous nowcast simulation (from 12:00 to 18:00). The nowcast is then run from 18:00UTC to 00:00UTC and a hotstart file is output. This hotstart file is then used to initialize the forecast and the same hotstart file will be used to initialize the nowcast of the next (06:00UTC) cycle.

SSMS cycles are event-based and can be triggered by different events. For example, 24/7 simulations can be triggered by the timer once a day at 00:00UTC. The storm surge simulations

are triggered by NHC forecast advisories. Once a forecast advisory is received it is analyzed and SSMS determines if at any time during the forecast the storm is close (within 300 nautical miles) to any of the SSMS domains and then the affected domains are scheduled to be included in the simulation. Limited resource environment is the reason for excluding the domains that are not forecasted to be affected by the storm.

SSMS Scenarios

As described in Chapter 1, there are two base scenarios: Full3D and Fast2D. The focus of a Full3D scenario is to provide the most accurate forecast possible, including predictions of salinity transport and baroclinic currents. The Fast2D scenario focuses on the speed and being able to produce a prediction in the shortest time possible, but possibly at the expense of physics complexity and accuracy of prediction. Since SSMS is a very flexible system and allows a variety of components to be used in different combinations - several scenarios can be derived. Table 4-3 lists various scenarios that can be conducted using SSMS and typical times required to complete these simulations. Every scenario consists of regional and coastal models as well as a combination of wind fields. The total time required to produce a prediction for a scenario consists of the following:

- time required to obtain (download) all data that is used to force models, such as official track, NOGAPS wind, WaveWatch III wave predictions, HYCOM predictions of water level and salinity, etc. Since all download processes are independent the time to obtain all needed data is equal to the maximum time needed to obtain either one of the datasets.
- time required to produce a resultant wind field for each model (ADCIRC, CH3D, SWAN)
- time required to run ADCIRC/CH3D/SWAN simulations. All models are dynamically coupled therefore the amount of time required to run all simulations is limited by the slowest model. This time consists of the time needed to run a nowcast simulation added to the time needed to complete a forecast simulation.
- time required to run post-processing, archive and catalog the results (typically ~5 minutes)

Table 4-3. SSMS scenarios setup and typical times required to obtain a 60-hours forecast for each scenario

Scenario	Regional surge model	Regional wave model	Coastal surge model	Coastal wave model	Storm wind	Background wind	CH3D domain	Cycle completion time (hours:min)
Fast2D	ADCIRC	---	CH3D-2D	---	ANA2	---	EC	01:10
							SW	01:10
Fast2D+Waves	ADCIRC	WWIII	CH3D-2D	SWAN	ANA2	---	EC	06:50
							SW	06:50
Fast2D-ANA	ADCIRC	---	CH3D-2D	---	ANA	---	EC	01:10
							SW	01:10
Full3D	ADCIRC	---	CH3D-3D	---	ANA2	---	EC	04:05
							SW	02:35
Full3D-HYCOM	HYCOM	---	CH3D-3D	---	ANA2	NOGAPS	EC	17:45
							SW	16:15
Full3D+Waves	ADCIRC	WWIII	CH3D-3D	SWAN	ANA2	---	EC	10:45
							SW	09:35
Full3D-NCOM	NCOM	---	CH3D-3D	SWAN	ANA2	NOGAPS	EC	25:45
							SW	24:15

Table 4-3 shows the best scenario that can be accomplished by SSMS in less than 8 hours - Fast2D+Waves. Both EC and SW domains can be typically completed in 7 hours or less which allows for an extra hour of time for unexpected delays. A Full3D-HYCOM scenario can be completed in less than 18 hours for both domains and a Full3D-NCOM in less than 26 hours. Full3D-NCOM scenario not only requires longer to obtain, but NCOM model output does not provide precipitation forecasts which makes HYCOM a better choice for salinity predictions as was shown by verification with Tropical Storm Fay.

Available Computing Resources

As described in Chapter 2, SSMS can use a variety of computing resources that use different access methods. Currently SSMS has multiple resources that are located locally as well as distributed resources. There are four dual-CPU Intel Pentium-D 3.6Ghz servers with 4GB of RAM and one dual-CPU Intel Xeon server (4 cores) with 4GB of RAM that are dedicated to the SSMS model simulations. An 8-core (dual CPU) Intel Xeon 2.5Ghz server with over 2TB of disk space is used to run all of the service tasks of SSMS, such as data downloads and processing, data archive and catalog, job setup and submission, monitoring, post-processing and archival and it is also used to run the interactive SSMS website.

Results and Products

SSMS forecast results are stored in the archive and recorded in a catalog. Stored results usually include time-series output at NOAA stations at with 6-minute resolution, hourly water level snapshots, 3-hourly salinity snapshots, and a MEOW (maximum envelope of water). All the output is stored in compressed (with gzip) NetCDF files, which internally use CF conventions. These results can be made accessible via the web directly as well as converted to geo-referenced form and displayed using the interactive GIS-based SSMS website (SSMS Team, 2009).

2008 Hurricane Season

SSMS was running semi-operationally during the 2008 hurricane season with little downtime that was required for maintenance and upgrades. The hurricane season of 2008 had 17 names storms (Figure 4-10) with only one storm - Tropical Storm Fay directly impacting Florida. Tropical Storm Eduard was the next closest to Florida storm; however, it passed almost a hundred miles to the east of Florida and did not impact the state. The results obtained during the 2008 season for Tropical Storm Fay as well as further developments and verification of SSMS using Fay are discussed in Chapter 6.

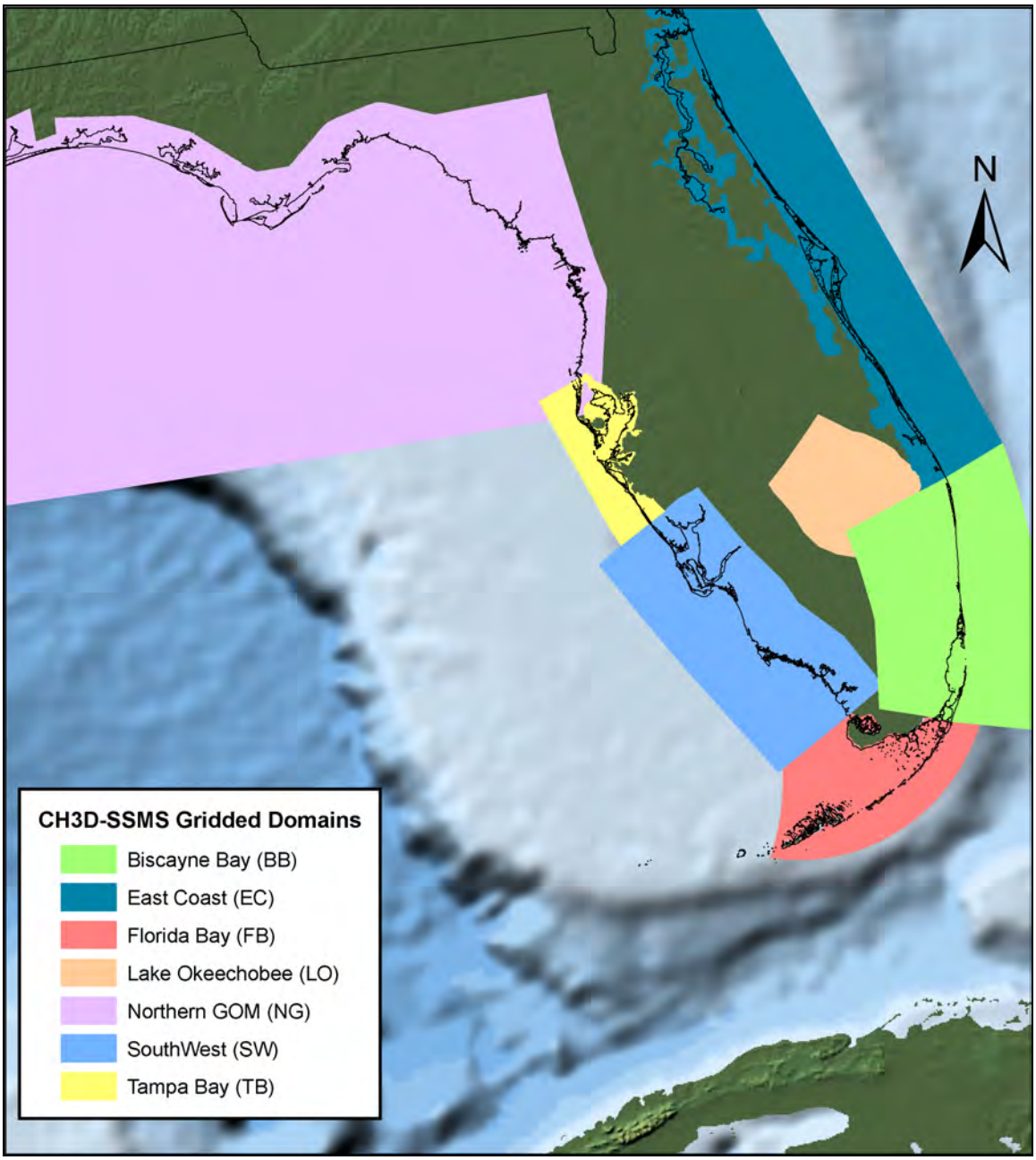

Figure 4-1. CH3D model domains

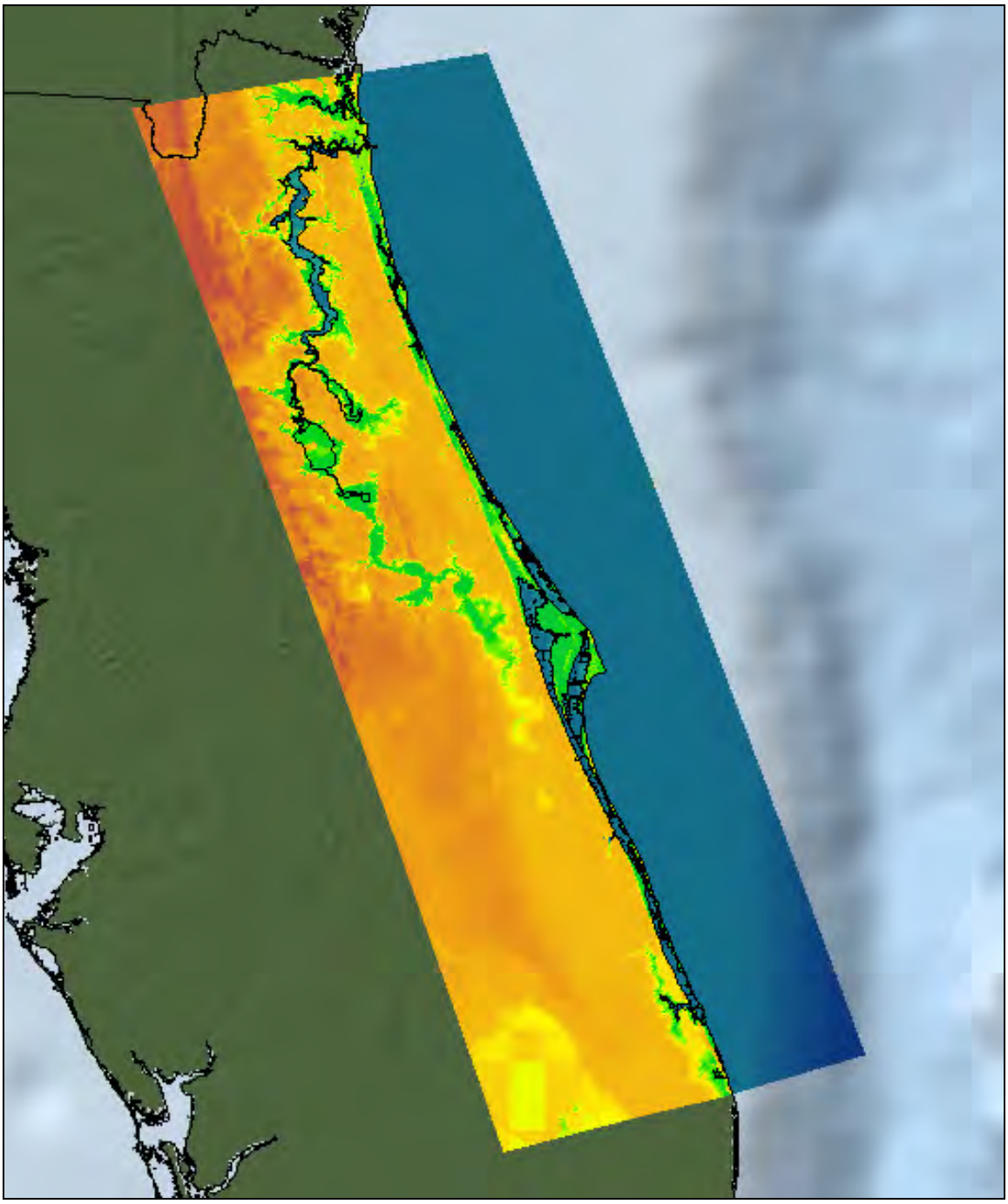

Figure 4-2. East coast of Florida CH3D grid (EC)

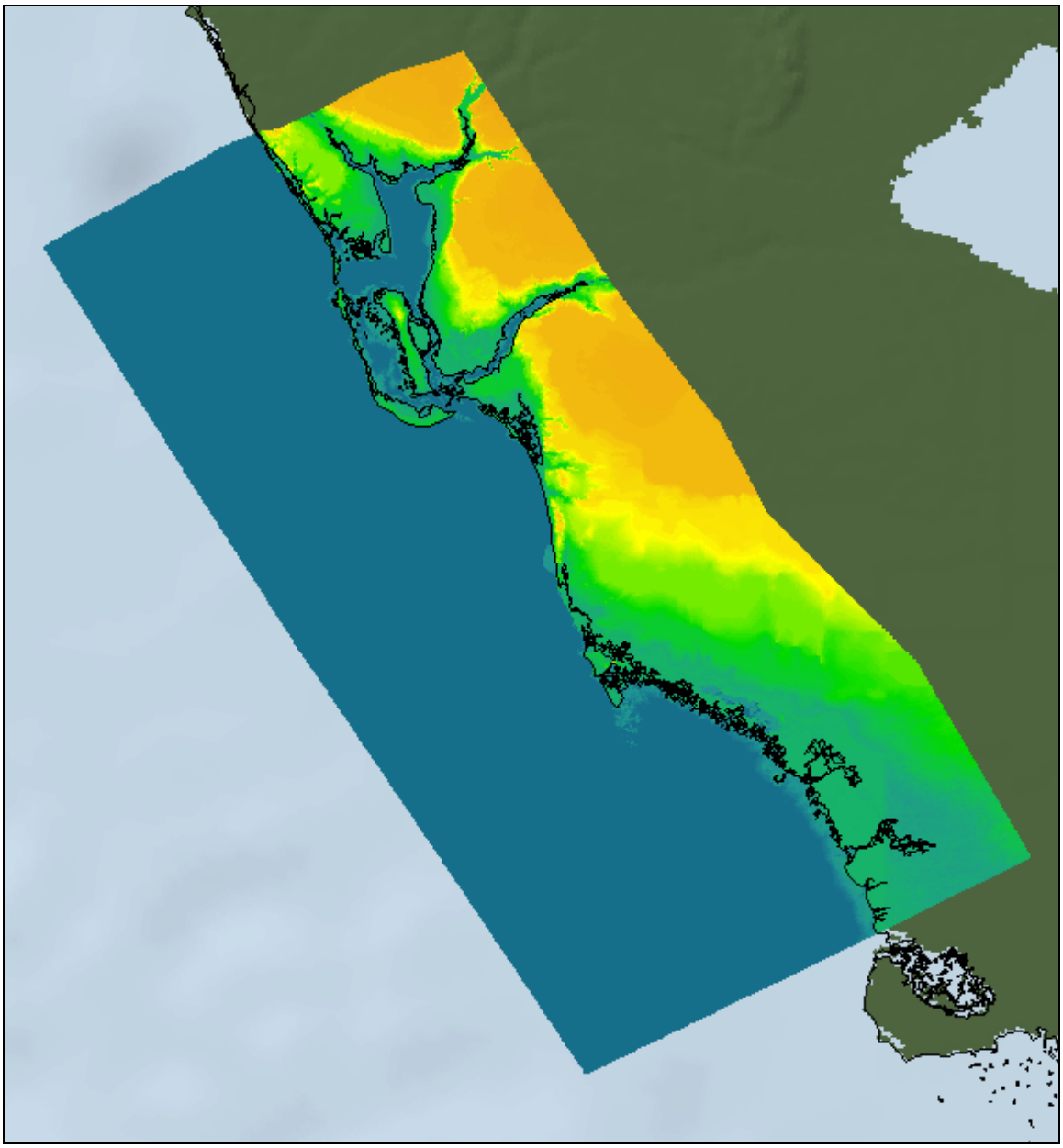

Figure 4-3. Southwest coast of Florida CH3D domain (SW)

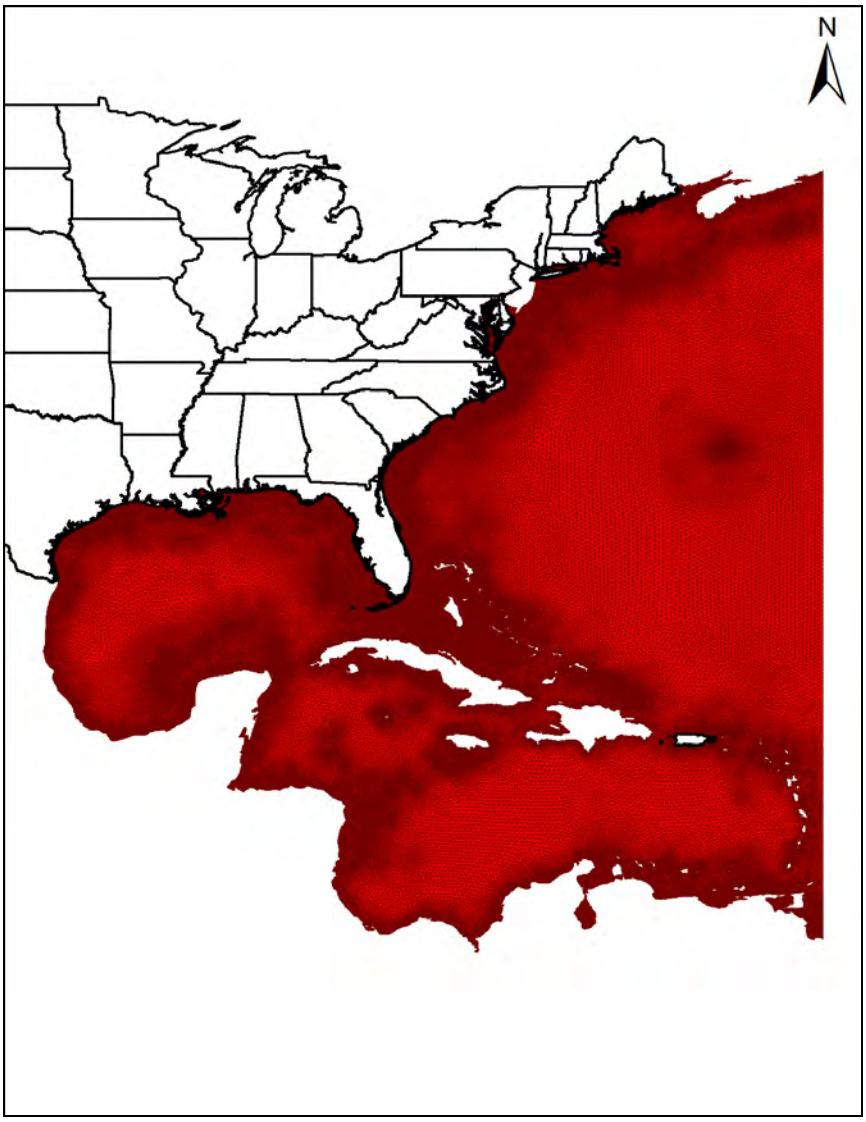

Figure 4-4. ADCIRC grid domain

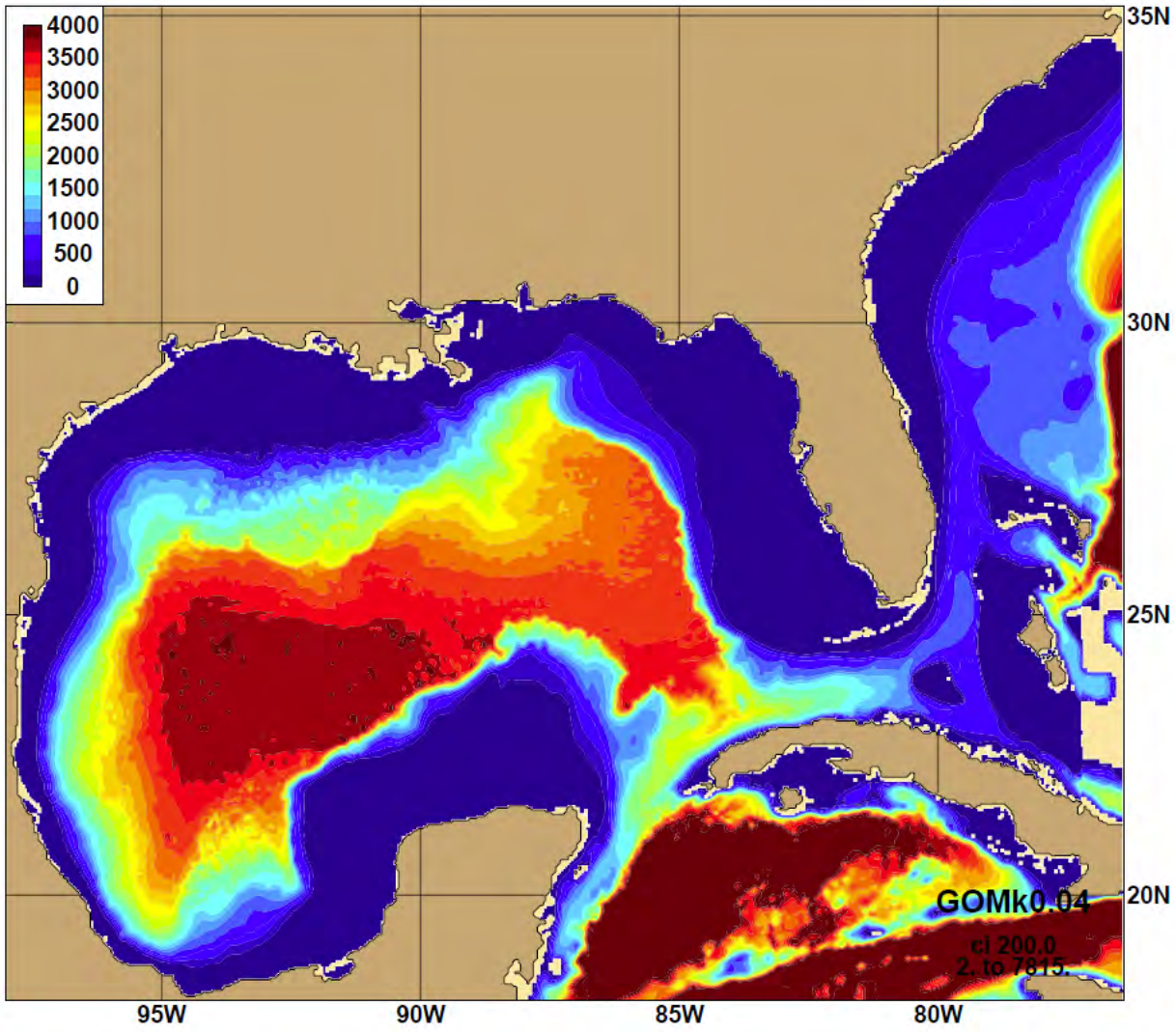

Figure 4-5. HYCOM Southeast United States domain (image courtesy of NRL)

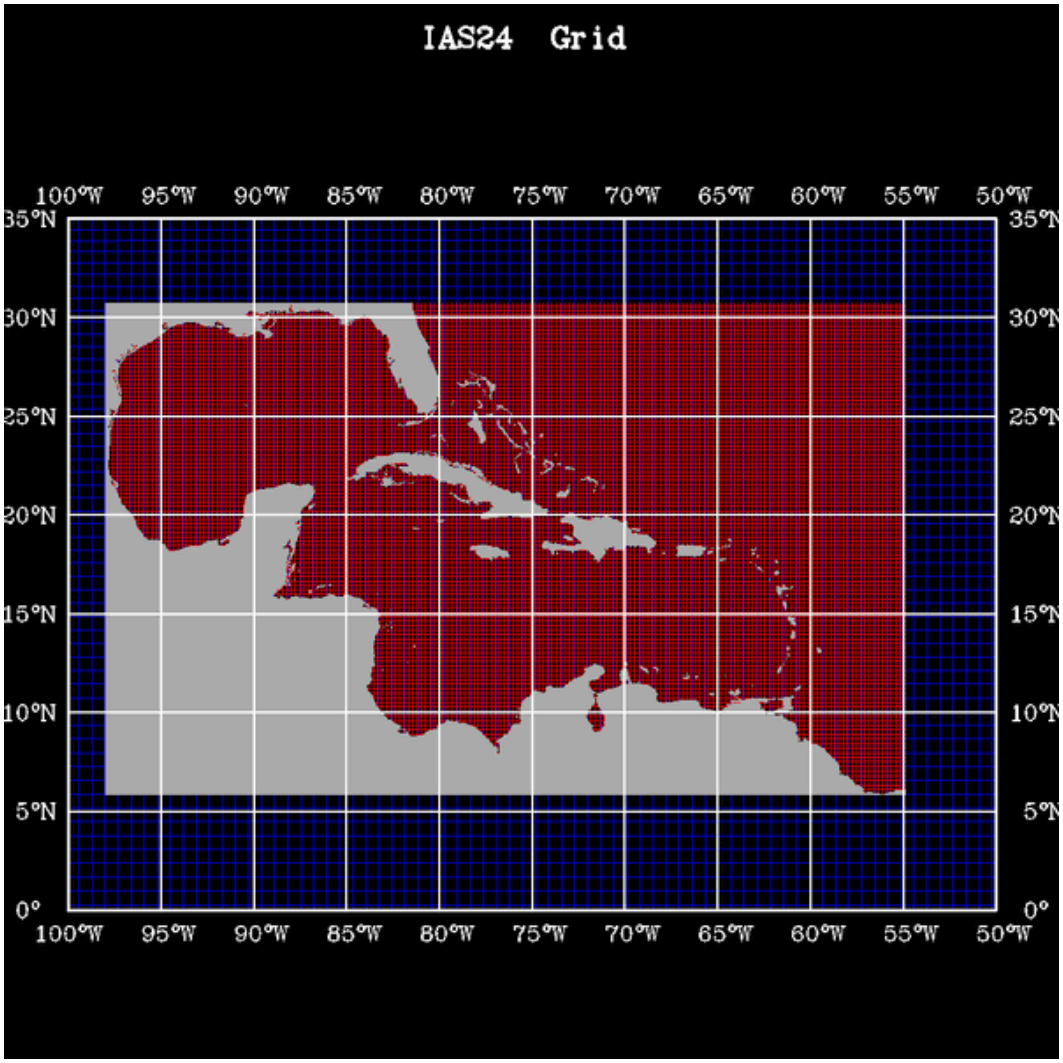

Figure 4-6. NCOM IASNFS computational grid (image courtesy of NRL)

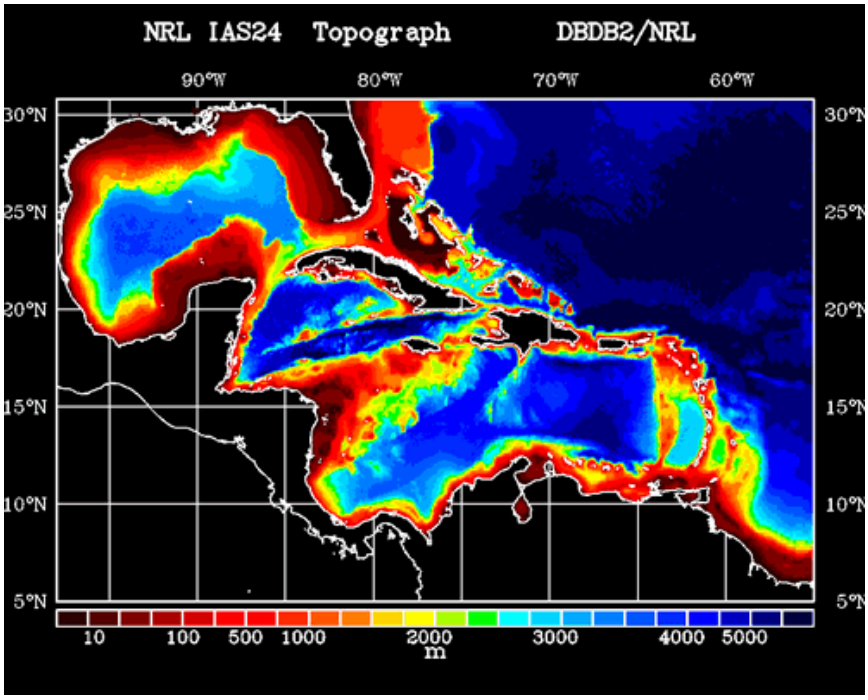

Figure 4-7. NCOM IASNFS topography (image courtesy of NRL)

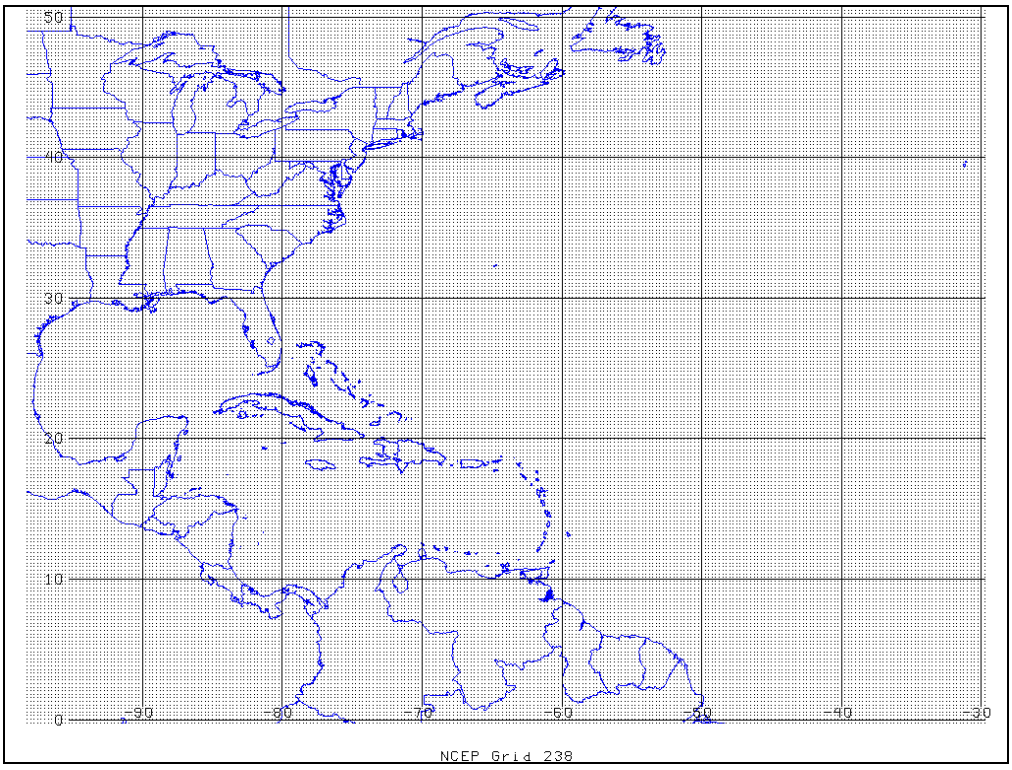

Figure 4-8. WaveWatch III Western North Atlantic (WNA) domain (image courtesy of NOAA)

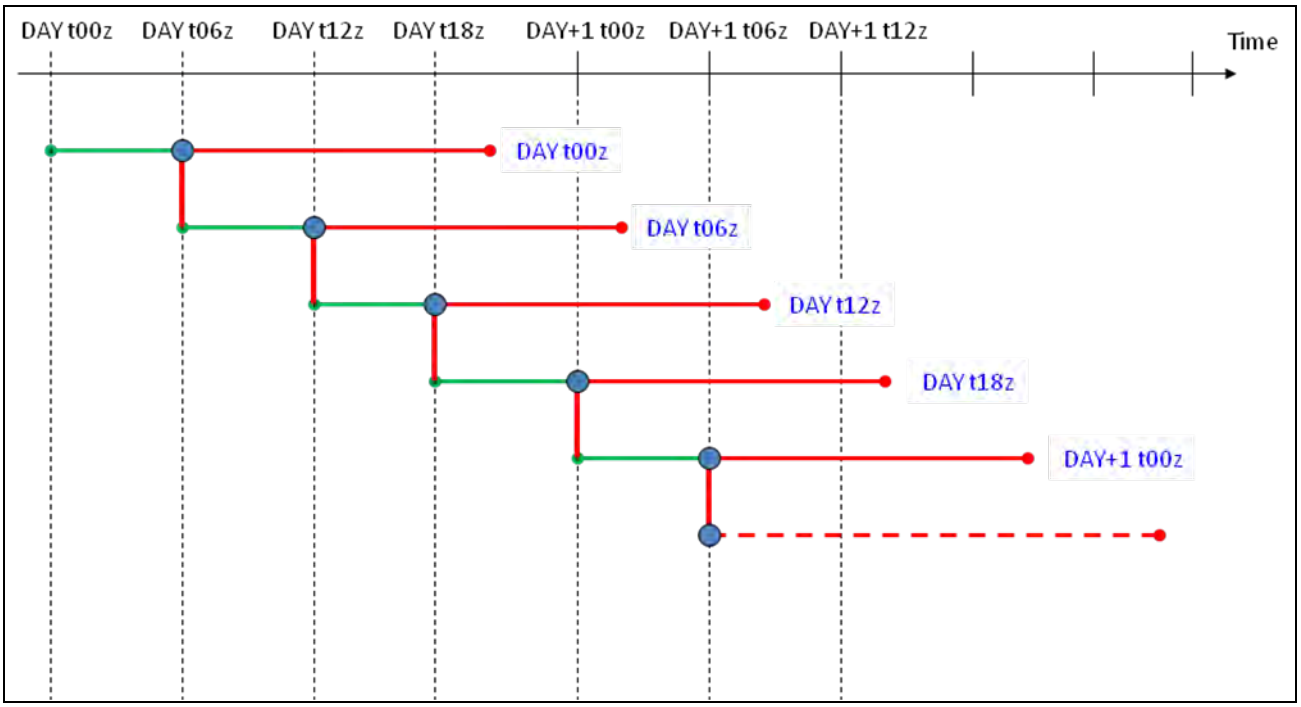

Figure 4-9. SSMS cycle structure: nowcasts (green horizontal lines) and forecasts (red horizontal lines).

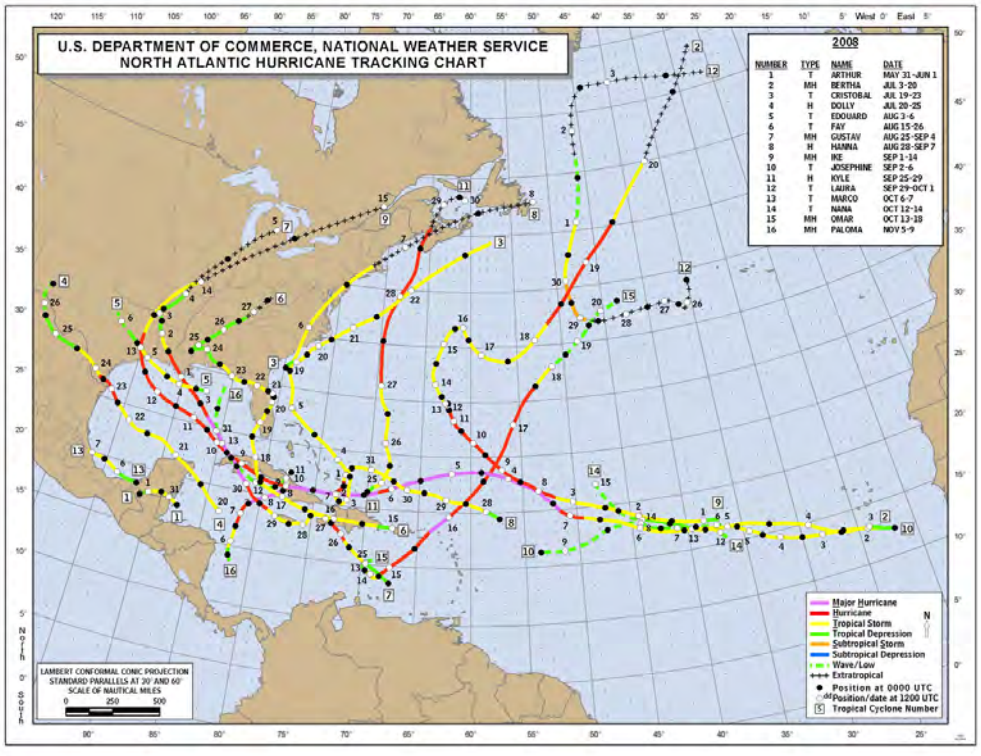

Figure 4-10. 2008 Atlantic hurricane season track map (image courtesy of NOAA/NWS).

CHAPTER 5
VERIFICATION OF SSMS: HURRICANE WILMA

Model verification is a complicated process, generally limited by data availability. It is especially true when it applies to tropical storms. Collecting a good dataset during and after a storm is both complicated and costly; since storm track and intensity forecasting is still very error prone and it is the quality of storm track forecasting that determines how successful a data collection event can be. Surge data from the coastal zone is often very scarce. Validation of the extent and dynamics of flooding has been literally impossible due to lack of data. High water marks often do not provide accurate elevation information and generally do not contain timing information. Installation of surge sensors before hurricanes is very challenging because hurricane paths are hard to predict and the amount of time allowed for instrument setup is small. Once installed, it is impossible to move the installed instruments quickly if a hurricane does not follow the forecasted path. Strong winds and surge currents are also capable of destroying instruments and often there are several instruments that could capture the water level that stop working during the storm. Therefore typical data collected during hurricanes has very low spatial resolution of measurements and makes it impossible to follow the evolution of surge and flood. Little temporal data have been collected in inland areas which have a potential to be flooded.

Generally, for every historical storm there are a few NOAA tidal gauges that are in the vicinity of the hurricane landfall that can capture the effects of the storm at the coast, however, these data are very sparse and there are very few such stationary devices inland of the coastal and in the estuarine zone. High water marks that are usually collected after the storm often do not provide accurate elevation information and carry no temporal information at all, which can be very important as will be shown later in this chapter. Coastal stations data even when combined with the high water marks data often make it very hard to impossible to follow the evolution of

flooding and inundation processes and leaves a lot of room for speculation. Hurricane Wilma is one of the few exceptions. US Geological Survey (USGS) has successfully conducted a data survey during Wilma. The USGS had setup almost 30 gauges capable of sensing storm surge on the west coast of Florida where Wilma was predicted to make a landfall. Gauges covered over 100km of the coastline and even though the track shifted slightly from its forecasted location and most gauges ended up located on the north side of the storm they still collected extremely useful data that can help us better understand the nature of processes of flooding and inundation.

Hurricane Wilma

Hurricane Wilma (Pasch et al., 2006) was the most intense hurricane ever recorded in the Atlantic basin. It was the twenty third named storm, thirteenth hurricane, sixth major hurricane and fourth Category 5 hurricane of a record breaking 2005 hurricane season. Hurricane Wilma was responsible for at least 63 deaths and over $29 billion in damage making it the third costliest hurricane to hit the U.S. after Katrina and Andrew.

Wilma spawned as a tropical storm over the western Caribbean Sea on October 15th. It was moving west at approximately 3 miles per hour and strengthening and on October 18th the NHC upgraded Wilma to a category two hurricane. Wilma strengthened further to a category five on October 19th and on the 21st passed Cozumel as a category four hurricane. It was drifting northward slowly until on the 23rd it picked up the pace and started moving northeast towards southwest Florida. Hurricane Wilma reached Florida Keys on the 24th with an 8-10 foot surge impacting the north coast of Cuba on the way, it made landfall near Cape Romano in Collier County, Florida around 10:30 UTC bringing near 10-foot surge in the region of Ten Thousand Islands. Accelerating continuously, the hurricane crossed Florida in about 4.5 hours moving at 20-25kt, weakened to Category 2 (95kt winds) and later that day Wilma emerged on the east coast of Florida near Jupiter at 15:00 UTC where it quickly re-intensified once again to a

category three storm and went quickly northeastward across the North Atlantic Ocean becoming a large extratropical storm and moving away from North America. The track of hurricane Wilma is shown on Figure 5-1.

H*Wind snapshots (Figures 5-2 to 5-5) to the north of the Cape Sable show maximum 1-minute sustained winds of over 90kts and direction onshore. The storm center passed just south of Marco Island where winds weren't as strong (50-60kts) and were directed offshore. Therefore the highest wind-induced surge is expected in the Keys and the area of Ten Thousand Islands, while in the area north of the Marco Island one might expect a setdown due to the offshore wind (see Figure 5-6 for wind data at Naples, FL wind station with winds primarily n the offshore direction).

Model Domains and Measured Data Availability

The model domains used for the SSMS CH3D model simulations are the East Coast (EC, Figure 5-7) and the South West Coast (SW, Figure 5-8 and a zoom-in on Captiva Island area on Figure 5-9) mentioned in the previous chapter. The ADCIRC simulations use two unstructured grids: EC95d (Figure 5-10) and a modified version of EC2001e (Mukai et al., 2002, Figure 5-11). Both grids cover the same region – the western North Atlantic and the Gulf of Mexico. The EC95d grid consists of 31,435 nodes and features 5-15 km resolution near the coast. The modified EC2001e grid is much finer and contains 254,774 nodes with 700 m-2 km resolution near the coast.

In order to get accurate representation of high surge levels at the southern part of Florida, the ADCIRC model was employed to simulate the surge outside the CH3D domain. ADCIRC model was forced only by wind and atmospheric pressure, providing surge values for CH3D model at its open boundary. Initially, a rather coarse EC95d grid, which covers the western North Atlantic and the Gulf of Mexico, was used for ADCIRC simulations. The EC95d grid did not

capture the wave propagation well due to its low coastal resolution. The EC2001e ADCIRC grid with much finer resolution was used later for simulations to obtain more satisfactory results in the Key West area. However, the EC2001e grid does not cover the Charlotte Harbor area. Hence the EC2001e grid was modified to include the Charlotte Harbor are and to refine the grid near Key West and Vaca Key with appropriate bathymetry (Figure 5-12) data to allow the model to better capture the surge in the Keys.

There is a good amount of data available for Hurricane Wilma including measured wind at FCMP (Florida Coastal Monitoring Program, FCMP, 2009) stations and NOAA-NOS (National Oceanic and Atmospheric Administration National Ocean Service) stations, analysis wind by HRD (Hurricane Research Division) also known as H*Wind, water level at coastal NOAA-NOS and COAMPS (Coupled Ocean / Atmosphere Mesoscale Prediction System by Naval Research Laboratory, Monterey Marine Meteorology Division) stations as well as surge gauges data set up and collected by USGS (United States Geological Survey). Availability of USGS surge data which allows for better validation of SSMS flooding and inundation capabilities plus the wind patterns that have winds directed offshore at most locations where measured water levels are available, allowing to test the wind-land interaction implemented in SSMS, was a deciding factor to use Hurricane Wilma for verification of the SSMS.

Wind data

HRD analysis of hurricane Wilma winds is available and unlike H*Wind datasets for most storms that are not tracked by HRD once they make landfall wind analysis for Wilma tracked the hurricane as it moved through the state and emerged on the east coast. The H*Wind data shows sustained (1-min avg.) 10-meter winds of 60-80kt across the Florida Keys during the peak of the storm (Figure 5-2) which is consistent with the NOAA-NOS measurements at the Key West station (ID: 8724580) with peak winds reaching about 75kt (Figure 5-13). HRD analysis winds

can be very useful for hindcasting, however, they are not available in real-time for nowcasting or forecasting and therefore the H*Wind data will only be used to validate the model wind forcing that is used to drive Hurricane Wilma simulations.

Wind measured by FCMP is another dataset that is very useful when validating the Hurricane Wilma simulated winds. Since wind is the primary driver for the surge and it needs to be as accurate as possible in order to produce accurate surge estimates. Unlike NOAA-NOS data that is available at 6-min intervals – the FCMP data is sampled at a very high frequency and data is available at 10-sec intervals, however, as it was shown in the chapter on development of WMS - 10-min average winds should be used for storm surge modeling. FCMP as well as NOAA-NOS station locations are shown on Figures 5-7 and 5-8.

Water Level Data

There are two NOAA-NOS stations in the SW domain – Naples and Fort Myers, both stations provide 6-min water level data and will be used for model verification. Also, there is a flow control structure S79 that has water level data available at 10-min intervals during Hurricane Wilma passage.

The East Coast domain, unfortunately, does not have as many data points available (Figure 5-7); however, since both domains would be included in the real-time nowcast/forecast simulation during Wilma it is essential to attempt to validate the model with the data available. On the East Coast the storm center emerged near Jupiter and given its large size the Trident Pier station on the east coast experienced 40 to 50kt winds according to the H*Wind data (Figures 5-2 and 5-3). It should be noted that all measured water level data were either obtained in reference to the NAVD88 datum or converted to the NAVD88 using the method described in the Vertical Datums section of Chapter 2.

USGS Surge Data

The USGS data set is by far the richest of the datasets measuring surge for hurricanes that made their landfall in Florida. Almost 30 Hobo water loggers surge were installed covering a span of over 100km of the coastline from Everglades City to Captiva Island (Figure 5-8, Table 5-1). The instruments were deployed both on the coastline and in the inlets and estuaries. The S-sensors with the nominal accuracy of 4.1 cm and the range of 30 meters were deployed at all locations. The B-sensors with the nominal accuracy of 2.1 cm and the range of 9 meters were installed at about 60% of all stations. The sensors were deployed on October 22 and retrieved through October 31. The temporal resolution of collected data is 30 seconds and all the data are referenced to NAVD88.

According to the USGS data, significant surge was found at most of the stations shown in Figure 5-8. As an example Figure 5-14 shows the observed surge at Goodland (station 27), Naples (station 22) and Wiggins Pass (station 20). As the center of Wilma was nearing landfall around 10:30 UTC on October 24th, Wiggins Pass had a setdown due to strong offshore-directed wind, a peak surge was found at Goodland due to strong onshore-directed wind, while Naples had a modest surge due to wind from the northwest. Figure 5-14 also shows that, 4-6 hours after Wilma landfall, there was a very pronounced second surge at all three locations, when the storm had already travelled to the east coast of Florida.

As shown in Figure 5-14, the second peak in storm surge appeared at station 27 first, followed by stations 22 and 20. Thus it appears that the second peak is associated with propagation of a “dome of water” along the coast from south to north when Wilma had already left the region. Although there exists no offshore water level data to validate this, it will be shown later via numerical modeling that this is indeed the case. It should be noted that at the

time of the second peak, the wind had already subsided at these coastal stations and many residents who thought the worst of the storm was over were caught by surprise.

Table 5-1. Locations of USGS Surge Measurement Stations

Station Name	Station Number
Captiva Island at South Seas Resort	8
Caloosahatchee River at Redfish Point	9
Downtown Fort Myers Yacht basin	10
Punta Rassa Boat Ramp	11
Matanzas Pass Bridge	13
Mullock Creek at Marina	14
Big Carlos Pass	15
Estero Bay at Coconut Point Marina	16
Estero River at US41	17
Spring Creek at US41	18
Imperial River at US41	19
Wiggins Pass State Park	20
Cocahatchee River at US41	21
Naples Pier	22
Naples Bay at US41 Gordon River Bridge	23
Henderson Creek (Downstream) at KOA Campground	24
Henderson Creek (Upstream) at US41	25
Marco Island at MIYC (Bayside)	26A
Marco Island at Tigertail Beach (Gulfside)	26B
Goodland	27
Blackwater River at Collier Seminole State Park	28
Faka Union Canal	29
Everglades City at Ranger Station	30

Precipitation and Run-off

According to Byrne (2006) storm rainfall during Hurricane Wilma was quite low and the highest contribution from rain averaged 1-2 inches across the Florida Keys therefore one can assume that the rainfall and runoff were not major contributors to the surge levels and did not cause major flooding in the area.

Waves

Waves were significant during the Hurricane Wilma, but only in the keys area (Figure 5-15) and near the keys and since no water level/surge measurements are available it is impossible

to validate the waves there. Preliminary simulations were done and near the coast in the area of interest, close to the landfall of the storm and to the north of it, the waves were not significant and did not affect the surge. Most likely this is due to the fact that the winds are primarily blowing offshore and do not create a significant setup locally. The east coast simulation was coupled with the wave model since the fetch in the Trident Pier area (the station available for water level comparison) was favorable for the wave action and setup (Figure 5-16).

Model Setup, Forcing and Boundary Conditions

SSMS was setup as described in Chapter 4 for both EC and SW modeling domains. Available data is limited to water levels at different locations. There are no observed currents or salinity available for Hurricane Wilma, also the NCOM/HYCOM data availability is limited to the years 2008 and after. Therefore, not only the Full3D scenario would be impossible to validate but obtaining boundary conditions to drive the 3D version of the CH3D model to simulate salinity transport would be problematic. The Fast2D scenario seems to be more applicable in this case. Also, the effect of waves is limited as it was shown above and therefore Fast2D+Waves scenario would be tested in addition to the Fast2D scenario. Duration of simulations of both SW and the EC domains is five days, which is consistent with a typical forecast cycle for the SSMS. Hurricane Wilma made landfall on October 24 to allow for the spin up time for models as well as the time for the surge to retreat, the simulation period was selected to be from October 22, 00:00 UTC to October 27, 00:00 UTC.

Wind Forcing

Wind is the primary forcing for storm surge simulations, the WMS described in Chapter 4 was used to produce consistent wind fields for Hurricane Wilma simulations. WMS was setup using the best track data for Hurricane Wilma obtained from ATCF (Table 5-2). The track information was extracted from the best track file and only variables pertinent to the WMS were

retained: date and time, position of the hurricane maximum sustained wind speed in knots (Vmax), minimum sea level pressure in millibars (MLSP), wind intensity for the radii defined in this record (RAD) in knots, radius of specified wind intensity for the North-East quadrant (RAD1), South-East quadrant (RAD2), South-West quadrant (RAD3) and the North-West quadrant (RAD4) in nautical miles, and the radius to maximum winds in nautical miles.

Table 5-2. Best track of Hurricane Wilma extracted from the ATCF data

Date/Time YYYYMMDDHH	Lat	Lon	Vmax (kt)	MLSP (MB)	RAD (kt)	RAD1 (nm)	RAD2 (nm)	RAD3 (nm)	RAD4 (nm)	RMW (nm)
2005101706	169N	796W	35	1000	34	0	0	40	0	35
2005101712	163N	797W	40	999	34	0	60	40	0	35
2005101718	160N	798W	45	997	34	30	60	60	30	35
2005101800	158N	799W	55	988	34	60	60	60	60	20
2005101800	158N	799W	55	988	50	20	20	20	20	20
2005101806	157N	799W	60	982	34	60	60	50	60	20
2005101806	157N	799W	60	982	50	20	20	20	20	20
2005101812	162N	803W	65	979	34	105	75	50	105	15
2005101812	162N	803W	65	979	50	30	20	20	30	15
2005101812	162N	803W	65	979	64	15	15	0	15	15
2005101818	166N	811W	75	975	34	120	75	60	120	15
2005101818	166N	811W	75	975	50	50	30	30	50	15
2005101818	166N	811W	75	975	64	15	15	15	15	15
2005101900	166N	818W	130	946	34	135	90	90	135	10
2005101900	166N	818W	130	946	50	60	30	30	60	10
2005101900	166N	818W	130	946	64	15	15	15	15	10
2005101906	170N	822W	150	892	34	140	90	90	140	10
2005101906	170N	822W	150	892	50	60	30	30	60	10
2005101906	170N	822W	150	892	64	30	15	15	30	10
2005101912	173N	828W	160	882	34	170	125	90	140	10
2005101912	173N	828W	160	882	50	70	45	45	70	10
2005101912	173N	828W	160	882	64	45	20	20	45	10
2005101918	174N	834W	140	892	34	200	200	100	150	5
2005101918	174N	834W	140	892	50	75	60	60	75	5
2005101918	174N	834W	140	892	64	50	40	40	50	5
2005102000	179N	840W	135	892	34	200	200	110	150	5
2005102000	179N	840W	135	892	50	75	75	60	75	5
2005102000	179N	840W	135	892	64	60	40	40	60	5
2005102006	181N	847W	130	901	34	200	200	110	150	5

Table 5-2. Continued

2005102006	181N	847W	130	901	50	75	75	60	75	5
2005102006	181N	847W	130	901	64	60	40	40	60	5
2005102012	183N	852W	130	910	34	200	150	110	175	25
2005102012	183N	852W	130	910	50	110	85	60	110	25
2005102012	183N	852W	130	910	64	75	75	45	75	25
2005102018	186N	855W	130	917	34	175	150	120	175	25
2005102018	186N	855W	130	917	50	110	90	75	110	25
2005102018	186N	855W	130	917	64	75	75	60	75	25
2005102100	191N	858W	130	924	34	175	150	120	175	20
2005102100	191N	858W	130	924	50	110	90	75	110	20
2005102100	191N	858W	130	924	64	75	75	60	75	20
2005102106	195N	861W	130	930	34	175	150	120	175	20
2005102106	195N	861W	130	930	50	110	90	75	110	20
2005102106	195N	861W	130	930	64	75	75	60	75	20
2005102112	201N	864W	125	929	34	175	175	120	150	20
2005102112	201N	864W	125	929	50	100	90	75	100	20
2005102112	201N	864W	125	929	64	75	75	60	75	20
2005102118	203N	867W	120	926	34	175	175	120	150	20
2005102118	203N	867W	120	926	50	100	100	75	100	20
2005102118	203N	867W	120	926	64	75	75	60	75	20
2005102200	206N	868W	120	930	34	175	175	120	150	15
2005102200	206N	868W	120	930	50	100	100	75	100	15
2005102200	206N	868W	120	930	64	75	75	60	75	15
2005102206	208N	870W	110	935	34	175	175	120	150	15
2005102206	208N	870W	110	935	50	100	100	75	100	15
2005102206	208N	870W	110	935	64	75	75	60	75	15
2005102212	210N	871W	100	947	34	175	175	120	150	20
2005102212	210N	871W	100	947	50	100	100	75	100	20
2005102212	210N	871W	100	947	64	75	75	60	75	20
2005102218	213N	871W	85	958	34	175	175	120	150	30
2005102218	213N	871W	85	958	50	100	100	75	100	30
2005102218	213N	871W	85	958	64	75	75	50	75	30
2005102300	216N	870W	85	960	34	175	175	120	150	30
2005102300	216N	870W	85	960	50	100	100	75	90	30
2005102300	216N	870W	85	960	64	60	60	50	60	30
2005102306	218N	868W	85	962	34	175	175	125	175	30
2005102306	218N	868W	85	962	50	100	100	75	90	30
2005102306	218N	868W	85	962	64	60	60	40	40	30
2005102312	224N	861W	85	961	34	200	200	125	175	30
2005102312	224N	861W	85	961	50	100	100	75	90	30

Table 5-2. Continued

2005102312	224N	861W	85	961	64	60	60	40	40	30
2005102318	231N	854W	90	963	34	200	200	150	150	30
2005102318	231N	854W	90	963	50	125	125	90	90	30
2005102318	231N	854W	90	963	64	65	75	50	50	30
2005102400	240N	843W	95	958	34	200	200	150	150	30
2005102400	240N	843W	95	958	50	125	125	90	90	30
2005102400	240N	843W	95	958	64	65	75	50	50	30
2005102406	250N	831W	110	953	34	200	200	175	150	30
2005102406	250N	831W	110	953	50	125	125	100	90	30
2005102406	250N	831W	110	953	64	75	80	75	50	30
2005102412	262N	810W	95	950	34	200	225	200	150	30
2005102412	262N	810W	95	950	50	125	150	100	90	30
2005102412	262N	810W	95	950	64	75	90	75	40	30
2005102418	280N	788W	105	955	34	200	225	200	150	35
2005102418	280N	788W	105	955	50	125	150	100	90	35
2005102418	280N	788W	105	955	64	75	90	75	40	35
2005102500	301N	760W	110	955	34	200	225	250	150	35
2005102500	301N	760W	110	955	50	125	150	100	90	35
2005102500	301N	760W	110	955	64	75	90	75	40	35
2005102506	333N	720W	100	963	34	200	275	375	150	35
2005102506	333N	720W	100	963	50	125	150	100	75	35
2005102506	333N	720W	100	963	64	75	90	60	40	35
2005102512	368N	679W	90	970	34	200	300	375	175	35
2005102512	368N	679W	90	970	50	125	150	100	75	35
2005102512	368N	679W	90	970	64	75	90	60	40	35
2005102518	405N	635W	75	976	34	200	300	375	175	45
2005102518	405N	635W	75	976	50	125	150	100	75	45
2005102518	405N	635W	75	976	64	60	75	45	45	45

WMS produces wind and pressure fields at 5-min intervals, which are then interpolated onto each model grid and passed to the three models: ADCIRC, CH3D and SWAN. The wind produced by the WMS is based on a synthetic model by Xie (2006) with the reduction factors due to land dissipation applied to it. The wind and pressure fields computed by the WMS are based only on parameters that are listed in Table 5-2 and are available from the ATCF system for forecasting. WMS wind produced by WMS compare well with the analysis H*Wind data

obtained from HRD (Figure 5-17). Validation of WMS and wind and pressure fields is described in detail in Chapter 3.

Additionally, sensitivity tests were done running simulations using the GFDL and HRD winds were made and results were compared to the results obtained using the synthetic wind model ANA with and without land-induced wind dissipation.

Water Level

Water level boundary conditions for CH3D model were obtained as a linear combination of the surge levels based on the ADCIRC model simulation, which in turn was driven by the same WMS generated wind field as CH3D, with tides computed based on the tidal constituents supplied to the model at the open boundary. To validate tidal constituents used for open boundary a period of time with very low winds was selected (about two months prior to Wilma landfall) and a simulation using tidas constituents as the only forcing was performed. Figure 5-18 shows the comparison of simulated tides at the NOAA-NOS station located at Naples, FL, tidal simulation was a 20-days long simulation that covered a time span with rather low winds just before the Hurricane Wilma arrival. Simulated tides show good agreement with measured data.

Waves

For the Fast2D+Waves scenario the inclusion of SWAN is necessary, SWAN was run in a non-stationary mode with a 5-second time step and is forced with the same wind produced by the WMS as the wind used for the ADCIRC and CH3D models. The open boundary conditions for SWAN are obtained from WaveWatch III model output. SWAN boundary conditions assume a Gaussian distribution and provide significant wave height, period and direction of waves based on the WaveWatch III model output.

Simulating the Storm

The H*wind snapshots as well as time-series of wind data at Naples, FL (Figure 5-6) show that as the storm made landfall just south of Marco Island winds were directed offshore along the coastline north of the storm landfall location. With an offshore wind acting for a prolonged period of time one would expect to see a setdown at most of the USGS stations, however, the data shows that there is significant storm surge according to the data collected by USGS, as shown on Figure 5-14, for example at Goodland (27), Naples (22), and Wiggins Pass (20), all other stations show similar behavior. Also there is a very pronounced second peak that can be seen after the storm has passed around 17:00-18:00UTC on October 24, 2005, depending on the location, that is the time when the storm center was already on the east coast of Florida.

It should be further noted that the observed surge could have been higher and more damaging had the peak surge coincided with the high tide. As shown in Figure 5-19, the second surge peak at Naples coincided with low tide conditions according to NOAA predicted tides, which are based only on astronomical tidal constituents. Had the landfall occurred during high tide conditions, one can expect the surge to be significantly higher and flooding to be more extensive.

As it was mentioned previously, Hurricane Wilma was simulated using two scenarios: Fast2D and Fast2D+Waves. Additional simulations were performed to study the effect on the results of each component of SSMS and to show the importance of coupling of CH3D coastal domain to a regional scale model (ADCIRC) as well as the effects of waves.

The preliminary results have shown that the difference between the Fast2D and Fast2D+Waves scenarios on the west coast is minimal based on the comparison of simulation results to the measured data (since there are no measurements available in the areas where wave action is very significant) and therefore the Fast2D+Waves simulation was discarded since the

results are almost identical and it takes a significant amount of CPU time to run a wave model. However, there was a difference between the two simulations of the east coast where the winds were blowing onshore and creating the fetch that is favorable for wave generation.

Regional Model Simulation

First, uncoupled simulations of Hurricane Wilma were performed using ADCIRC and CH3D models within the SSMS framework. The results show that neither model can successfully simulate surge and inundation due to the storm. The ADCIRC grid is significantly coarser and does not feature flooding and drying neither does it cover land, creeks or estuaries, therefore comparisons to the USGS data would be unfair or impossible depending on the location. It can be observed from the ADCIRC simulations (Figures 5-20 and 5-21) that high surge accumulates between the southern tip of the Keys and the Thousand Island area outside the CH3D domain. The CH3D domain coverage is insufficient to accurately simulate Hurricane Wilma on its own. Extending the CH3D grid significantly offshore to include the Keys, while keeping the same high resolution, would significantly increase the simulation time required. Coupling CH3D with a regional scale ADCIRC model to obtain the surge at the open boundary, however, effectively solves the problem of domain coverage with much less computational time than that required for a high resolution CH3D or ADCIRC with a domain that includes the coastal domain and the Keys.

Simulations provide confirmation that the second peak observed in the data is formed by a long wave travelling alongshore. Figure 5-22 shows surge elevations at selected USGS stations and three stations (A1, A2, and A3) selected for model output but without measured data for comparison. This figure allows one to track the second peak as a large long wave: originating with a crest between the Ten Thousand Islands area and just north of the Keys, then propagating alongshore while creating the second peak in surge on its way to Captiva Island in the north. The

surge wave starts travelling north from approximately Cape Sable, then quickly reaches station A3, then Everglades City where it creates the second peak as wind has changed direction when the wave arrives, followed by Goodland, Naples Bay, Matanzas Pass and Captiva Island (Figure 5-22). The propagation speed of the wave is nearly constant and the time lag between the second peaks at stations is consistent with the distance between them, with Everglades and Goodland being the only exception – this is because the time when the wave passed the Everglades City almost coincided with the time when hurricane eye passed very close to Everglades City and wind directions quickly changed from onshore to longshore (south-south-east), which affected the water level. The use of a refined EC2001e model grid made it possible to accurately simulate the longshore wave, but earlier simulations using the coarser EC95d grid was unsuccessful (Figure 5-23). Obviously, using the coastal model grid alone without the offshore grid would not be able to simulate the second peaks in storm surge due to inability to capture the surge wave development and propagation after the hurricane landfall.

Local Model Simulation

The two model scenarios employed for the SSMS were simulated and CH3D surge results were compared with the data in addition the west coast domain having more available data was used to perform a sensitivity test of storm surge results to the wind that is used to drive the modeling system. As described in Chapter 3 – different winds are available for use with the SSMS; however, the synthetic wind model ANA2 by Xie et al. (2006) was selected for forecasting. While other models are available to be used it will be shown that even the results provided by the synthetic model ANA by Wilson (1960) are plausible when land-induced wind dissipation is applied if compared to other sources of wind. The effect of waves was studied using the east coast domain where wave action created more significant setup. Finally, the results

were validated using the surge data measured by the USGS providing good agreement with the data.

Validation With USGS Surge Data

Figures 5-24 to 5-29 show simulated vs. measured water level at USGS surge stations. Both magnitude and timing of the peaks are well simulated. The simulated second peaks show slight phase lead and lower magnitude compared to the measured data, probably due to rather low alongshore spatial resolution of bathymetry and topography. The second peak is caused by a surge wave that comes from the south and travels significant distance before arriving at these stations. The wave speed in shallow water is a function of bathymetry only: $c = \sqrt{gh}$. Discrepancy between model and real bathymetry is the most likely reason for simulated results being slightly off.

Figure 5-30 shows a regression analysis of errors in peak elevations between the simulated surge and the measured surge at the 23 USGS stations and Figure 5-31 shows an inundation map. Overall the comparison is good with R^2 of about 0.84. The relatively large errors at a few stations can be attributed to discrepancy in local topography and a variety of rather small features that cannot be represented by the CH3D model (e.g., some gauges are located in semi-enclosed locations, on piers and surrounded by other fine-scale features). In addition, most of the USGS stations are located near rivers and creeks and even though the rainfall was not very significant, runoff as well as flows from creeks and small rivers could contribute to the overall surge levels at these locations but, unfortunately, neither the run off data nor the flow rate for very small rivers is currently available.

The Sensitivity of Simulations to Wind Forcing

Wind-sensitivity tests were done using a variety of winds described above (GFDL, HRD H*Wind, ANA with and without land dissipation) the results of these simulations are presented in Figures 5-32 and 5-33. These tests confirmed that land dissipation has significant effect on hurricane wind and resulting storm surge. Wind fields without land dissipation led to overestimation of the offshore-directed wind after Wilma made landfall and overestimation of the setdown caused by the strong offshore-directed wind.

The Effect of Waves on the Simulation

Unfortunately data availability was very limited for the east coast domain and only the Trident Pier station was affected by the Hurricane Wilma. This station was used to verify model results. The station has no NAVD88 datum established for it and measured water level is provided in reference to the mean sea level. Datum correction was applied to the station data based on the datum information at the nearby stations (Appendix C) prior to making comparisons. Figure 5-34 shows the comparison of the two simulations – with and without waves to the measured data. Overall the agreement is good with the peak being well-timed and slightly over-predicting the peak water level by about 10 cm for the Fast2D+Waves simulation.

Summary and Conclusions

Hurricane Wilma provides an excellent example that storm surge can occur in areas where it's not expected or have a much greater than expected magnitude, after hurricane landfall and wind subsided. In the northern hemisphere a hurricane making its way perpendicular to the coastline should not cause significant flooding on the left side of it, but a large long surge wave can travel significant distance alongshore and cause flooding along its path. It can be especially damaging given the time it takes for the wave to propagate as with Wilma the surge occurred hours after the winds have weakened. The effect of surge could have been more pronounced had

Wilma made its landfall during high-tide conditions instead of the low-tide – This could have caused significantly higher surge around and just south of Naples as Wilma's peak surge almost exactly coincided with the lowest tide at Naples.

Hurricane Wilma was successfully simulated using SSMS. Peak surge levels (both magnitude and direction) measured by USGS were accurately simulated by the model. Second peak in the data was found to be caused by a surge wave which developed in the south near Cape Sable and propagated alongshore towards the north. Detailed analysis of the simulated and measured water level data at the USGS stations confirmed that the surge wave propagated along the coast from Cape Sable to Captive Island with a constant speed of $c = \sqrt{gh}$.

To accurately simulate the observed USGS data, it was necessary to have an adequate model domain and sufficient model grid resolution. In this study, the model domain includes a high resolution coastal domain for CH3D, which is coupled to a refined ADCIRC grid. The refined ADCIRC grid, modified EC2001e, enabled resolution of the offshore water and Florida Keys where the surge wave, i.e., "dome of water" was first developed and later propagated into the CH3D domain along the coast, causing the simulated second peaks in storm surge at the USGS stations. Without the refined EC2001e grid, it was not possible to simulate the observed second peaks in storm surge. Using a coastal domain alone without the offshore grid would make it impossible to simulate the second peaks in storm surge as well.

The USGS data provided an excellent opportunity to better calibrate and validate storm surge modeling systems such as SSMS. These USGS data, unlike the typical "high water marks", provide temporal information which is missing in "high water marks". For example, "high water marks" during Wilma would have only captured one peak and could falsely lead to a conclusion that flooding was wind-induced in areas that are not normally inundated. The USGS data

allowed better validation of the simulated dynamics of flooding and drying process over a large area. Comparisons of USGS data vs. simulated results show slightly slower drying process thus simulated by the SSMS model. This issue could be addressed in the future by coupling SSMS with hydrologic, runoff and/or groundwater models, and expanding the CH3D domain. Of course, model results could be further improved if more accurate topography data become available in areas where model results did not match the observed data so well.

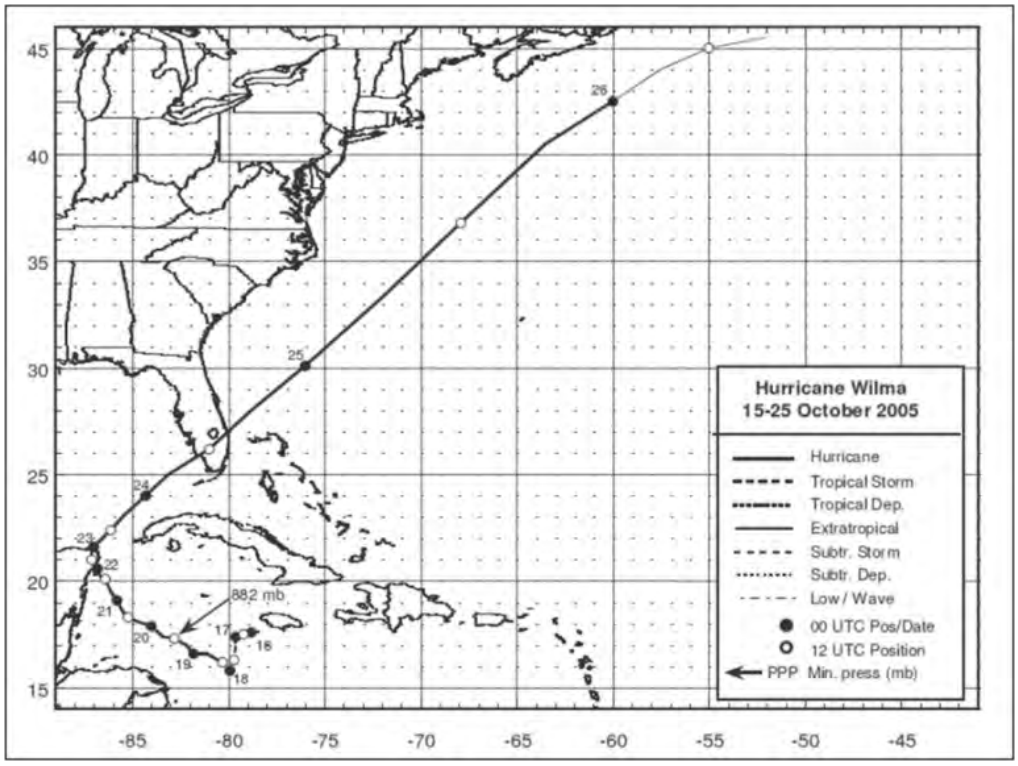

Figure 5-1. Hurricane Wilma path

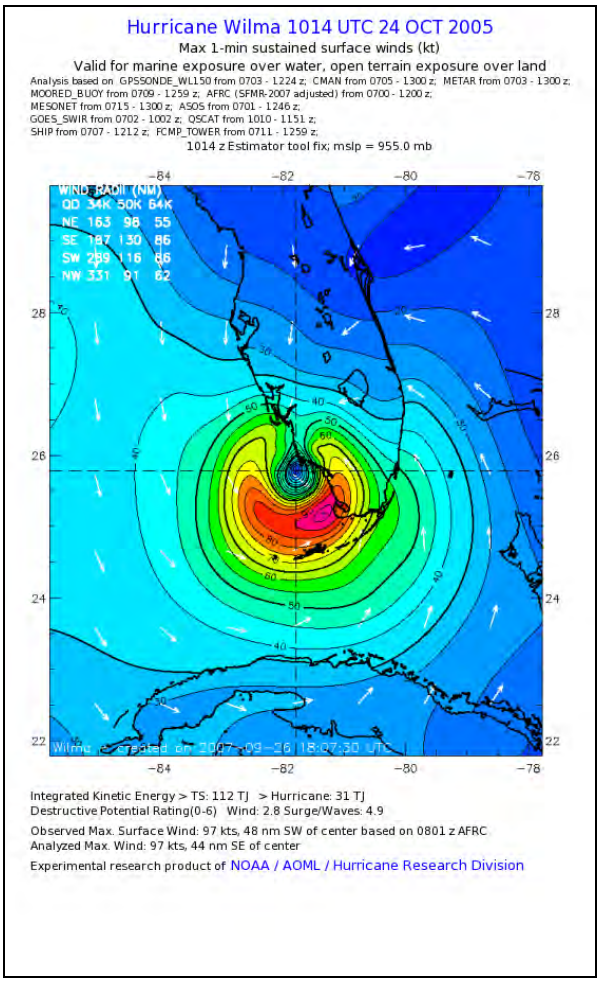

Figure 5-2. Hurricane Wilma H*Wind snapshot. Oct. 24, 2005 10:14UTC

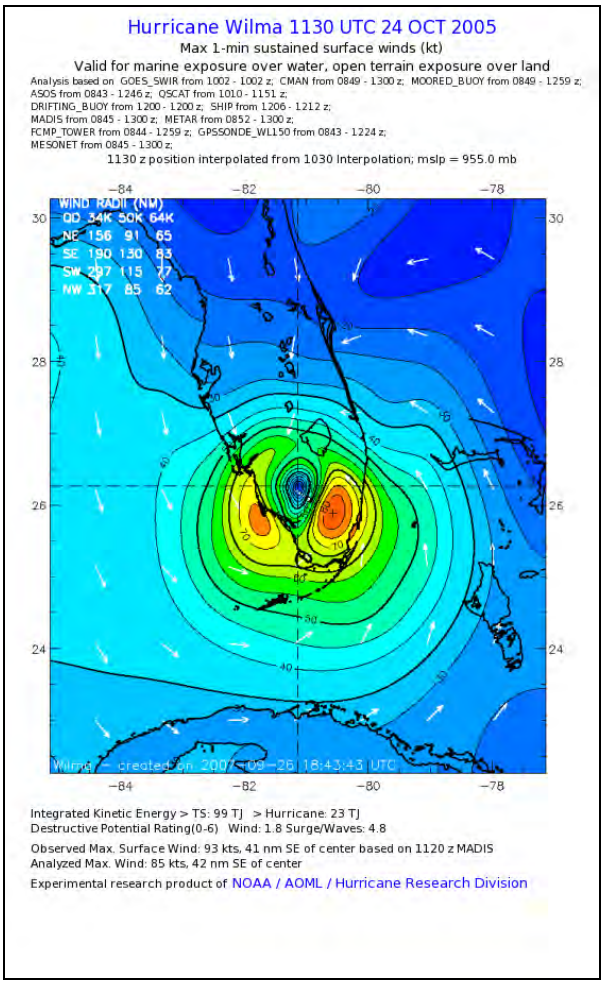

Figure 5-3. Hurricane Wilma H*Wind snapshot. Oct. 24, 2005 11:30UTC

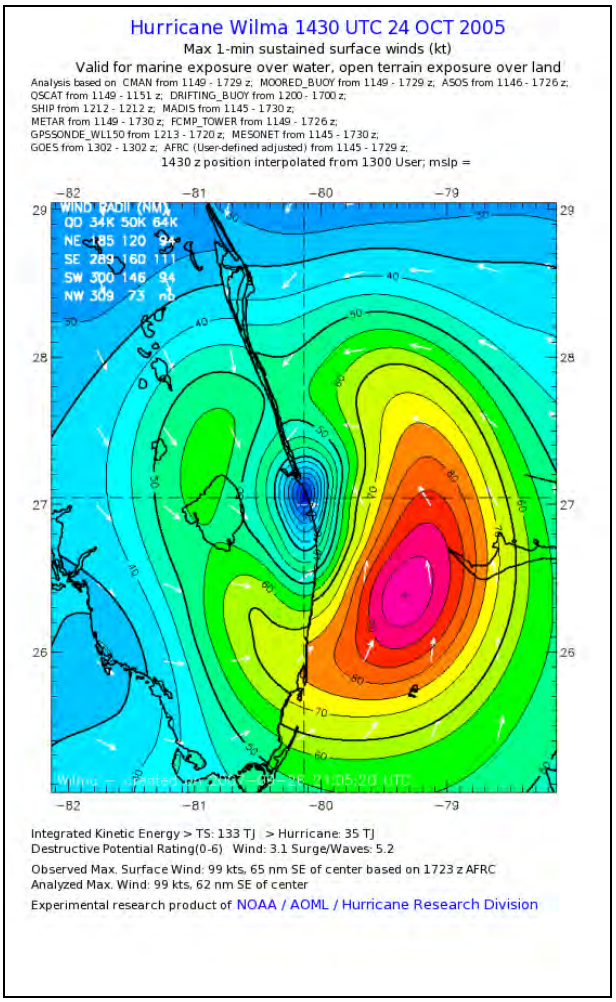

Figure 5-4. Hurricane Wilma H*Wind snapshot. Oct. 24, 2005 14:30UTC

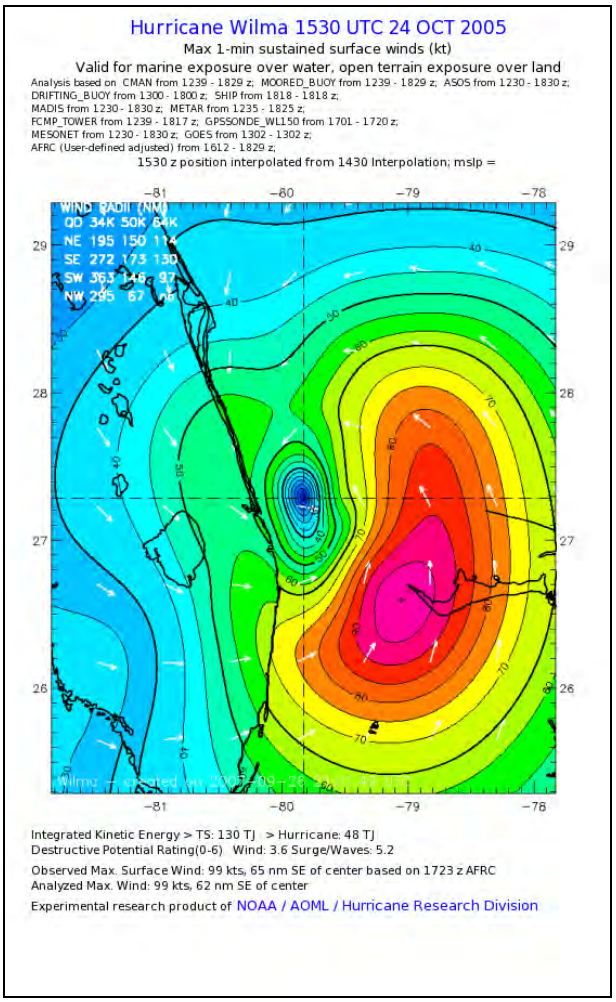

Figure 5-5. Hurricane Wilma H*Wind snapshot. Oct. 24, 2005 15:30UTC

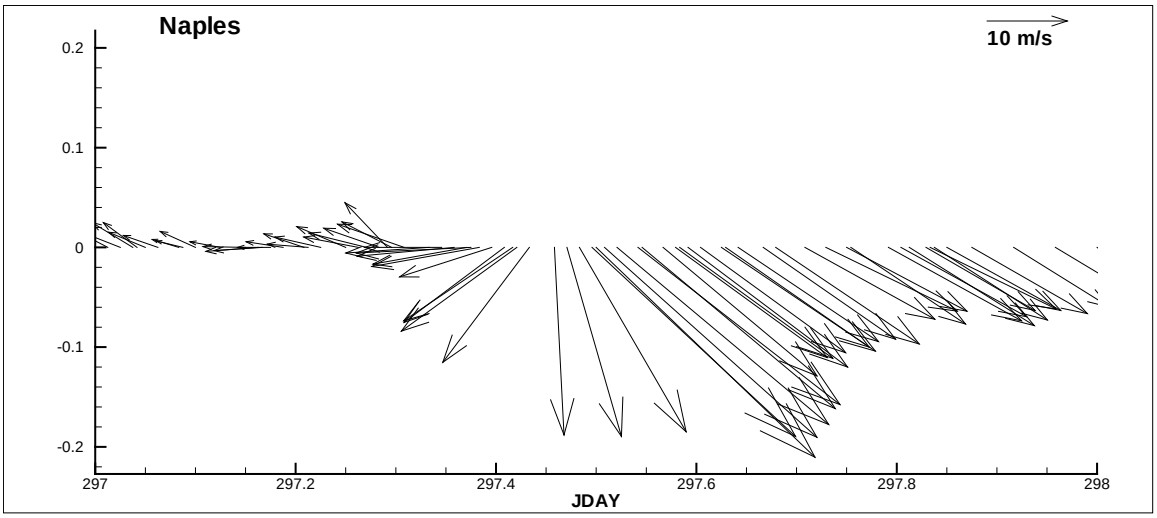

Figure 5-6. Wind measured at the NOAA CO-OPS stations located at Naples, FL during Wilma

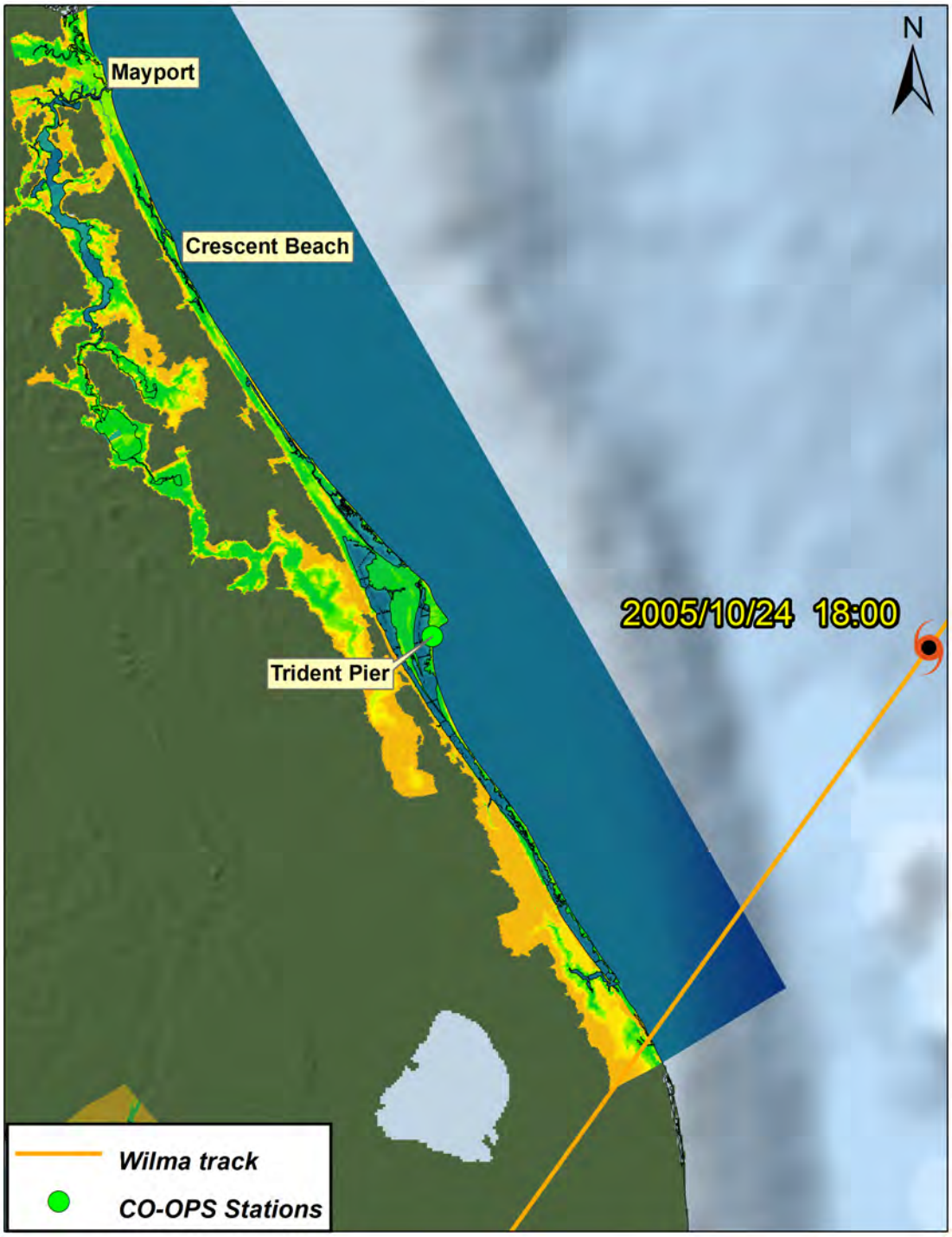

Figure 5-7. Map of the east coast of Florida with CH3D east coast (EC) modeling domain, Hurricane Wilma track, locations of FCMP stations, and NOAA CO-OPS stations.

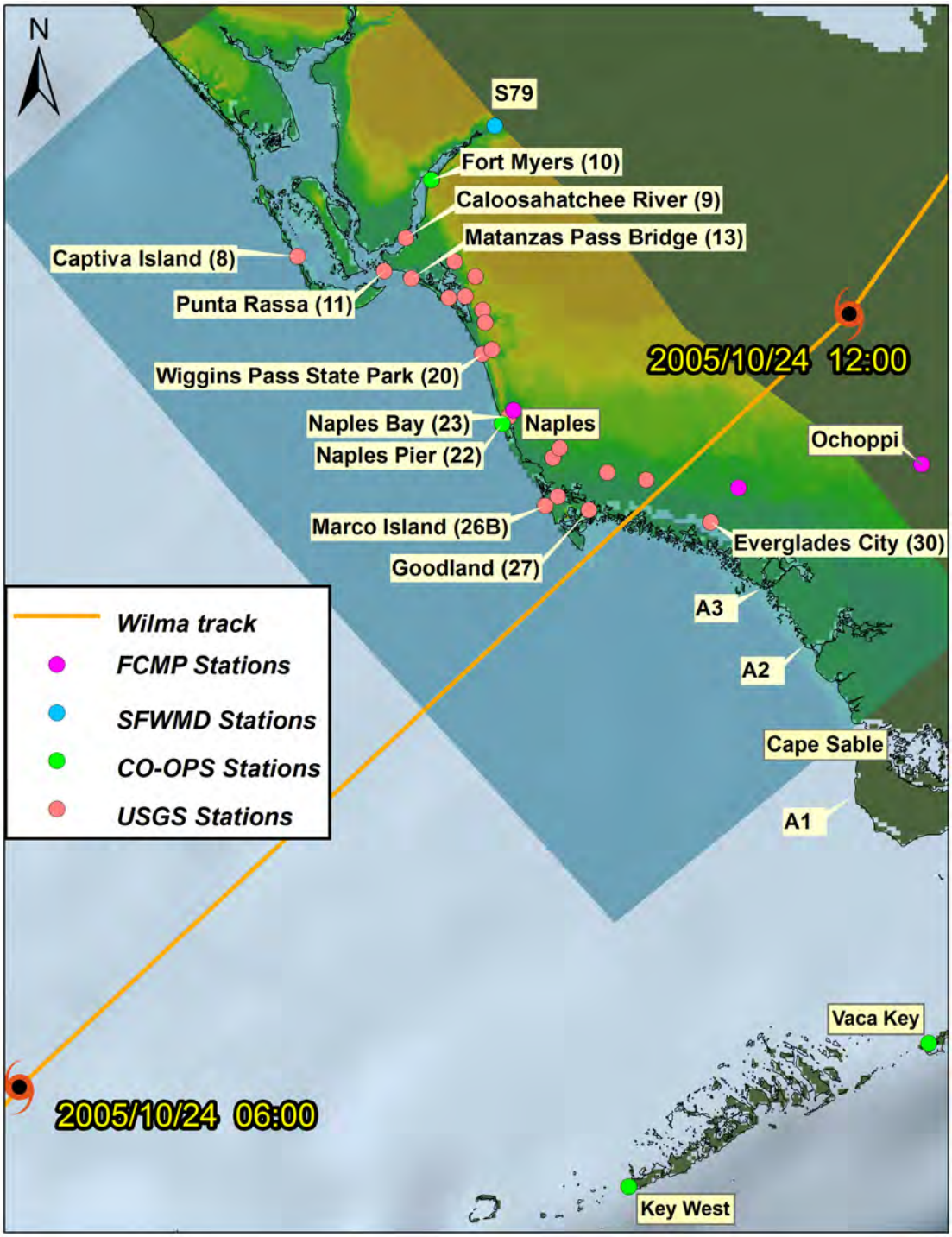

Figure 5-8. Map of southwest Florida with CH3D southwest (SW) modeling domain, Hurricane Wilma track, locations of FCMP stations, NOAA CO-OPS stations, USGS surge stations, SFWMD station and locations of model output (A1-A3).

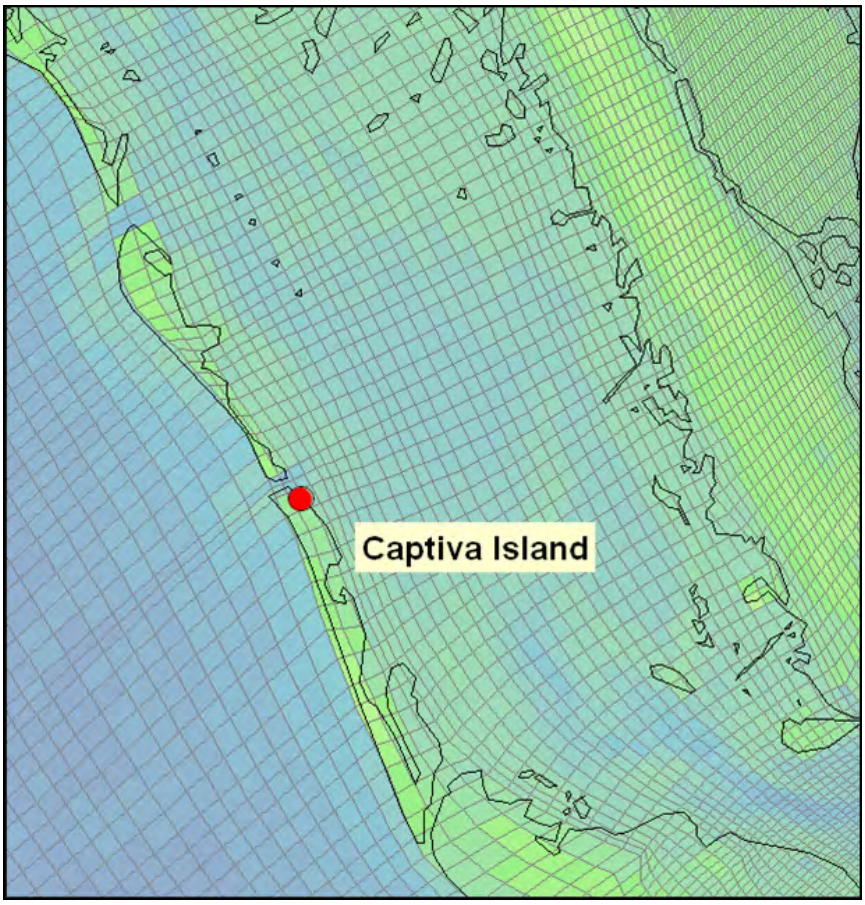

Figure 5-9. CH3D model grid in the vicinity of Captiva Island, Charlotte Harbor, Florida

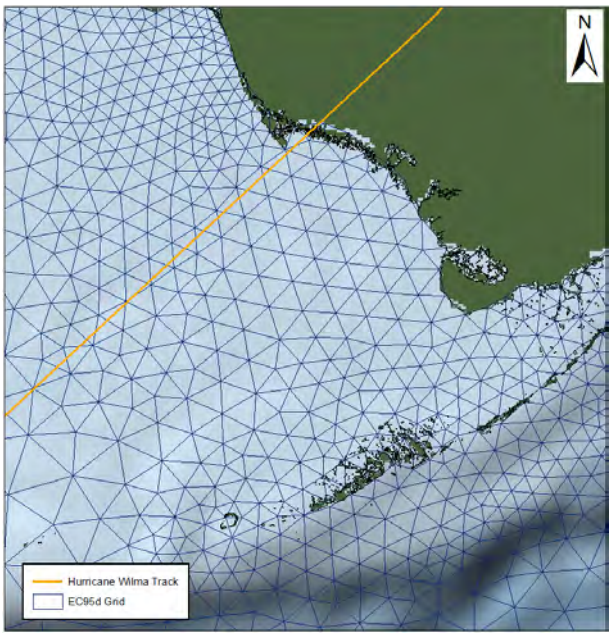

Figure 5-10. ADCIRC model grid EC95d

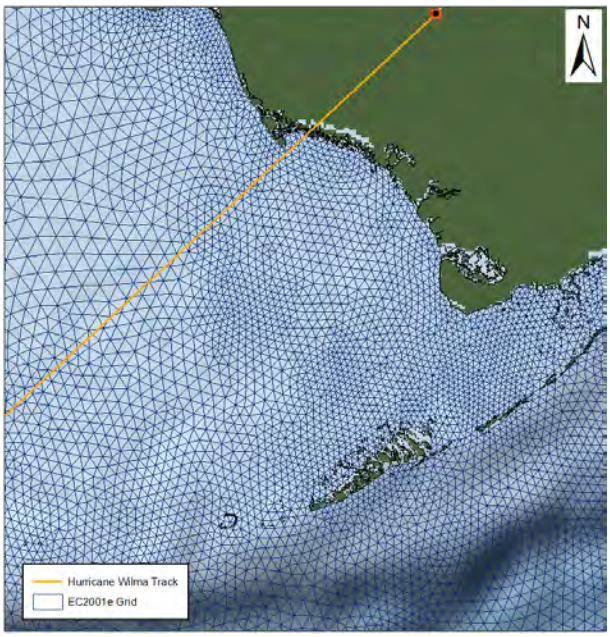

Figure 5-11. Modified ADCIRC model grid EC2001e

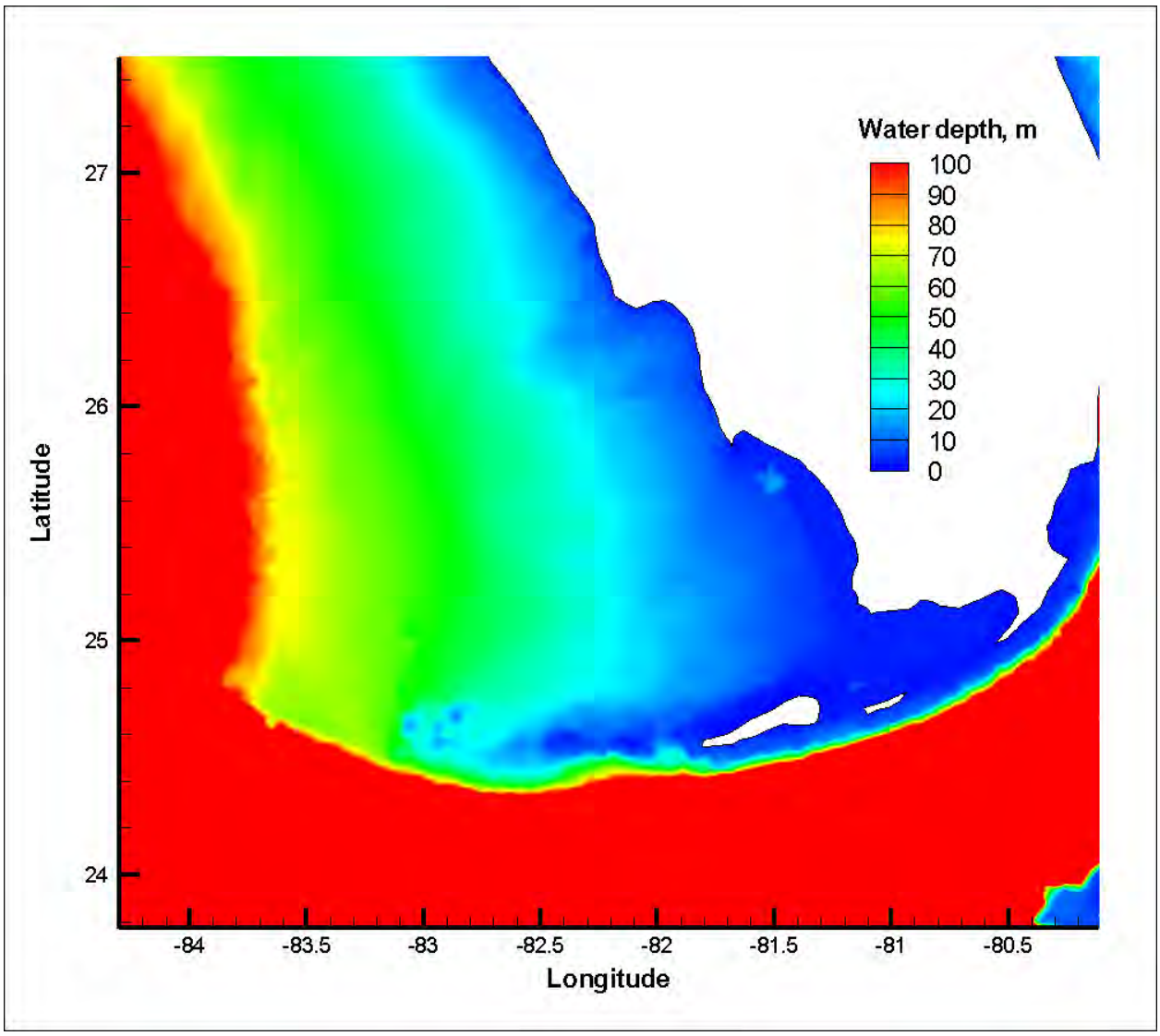

Figure 5-12. ADCIRC modified EC2001e grid bathymetry (meters, MSL)

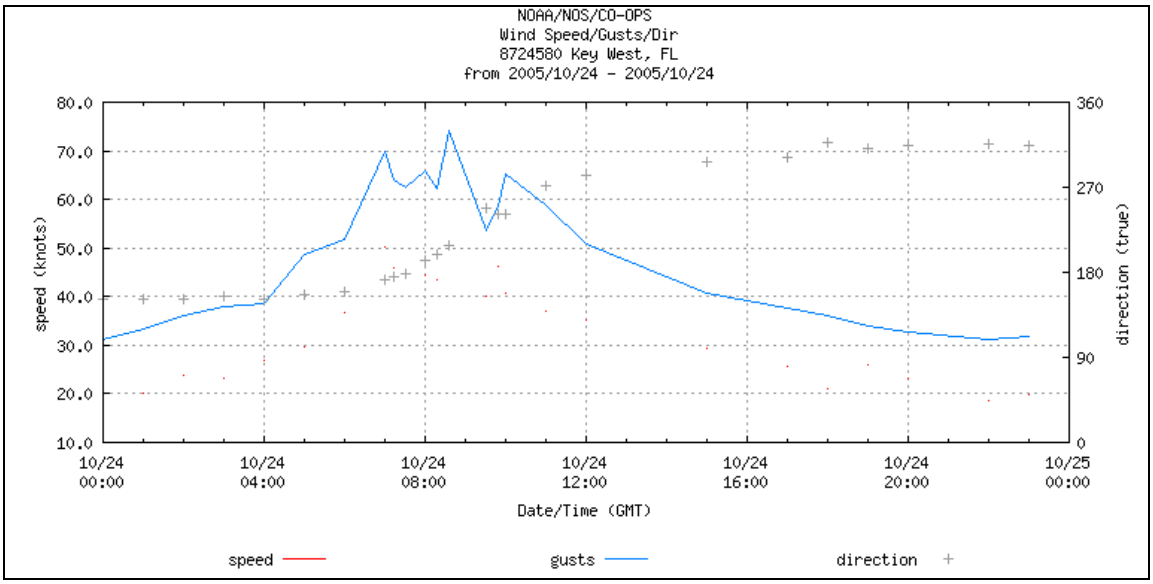

Figure 5-13. Measured wind speed and direction at Key West, FL NOAA-NOS station ID: 8724580 during Hurricane Wilma

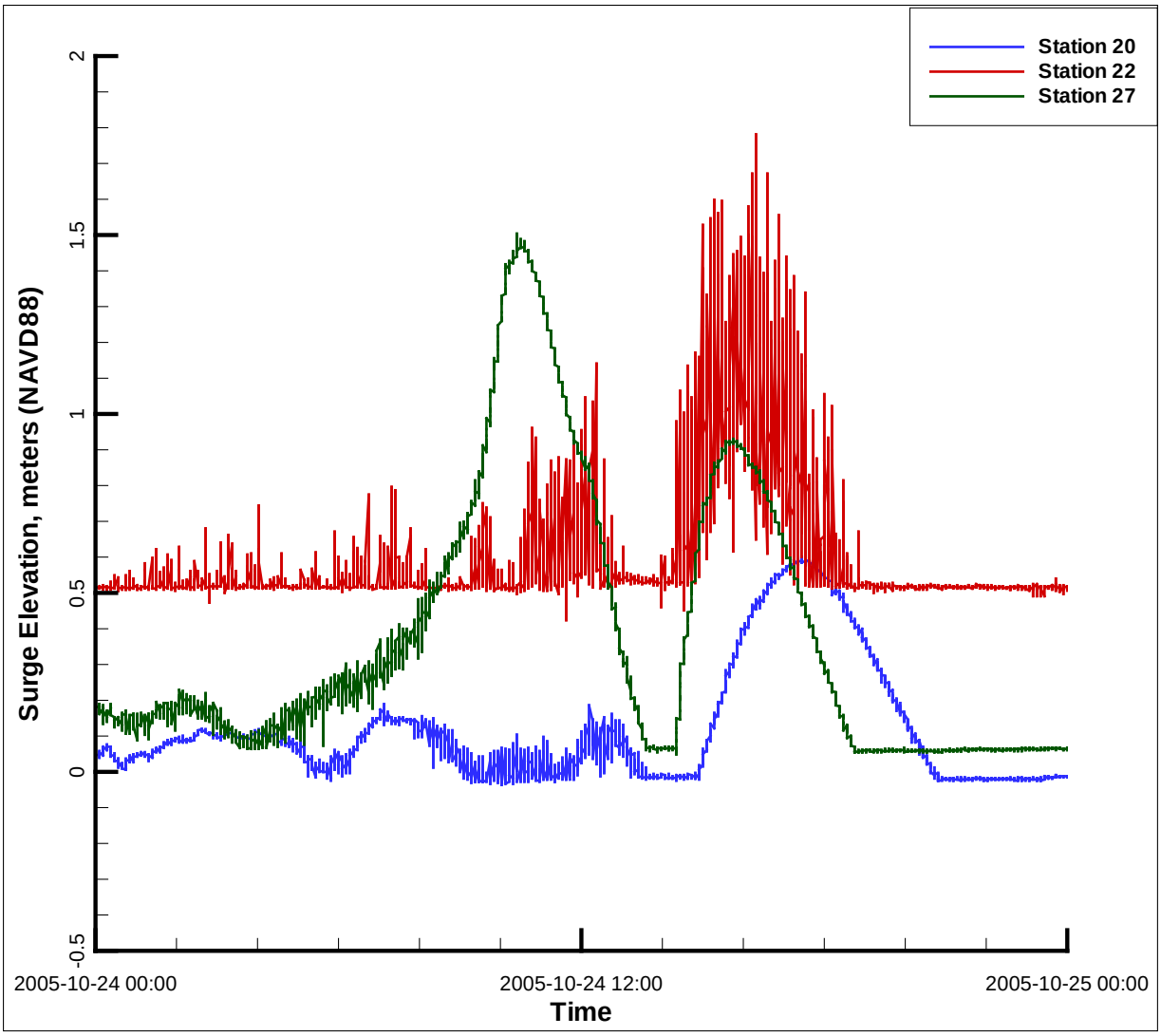

Figure 5-14. Surge levels at selected USGS stations (time in UTC)

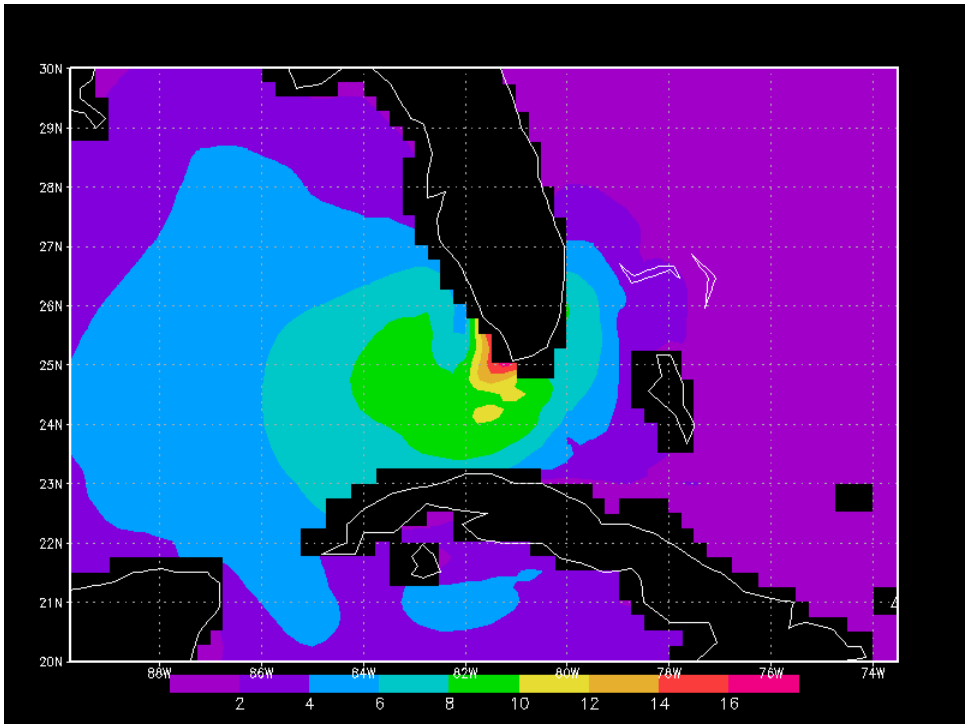

Figure 5-15. WaveWatch III nowcast on October 24, 2005 12:00 UTC, significant wave height in meters

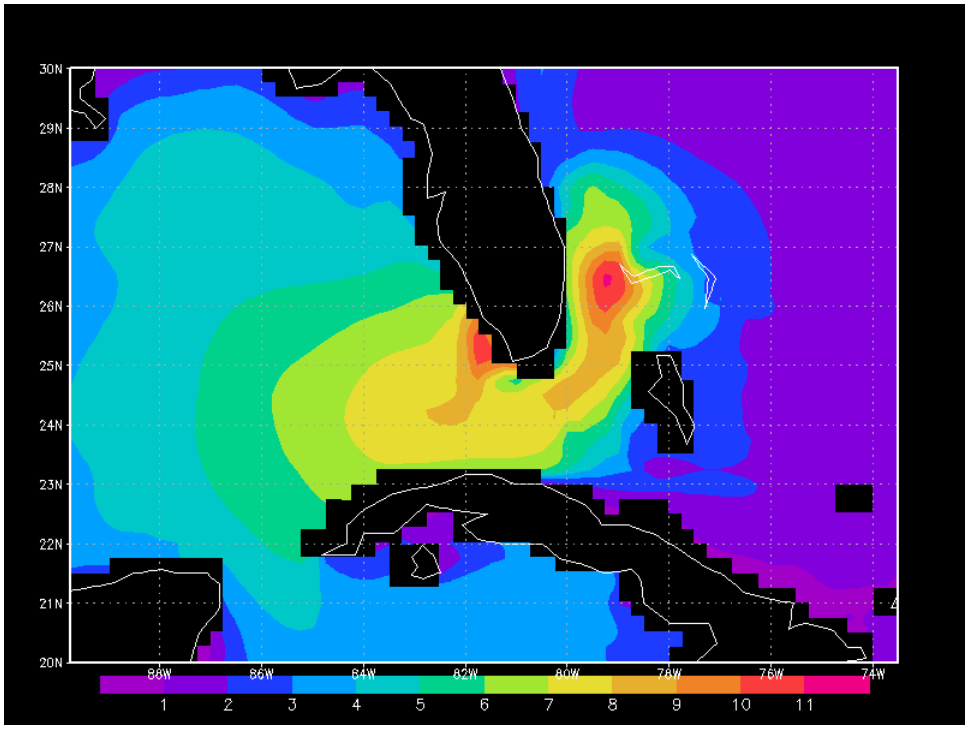

Figure 5-16. WaveWatch III nowcast on October 24, 2005 15:00 UTC, significant wave height in meters

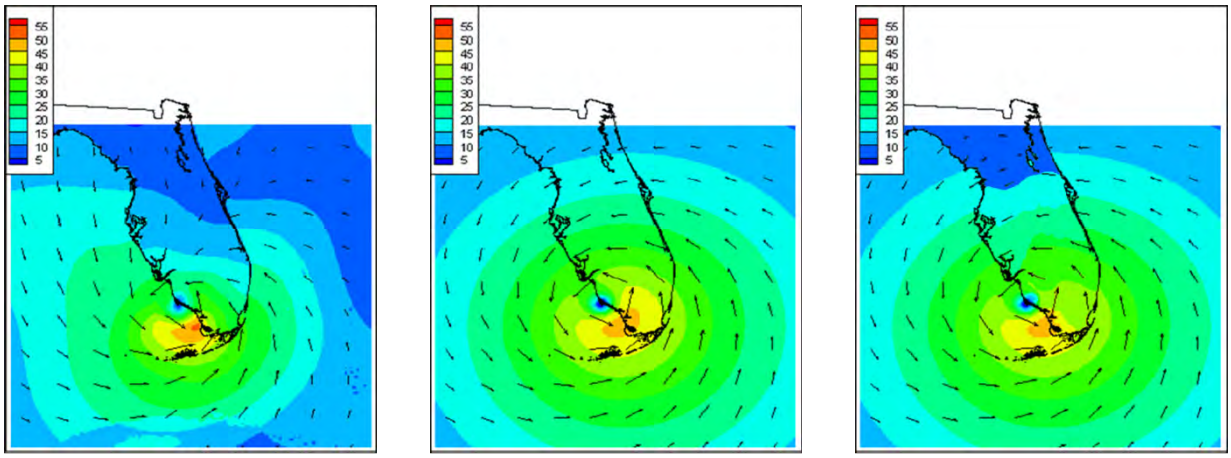

Figure 5-17. Wind fields used for SSMS simulations of Hurricane Wilma a) H*Wind snapshot; b) synthetic wind without land-induced dissipation and c) synthetic wind with land-induced dissipation

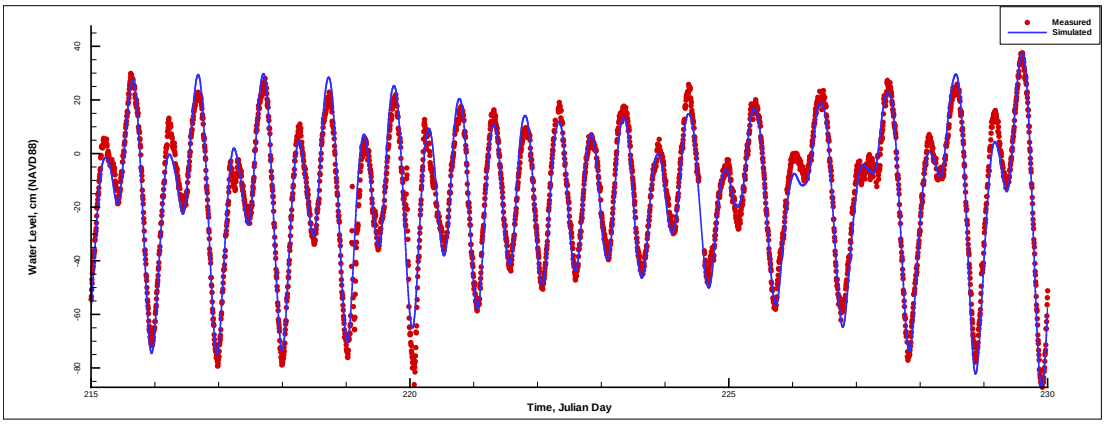

Figure 5-18. Simulated and measured tides at Naples, FL NOAA-NOS station

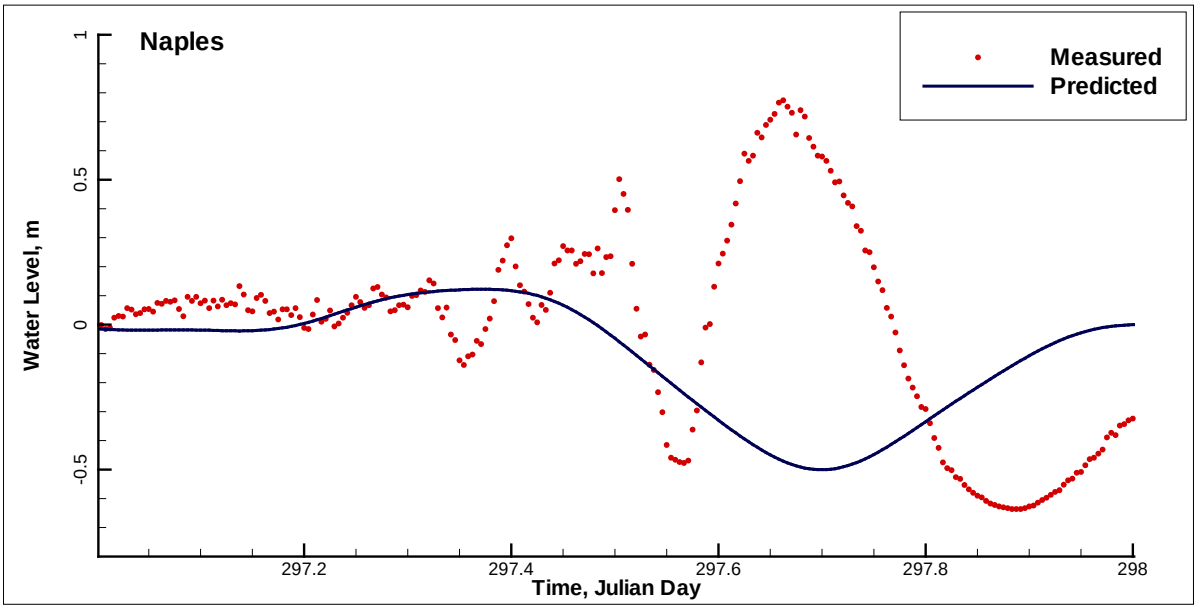

Figure 5-19. NOAA predicted tide and observed water level at Naples, FL NOAA-NOS station during Hurricane Wilma

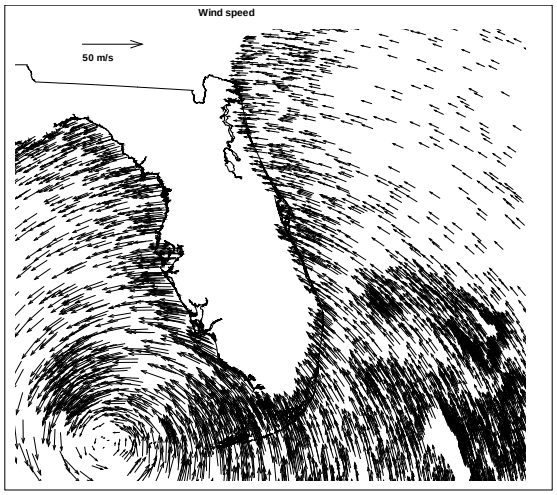

Figure 5-20(a). Wind field at 03:30UTC

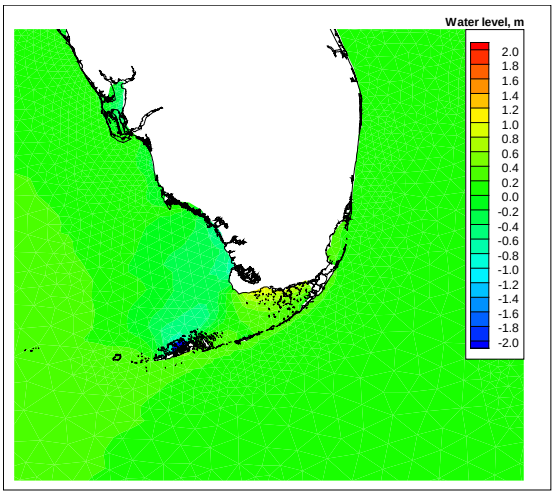

Figure 5-21(a). Water level at 03:30UTC

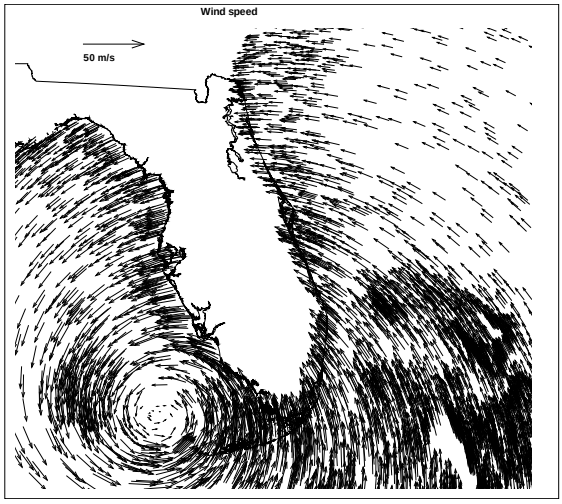

Figure 5-20(b). Wind field at 07:00UTC

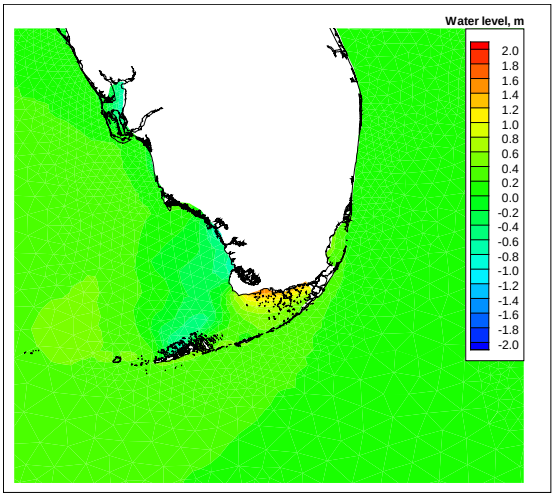

Figure 5-21(b). Water level at 07:00UTC

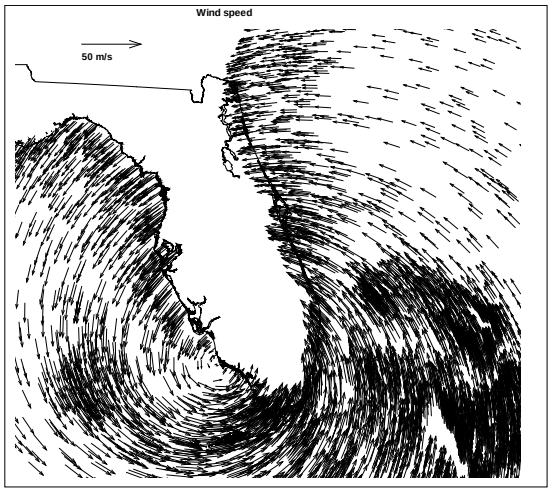

Figure 5-20(c). Wind field at 10:30UTC

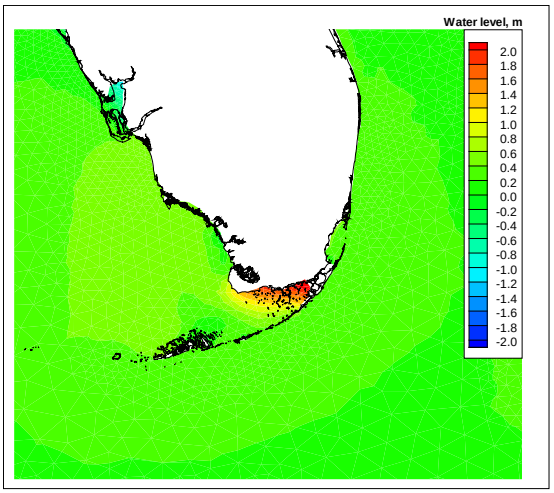

Figure 5-21(c). Water level at 10:30UTC

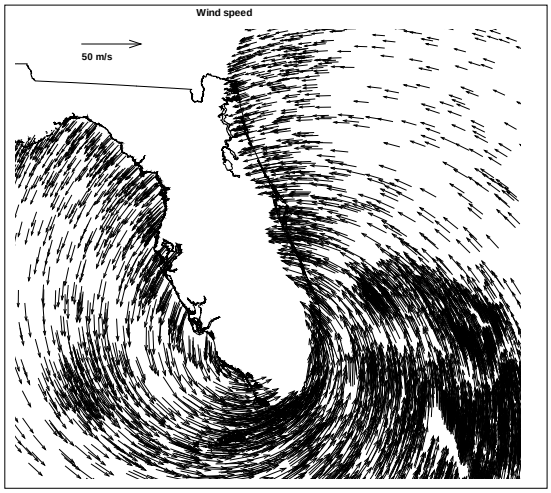

Figure 5-20(d). Wind field at 11:30UTC

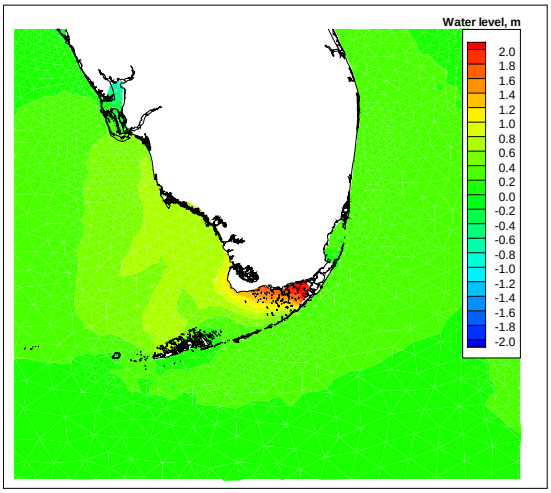

Figure 5-21(d). Water level at 11:30UTC

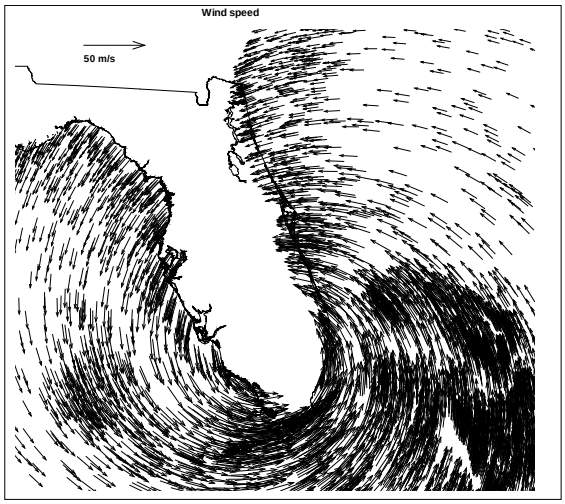

Figure 5-20(e). Wind field at 12:00UTC

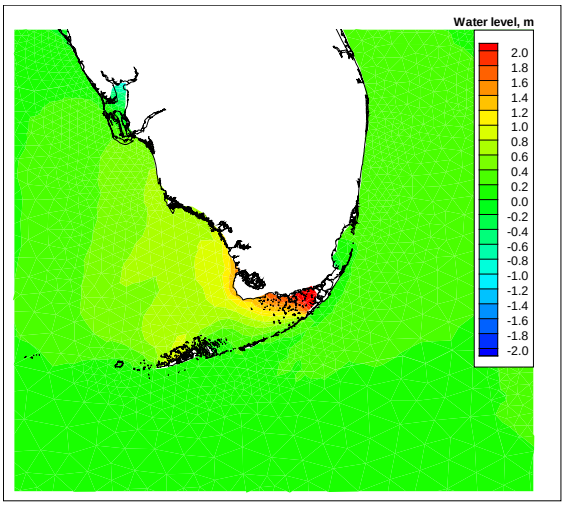

Figure 5-21(e). Water level at 12:00UTC

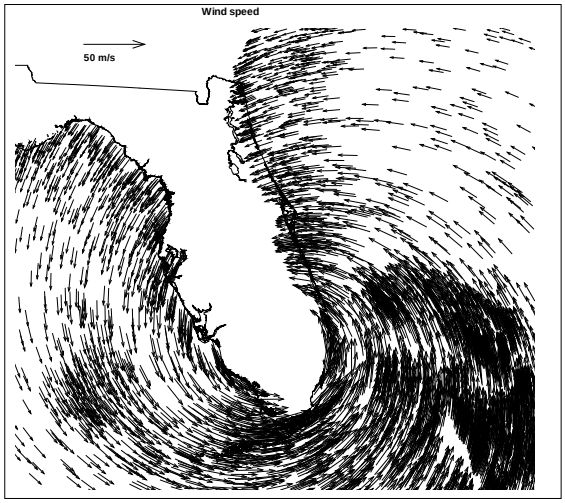

Figure 5-20(f). Wind field at 12:30UTC

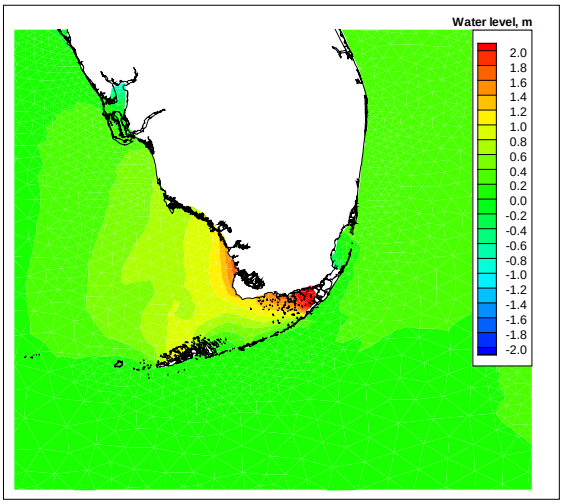

Figure 5-21(f). Water level at 12:30UTC

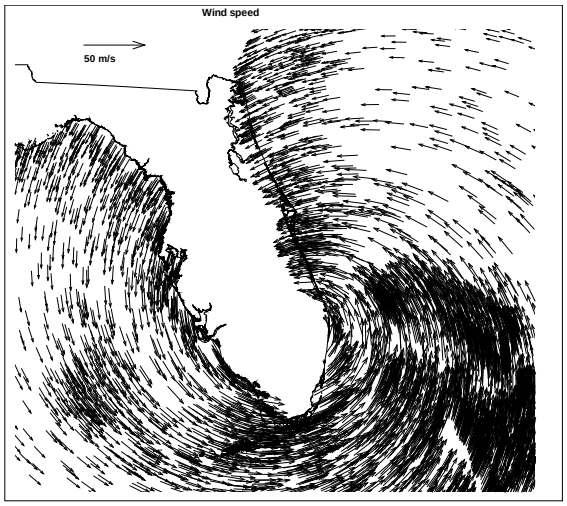

Figure 5-20(g). Wind field at 13:30UTC

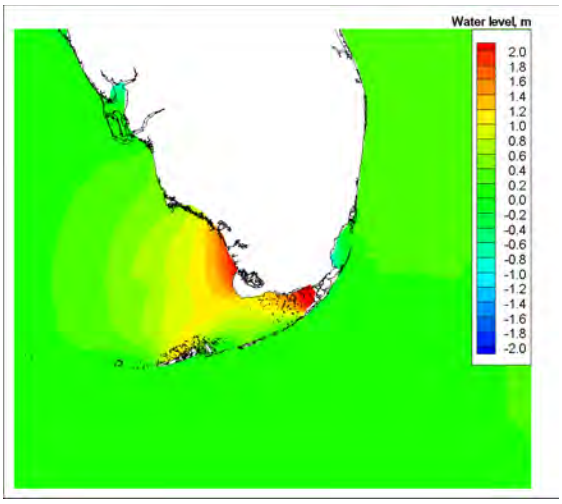

Figure 5-21(g). Water level at 13:30UTC

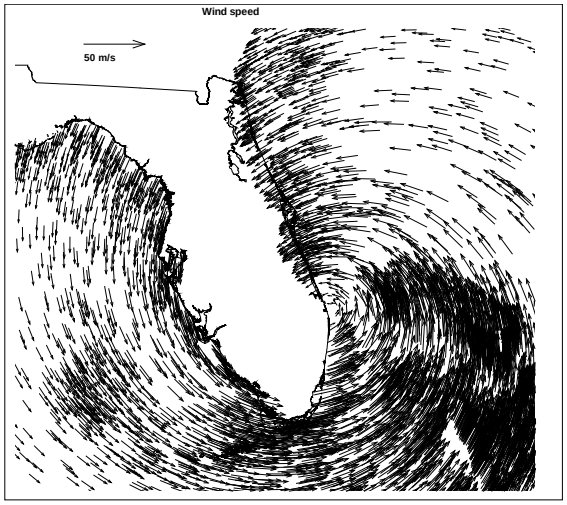

Figure 5-20(h). Wind field at 14:30UTC

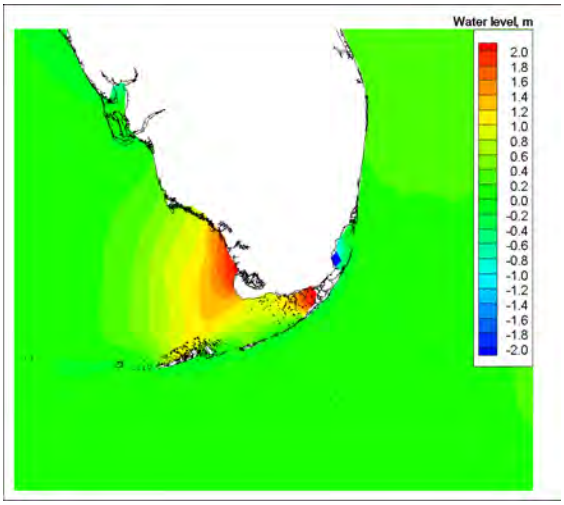

Figure 5-21(h). Water level at 14:30UTC

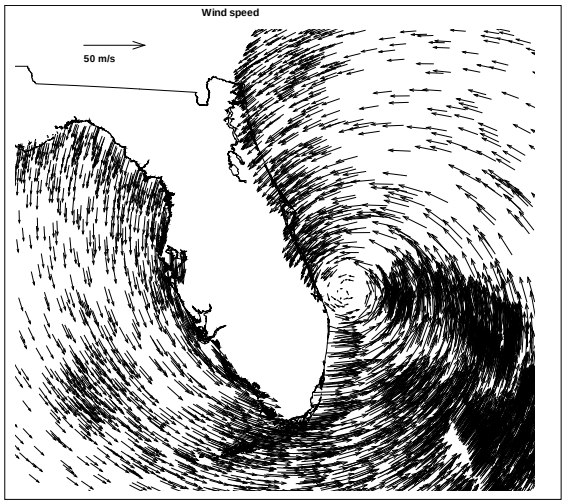

Figure 5-20(i). Wind field at 15:30UTC

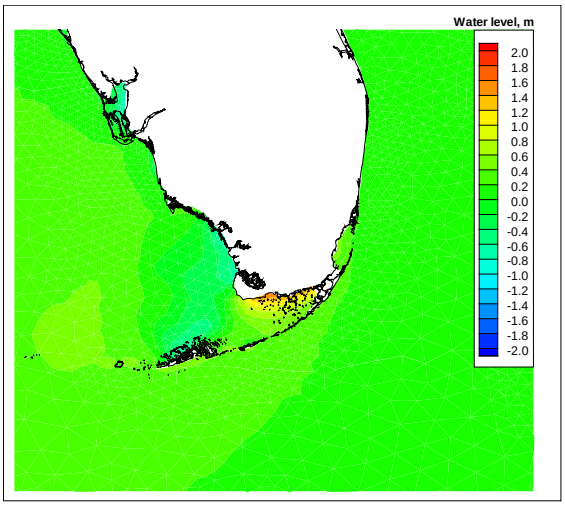

Figure 5-21(i). Water level at 15:30UTC

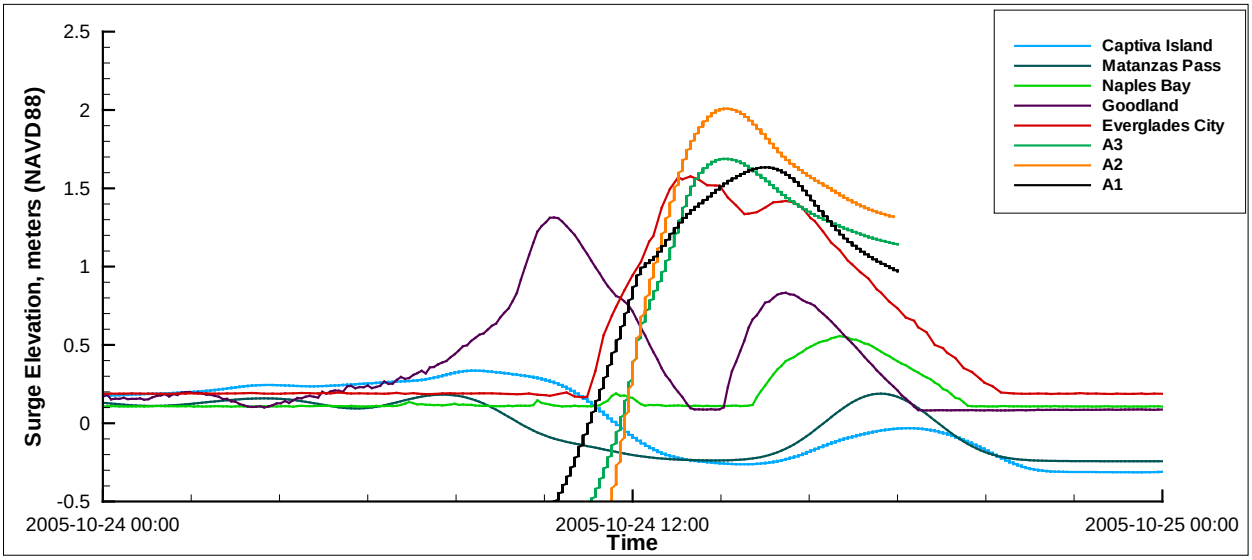

Figure 5-22. Simulated surge at USGS stations and the three output stations (A1-A3)

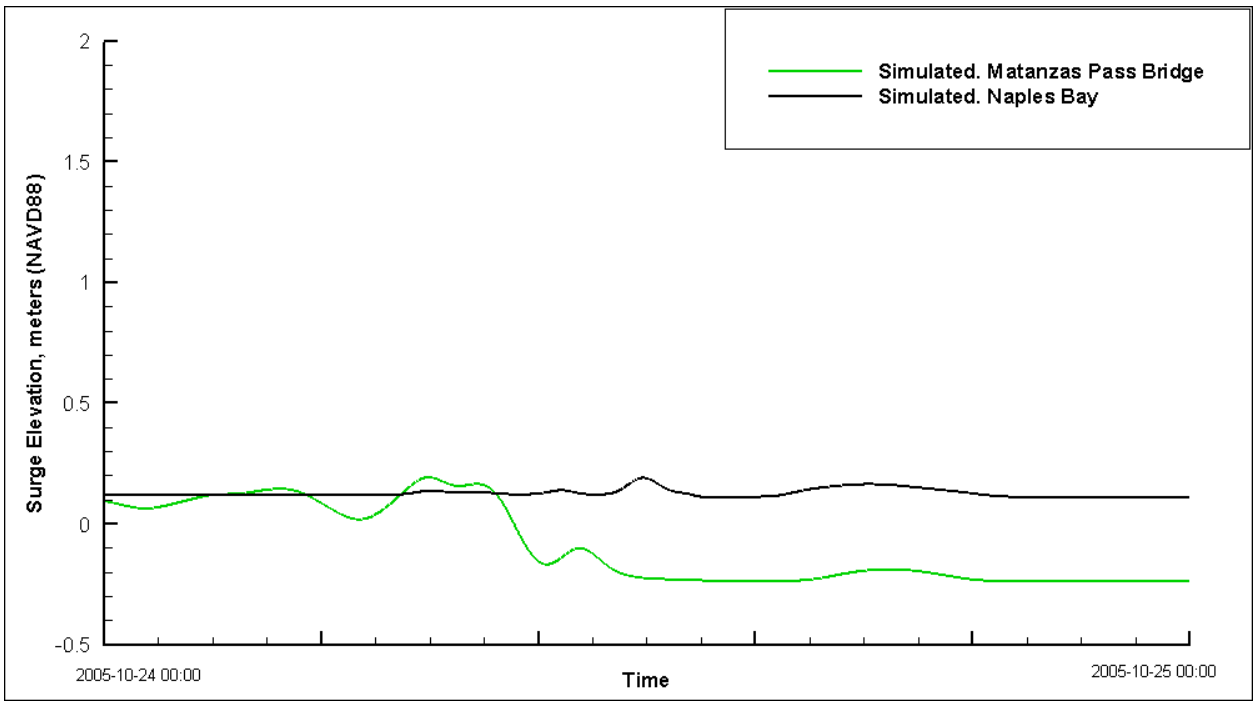

Figure 5-23. Simulated surge at USGS stations Matanzas Pass Bridge (13) and Naples Bay (23) using the coarse EC95d ADCIRC grid

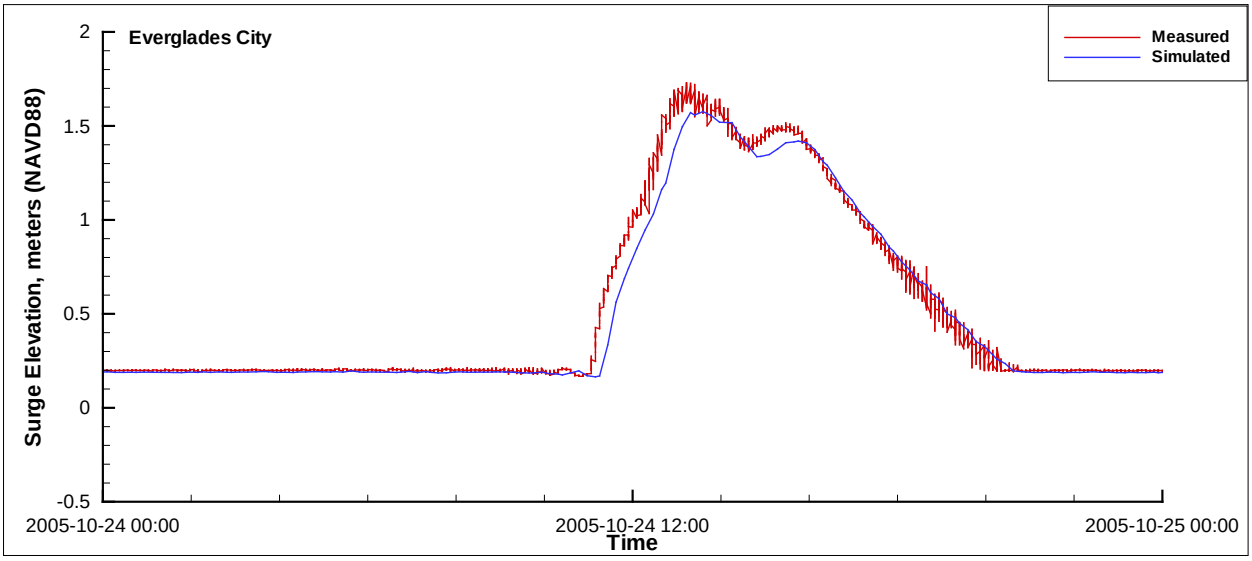

Figure 5-24. Surge comparison at USGS station Everglades City (30)

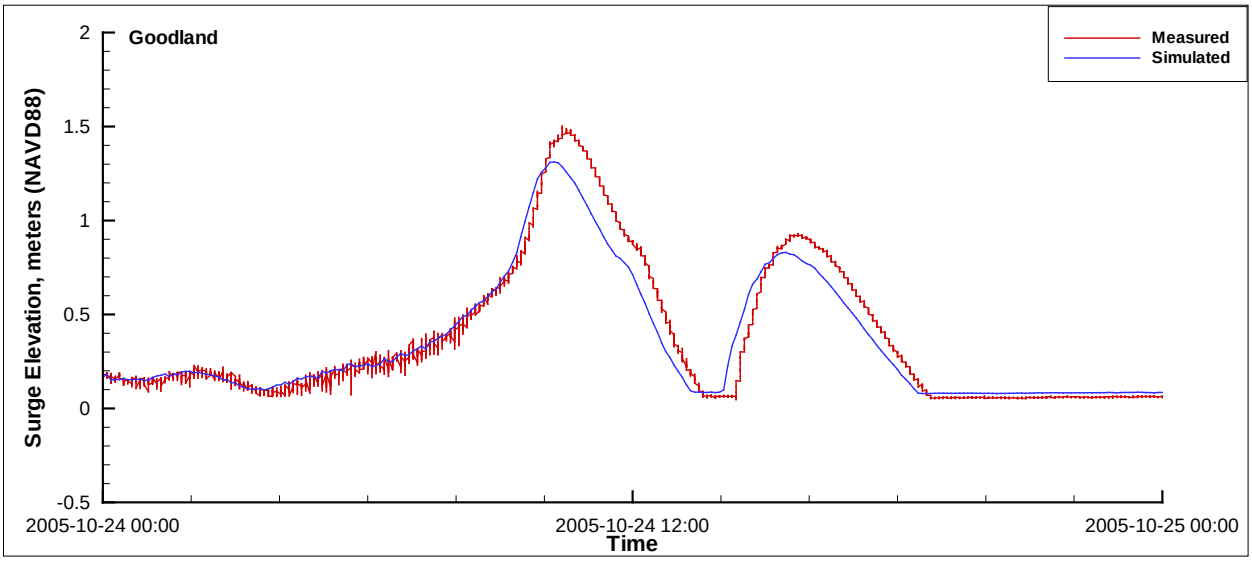

Figure 5-25. Surge comparison at USGS station Goodland (27)

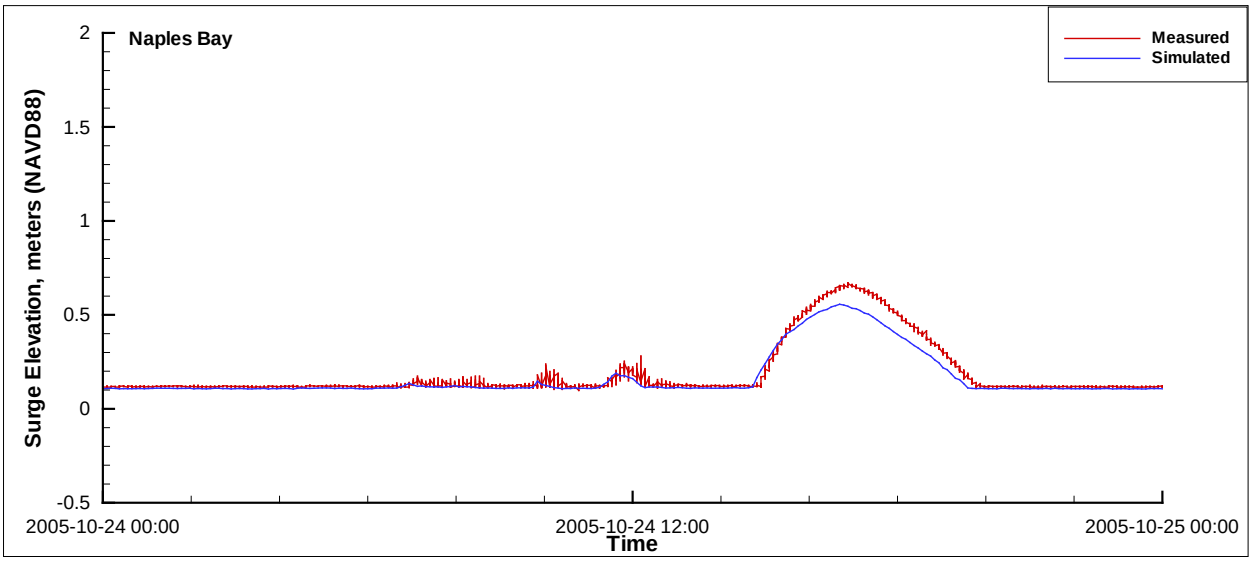

Figure 5-26. Surge comparison at USGS station Naples Bay (23)

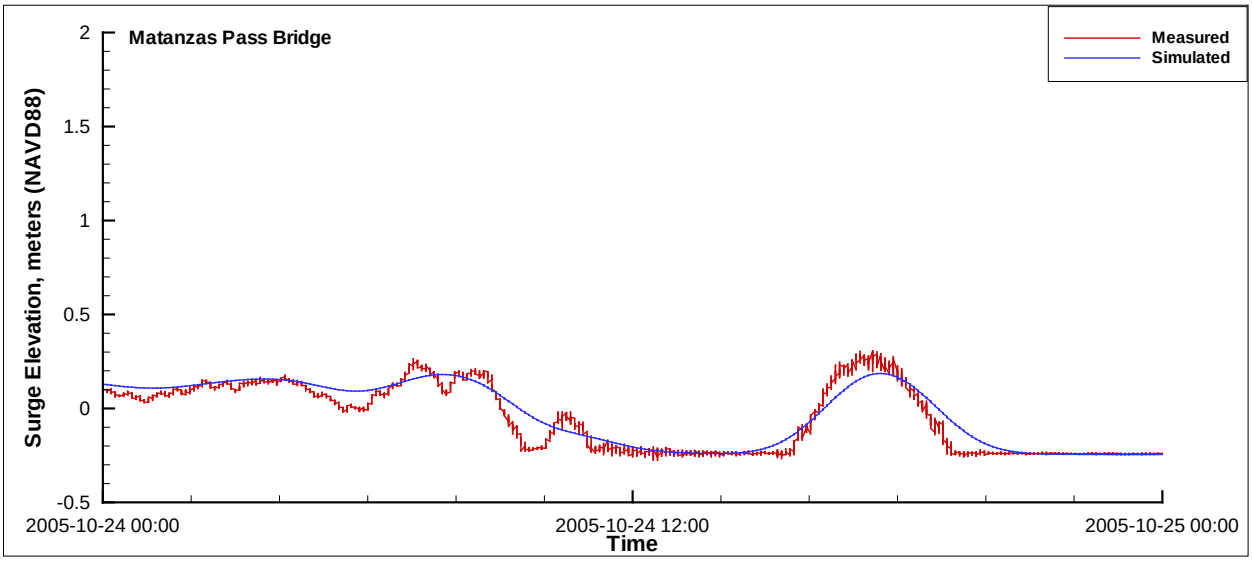

Figure 5-27. Surge comparison at USGS station Matanzas Pass Bridge (13)

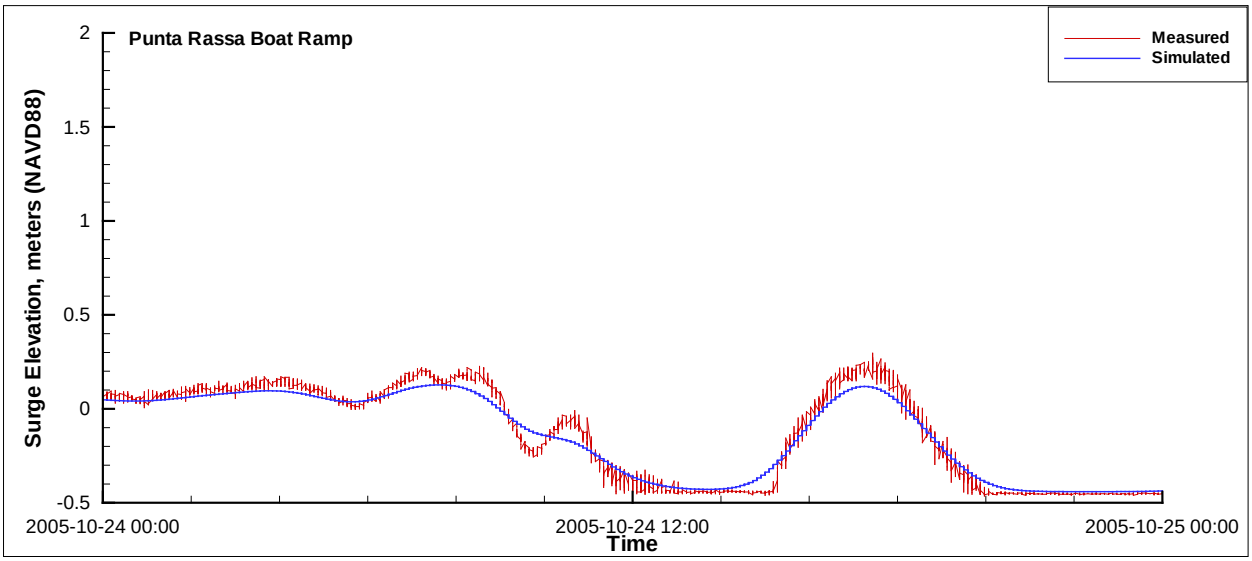

Figure 5-28. Surge comparison at USGS station Punta Rassa (11)

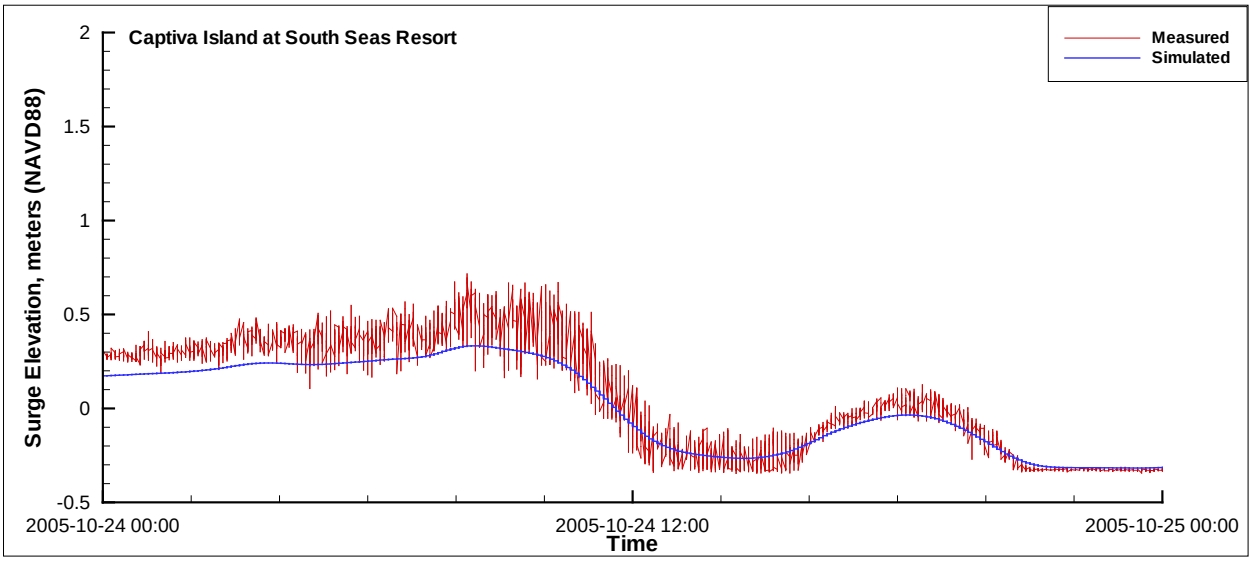

Figure 5-29. Surge comparison at USGS station Captiva Island (08)

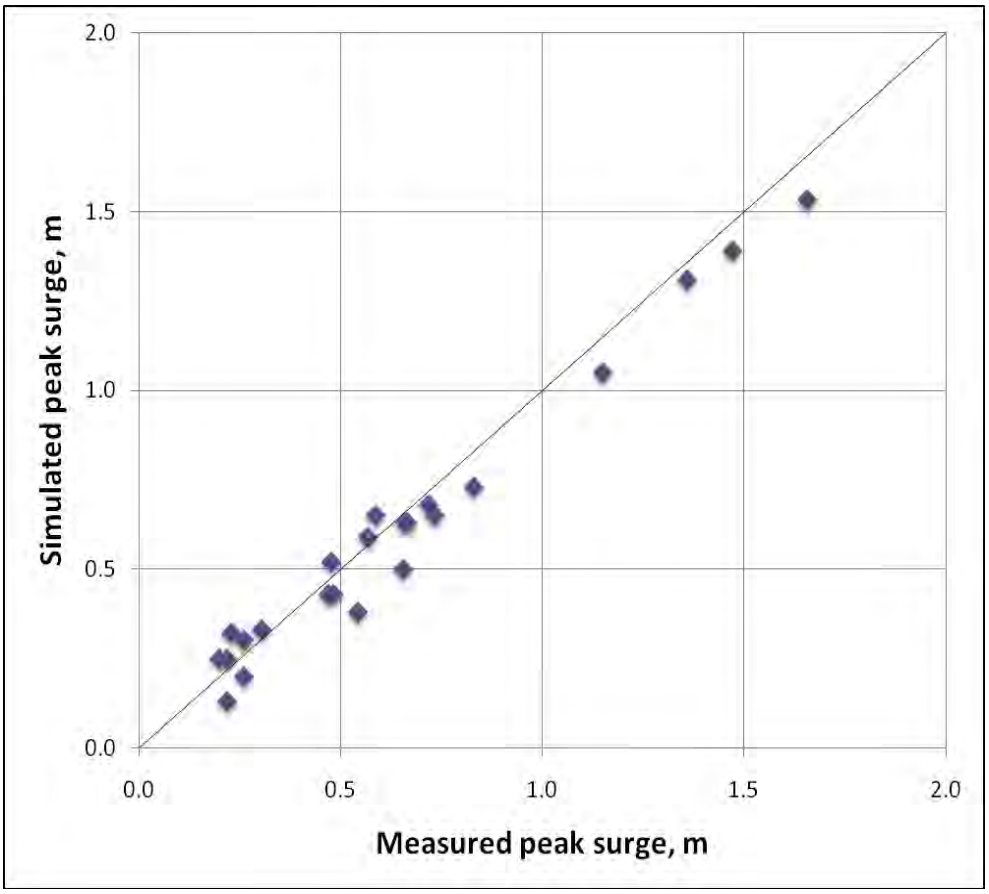

Figure 5-30. USGS stations peak comparisons summary

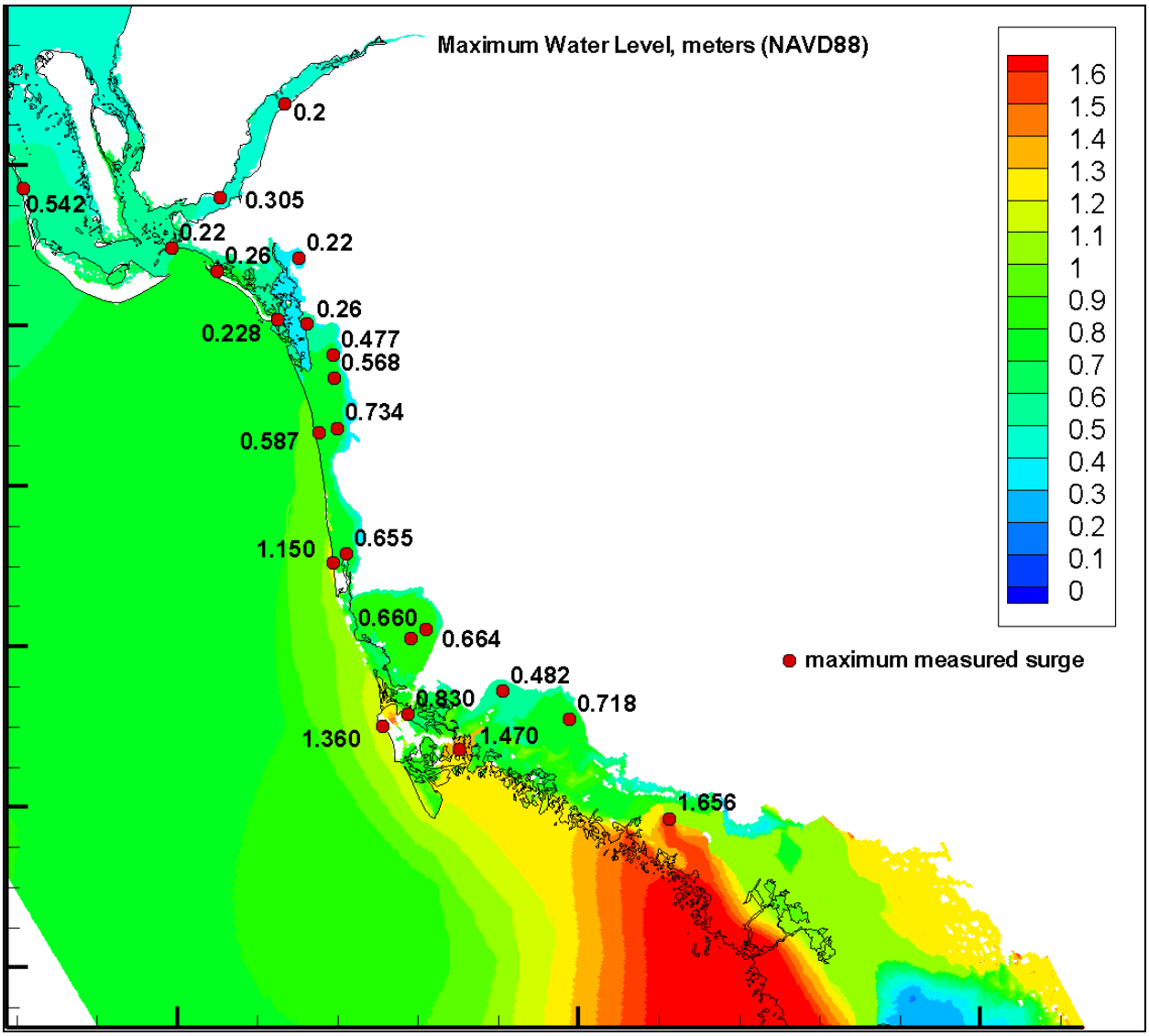

Figure 5-31. MEOW (Maximum Envelope of Water) during Hurricane Wilma simulation and peak observed values at water level measurement stations.

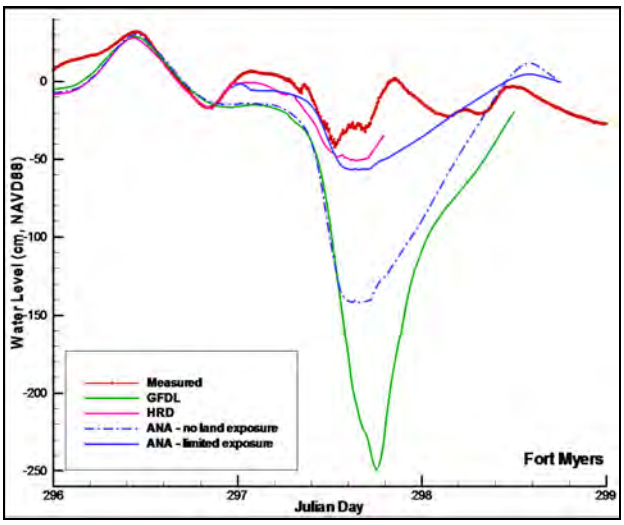

Figure 5-32. Simulated surge using different wind fields at Fort Myers, Charlotte Harbor, FL from October 23, 2005 (Julian Day 296) to October 26, 2005 (Julian Day 299)

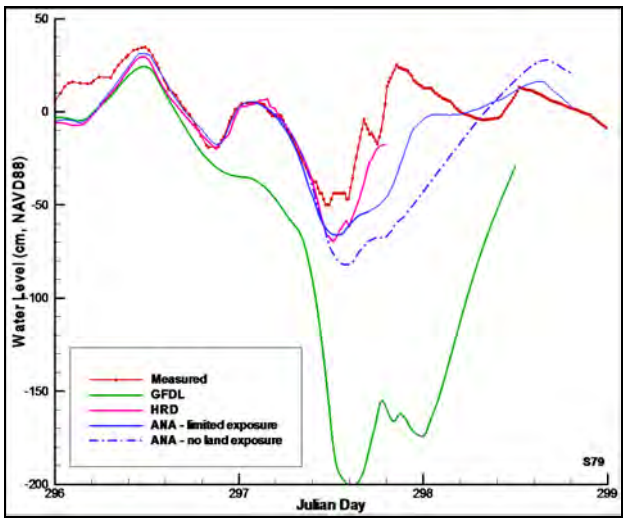

Figure 5-33. Simulated surge using different wind fields at S79 structure, FL from October 23, 2005 (Julian Day 296) to October 26, 2005 (Julian Day 299)

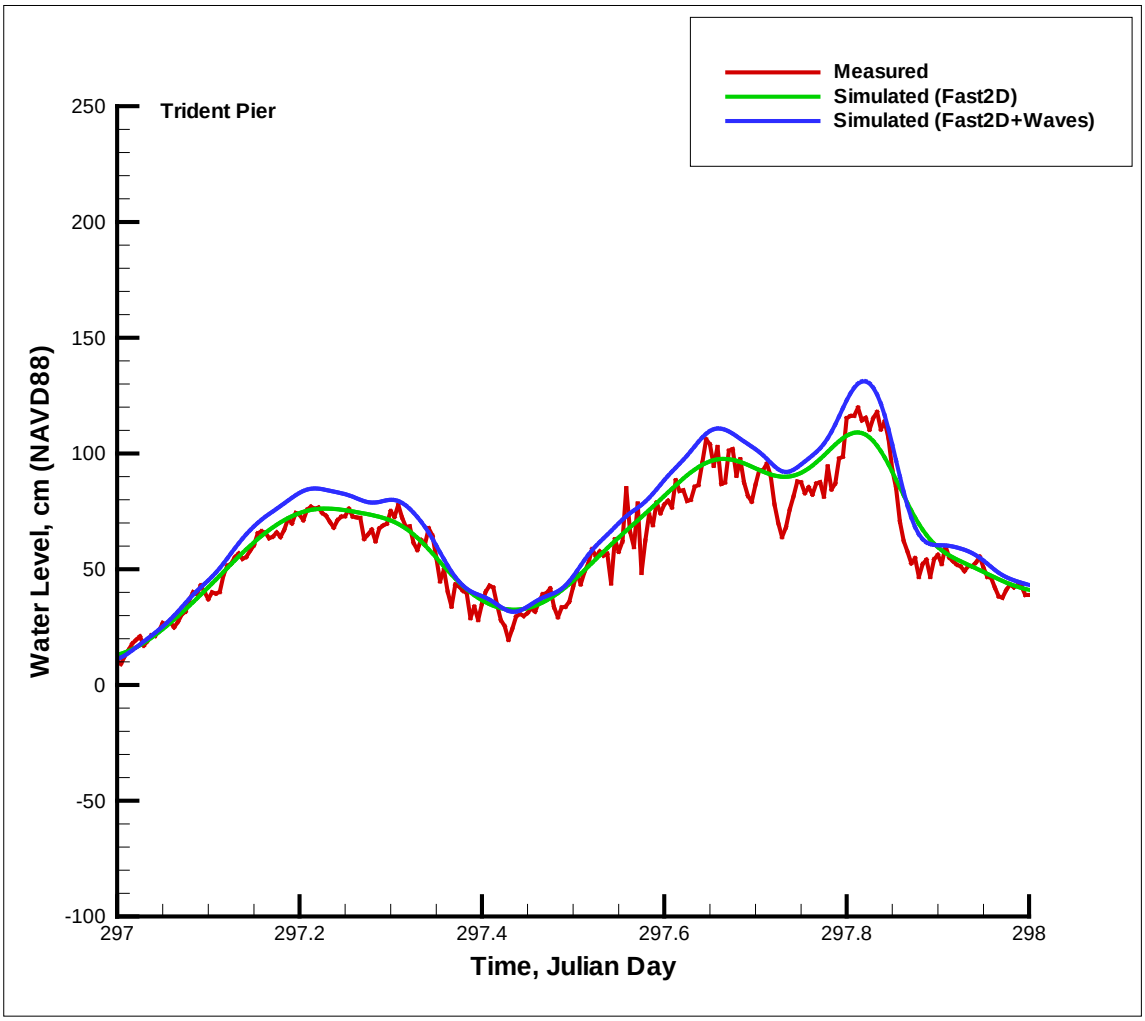

Figure 5-34. Simulated water level at the Trident Pier station (EC domain) for the two scenarios: Fast2D and Fast2D+Waves and the measured data at the station corrected to the NAVD88 datum.

CHAPTER 6
VERIFICATION OF SSMS: TROPICAL STORM FAY

Tropical Storm (TS) Fay (2008) is another storm that has been selected for SSMS verification. Fay crossed Florida and affected almost every part of Florida, including the two domains that were selected for verification of the SSMS. The data available for Fay is fairly limited, but being the only storm that directly affected Florida in 2008, Fay is the first and best choice candidate for SSMS verification.

Despite being forecast multiple times to reach hurricane strength, TS Fay never became one. However, although it did not cause massive damage with strong winds and high surge, Fay brought a good amount of flood due to extended rainfall which had a noticeable effect on circulation and salinity, thus making it very suitable for verification of the 3D and baroclinic prediction of the SSMS. Fay impacted a few salinity stations on the east coast , as it was almost stationary for an extended amount of time (about two days) with pouring rain. The amount of rainfall and flooding that Fay produced underscores the importance of incorporating precipitation and river runoff into a forecasting system. Flooding and inundation can be caused by a combination of storm surge, precipitation and river runoff. Most current surge and inundation forecasting systems, as it was shown in Chapter 1 do not include precipitation and river runoff.

Tropical Storm Fay

Fay (Figure 6-1) was a long-lived tropical storm that made four landfalls (a record!) in Florida and produced a great amount of rainfall that caused extensive flooding in Florida. Fay spawned from a tropical wave at the African coast on August 6, 2008. It was a rather slow moving storm which made eight landfalls, four of which were in Florida, along its path and went through many re-intensifications. It was forecast to reach hurricane strength multiple times but it never became one. Fay reached Cuba early on August 18 and later that day crossed over the

Straits of Florida and made landfall near Key West. Passing the warm waters of the Florida Bay, Fay intensified and made landfall near Everglades City early on the 19th (Figure 6-2) reaching 55 kt winds according to the H*Wind data. Despite interaction with land, the storm intensified slightly to 60 kt winds and kept a well-defined eye moving towards Lake Okeechobee (Figures 6-3 and 6-4). Afterwards it weakened slowly until it reached the waters off the Florida east coast (Figure 6-5). Reaching the east coast the storm skirted coastal region near Cape Canaveral moving at a speed of 3-4 knots with heavy rainfall in excess of 20 in total. In Brevard County, and finally made its third landfall in Florida late on the 21st moving west (Figures 6-6 and 6-7). Fay maintained a westward motion emerging again on the west Florida coast at the north-eastern Gulf of Mexico (Figures 6-8 to 6-11) and making its final landfall in the morning of August 23 near Carrabelle in the Florida Panhandle (Stewart and Beven II, 2009).

Storm surge and wave action from Fay were relatively minimal, with surge heights on the southwest coast around 1-2 ft above the NGVD29 and slightly higher surge on the east coast of Florida reaching 2-4 ft due to a prolonged onshore flow from the Atlantic Ocean (Stewart and Beven II, 2009).

Model Domains and Data Availability

The model domains used to simulate TS Fay are the same two domains that were used for Wilma simulations: the East Coast and the Southwest Coast domains (Figure 6-12). Both domains were directly impacted by the storm but neither had significant surge-induced inundation as most of the flooding was caused by the rainfall. There is some data available for Fay which includes H*Wind products from the Hurricane Research Division, water level from NOAA-NOS and salinity measurements on the east coast provided by the Guana-Tolomato-Matanzas National Estuarine Research Reserve (GTM-NERR).

Wind Data

HRD wind of TS Fay is available for the duration when the storm was moving throughout Florida and in its vicinity. In addition the best track was obtained from ATCF and used to drive the synthetic wind model. The best track data shows the peak wind for Fay to be around 60 kt consistent with the H*Wind of Fay which shows sustained 1-min average winds at 10 meter elevation in (Figures 6-2 to 6-11). Time-series of wind are available at Trident Pier NOAA-NOS station (ID 8721604, Figure 6-12) on the east coast showing gusts up to 50 kt, in good agreement with the H*Wind data. Similar to model verification of hurricane Wilma, H*Wind data is used only to verify the quality of synthetic wind field used to drive the SSMS simulations of TS Fay. Since H*Wind data is only available for hindcasting, the SSMS in forecasting mode has to rely on the synthetic wind model to provide the wind forcing.

Water Level Data

Unfortunately many NOAA-NOS stations for measurements of water level on the east coast of Florida went offline before 2008. Available water level during Fay is limited to the Trident Pier and Ponce De Leon (Figure 6-13) stations on the east coast and one station at the I-295 Bridge in the St. Johns River. Two NOAA-NOS stations (Mayport and Vilano Beach) have NOAA predicted tidal data which gives a good representation of tides in the area. These data are used to verify the tidal boundary conditions for the East Coast domain.

On the southwest coast of Florida, water level data available at Fort Myers and Naples stations are used to verify model results.

All of the NOAA-NOS data is available at 6-minute intervals. It should also be noted that all measured water level data were either obtained in reference to the NAVD88 datum or converted to the NAVD88 using the method described in Chapter 3 in Vertical Datums section.

Salinity Data

Salinity data at 15-min intervals, was collected and QA/QC'd by the GTM-NERR, is available at four locations: Fort Matanzas, Pine Island, Pellicer Creek and San Sebastian during Fay (Figure 6-14).

Precipitation and Run-off

Precipitation and run-off have been shown to be quite important in simulating Fay and especially the impact of Fay on the east coast where in Breward County Fay brought over 20 in of rain hence significantly affected salinity in estuaries. The SSMS uses river forecasts and observations provided by the National Weather Service's Advanced Hydrologic Prediction Service (AHPS, 2009). Whenever possible forecast data is used and observed values are used otherwise. If the period of forecast for a river condition is shorter than the SSMS forecast time then the last forecast or observation value available is extended to provide boundary condition for the rest of the forecast simulation.

Waves

Wave effects are included in Fay simulations although the wave action was rather small due to moderate winds. The SWAN model is run in a non-stationary mode with a 10-second time step and is forced with the same wind produced by the WMS and used for the ADCIRC and CH3D models. The open boundary conditions for SWAN are obtained from WaveWatch III model output. SWAN boundary conditions assume a Gaussian distribution and provide significant wave height, period and direction of waves based on the WaveWatch III model forecast.

Model Setup, Forcing and Boundary Conditions

For TS Fay simulations the SSMS is setup as described in Chapter 4 for both the EC and SW model domains. Two scenarios, described in Chapter 3, are chosen for SSMS simulation of

TS Fay: Fast2D and Full3D-HYCOM. Two additional scenarios: Fast2D+Waves and Full3D-HYCOM+Waves are run to show that the effect of waves during Fay was not significant. The chosen scenarios allow verification of simulated water level and salinity versus the measured data, as well as a comparison of computational times required to run the scenarios. They also help to estimate the computational time required to obtain a salinity forecast. A typical forecast cycle of 5 days is used as the duration of simulation in both domains and each scenario. Since salinity simulations require significant spin-up time, a two-month spin-up simulation prior to the storm simulation is performed. After the spin-up the storm simulation period from August 18, 00:00 UTC to August 23, 18:00 UTC is slightly longer than a typical 3-day or 5-day forecast cycle, but this allows tracking of changes in salinity for a longer time after the storm. Forcing functions for the storm simulations include: wind forcing, tides at the open boundary, surge from a large scale model at the open boundary (which is then combined with tides) and salinity at the open boundary for Full3D simulations.

Wind Forcing

Wind is the primary forcing for storm surge simulations, the WMS described in Chapter 4 was used to produce consistent wind fields for Hurricane Wilma simulations. WMS is set up using the best track data for TS Fay obtained from ATCF (Table 6-1). The track information is extracted from the best track file and only variables pertinent to the WMS are retained: date and time, position of the hurricane maximum sustained wind speed in knots (Vmax), minimum sea level pressure in millibars (MLSP), wind intensity for the radii defined in this record (RAD) in knots, radius of specified wind intensity for the northeast quadrant (RAD1), southeast quadrant (RAD2), southwest quadrant (RAD3) and the northwest quadrant (RAD4) in nautical miles, and the radius to maximum winds in nautical miles.

Table 6-1. Best track of Tropical Storm Fay extracted from the ATCF data

Date/Time YYYYMMDDHH	Lat	Lon	Vmax (kt)	MLSP (MB)	RAD (kt)	RAD1 (nm)	RAD2 (nm)	RAD3 (nm)	RAD4 (nm)	RMW (nm)
2008081518	185N	688W	35	1009	34	75	0	0	75	60
2008081600	186N	702W	40	1008	34	90	60	0	75	60
2008081606	187N	714W	40	1008	34	90	60	0	75	50
2008081612	188N	729W	40	1007	34	90	60	0	75	50
2008081618	191N	746W	40	1007	34	90	60	0	0	75
2008081700	193N	757W	45	1005	34	90	60	0	0	75
2008081706	196N	769W	45	1004	34	90	50	0	0	50
2008081712	200N	781W	45	1003	34	90	50	0	0	50
2008081718	207N	796W	45	1006	34	90	90	0	0	60
2008081800	211N	803W	45	1001	34	90	90	0	0	60
2008081806	219N	808W	45	1003	34	30	90	0	0	60
2008081812	232N	812W	50	1002	34	100	90	0	0	60
2008081812	232N	812W	50	1002	50	65	0	0	0	60
2008081818	243N	817W	50	1000	34	110	90	30	30	30
2008081818	243N	817W	50	1000	50	60	0	0	0	30
2008081900	250N	819W	50	997	34	110	90	30	30	30
2008081900	250N	819W	50	997	50	60	0	0	0	30
2008081906	255N	818W	55	994	34	110	90	30	30	20
2008081906	255N	818W	55	994	50	60	60	15	0	20
2008081912	264N	814W	55	988	34	100	90	30	30	20
2008081912	264N	814W	55	988	50	30	30	0	0	20
2008081918	270N	811W	60	986	34	120	150	30	30	20
2008081918	270N	811W	60	986	50	20	20	0	0	20
2008082000	275N	809W	55	988	34	120	120	30	30	20
2008082000	275N	809W	55	988	50	20	20	0	0	20
2008082006	280N	806W	50	992	34	120	100	30	40	30
2008082006	280N	806W	50	992	50	20	20	0	0	30
2008082012	284N	806W	45	994	34	100	90	0	0	30
2008082018	287N	806W	45	997	34	120	100	0	30	30
2008082100	289N	805W	50	993	34	130	100	40	100	30
2008082100	289N	805W	50	993	50	40	40	0	0	30
2008082106	291N	807W	50	993	34	130	100	40	100	50
2008082106	291N	807W	50	993	50	60	40	0	0	50
2008082112	292N	807W	50	993	34	130	100	40	100	50
2008082112	292N	807W	50	993	50	60	40	0	0	50
2008082118	293N	810W	55	993	34	130	100	40	100	50
2008082118	293N	810W	55	993	50	60	40	0	0	50

Table 6-1. Continued

2008082200	293N	812W	50	994	34	150	130	50	100	50
2008082200	293N	812W	50	994	50	50	40	0	0	50
2008082206	295N	819W	50	995	34	150	120	0	0	50
2008082206	295N	819W	50	995	50	40	30	0	0	50
2008082212	296N	824W	45	996	34	120	100	0	0	50
2008082218	298N	830W	40	997	34	120	100	40	0	50
2008082300	297N	838W	45	996	34	0	80	80	0	45
2008082306	298N	847W	45	997	34	0	80	80	0	45
2008082312	300N	852W	40	998	34	0	80	80	0	45
2008082318	305N	859W	40	999	34	0	80	30	0	45

WMS produces wind and pressure fields at 5-min intervals which are then interpolated onto CH3D model grid and passed to CH3D and SWAN.

For a Fast2D scenario the wind produced by the WMS is based on a synthetic model by Xie (2006) with the reduction factors due to land dissipation applied to it. The wind and pressure fields computed by the WMS are based only on parameters that are listed in Table 6-1 which are available from the ATCF system for forecasting. WMS wind compares well with the H*Wind obtained from HRD. For a Full3D scenario the aforementioned WMS wind field is blended with the NOGAPS wind field as described in Chapter 4 to allow for background wind and for consistency at the open boundary where CH3D obtains its conditions from the HYCOM model which is run using the NOGAPS wind. The spin-up simulation is based purely on NOGAPS wind as TS Fay had no effect on the domain prior to August 18. In a real-time forecasting mode, as described in Chapter 3, continuous nowcast simulations are done automatically before each forecasting cycle (every 6 hours) so that the initial conditions are the same as in a real-time system.

Water Level

Water level boundary conditions for CH3D model are obtained as a linear combination of the tidal constituents supplied to the model at the open boundary and surge levels simulated by the ADCIRC model for the Fast2D scenario, or the HYCOM for the Full3D scenario. The ADCIRC model that provides open boundary conditions for the Fast2D scenario is driven by the same WMS wind field as CH3D, while HYCOM is driven by the NOGAPS wind field.

A simulation with tides only is performed to validate the tidal constituents and Figures 6-15 and 6-16 show the comparison of simulated tides versus predicted tides at the NOAA-NOS stations Vilano Beach and Mayport, respectively. Results of the 20-day tidal simulation show reasonable comparison between the simulated tides and the NOAA predicted tides.

Waves

Waves are included in all scenarios. SWAN is run in a non-stationary mode with a 10-second time step and is forced with the same as WMS wind used by the ADCIRC and CH3D models. The open boundary conditions for SWAN are obtained from WaveWatch III model output. SWAN boundary conditions assume a Gaussian distribution of spectra and provide significant wave height, period and direction of waves based on the WaveWatch III model output.

Salinity

The salinity boundary conditions for the Full3D scenario are based on the HYCOM model output and salinity values from the HYCOM model are interpolated onto the CH3D open boundary throughout the water column. The salinity boundary conditions at river boundaries are set to the latest measured salinity value for the duration of forecast and fresh water where measurements are not available. Precipitation forecasted by the HYCOM is also used, which will be shown to be quite important during Fay simulations.

Simulating the Storm

The four scenarios: Fast2D, Fast2D+Waves, Full3D-HYCOM and Full3D-HYCOM+Waves are simulated and results analyzed for the TS Fay. Simulated results of various scenarios are compared to each other and to measured data to see if any improvement is achieved due to the inclusion of precipitation, which was not included in the real-time forecasting conducted in 2008.

It is hypothesized that improvement in water level prediction can be achieved by using a more accurate wind model, and salinity prediction at GTM-NERR stations can be improved by adding precipitation to the model. It is also hypothesized that waves do not have a major effect on prediction of either water level or salinity, since both Fay reports and observations indicated that waves and surge were rather minimal during Fay.

There is little difference between simulated water levels using a Fast2D and Fast3D scenarios. Given that the wave action was very mild and wave-current interaction was therefore insignificant, it seems logical that the differences between the 2D and 3D simulations would be rather small. However, 3D simulation is needed for more accurate simulation of salinity and currents. A 2D model can only produce vertically-averaged salinity and currents which cannot be compared with data easily

It should be noted that wave action is rather mild and it can be seen from the comparisons that, both on the southwest coast and the east coast (Figures 6-17 and 6-18), waves did not have a major effect on setup/setdown.

The simulation of Fay on the southwest Florida coast yields reasonable comparison between simulated and measured water levels. Both Fort Myers (Figure 6-19) and Naples (Figure 6-20) stations experienced a small setdown early on the 19th of August, which is

expected as the winds were to the offshore (Figures 6-3 and 6-4) and hence moving the water offshore creating the setdown.

On the east coast, the winds were moving the water onshore, although the surge is not very high due to rather weak winds. Surge and waves at Trident Pier (Figure 6-21) and Ponce De Leon (Figure 6-22) stations were very low and water levels stay mostly within their normal tidal range.

It is interesting to note, that the surge at the I-295 Bridge in St. Johns River, as shown in Figure 6-23, started building up slowly on August 22 due to onshore wind (Figures 6-8 to 6-10) that built up the surge at the coast near St. Johns River mouth forcing the water into the estuary. These winds are fairly weak with onshore component ranging from 10 to 35-40 kt, but persistence over a prolonged time pushed the water into the fairly shallow St. Johns River thus creating a surge wave. At the same time winds over the St. Johns River have a significant northerly component (Figure 6-10) which helped to push the water south, further up the St. Johns River. Winds during Fay were not very strong but the storm was located over the east coast for a prolonged time and continuous exposure to such winds slowly built up rather significant surge up the St. Johns River. These processes are confirmed via personal conversations with the staff of the NWS office in Jacksonville who observed such processes in the St. Johns River. To illustrate this point more clearly a simulation without tides was conducted so that a pure surge wave can be observed without surge / tide interaction. The surge starts building up on August 21 (Figure 6-24) as the storm is located off the east coast and is almost stationary. The northerly wind component over the St. Johns River helps to move the water further upstream. Then, on the 22nd the storm starts moving inland and wind direction starts switching from northerly to southerly (Figures 6-25 and 6-26). Since the St. Johns River is fairly shallow it creates even higher surge

and some flooding on the left bank of the river. Figures 6-27 and 6-28 show a transect along the St. Johns River and storm surge evolution along that transect in time. It can be observed that between August 21 22:00 and August 22 09:00 the St. Johns River fills up with water, this is due to the rivers and run off flows being blocked by the winds directed up the river. Then on August 22 21:00 as the wind direction changes to southerly the water from the upstream starts moving towards the ocean.

The accuracy of salinity simulations is severely limited by availability of river flow data and run-off data. For example, at the Fort Matanzas station (Figure 6-29) near the ocean and not being affected very significantly by the fresh river discharge. However, simulated salinity is not as good at other stations such as Pellicer Creek (Figure 6-30), Pine Island (Figure 6-31) and San Sebastian (Figure 6-32).

Adding precipitation effect to the system helped improve the salinity simulation. For example, simulated salinity at Pellicer Creek and San Sebastian (Figures 6-33 and 6-34, respectively) is significantly more accurate when precipitation is included. The Pellicer Creek station shows almost no change in simulated salinity during Fay without precipitation. While inclusion of precipitation allows the nearby areas to accumulate water from rainfall and the salinity to decrease significantly, it is apparent that the amount of fresh water discharge into the system is insufficient and smaller than what it is in reality since the model domain does not cover the entire watershed which is affected by the rainfall, therefore the model is not able to provide a sufficient amount of fresh water for salinity to decrease to the measured values during Fay.

Figure 6-35 demonstrates one of the products that could be generated using SSMS – GIS-based inundation map for the storm, combining high-resolution maximum simulated water level, high-resolution topography data and aerial imagery.

Summary and Conclusions

One of the lessons learned from the simulations and analysis of the TS Fay is the need to incorporate more processes into existing storm surge modeling systems. Accurate simulation of salinity during Fay was impossible without inclusion of precipitation into the model. Yet the lack of accurate run-off data for the model domain prevents the SSMS from achieving the desired accuracy in salinity simulations. There are no flooding data during Fay but it could be speculated that inclusion of a watershed model into the SSMS will enable accurate simulation of rain-induced flooding and will enable simulation of flooding due to rainfall and surge.

The performance of SSMS has been evaluated using the data from TS Fay, which is the only storm of the 2008 hurricane season that had a significant effect on Florida. Predicted water levels compare well with observed data yielding small errors. The SSMS results show that rather significant surge developed in the St. Johns River due to favorable wind conditions while setdown was simulated on the west coast of Florida where the storm did not produce significant surge.

The salinity prediction at the GTM-NERR stations appears to be reasonable, yet still has room for improvement. The results presented here show significant improvement compared to the real-time forecasting results that were obtained during the 2008 season, due to the inclusion of precipitation. It is hypothesized that further improvements in salinity can be achieved by including a watershed model which would provide more accurate run-off to the rivers and streams. Adding a watershed model to the SSMS is outside the present scope of this work, but should be considered for future enhancement of the SSMS.

The effects of waves were found to be rather insignificant during Fay primarily due to rather weak winds. Model results show very little difference in all simulated variables when comparing simulations with and without wave effects. However, it should be noted that the significance of waves were clearly shown for several past hurricanes including Hurricane Isabel in Chesapeake Bay (2003) by Sheng et al. (2009).

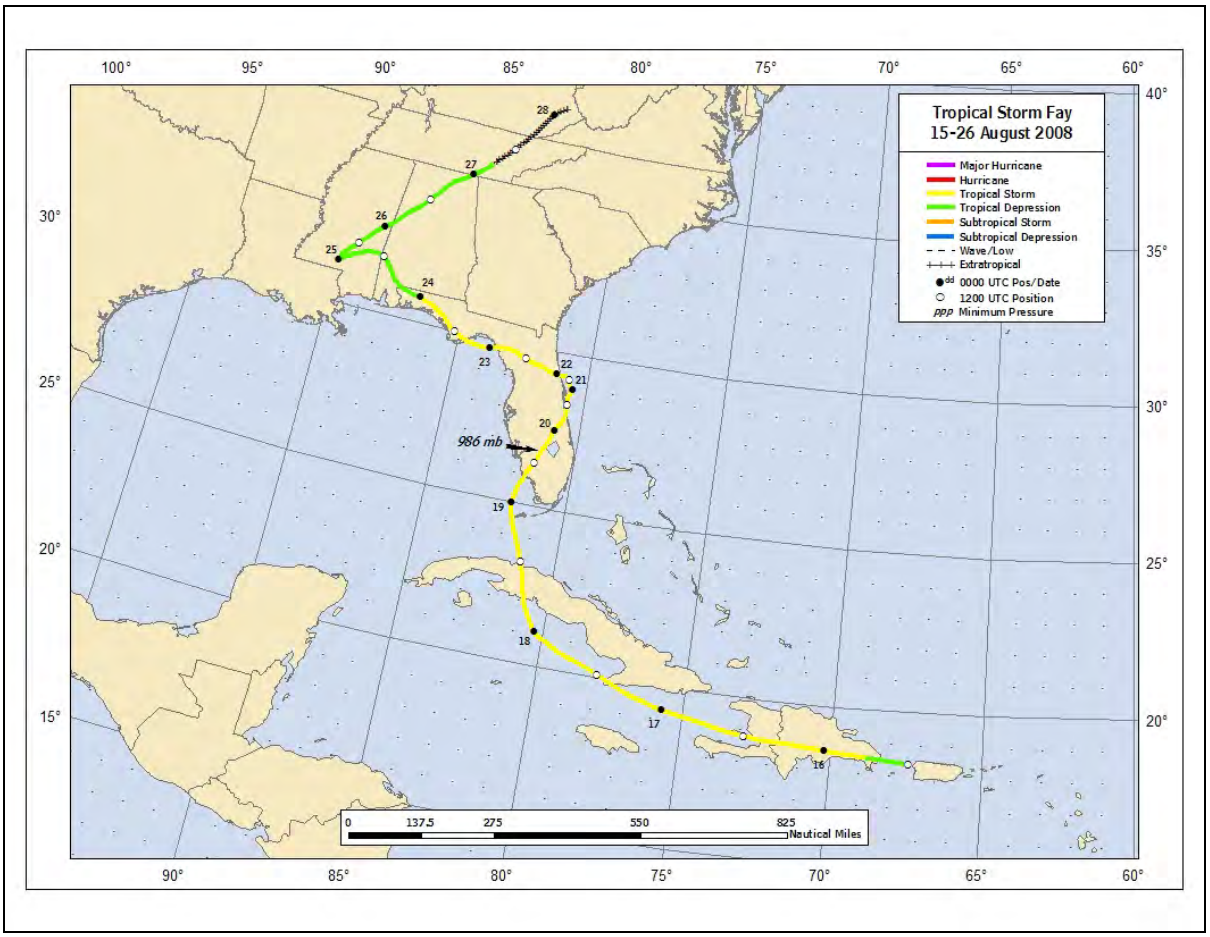

Figure 6-1. Best track for Tropical Storm Fay

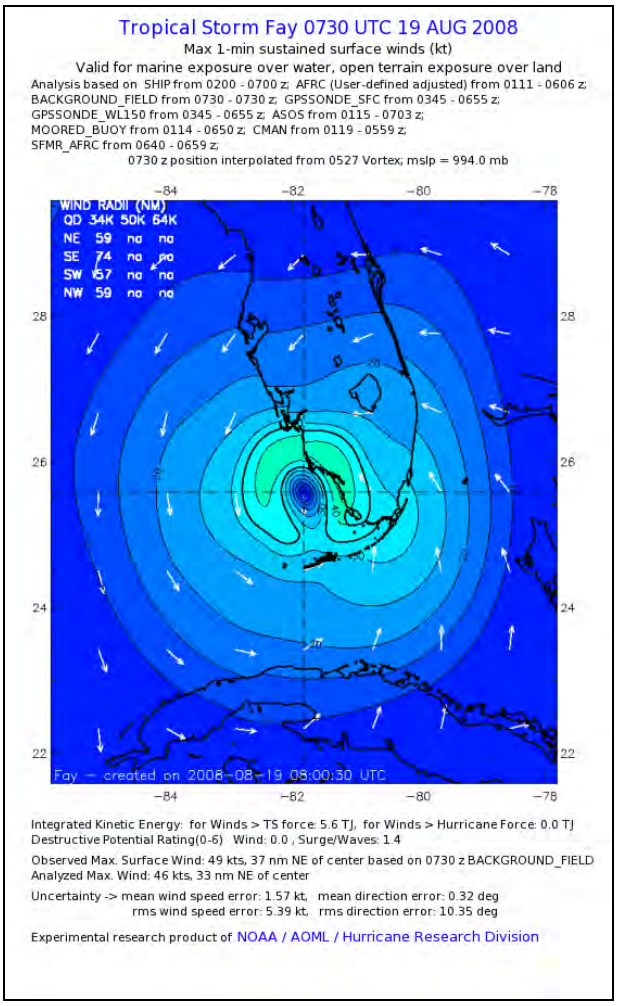

Figure 6-2. Tropical storm Fay H*Wind snapshot. Aug. 19, 2008 07:30UTC

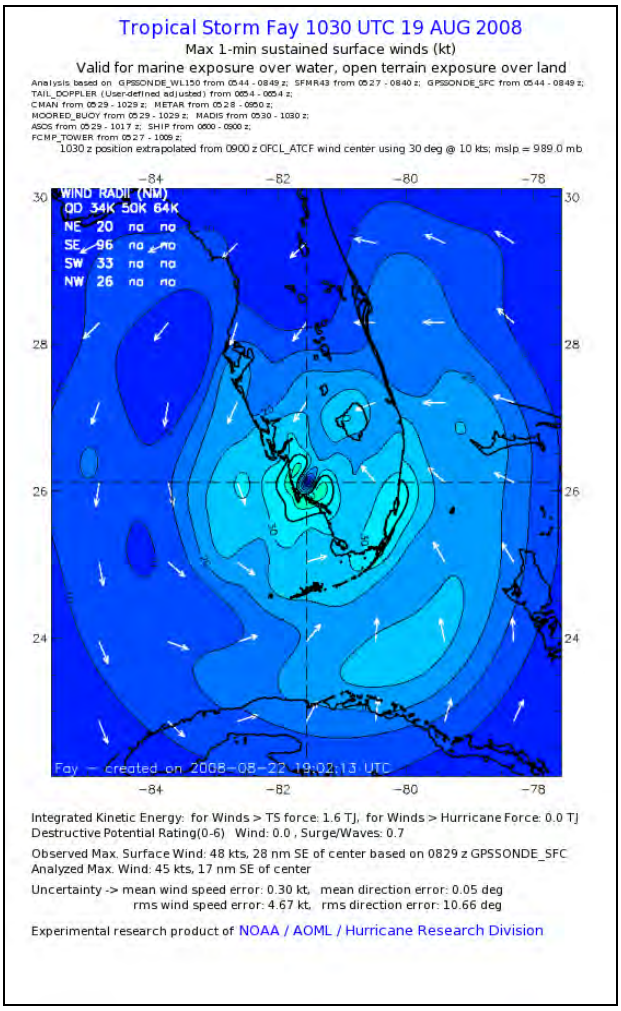

Figure 6-3. Tropical storm Fay H*Wind snapshot. Aug. 19, 2008 10:30UTC

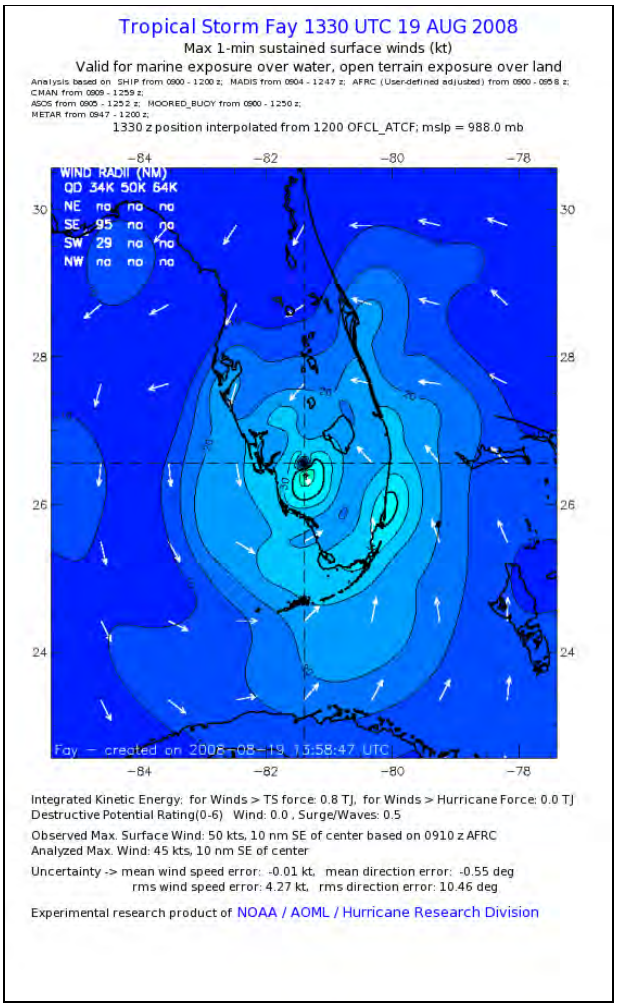

Figure 6-4. Tropical storm Fay H*Wind snapshot. Aug. 19, 2008 13:30UTC

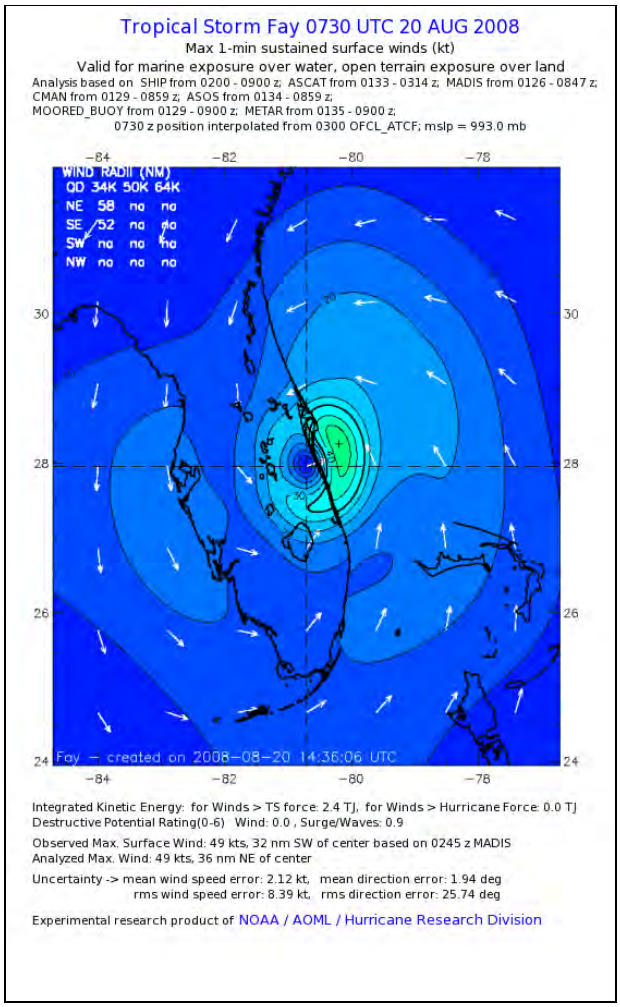

Figure 6-5. Tropical storm Fay H*Wind snapshot. Aug. 20, 2008 07:30UTC

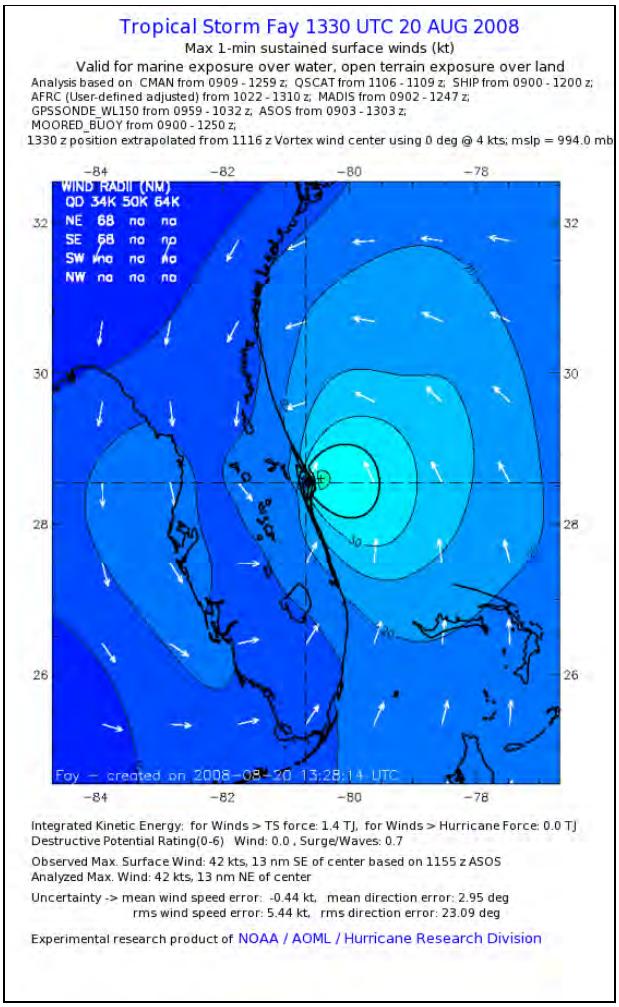

Figure 6-6. Tropical storm Fay H*Wind snapshot. Aug. 20, 2008 13:30UTC

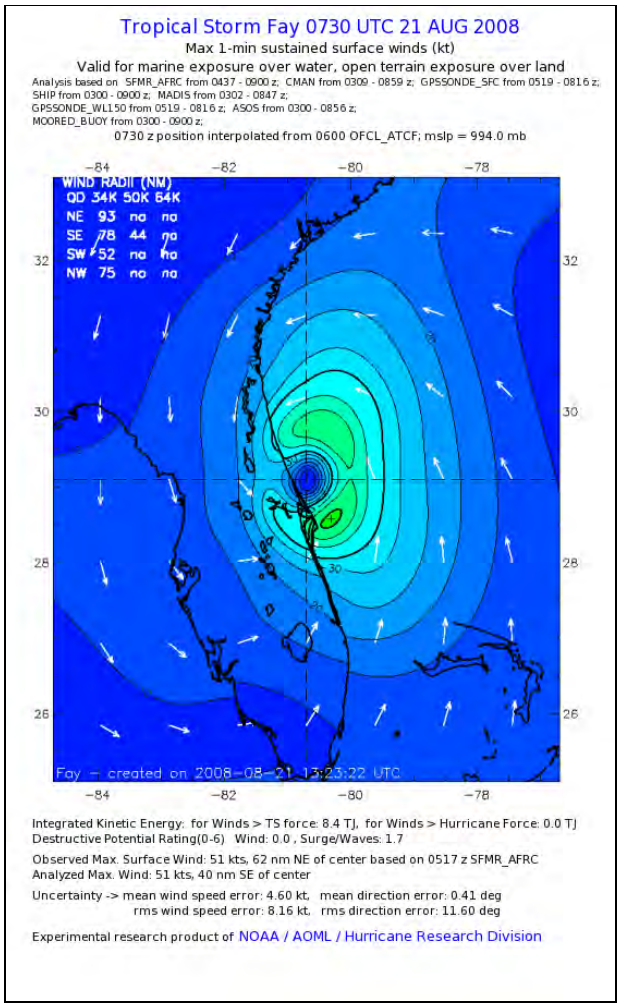

Figure 6-7. Tropical storm Fay H*Wind snapshot. Aug. 21, 2008 07:30UTC

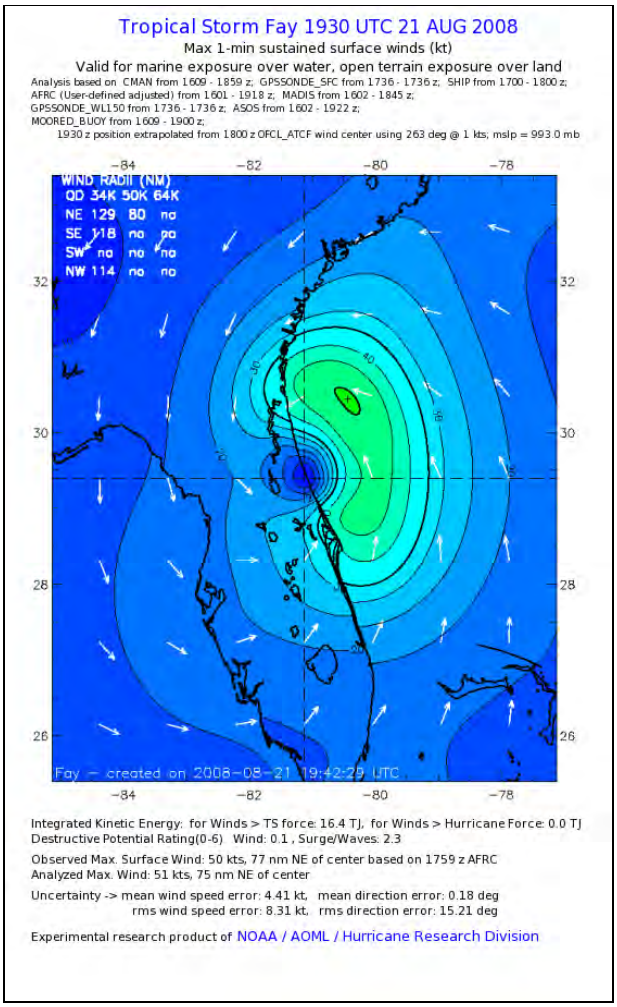

Figure 6-8. Tropical storm Fay H*Wind snapshot. Aug. 21, 2008 19:30UTC

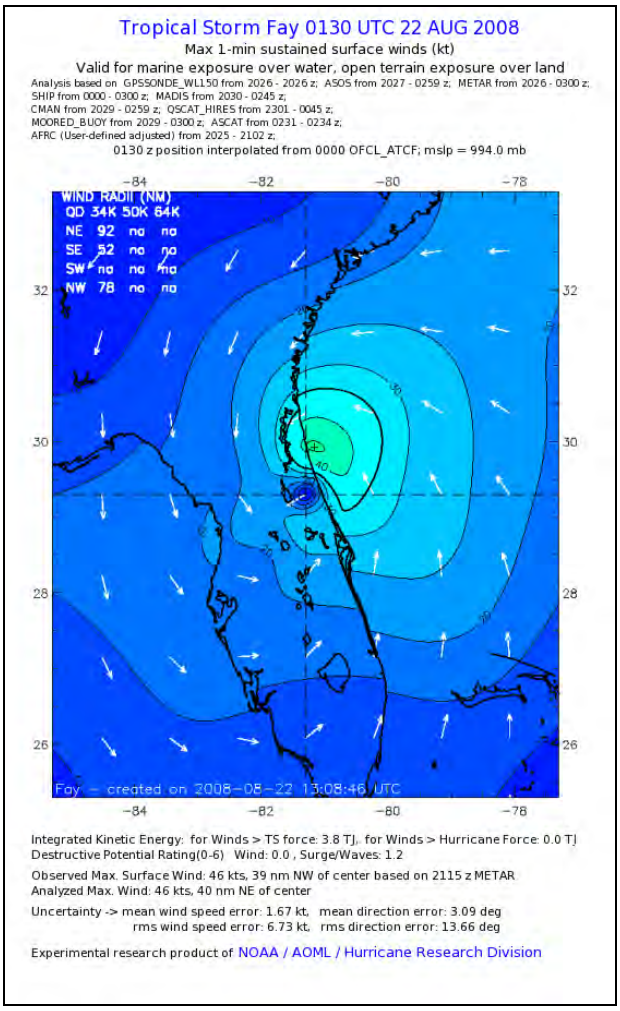

Figure 6-9. Tropical storm Fay H*Wind snapshot. Aug. 22, 2008 01:30UTC

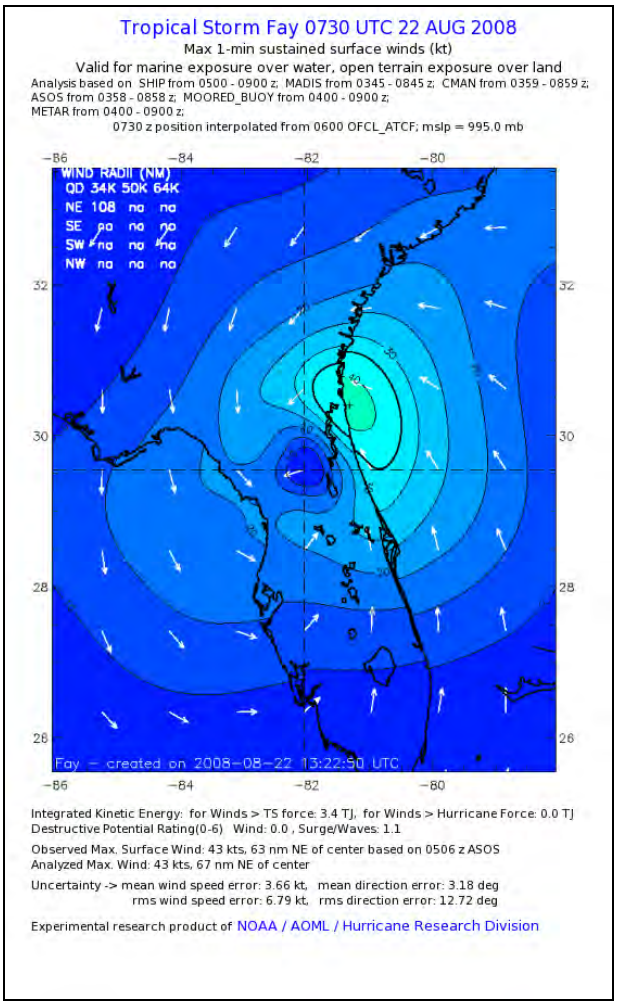

Figure 6-10. Tropical storm Fay H*Wind snapshot. Aug. 22, 2008 7:30UTC

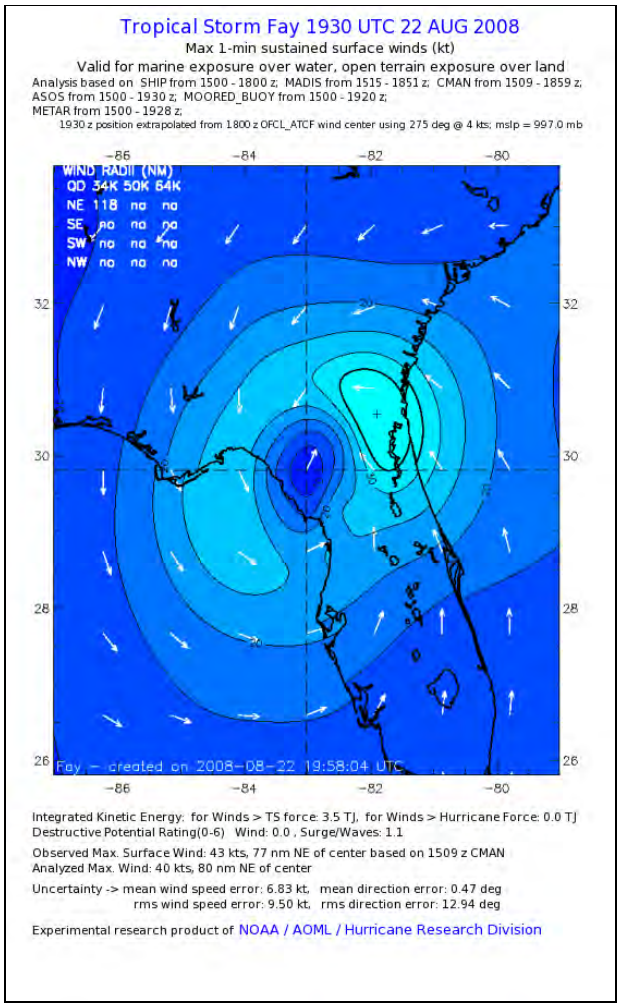

Figure 6-11. Tropical storm Fay H*Wind snapshot. Aug. 22, 2008 19:30UTC

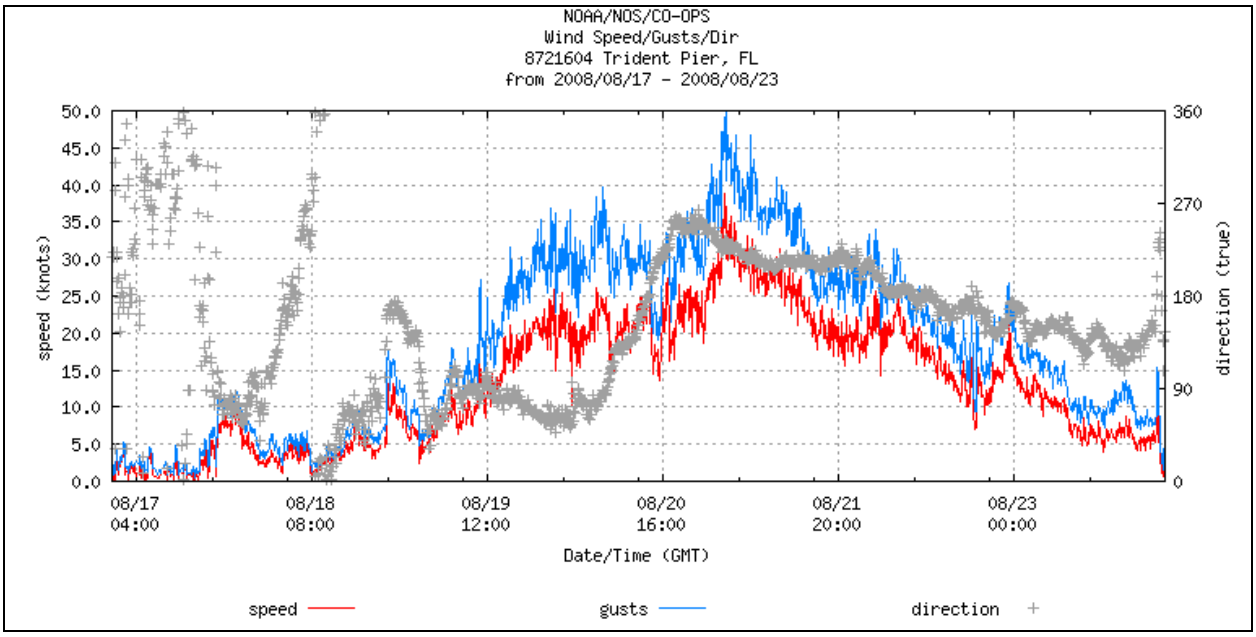

Figure 6-12. Wind speed and direction at NOAA-NOS station 8721604 - Trident Pier during tropical storm Fay (NOAA-NOS)

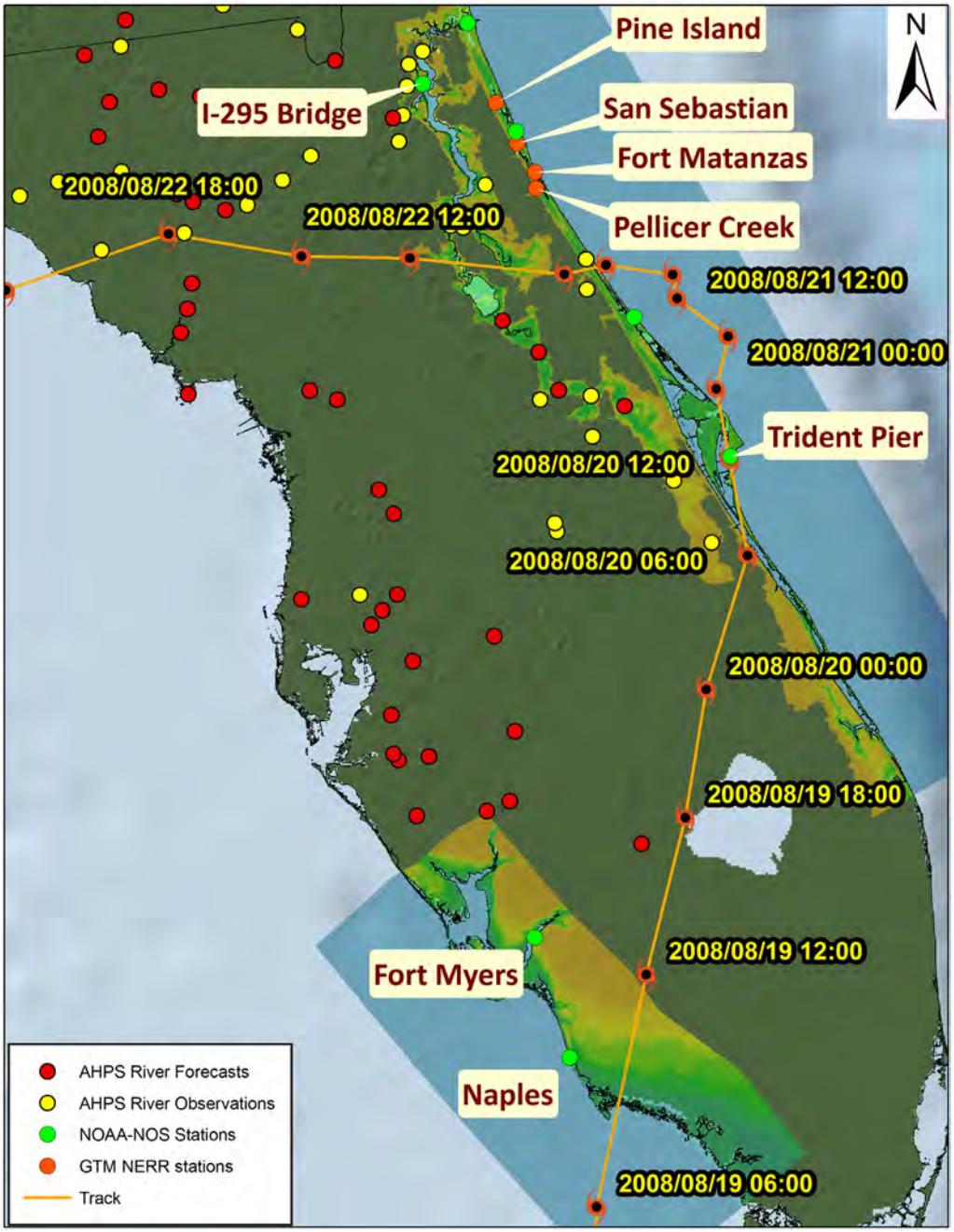

Figure 6-13. SSMS domains (EC and SW) used for verification of the system with Tropical Storm Fay

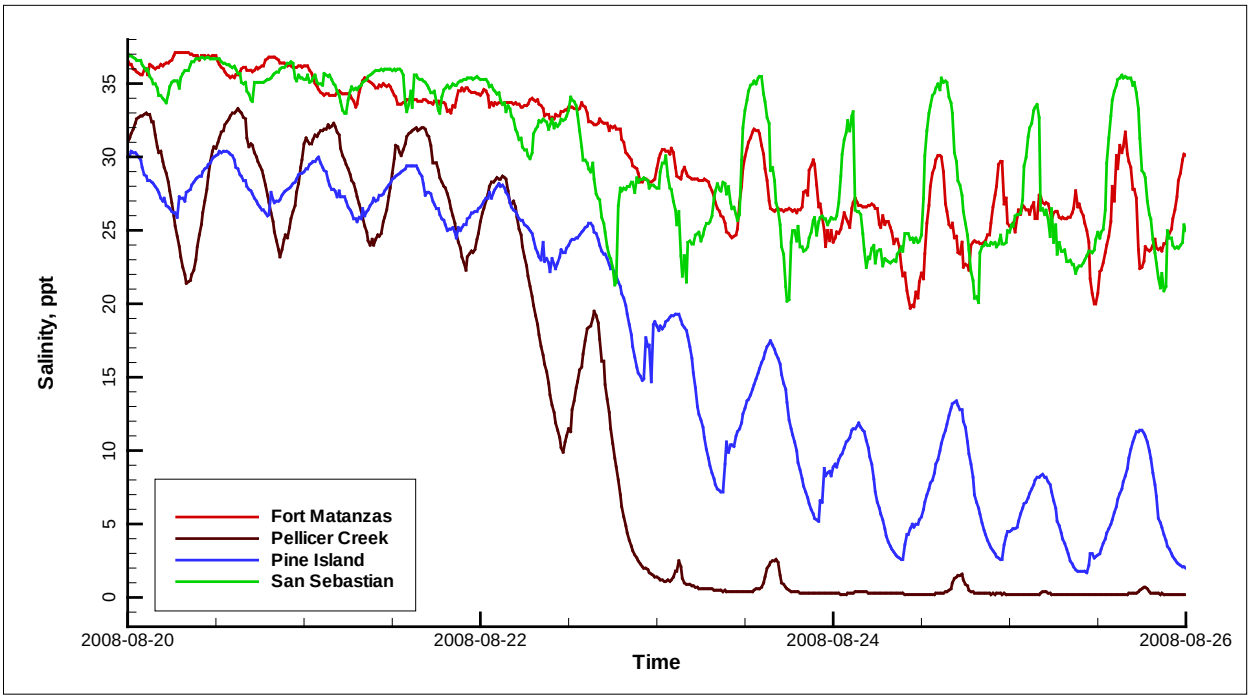

Figure 6-14. Measured salinity at Guana-Tolomato-Matanzas National Estuarine Research Reserve stations during tropical storm Fay

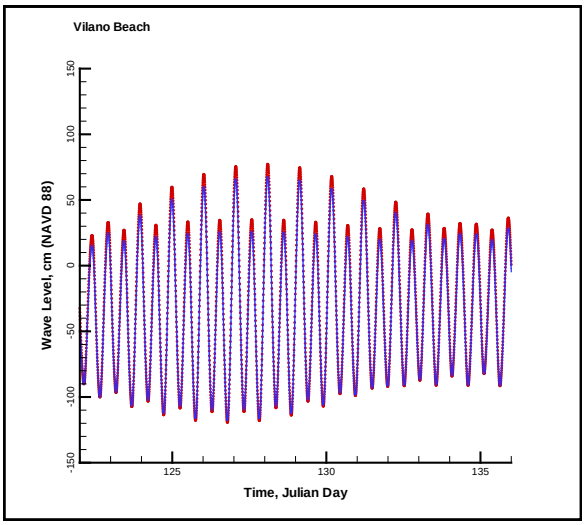

Figure 6-15. NOAA-NOS Station 8720554 – Vilano Beach. Simulated and predicted tides

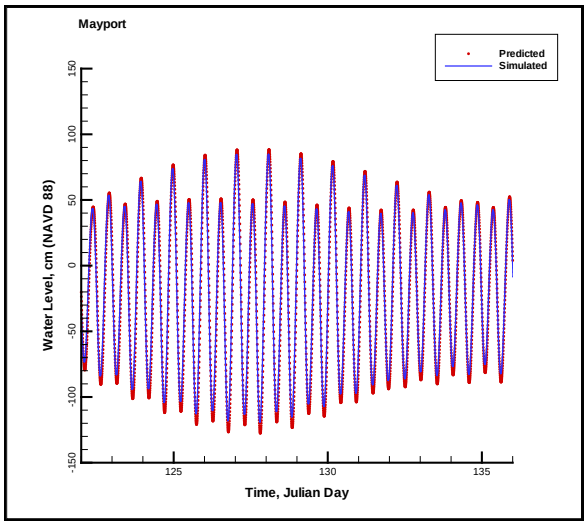

Figure 6-16. NOAA-NOS Station 8720211 - Mayport. Simulated and predicted tides

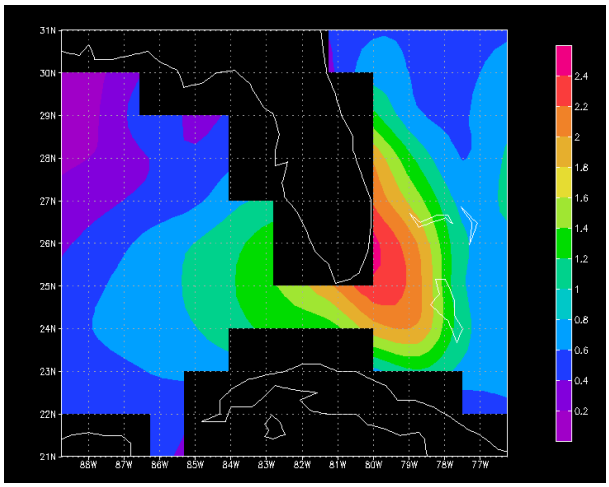

Figure 6-17. WaveWatch III significant wave height August 19, 2008 15:00UTC

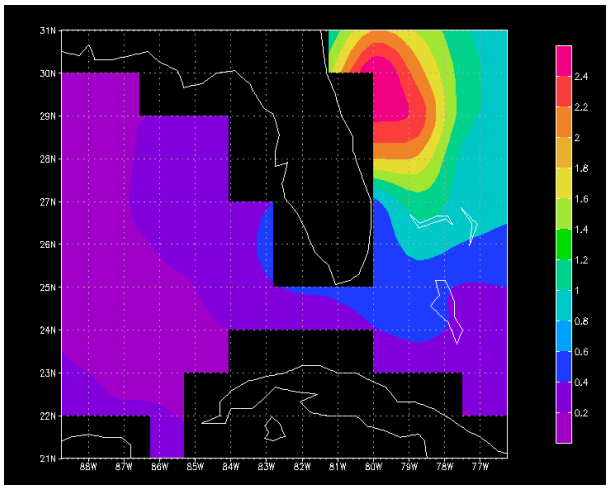

Figure 6-18. WaveWatch III significant wave height August 20, 2008 21:00UTC

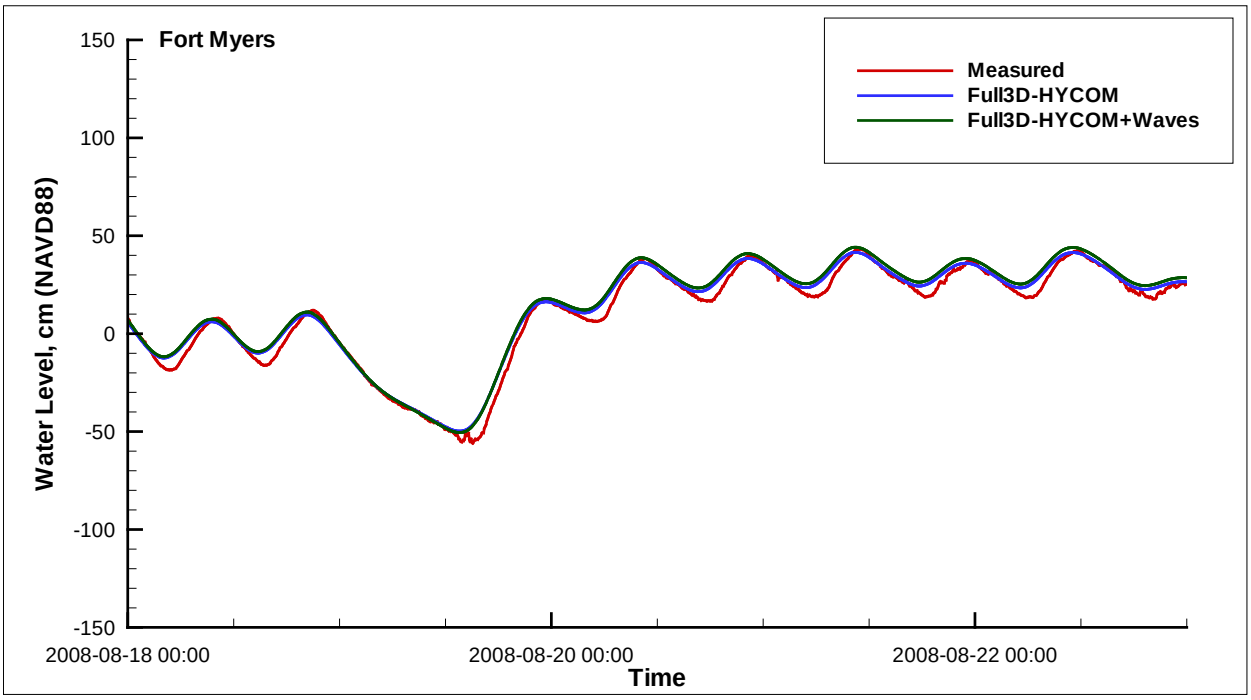

Figure 6-19. Measured and simulated water level during tropical storm Fay at Fort Myers station

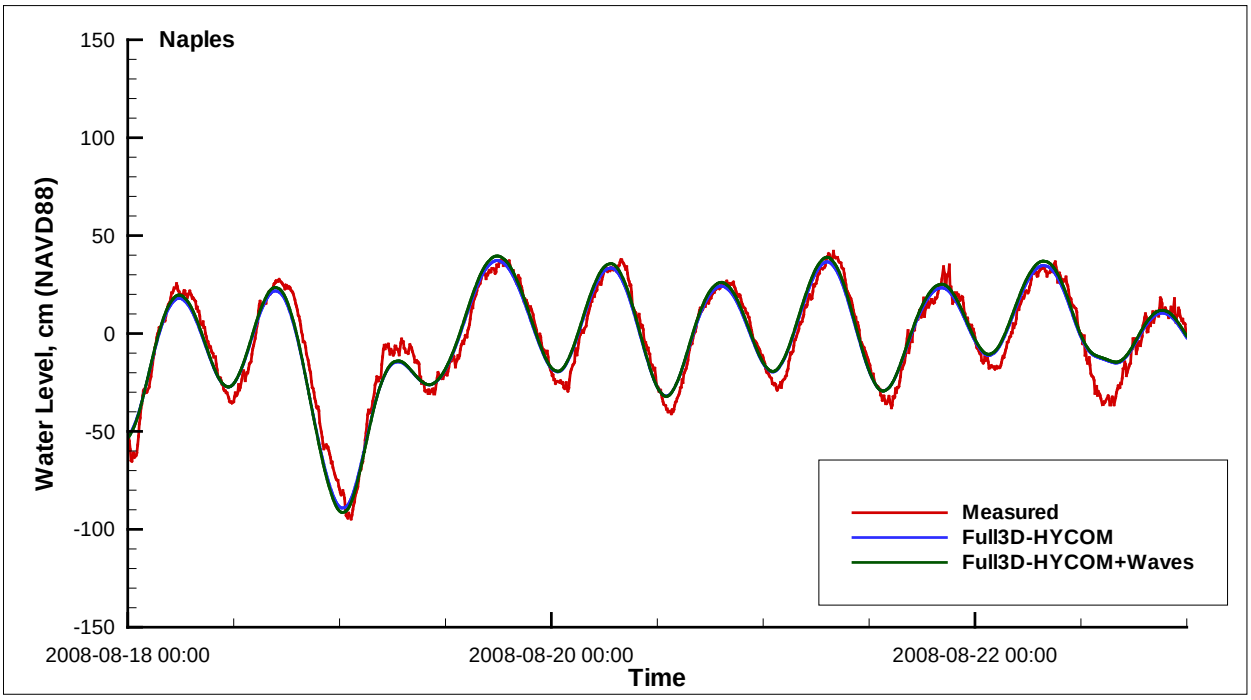

Figure 6-20. Measured and simulated water level during tropical storm Fay at Naples station

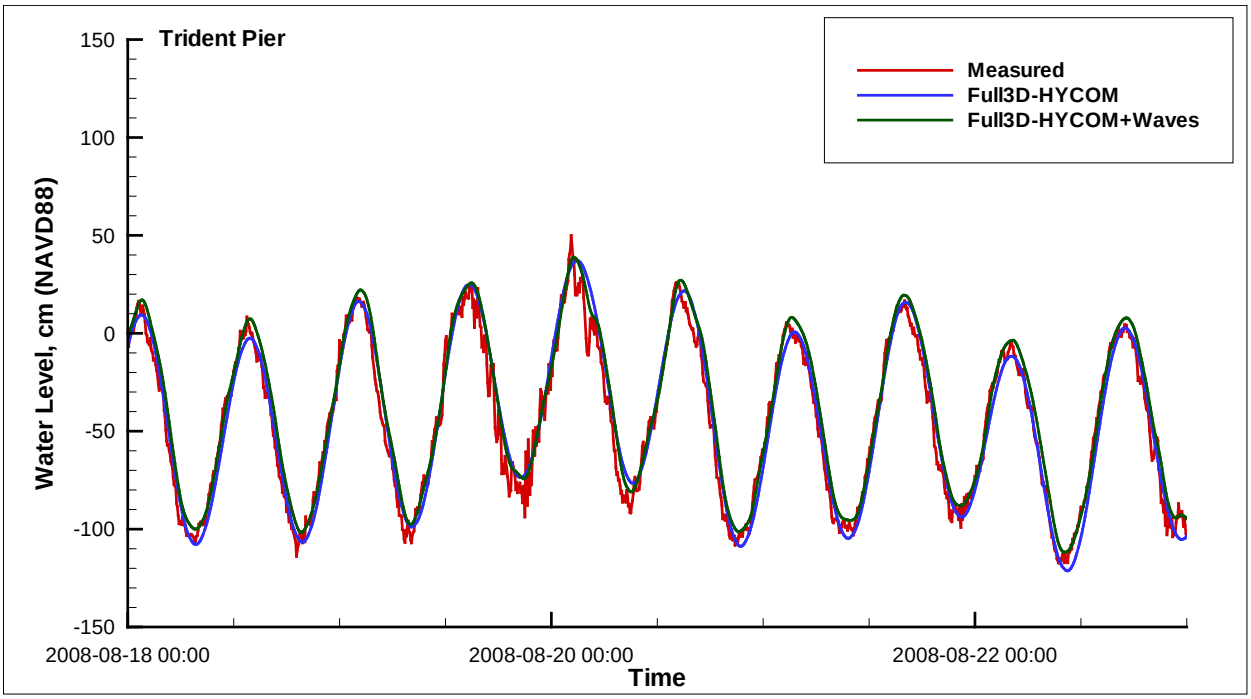

Figure 6-21. Measured and simulated water level during tropical storm Fay at Trident Pier station

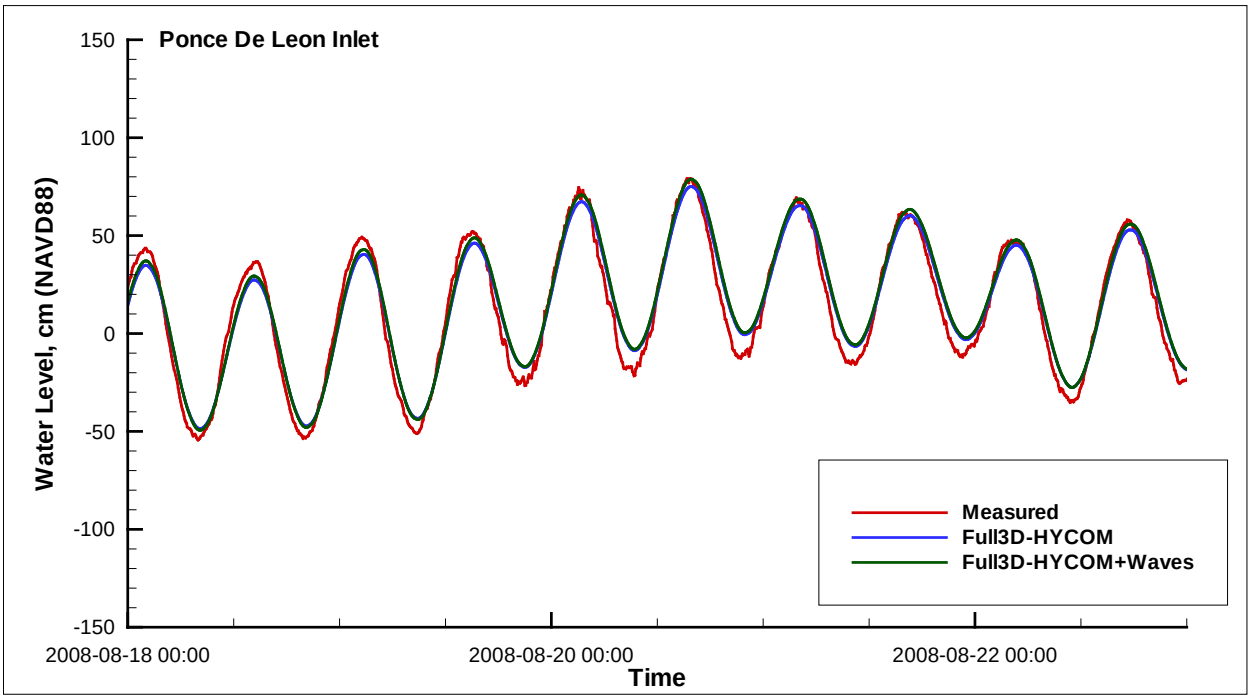

Figure 6-22. Measured and simulated water level during tropical storm Fay at Ponce De Leon Inlet station

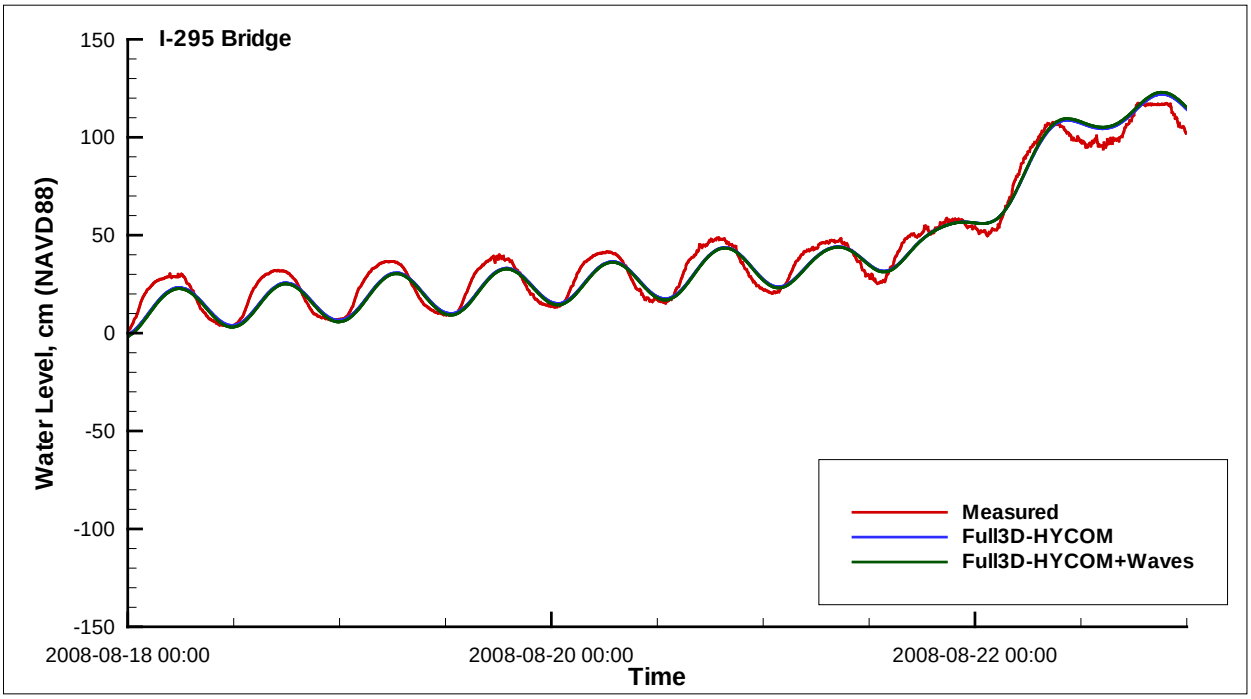

Figure 6-23. Measured and simulated water level during tropical storm Fay at I-295 Bridge at St. Johns River station

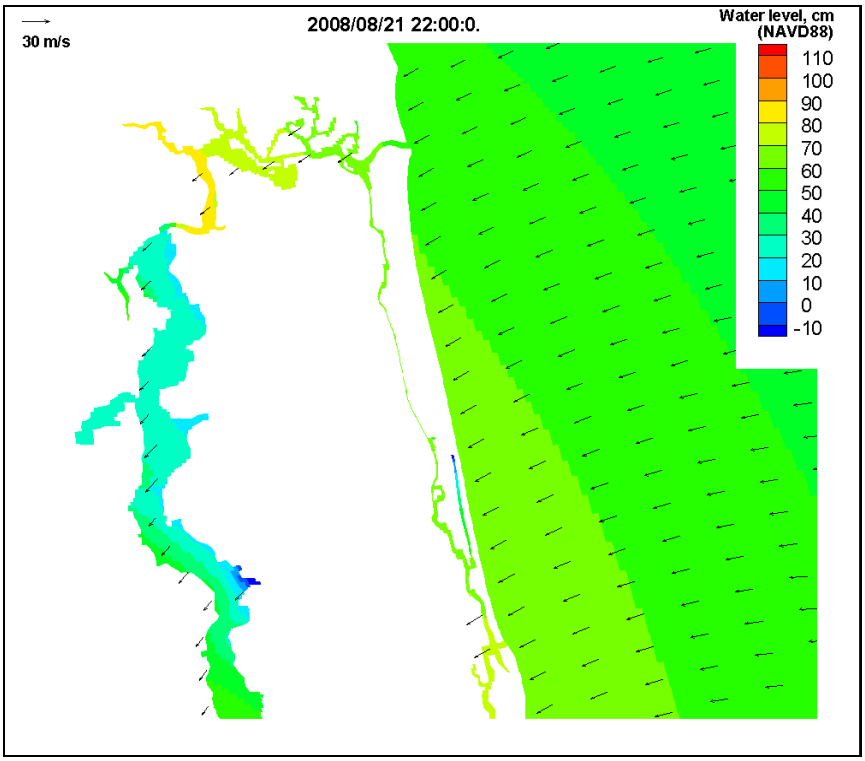

Figure 6-24. Contours of water level in the lower St. Johns River on August 21, 2008 at 22:00UTC

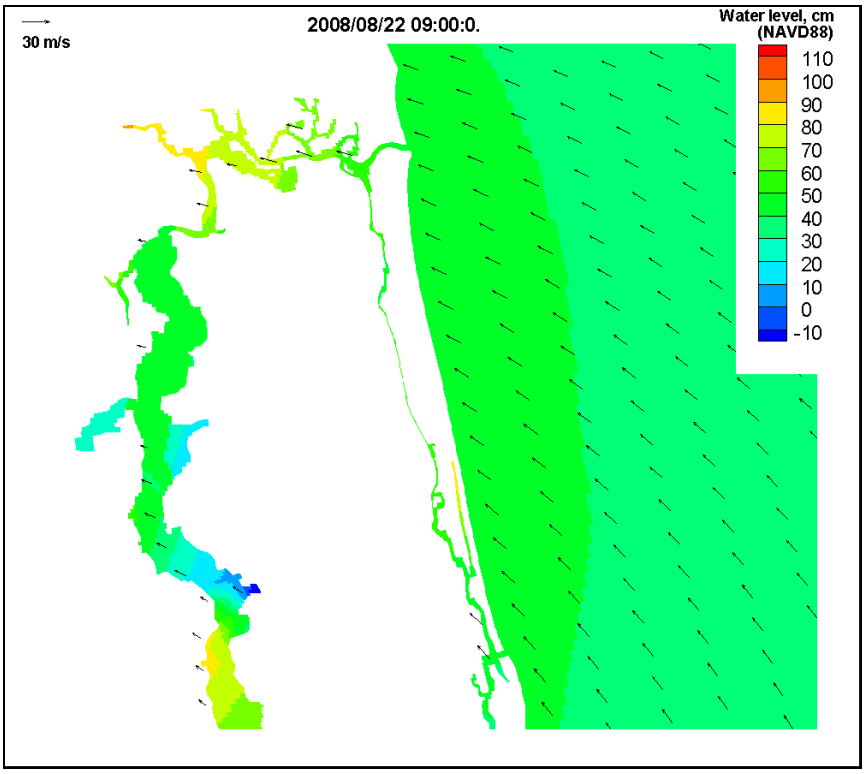

Figure 6-25. Contours of water level in the lower St. Johns River on August 22, 2008 at 09:00UTC

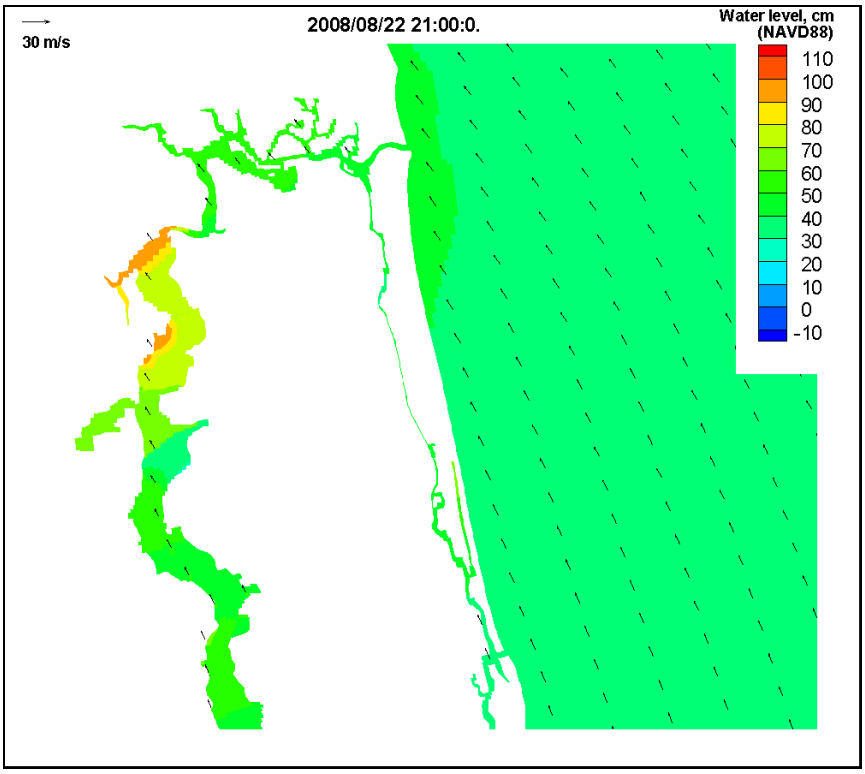

Figure 6-26. Contours of water level in the lower St. Johns River on August 22, 2008 at 21:00UTC

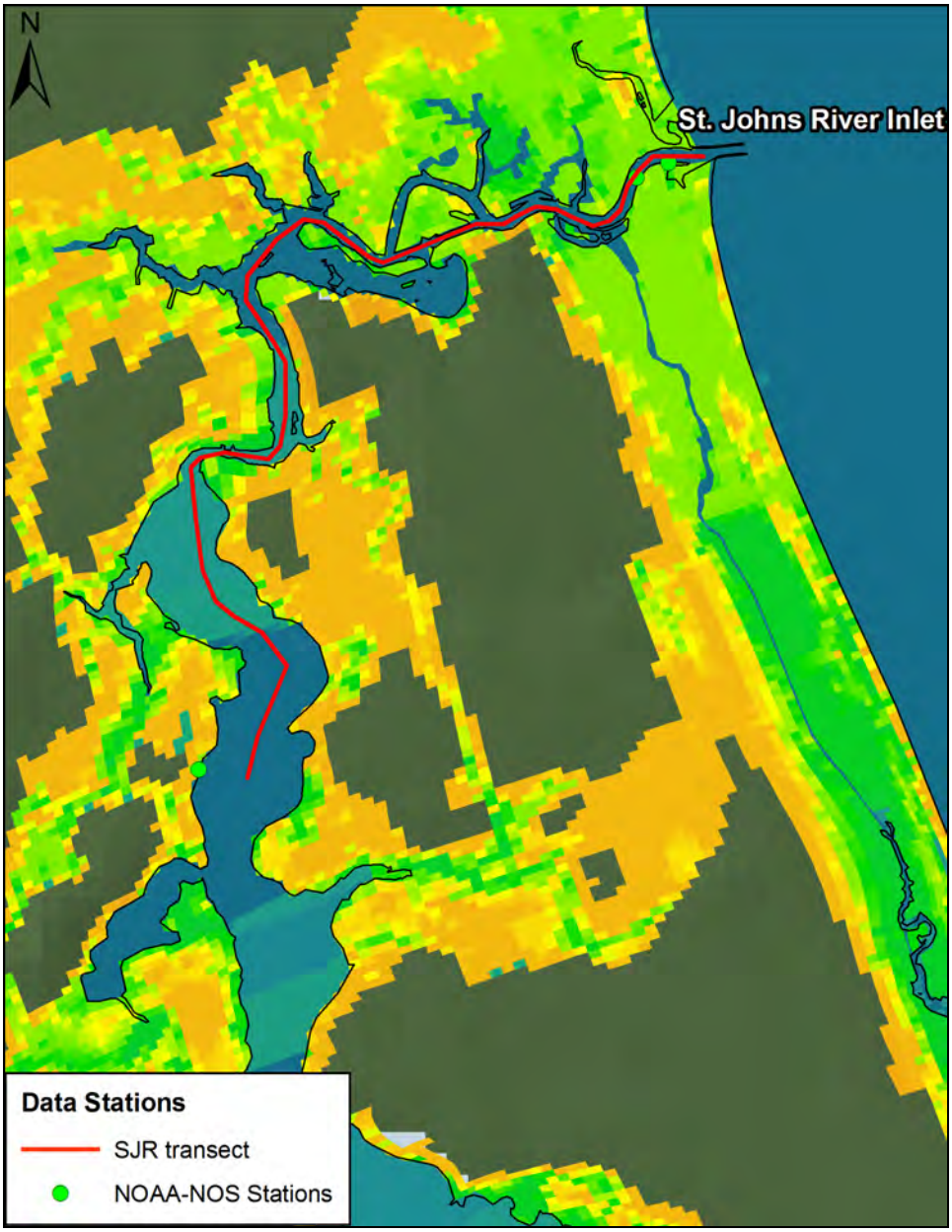

Figure 6-27. Map of the St. John River transect

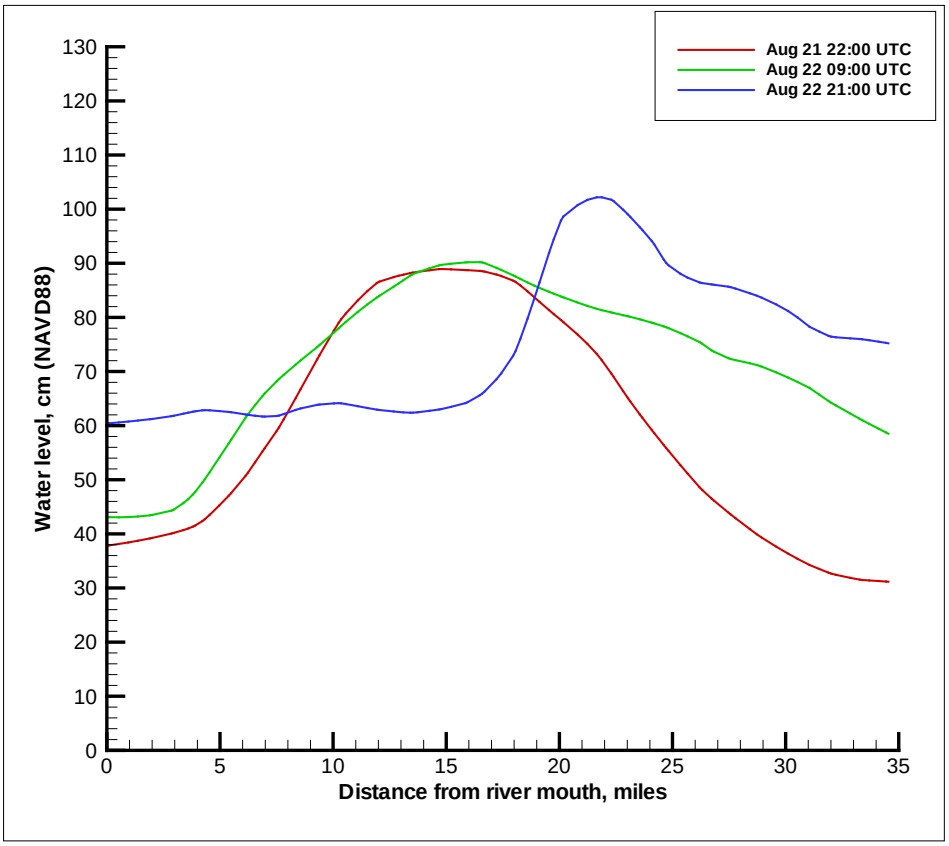

Figure 6-28. Water level along the transect of the St. Johns River during tropical storm Fay

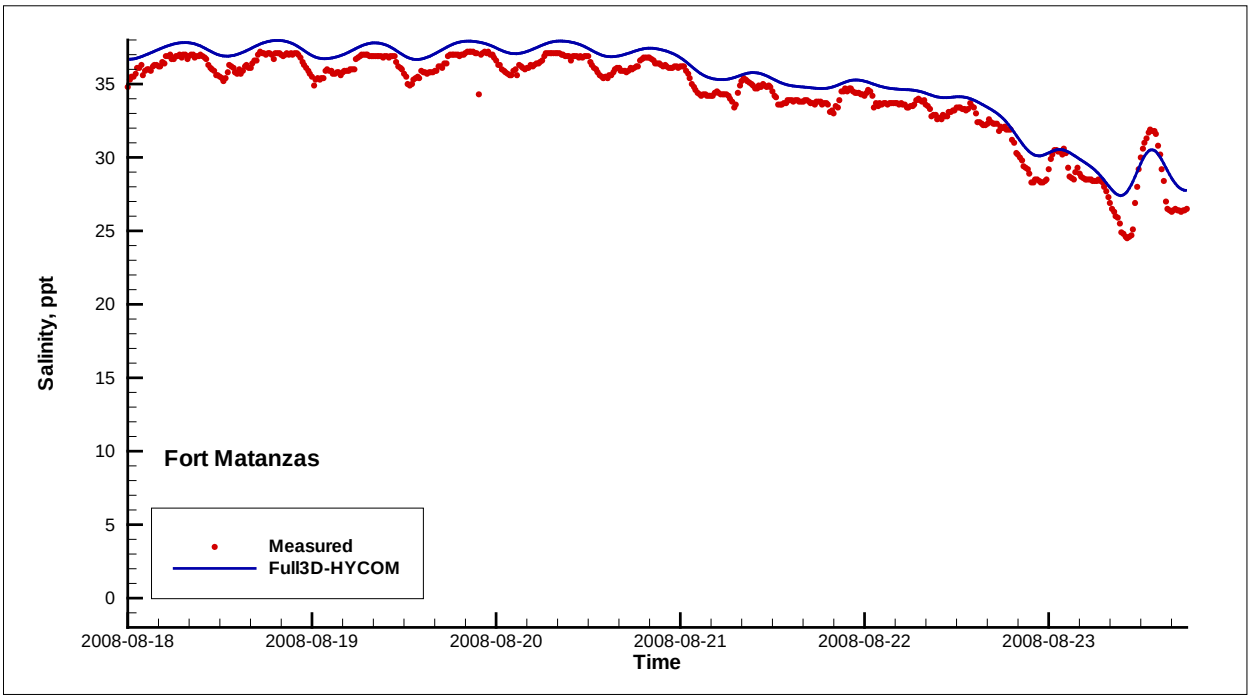

Figure 6-29. Measured and simulated salinity during tropical storm Fay at Fort Matanzas station

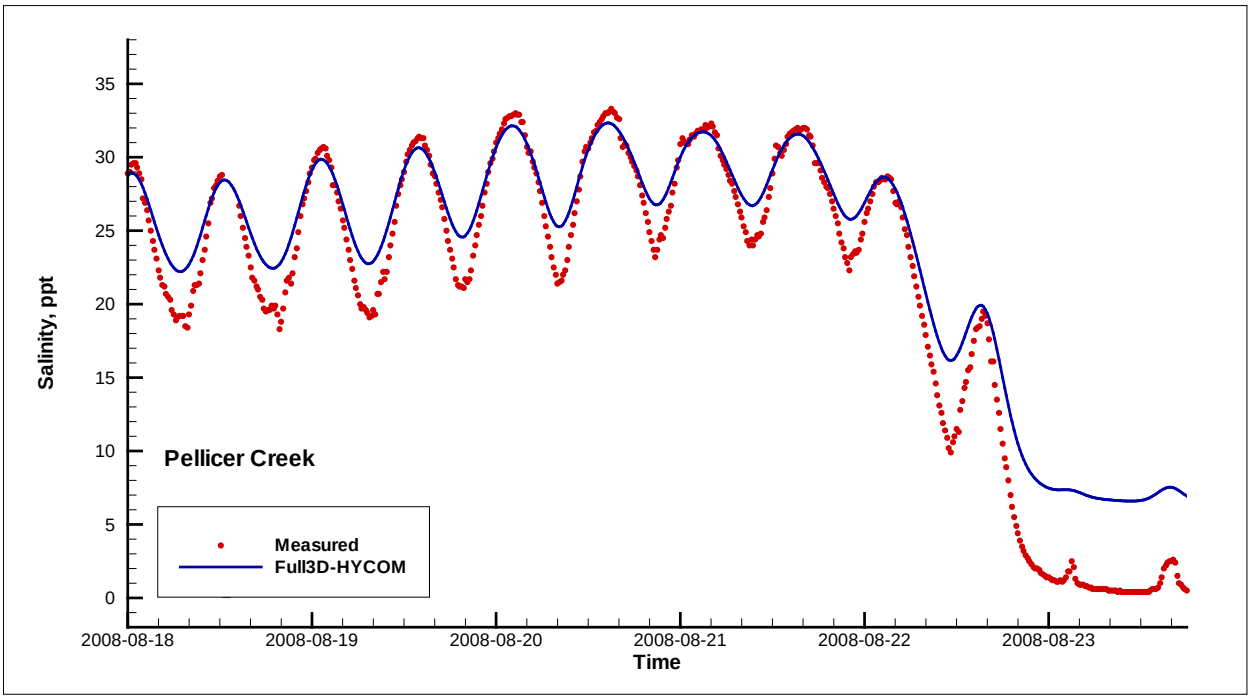

Figure 6-30. Measured and simulated salinity during tropical storm Fay Pellicer Creek station

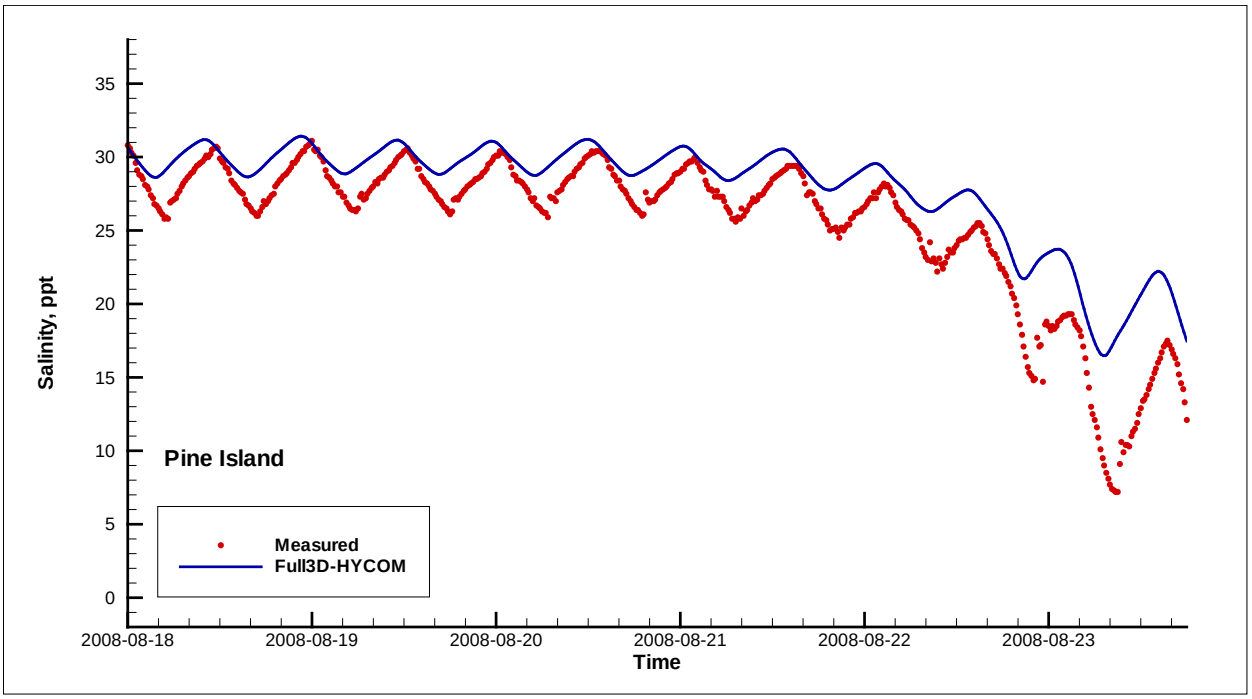

Figure 6-31. Measured and simulated salinity during tropical storm Fay at Pine Island station

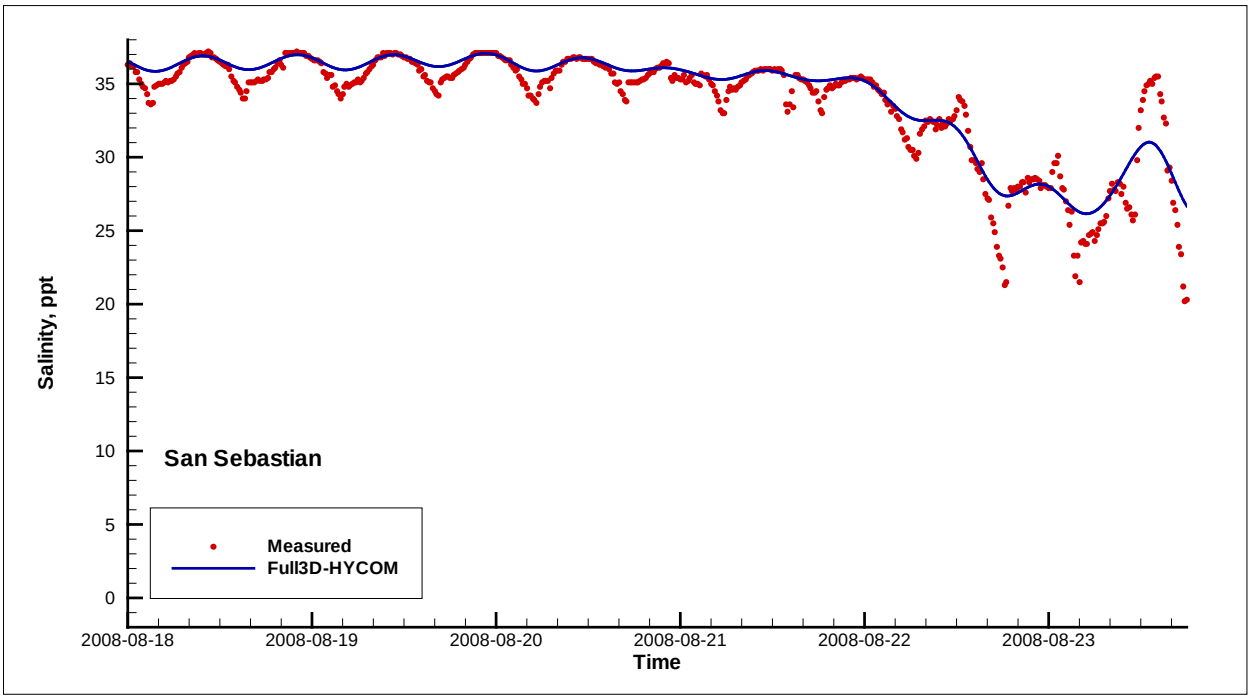

Figure 6-32. Measured and simulated salinity during tropical storm Fay at San Sebastian station

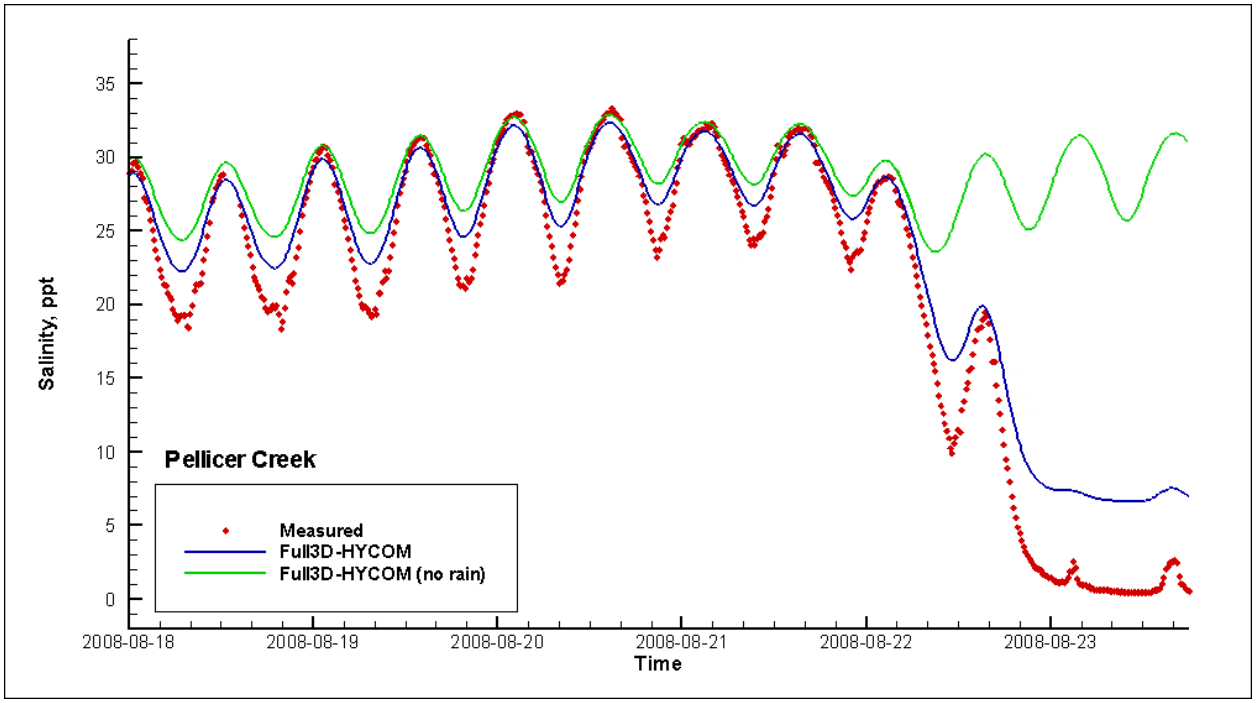

Figure 6-33. Comparison of simulated salinity during tropical storm Fay at Pellicer Creek station using the Full3D-HYCOM scenario with and without added precipitation

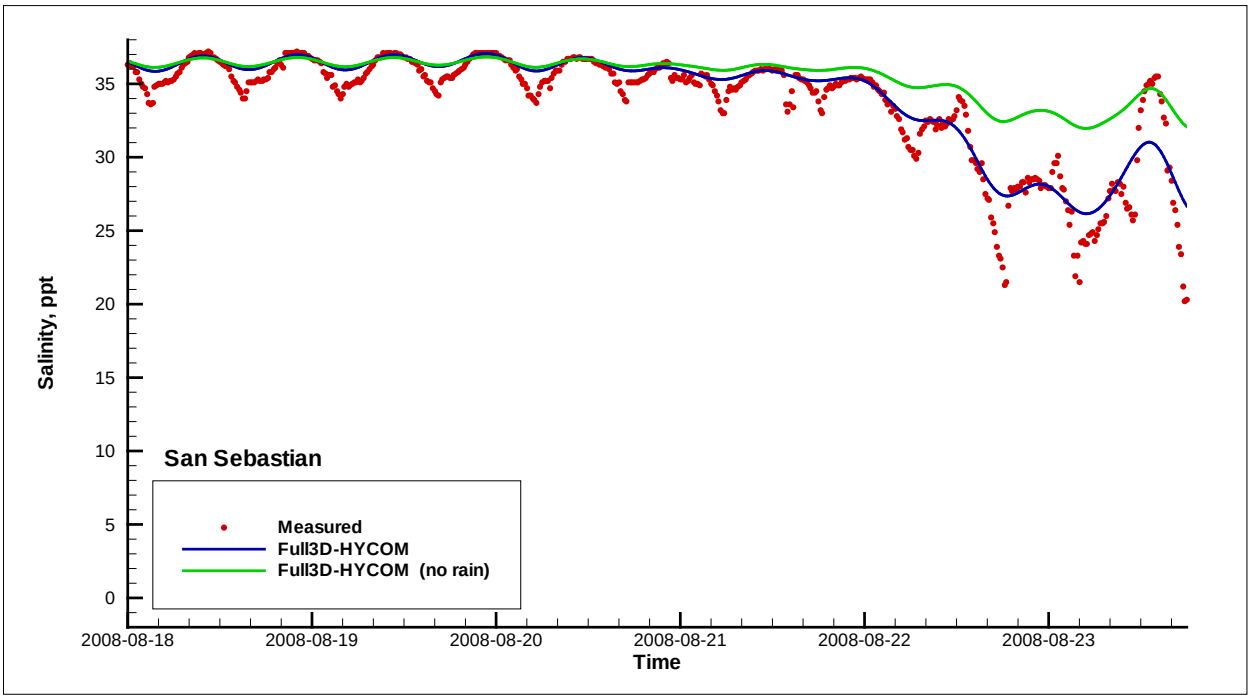

Figure 6-34. Comparison of simulated salinity during tropical storm Fay at San Sebastian station using the Full3D-HYCOM scenario with and without added precipitation

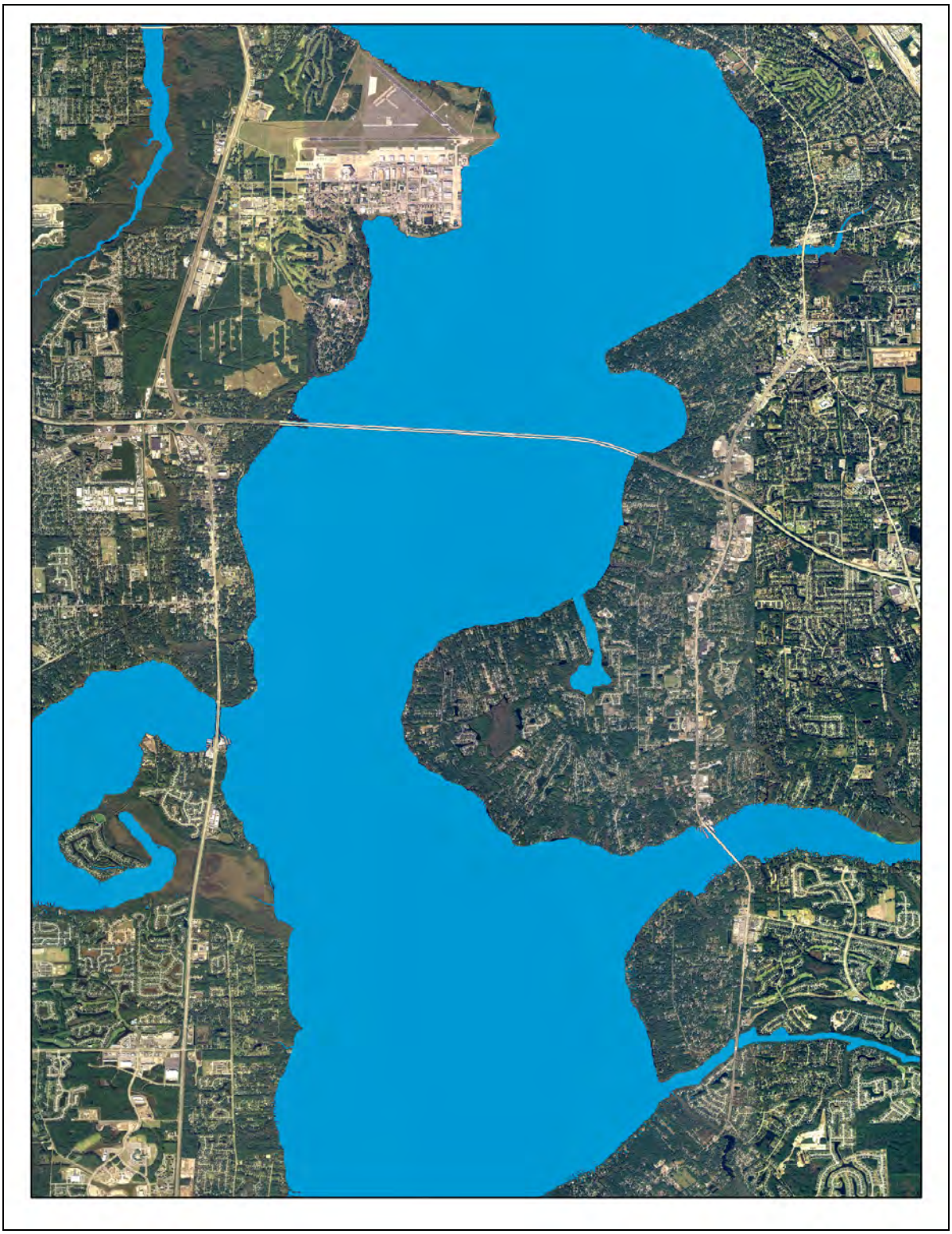

Figure 6-35. Inundation map of Tropical Storm Fay in the vicinity of the I-295 Bridge.

CHAPTER 7
SUMMARY

Summary and Conclusions

This work sought to achieve the following goals:

I) Improve the physics of the SSMS;
II) Improve the performance of SSMS to create a semi-operational forecast system;
III) Validate SSMS with the new data since 2005.

The first goal was achieved by:

a. Developing a wind modeling system (WMS), which contains two parametric synthetic models (ANA and ANA2) and can use a variety of publicly available forecast and analysis wind fields such as GFDL, HWRF, H*Wind, etc. The WMS is a flexible system and allows generating wind forcing fields for ADCIRC, CH3D and SWAN models. It has capabilities for Lagrangian interpolation, wind field blending, and data assimilation. It can also adjust wind fields according to water/land exposure taking advantage of land use data.

b. One-way coupling of a 3D version of CH3D model to NCOM and HYCOM models, thus enabling forecasting of 3D baroclinic flow and salinity transport as well as one-way coupling to a 2D ADCIRC model which allows for fast forecasts of storm surge and inundation.

c. Adding precipitation to the model was found to be particularly useful in simulating Tropical Storm Fay.

The second goal was achieved by:

a. Parallelization of the flooding and drying version of CH3D model and the WMS using OpenMP technique allowing it to take advantage of multiple processors for computing.

b. A job scheduling / submission system was designed, which takes into account properties of SSMS and its models and is able to interact with different popular scheduling / job submission software (Condor, PBS) as well as being able to make use of dedicated local resources accessed via SSH.

c. Automation of data collection, model configuration, pre- and post-processing of data, archival and publishing of the results, which created a semi-operational system that can function for a prolonged amount of time without human intervention.

To achieve the third goal, SSMS was validated with the new data from:

a. Hurricane Wilma (2005) and
b. Tropical Storm Fay (2008).

Comparisons to the data showed that asymmetric parametric synthetic wind model (ANA2) combined with land dissipation effects can provide an adequate wind field for accurate predictions of storm surge and inundation. Verification of SSMS using Fay data demonstrated that inclusion of precipitation and run-off can be very important for accurate prediction of salinity. It was also shown that a 60-hour SSMS forecast in a Fast2D-Waves configuration can be conducted in less than 7 hours and can provide timely warnings that would meet the NWS evacuation clearance times for all Florida counties except Dade County during a Category 5 hurricane. It takes up to 18 hours to provide the most accurate 60-hour forecast possible (Full3D-HYCOM) which includes salinity predictions. While 18 hours is not sufficient to meet the NWS evacuation clearance times for some counties it could be improved in the future as computing resources become more powerful and capable of processing the data faster. It is reasonable to expect to see that time reduced to 8 hours in the next several years and even at 18 hours the forecast can still be useful as it is over 40 hours ahead of event for a 60 hour forecast.

Simulation of Hurricane Wilma demonstrated that dynamic inclusion of tides and model domain resolution can be very important, while simulation of Hurricane Isabel (Sheng et al., 2009) demonstrated that inclusion of wave effects can be very important for accurate prediction of storm surge and inundation. It was also shown that a parametric model based on NHC forecast advisories combined with land-induced wind dissipation can be used to accurately represent the wind field during a storm.

Storm surge and inundation can be predicted accurately, which was shown by comparison with data from Hurricane Wilma (2005) and Tropical Storm Fay (2008), but salinity transport simulation could still be improved by gathering additional precipitation and river flow data in the future.

Discussion and Recommendation

SSMS is a useful tool which can be used to accurately predict storm surge and inundation in the coastal zone. Meeting the NWS evacuation goals, it could become a useful tool for emergency managers, while scientists could find more complex 3D simulations more appealing for studying the effects of storms on the coast and estuaries.

SSMS salinity predictions need to be improved. The main obstacle is the lack of flow data at rivers and streams. That obstacle could be overcome by coupling CH3D model to an existing watershed model which would result in significantly better boundary conditions and have a dramatic effect on accuracy of salinity and baroclinic flow predictions. Therefore, hurricane track and intensity forecast remain the weakest point of the forecast, however, in the past years the accuracy of storm track predictions increased dramatically (Figure 7-1) and NHC has recently been focused on improvement of storm intensity forecasts. Improvements in storm track and intensity forecasting would lead to increasing accuracy of storm surge, inundation as well as salinity predictions.

The accuracy of predictions could also be addressed in a probabilistic sense by producing an ensemble of wind fields based on historical errors (Davis et al., 2007) and conducting simulations for each member of the ensemble to compute a probability of exceeding a certain level or levels of confidence in a forecast based on historical errors.

Two-way coupling between one of the regional models (ADCIRC/HYCOM/NCOM) could be another option to improve the model. Currently, the coastal CH3D model is driven by a regional model at the open boundary, but the coastal model does not feed any information back to the regional model. Such two-way coupling should increase the accuracy of the regional model by providing improved water level and salinity near the shore and inland which in turn would have a positive effect on the results of the coastal model.

Another possible improvement for the SSMS could be the implementation of dynamic model domain. Currently existing model domains (Figure 7-2) could be joined into a continuous domain covering the entire coast of Florida and establishing several lines for dissecting the domain (for example approximately at 50 mile intervals along the coastline, avoiding inlets and complex coastal and estuarine features). Then a domain could be selected automatically based on the area that can potentially be affected by the storm, for example if a storm were to take its path to the Charlotte Harbor and the radius of the storm is estimated at 80 miles the system would select a domain which is limited by preselected dissection lines and extends at least 100 miles in each direction along the coastline such that the entire storm is contained within the coastal domain.

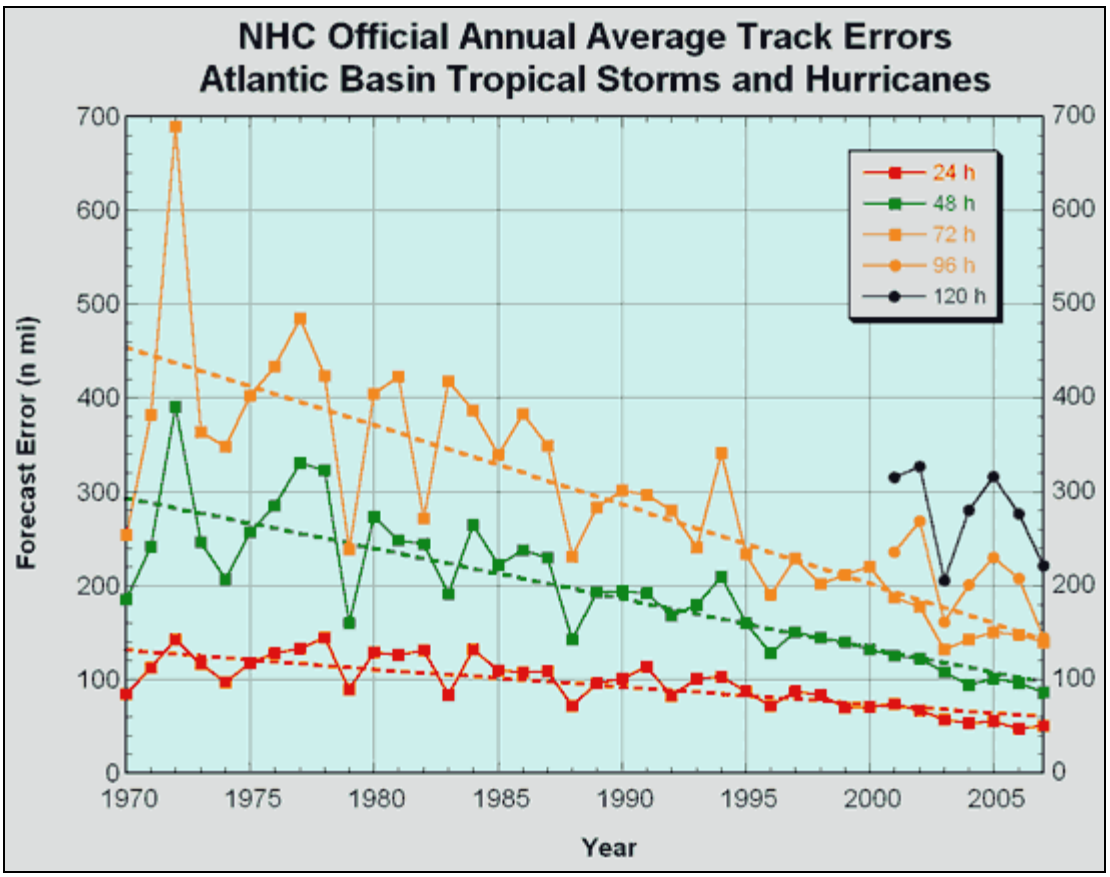

Figure 7-1. NHC official annual average track errors for tropical storms and hurricanes in the Atlantic basin (image courtesy of NHC NOAA)

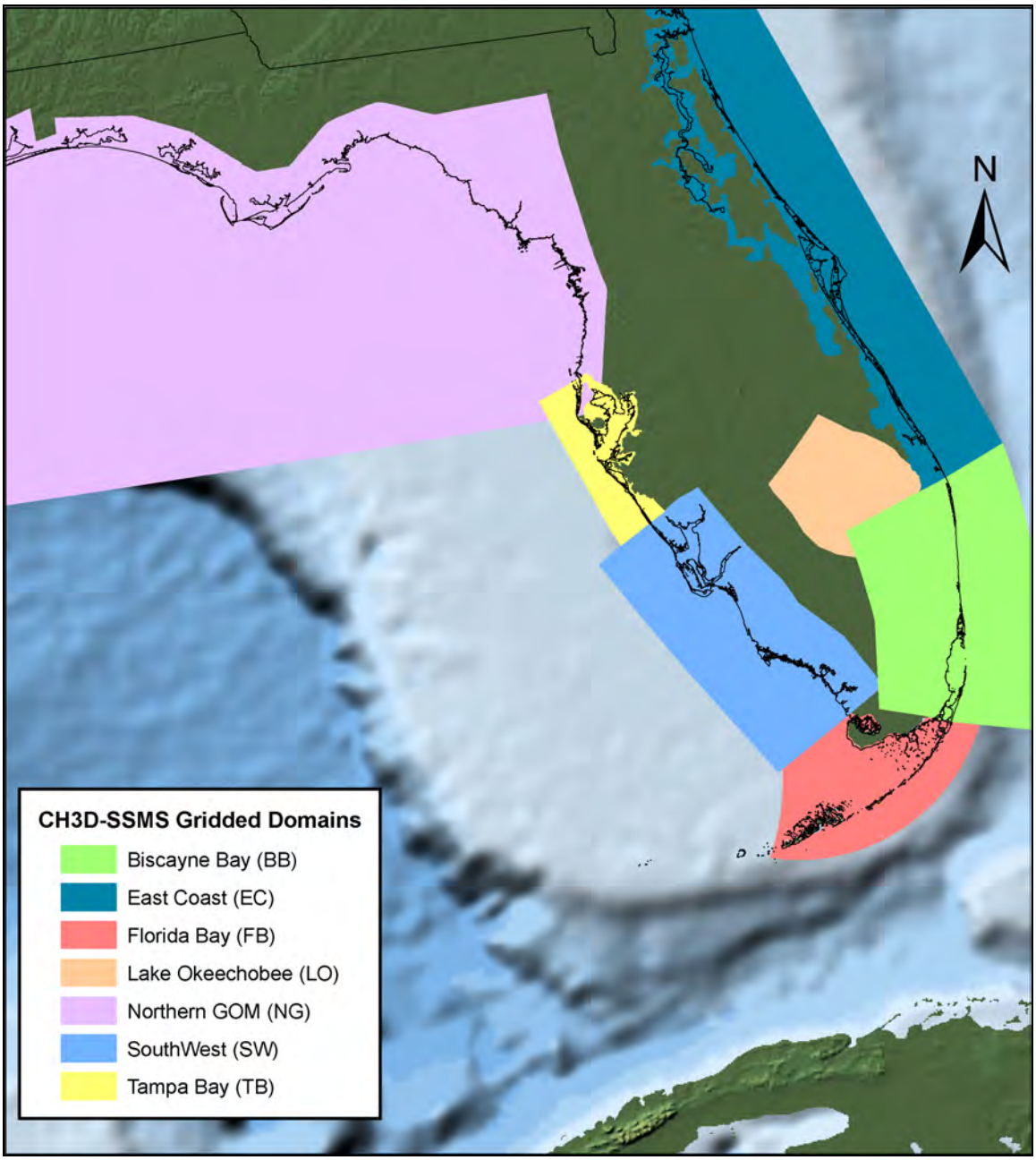

Figure 7-2. CH3D model domains

APPENDIX A
ESTIMATED EVACUATION CLEARANCE TIMES FOR THE STATE OF FLORIDA COUNTIES.

Table A-1 provides estimates of evacuation clearance times for evacuation in case of hurricane event and it was derived from the Appendix F. Estimated Evacuation Clearance Times of the Weather Service Operation Manual (WSOM, 2001).

Table A-1. Estimated evacuation clearance times for the state of Florida counties

County	Cat 1	Cat 2	Cat 3	Cat 4	Cat 5
Note: Longer times for the following counties reflect both slower response times and higher tourist occupancy.					
Escambia	13-17	13-17	16-19	16-19	16-19
Santa Rosa	7-11	7-11	8-13	8-13	8-13
Okaloosa	13-17	13-17	15-19	15-19	15-19
Walton	7-13	7-13	8-15	8-15	8-15
Bay	22-30	22-30	26-34	26-34	26-34
Note: Longer times for the following counties reflect slower response times only.					
Gulf	11-21	11-21	12-24	12-24	12-24
Franklin	11-24	11-24	13-30	13-30	13-30
Wakulla	5-11	5-11	5-11	5-11	5-11
Jefferson	5-11	5-11	5-11	5-11	5-11
Leon (Inland)	5-11	5-11	7-11	7-11	7-11
Gadsen (Inland)	5-11	5-11	5-11	5-11	5-11
Liberty (Inland)	5-11	5-11	5-11	7-11	7-11
Calhoun (Inland)	5-11	5-11	5-11	5-11	5-11
Jackson (Inland)	5-11	5-11	5-11	5-11	5-11
Note: The following counties have no "official" evacuation clearance times.					
Taylor					
Dixie					
Note: Longer lead times for the following counties reflect background traffic evacuating from other regions.					
Levy	14-20	14-20	15-41	16-42	17-43
Citrus	13-23	12-23	17-42	18-43	19-43
Hernando	14-27	14-28	18-44	17-43	19-45
Note: Longer times for the following counties reflect slower response times only.					
Pasco	11-16	11-16	19	19	19
Pinellas	13-16	13-16	18-24	18-24	18-24
Hillsboro	13-16	13-16	18-22	18-22	18-22
Manatee	14	14	14-18	14-18	14-18

Table A-1. Continued

Note: Longer lead times for the following counties reflect no traffic management.					
Sarasota	6-9	6-9	8-10	10-13	10-13
Charlotte	7-13	7-19	11-31	11-31	11-31
Lee	9-13	18-27	23-31	23-31	23-31
Note: Slow response times based on normal summer occupancy (first time listed) to peak fall occupancy (second time listed) assuming 50% evacuation on non-surge population.					
Collier	12	10-17	13-20	14-20	14-20
Note: Longer times for the following counties reflect slower response times only.					
Monroe (Middle and Upper Keys)	11-17	11-17	19-27	19-27	19-27
Monroe (Lower and Middle Keys)	11-17	11-17	21-30	21-30	21-30
Monroe (All Keys)	17-25	17-25	29-38	29-38	29-38
Note: Slow response times based on normal summer occupancy (first time listed) to peak fall occupancy (second time listed) assuming 50% evacuation on non-surge population.					
Dade	28-33	46-52	46-52	71-81	71-81
Broward	21	21	26	26	26
Palm Beach	16	16	16	16	16
Note: Times for the following counties are based on specific hurricane landfall scenarios--not on Sea, Lake, and Overland Surge or Maximum Envelope Of Water models.					
Martin	7-11	7-11	9-17	9-17	9-17
St. Lucie	8	8	14	14	14-20
Indian River	12	12	12	12	12
Note: Longer times for the following counties reflect slower response times only.					
Brevard	8-12	8-12	8-12	8-12	8-12
Volusia	5-10	5-10	9-17	9-17	9-17
Putnam	4-9	4-9	4-9	4-9	4-9
Flagler	4-9	4-9	4-9	4-9	4-9
St. Johns	4-10	4-10	15-17	15-17	15-17
Duval	7-10	7-10	15-17	15-17	15-17
Nassau	5-10	5-10	5-10	5-10	5-10

APPENDIX B
NOAA NOS SKILL ASSESSMENT PROCEDURES

The following variables for model skill assessment and acceptance criteria for these variables are listed in the tables below. Table B-1 defines in detail each variable that is used in the skill assessment procedures. Table B-2 lists the acceptance criteria for each one of these variables, while Table B-3 contains the components that are required for model skill assessment of water level.

Table B-1. Skill assessment variables

Variable	Explanation
Error	The error is defined as the predicted value p minus the observed (or reference) value r: $e_i = p_i - r_i$
SM	Series Mean. The mean value of a time series of y. Calculated as $\overline{y} = \frac{1}{N}\sum_{i=1}^{N} y_i$
RMSE	Root Mean Square Error. Calculated as $RMSE = \sqrt{\frac{1}{n}\sum_{i=1}^{N} e_i^2}$
SD	Standard Deviation. Calculated as $SD = \sqrt{\frac{1}{N-1}\sum_{i=1}^{N}\left(e_i - \overline{e}\right)^2}$
CF(X)	Central Frequency. Fraction (percentage) of errors that lie within the limits $\pm X$.
POF(X)	Positive Outlier Frequency. Fraction (percentage) of errors that are greater than X.
NOF(X)	Negative Outlier Frequency. Fraction (percentage) of errors that are less than $-X$.

Table B-1. Continued

MDPO(X)	Maximum Duration of Positive Outliers. A positive outlier event is two or more consecutive occurrences of an error greater than X . MDPO is the length (number of consecutive occurrences) of the longest event.
MDNO(X)	Maximum Duration of Negative Outliers. A negative outlier event is two or more consecutive occurrences of an error less than $-X$. MDNO is the length (number of consecutive occurrences) of the longest event.
WOF(X)	Worst Case Outlier Frequency. Fraction (percentage) of errors that, given an error of magnitude exceeding X , that (1) the simulated value of water level is greater than the astronomical tide and the observed value is less than the astronomical tide or (2) the simulated value of water level is less than the astronomical tide and the observed value is greater than the astronomical tide.
PCD	Principal Current Direction. For an eastward current u and northward current v (Preisendorfer,1988), $$PCD = \frac{1}{2}\arctan\left(\frac{2\sum_{i=1}^{N}(u_i-\bar{u})(v_i-\bar{v})}{\sum_{i=1}^{N}(u_i-\bar{u})^2-\sum_{i=1}^{N}(v_i-\bar{v})}\right)+m\frac{\pi}{2}$$ where m is either 0 or 1, whichever maximizes s^2 $$s^2(PCD)=\cos^2(PCD)\sum_{i=1}^{N}(u_i-\bar{u})^2+\sin(PCD)\cos(PCD)\sum_{i=1}^{N}(u_i-\bar{u})(v_i-\bar{v})+\sin^2(PCD)\sum_{i=1}^{N}(v_i-\bar{v})^2$$ PCD is counterclockwise from east and may represent either the flood or ebb direction.

Table B-2. Standard suite and standard criteria for skill assessment

Standard Suite of Skill Assessment Parameters { Given X }	Standard Criteria for Acceptance {Given N }
SM, RMSE, SD	None
CF(X)	CF(X) > 90%
POF(2X), MDPO(2X)	POF(2X) < 1%, MDPO(2X) < N
NOF(2X), MDNO(2X)	NOF(2X) < 1%, MDNO(2X) < N

Table B-3. Components of model skill assessment for water levels

Variable		Skill Assessment Parameters	Acceptance Criteria
Scenarios: Test Nowcast and Semi-operational Nowcast			
WL		Standard Suite {X=15cm} WOF(30cm)	Standard Criteria{N=24hr} WOF < ½%
AHW, ALW		Standard Suite {X=15cm}	Standard Criteria {N=3}
THW, TLW		Standard Suite {X=30min}	Standard Criteria {N=3}
Scenarios: Test Forecast and Semi-operational Forecast			
WL		Standard Suite {X=15cm} WOF(30cm)	Standard {N=3}, BPA WOF < ½% , BPA
AHW, ALW		Standard Suite {X=15cm}	Standard {N=3}, BPA
THW, TLW		Standard Suite {X=30min}	Standard {N=3}, BPA

APPENDIX C
VERTICAL DATUMS

The data in this appendix relates three datums: Mean Seal Level (MSL), Mean Lower Low Water Level (MLLW) and North American Vertical Datum established in 1988 (NAVD88). These elevations were used to convert water level data and bathymetry data from MSL and MLLW to NAVD88 at locations where NAVD88-based data is not available. Table C-1 and Table C-2 contain elevations for the East Coast (EC) and the Southwest (SW) modeling domains respectively. All elevations are in feet and are based on present Epoch 1983-2001. The data were obtained from the NOAA Tides and Currents website (NOAA Tides and Currents, 2009).

Table C-1. Datums for the East Coast of Florida domain (EC) from St. Lucie Inlet and to the Florida - Georgia border

Name	ID	Lat	Lon	NAVD88	MSL	MLLW
Peck Lake, St. Lucie Inlet , FL	8722404	27° 6.8' N	80° 8.7' W	4.89	3.98	3.20
Port Salerno , FL	8722383	27° 9.1' N	80° 11.7' W	3.05	2.04	1.47
Sewall Point. St. Lucie River , FL	8722371	27° 10.5' N	80° 11.3' W	5.14	4.13	3.53
Stuart, St. Lucie River , FL	8722357	27° 12' N	80° 15.5' W	4.12	3.30	2.75
North Fork, St. Lucie River , FL	8722334	27° 14.6' N	80° 18.8' W	2.35	1.45	0.82
Fort Pierce, South Jetty , FL	8722212	27° 28.2' N	80° 17.3' W	5.71	4.60	3.08
Vero Beach (Ocean) , FL	8722105	27° 40.2' N	80° 21.6' W	3.61	2.47	0.59
Wabasso, Ndian River , FL	8722059	27° 45.3' N	80° 25.5' W	3.40	2.49	2.26
Sebastian, Indian River , FL	8722029	27° 48.7' N	80° 27.8' W	4.36	3.47	3.25
Sebastian Inlet , FL	8722004	27° 51.6' N	80° 26.9' W	4.33	3.13	1.90
Micco, Indian River , FL	8721994	27° 52.4' N	80° 29.8' W	4.41	3.58	3.37
Turtle Mound , FL	8721223	28° 55.6' N	80° 49.5' W	3.69	3.29	3.11
Edgewater, Indian River , FL	8721191	28° 59.3' N	80° 54' W	4.19	3.70	2.68
Ponce De Leon Inlet South , FL	8721147	29° 3.8' N	80° 54.9' W	4.72	3.81	2.14
Halifax River, Ponce Inlet , FL	8721138	29° 4.9' N	80° 56.2' W	5.19	4.45	2.94
North Turnbull Bay , FL	8721136	29° 5' N	80° 58' W	3.73	3.19	2.55
Daytona Beach Shores , FL	8721120	29° 8.8' N	80° 57.8' W	5.25	4.46	2.39

Table C-1. Continued

Ormond Beach , FL	8720954	29° 17.1' N	81° 3.2' W	3.22	2.84	2.48
Fort Matanzas , FL	8720686	29° 42.9' N	81° 14.3' W	5.34	4.88	2.69
Anastasia Island , FL	8720623	29° 47.6' N	81° 16.3' W	4.79	4.43	1.92
St. Augustine Beach, Atlantic Ocean , FL	8720587	29° 51.4' N	81° 15.8' W	6.14	5.44	3.01
St. Augustine , FL	8720576	29° 53.5' N	81° 18.6' W	4.70	4.20	1.77
Oak Landing , FL	8720305	30° 15.2' N	81° 25.8' W	5.48	5.27	2.67
Jacksonville Beach , FL	8720291	30° 17' N	81° 23.2' W	9.36	8.77	6.22
Pablo Creek , FL	8720267	30° 19.4' N	81° 26.3' W	6.41	5.98	3.79
Little Talbot Island , FL	8720194	30° 25.8' N	81° 24.3' W	6.06	5.61	2.78
Fort George Island, FL	8720186	30° 26.4' N	81° 26.3' W	6.21	5.86	3.24
Simpson Creek, FL	8720168	30° 27.9' N	81° 25.9' W	5.71	5.25	2.53
Nassau River Entrance, FL	8720135	30° 31.1' N	81° 27.2' W	6.42	5.93	3.23
Sawpit Creek Entrance , FL	8720137	30° 30.8' N	81° 27.4' W	7.66	7.15	4.45
Amelia City, South Amelia River, FL	8720086	30° 35.2' N	81° 27.8' W	4.84	4.44	1.55
Kingsley Creek, Seaboard R.r., FL	8720058	30° 37.9' N	81° 28.6' W	5.32	4.84	1.57
Fernandina Beach, Amelia River, FL	8720030	30° 40.3' N	81° 27.9' W	5.52	4.99	1.70
Chester, Bells River, FL	8720023	30° 41' N	81° 32' W	5.92	5.55	2.03

Table C-2. Datums for the SouthWest modeling domain (SW) covering the coastline from the Everglades City to Captiva Island in the Charlotte Harbor

Name	ID	Lat	Lon	NAVD88	MSL	MLLW
Everglades City , FL	8724948	25° 51.5' N	81° 23.2' W	4.17	3.49	2.09
Marco Island, Caxambas Pass , FL	8724967	25° 54.5' N	81° 43.7' W	3.54	2.86	1.18
Marco, Big Marco River , FL	8724991	25° 58.3' N	81° 43.7' W	3.60	2.97	1.47
Mcilvaine Bay , FL	8724996	25° 59.1' N	81° 42.1' W	2.60	2.01	0.57
Keewaydin Island, Inside , FL	8725019	26° 1.5' N	81° 46.1' W	2.63	2.08	0.63
Naples Bay, North , FL	8725114	26° 8.2' N	81° 47.3' W	3.93	3.43	1.86
Naples, Gulf Of Mexico , FL	8725110	26° 7.8' N	81° 48.4' W	4.43	3.79	2.14
Water Turkey Bay , FL	8725222	26° 16.6' N	81° 49.5' W	4.76	4.23	3.03
Cocohatchee River, U.s. 41 , FL	8725228	26° 16.9' N	81° 48.1' W	4.94	4.46	3.27
Wiggins Pass, Inside , FL	8725235	26° 17.4' N	81° 49.1' W	2.83	2.35	1.08
Little Hickory Bay , FL	8725259	26° 19.8' N	81° 50.3' W	3.96	3.65	3.26
Fish Trap Bay , FL	8725272	26° 20.2' N	81° 50.7' W	2.69	2.35	1.88
Imperial River Entrance , FL	8725269	26° 20.2' N	81° 49.8' W	2.86	2.60	2.18
Imperial River, Headwaters , FL	8725271	26° 20.6' N	81° 46.8' W	3.95	3.68	3.26
Coconut Point, Estero Bay , FL	8725319	26° 24' N	81° 50.6' W	3.72	3.34	1.97
Estero Island, Estero Bay , FL	8725351	26° 26.3' N	81° 55.1' W	4.41	3.70	2.30
Matanzas Pass, Estero Island , FL	8725366	26° 27.4' N	81° 57.2' W	3.41	2.68	1.22
Fort Myers, Caloosahatchee River , FL	8725520	26° 38.8' N	81° 52.3' W	5.40	4.99	4.36
Bokellia, Charlotte Harbor , FL	8725541	26° 42.4' N	82° 9.8' W	4.65	3.95	3.02
Placida, Gasparilla Sound , FL	8725667	26° 50' N	82° 15.9' W	4.54	4.04	3.26
Englewood, Lemon Bay , FL	8725747	26° 56' N	82° 21.2' W	4.26	3.62	2.82
Manasota , FL	8725809	27° 0.7' N	82° 24.6' W	4.11	3.63	2.76
El Jobean, Myakka River , FL	8725769	26° 57.7' N	82° 12.6' W	3.45	2.93	1.84
Punta Gorda , FL	8725744	26° 55.7' N	82° 3.9' W	4.58	4.01	2.94
Harbour Heights, Peace River, FL	8725791	26° 59.3' N	81° 59.6' W	4.50	4.07	2.97
Shell Creek, Peace River , FL	8725781	26° 58.8' N	81° 57.6' W	4.42	4.03	2.87
Liverpool, Peace River , FL	8725835	27° 2.6' N	81° 59.2' W	4.96	4.58	3.40
Myakka River, Us 41 , FL	8725837	27° 2.7' N	82° 17.6' W	5.15	4.79	3.77
Venice, Gulf Of Mexico , FL	8725858	27° 4.3' N	82° 27.2' W	2.64	2.19	1.02

APPENDIX D
CH3D MODEL GOVERNING EQUATIONS

Governing equations

Governing equations in Cartesian coordinate system

In Cartesian coordinate system, the governing equations for water continuity, X-momentum, and Y-momentum equations are:

$$\frac{\partial u}{\partial x}+\frac{\partial v}{\partial y}+\frac{\partial w}{\partial z}=0 \tag{D-1}$$

$$\frac{\partial u}{\partial t}+\frac{\partial uu}{\partial x}+\frac{\partial uv}{\partial y}+\frac{\partial uw}{\partial z}+\frac{1}{\rho_w}\frac{\partial S_{xx}}{\partial x}+\frac{1}{\rho_w}\frac{\partial S_{xy}}{\partial y}$$
$$=-g\frac{\partial \zeta}{\partial x}-\frac{1}{\rho_w}\frac{\partial P_a}{\partial x}+fv+A_H\left(\frac{\partial^2 u}{\partial x}+\frac{\partial^2 u}{\partial y}\right)+\frac{\partial}{\partial z}\left(A_V\frac{\partial u}{\partial z}\right) \tag{D-2}$$

$$\frac{\partial v}{\partial t}+\frac{\partial uv}{\partial x}+\frac{\partial vv}{\partial y}+\frac{\partial vw}{\partial z}+\frac{1}{\rho_w}\frac{\partial S_{yx}}{\partial x}+\frac{1}{\rho_w}\frac{\partial S_{yy}}{\partial y}$$
$$=-g\frac{\partial \zeta}{\partial y}-\frac{1}{\rho_w}\frac{\partial P_a}{\partial y}-fu+A_H\left(\frac{\partial^2 v}{\partial x}+\frac{\partial^2 v}{\partial y}\right)+\frac{\partial}{\partial z}\left(A_V\frac{\partial v}{\partial z}\right) \tag{D-3}$$

where $u(x,y,z,t)$, $v(x,y,z,t)$ and $w(x,y,z,t)$ are the velocity vector components in x-, y-, and z-coordinate directions, respectively; t is time; $\varsigma(x,y,t)$ is the free surface elevation; g is the acceleration of gravity; A_H and A_V are the horizontal and vertical turbulent eddy coefficients, respectively; S_{xx}, S_{xy}, S_{yy} are radiation stresses, P_a is atmospheric pressure and f is the Coriolis parameter. A_V is calculated by the vertical turbulence model described in Sheng and Villaret (1989), and A_H by a Smargorinsky-type formula.

Non-dimensional equations in curvilinear coordinate system

The non-dimensional form of above equations in curvilinear, boundary-fitted grid system is (Sheng, 1987, 1990):

$$\frac{\partial \zeta}{\partial t}+\frac{\beta}{\sqrt{g_0}}\left[\frac{\partial}{\partial \xi}\left(\sqrt{g_0}Hu\right)+\frac{\partial}{\partial \eta}\left(\sqrt{g_0}Hv\right)\right]+\beta\frac{\partial H\omega}{\partial \sigma}=0 \tag{D-4}$$

$$\frac{1}{H}\frac{\partial Hu}{\partial t} = -(g^{11}\frac{\partial \zeta}{\partial \xi} + g^{12}\frac{\partial \zeta}{\partial \eta}) + -(g^{11}\frac{\partial P}{\partial \xi} + g^{12}\frac{\partial P}{\partial \eta}) + (\frac{g_{12}}{\sqrt{g_0}}u + \frac{g_{22}}{\sqrt{g_0}}v)$$
$$-\frac{R_0}{g_0}\left\{x_\eta\left[\frac{\partial}{\partial \xi}(y_\xi\sqrt{g_0}S_{xx} + y_\eta\sqrt{g_0}S_{xy}) + \frac{\partial}{\partial \eta}(y_\xi\sqrt{g_0}S_{xy} + y_\eta\sqrt{g_0}S_{yy})\right]\right.$$
$$\left. - y_\eta\left[\frac{\partial}{\partial \xi}(x_\xi\sqrt{g_0}S_{xx} + x_\eta\sqrt{g_0}S_{xy}) + \frac{\partial}{\partial \eta}(x_\xi\sqrt{g_0}S_{xy} + x_\eta\sqrt{g_0}S_{yy})\right]\right\}$$
$$-\frac{R_0}{g_0 H}\left\{x_\eta\left[\frac{\partial}{\partial \xi}(y_\xi\sqrt{g_0}Huu + y_\eta\sqrt{g_0}Huv) + \frac{\partial}{\partial \eta}(y_\xi\sqrt{g_0}Huv + y_\eta\sqrt{g_0}Hvv)\right]\right. \quad \text{(D-5)}$$
$$\left. - y_\eta\left[\frac{\partial}{\partial \xi}(x_\xi\sqrt{g_0}Huu + x_\eta\sqrt{g_0}Huv) + \frac{\partial}{\partial \eta}(x_\xi\sqrt{g_0}Huv + x_\eta\sqrt{g_0}Hvv)\right] - g_0\frac{\partial Hu\omega}{\partial \sigma}\right\}$$
$$+\frac{E_v}{H^2}\frac{\partial}{\partial \sigma}(A_v\frac{\partial u}{\partial \sigma}) + E_H A_H(\text{Horizontal Diffusion of } u)$$
$$-\frac{R_0}{F_r^2}\left[H\int_\sigma^0(g^{11}\frac{\partial \rho}{\partial \xi} + g^{12}\frac{\partial \rho}{\partial \eta})d\sigma + (g^{11}\frac{\partial H}{\partial \xi} + g^{12}\frac{\partial H}{\partial \eta})(\int_\sigma^0 \rho d\sigma + \sigma p)\right]$$

$$\frac{1}{H}\frac{\partial Hv}{\partial t} = -(g^{21}\frac{\partial \zeta}{\partial \xi} + g^{22}\frac{\partial \zeta}{\partial \eta}) - (g^{21}\frac{\partial P}{\partial \xi} + g^{22}\frac{\partial P}{\partial \eta}) - (\frac{g_{11}}{\sqrt{g_0}}u + \frac{g_{21}}{\sqrt{g_0}}v)$$
$$-\frac{R_0}{g_0}\left\{x_\xi\left[\frac{\partial}{\partial \xi}(y_\xi\sqrt{g_0}S_{yx} + y_\eta\sqrt{g_0}S_{yy}) + \frac{\partial}{\partial \eta}(y_\xi\sqrt{g_0}S_{yx} + y_\eta\sqrt{g_0}S_{yy})\right]\right.$$
$$\left. - y_\eta\left[\frac{\partial}{\partial \xi}(x_\xi\sqrt{g_0}S_{xx} + x_\eta\sqrt{g_0}S_{yx}) + \frac{\partial}{\partial \eta}(x_\xi\sqrt{g_0}S_{yx} + x_\eta\sqrt{g_0}S_{yy})\right]\right\}$$
$$-\frac{R_0}{g_0 H}\left\{x_\xi\left[\frac{\partial}{\partial \xi}(y_\xi\sqrt{g_0}Huv + y_\eta\sqrt{g_0}Hvv) + \frac{\partial}{\partial \eta}(y_\xi\sqrt{g_0}Huv + y_\eta\sqrt{g_0}Hvv)\right]\right. \quad \text{(D-6)}$$
$$\left. - y_\eta\left[\frac{\partial}{\partial \xi}(x_\xi\sqrt{g_0}Huu + x_\eta\sqrt{g_0}Huv) + \frac{\partial}{\partial \eta}(x_\xi\sqrt{g_0}Huv + x_\eta\sqrt{g_0}Hvv)\right] - g_0\frac{\partial Hv\omega}{\partial \sigma}\right\}$$
$$+\frac{E_v}{H^2}\frac{\partial}{\partial \sigma}(A_v\frac{\partial v}{\partial \sigma}) + E_H A_H(\text{Horizontal Diffusion of } v)$$
$$-\frac{R_0}{F_r^2}\left[H\int_\sigma^0(g^{21}\frac{\partial \rho}{\partial \xi} + g^{22}\frac{\partial \rho}{\partial \eta})d\sigma + (g^{21}\frac{\partial H}{\partial \xi} + g^{22}\frac{\partial H}{\partial \eta})(\int_\sigma^0 \rho d\sigma + \sigma p)\right]$$

where

η, ξ and σ are the transformed coordinates;

u, v, w are non-dimensional contra-variant velocities in curvilinear grid (η, ξ, σ).

$\sqrt{g_0}$ is the Jacobian of horizontal transformation;

$g^{11}, g^{22}, g_{11}, g_{12}, g_{22}$ are the metric coefficients of coordinate transformations;

β is non-dimensional parameter;

ζ is water level;

It can be shown (Sun and Sheng, 2008) that the wave-averaged equations (D-4) to (D-6) can be used throughout the water column by computing the wave radiation stress differently for two regions of it. The radiation stress is computed as vertically uniform and is based on Longuet-Higgins and Stewart (1964) which is valid for the region below the wave trough where there is no Stokes drift, in the region between the wave trough and the water free surface an additional term due to the wave roller that represents the Stokes drift is used.

The governing equations are written for three dimensions, however, in the numerical solution it is possible to only solve two dimensional vertically integrated equations which results in significant savings in computational time and results of a 2D model can still be very useful in many practical applications.

Model boundary conditions

The boundary condition of the CH3D model at the free surface is calculated using

$$\tau_x^w = \rho_a C_d u_w W_s \tag{D-7}$$

$$\tau_y^w = \rho_a C_d v_w W_s \tag{D-8}$$

where u_w and v_w are wind speed components, and W_s is the total wind speed. The drag coefficient, C_d is calculated using Garratt (1977) formulation:

$$C_d = 0.001 \times \left(0.75 + 0.067 W_s\right) \tag{D-9}$$

A cap is enforced on a C_d and it cannot be larger than 0.003 in which cased it is forced to the value of 0.003.

The boundary condition at the bottom is expressed in terms of bottom stress given by the quadratic law:

$$\tau_{\mathrm{bx}} = \rho_w C_d u_b \sqrt{u_b^2 + v_b^2} \tag{D-10}$$

$$\tau_{\mathrm{by}} = \rho_w C_d v_b \sqrt{u_b^2 + v_b^2} \tag{D-11}$$

where u_b and v_b are bottom velocities and C_d is the drag coefficient which is defined using the formulation by Sheng (1983):

$$C_d = \left(\kappa / \ln\left(z_1 / z_0\right)\right)^2 \tag{D-12}$$

where $\kappa = 0.4$ is the von Karman constant. The formulation states that the coefficient is a function of the size of the bottom roughness, z_0, and the height at which u_b is measured, z_1 is within the constant flux layer above the bottom. The size of the bottom roughness can be expressed in terms of the Nikuradse equivalent sand grain size, k_s, using the relation $z_0 = k_s / 30$.

In the two-dimensional mode, the bottom boundary conditions are given using the Chezy-Manning formulation:

$$\tau_{\mathrm{bx}} = \rho A_v \frac{\partial u_b}{\partial z} = \frac{g u_b \sqrt{u_b^2 + v_b^2}}{C_z^2} \tag{D-13}$$

$$\tau_{\mathrm{by}} = \rho A_v \frac{\partial v_b}{\partial z} = \frac{g v_b \sqrt{u_b^2 + v_b^2}}{C_z^2} \tag{D-14}$$

where C_z is the Chezy friction coefficient defined as

$$C_z = 4.64\frac{R^{\frac{1}{6}}}{n} \tag{D-15}$$

where R is the hydraulic radius which can be approximated by the total depth given in centimeters, and n is Manning's n.

Wave-enhanced surface roughness, z_0, and drag coefficient, C_{de}, developed by Donelan et al. (1993), are used to calculate wind stress at the free surface. Both the surface roughness and the drag coefficient are functions of wave age and roughness increases when the waves are young and makes the wind stress higher compared to when the waves are fully developed.

$$z_0 = 3.7 \cdot 10^{-5}\left(\frac{W_s^2}{g}\right)\left(\frac{W_s^2}{C_p}\right)^{0.9} \tag{D-16}$$

where W_s is the wind speed at 10 m above air-sea interface. Following the relation between z_0 and C_d, $z_0 = z \cdot \exp\left(-\kappa \Big/ \sqrt{C_d(z)}\right)$, yields the wave-enhanced drag coefficient

$$C_{de} = \left[\frac{\kappa}{\ln\left(3.7 \cdot 10^{-5}\left(\frac{W_s^2}{gz}\right)\left(\frac{W_s}{C_p}\right)^{0.9}\right)}\right]^2 \tag{D-17}$$

where C_p is wave phase speed and W_s/C_p represents the inverse wave age.

Wave-Enhanced Bottom Stress

Wave-enhanced bottom stress is implemented in CH3D using two methods. The first method uses a simplified formulation developed by Signell et al. (1990) based on the Grant and Madsen (1979) theory for a wave-averaged bottom boundary layer. The second method resolves a turbulent wave-current boundary level by using a comprehensive look-up table for wave-current bottom stress developed with a turbulent closure model of Sheng and Villaret (1989).

The Grant and Madsen (1979) formulation is given by the typical quadratic law with one distinction where C_{de} is the wave-enhanced drag coefficient.

$$\tau_{\mathrm{bx}} = \rho C_{de} u_b \sqrt{u_b^2 + v_b^2} \tag{D-18}$$

$$\tau_{\mathrm{by}} = \rho C_{de} v_b \sqrt{u_b^2 + v_b^2} \tag{D-19}$$

The main assumption used in the formulation is that for a co-linear flow, the maximum bottom shear stress is defined as

$$\tau_{b,\max} = \tau_c + \tau_w \tag{D-20}$$

where τ_c is the bottom stress due to current and τ_w is the maximum stress due to waves which can be determined from

$$\tau_w = \frac{1}{2} \rho f_w u_w^2 \tag{D-21}$$

where u_w is the near-bottom wave orbital velocity and f_w is the wave friction factor which depends on the bottom roughness, k_s. The final expression for the wave-enhanced drag coefficient at the reference height, z_r, chosen to lie above the wave boundary layer is

$$C_{de} = \left(\frac{\kappa}{\ln\left(30 z_r / k_{bc}\right)} \right)^2 \tag{D-22}$$

Following Signell et al. (1990), the reference height z_r was specified as 20 cm and $k_s = 0.1\,\mathrm{cm}$ was selected to correspond to a drag coefficient of $1.5 \cdot 10^{-3}$ at one meter above the bed in the absence of waves. The effective drag coefficient C_{de} is used to compute bottom stress as defined by equations (D-18) and (D-19).

The second formulation uses a turbulent closure model (Sheng and Villaret, 1989) to calculate the wave-current bottom shear stress inside a turbulent wave-current bottom boundary

layer. The wave-resolving governing equations for the combined wave-current bottom boundary layer are:

$$\frac{\partial u}{\partial t} = -\frac{1}{\rho}\frac{\partial p}{\partial x} + \frac{\partial}{\partial z}\left(A_v \frac{\partial u}{\partial z} \right) \tag{D-23}$$

$$\frac{\partial u}{\partial t} = -\frac{1}{\rho}\frac{\partial p}{\partial x} + \frac{\partial}{\partial z}\left(A_v \frac{\partial u}{\partial z} \right) \tag{D-24}$$

with the following bottom boundary conditions:

$$\tau_{bx} = A_v \frac{\partial u}{\partial z} = \rho C_d u_1 \sqrt{u_1^2 + v_1^2} \tag{D-25}$$

$$\tau_{by} = A_v \frac{\partial v}{\partial z} = \rho C_d u_2 \sqrt{u_1^2 + v_1^2} \tag{D-26}$$

where u_1, v_1 are velocity components at the lowest grid point, z_1, and C_d is computed by:

$$C_d = \left[\frac{\kappa}{\ln\left(z_1 / z_0 \right)} \right]^2 \tag{D-27}$$

where z_0 is the bottom roughness which was set to 0.1 cm and κ is the von Karman constant. The smallest grid spacing near the bottom is 0.03 cm.

Boundary conditions at the top of the bottom boundary layer, which was set to 30 cm, are:

$$\tau_{sx} = A_v \frac{\partial u}{\partial z} = 0 \tag{D-28}$$

$$\tau_{sy} = A_v \frac{\partial v}{\partial z} = 0 \tag{D-29}$$

To drive a wave-induced oscillatory motion inside the boundary layer, a pressure gradient from the linear wave theory is applied:

$$\left(-\frac{1}{\rho}\frac{\partial p}{\partial x} \right)_w = \frac{1}{2} gkH \frac{\cosh\left(kz \right)}{\cosh\left(kh \right)} \sin\varphi \cos\left(\sigma t \right) \tag{D-30}$$

$$\left(-\frac{1}{\rho}\frac{\partial p}{\partial y}\right)_w = \frac{1}{2} gkH \frac{\cosh(kz)}{\cosh(kh)} \cos\varphi \cos(\sigma t) \tag{D-31}$$

where g is gravitational acceleration, k is wave number, H is wave height, φ is wave direction, and σ is angular wave frequency.

To drive a current inside the boundary layer, a constant pressure gradient is applied in the y-direction:

$$\left(-\frac{1}{\rho}\frac{\partial p}{\partial y}\right)_c = \text{const} \tag{D-32}$$

The vertical turbulent eddy viscosity A_v inside the turbulent wave-current boundary layer is determined using a TKE closure model developed by Sheng and Villaret (1989) and a very small time step which is 1/100-th of the wave period. A total of 145,200 model runs (see Table D-1) are made, taking into account of various combinations of five different model parameters: water depth, wave height, wave period, wave direction and current magnitude. These runs resulted in a comprehensive "look-up table" of bottom shear stress in a wave-current boundary layer. During a CH3D simulation, the bottom stress value at each grid cell is determined by interpolation of the values in the "look-up table" in a five-dimensional space (i.e., water depth, wave height, wave period, wave direction, current magnitude). The current is specified at the lowest grid point, z_1, where CH3D calculates its currents.

Table D-1. Parameters used to create the "look-up" table for wave-enhanced bottom stress

Parameter	Values
Water Depth	0.5 m to 5.0 m with 0.5 m increments
Wave Height	0.0 m to 2.0 m with 0.2 m increments
Wave Period	2 s to 16 s with 1 s increments
Wave Direction	0 deg to 315 deg with 45 deg increments
Current	0.0 m/s to 1.0 m/s with 0.1 m/s increments

Therefore, the water depth within the 1-D model is defined as half of the vertical grid spacing subtracted by the roughness length, and the wave height corresponded to the z_1 point is determined according to the linear wave theory:

$$H_{(z=z_1)} = H_{(z=\zeta)} \frac{\sinh k(h+z_1)}{\sinh k(h+\zeta)} \tag{D-33}$$

where h is local water depth, ζ is water surface elevation, and $H_{(z=\zeta)}$ is wave height at the surface.

Wave-Induced Radiation Stress

The CH3D governing equations include wave-induced radiation stress terms which contribute to wave setup in the near shore region. The radiation stress formulation implemented in the CH3D model includes the classical vertically uniform radiation stress (Longuet-Higgins and Stewart, 1964) throughout the entire water column, plus a contribution (only in the region between the wave trough and the free surface) due to surface roller (Haas and Svendsen, 2000).

The vertically uniform radiation stress terms are:

$$S_{xx} = E\left[n\left(\cos^2\theta + 1\right) - \frac{1}{2} \right] \tag{D-34}$$

$$S_{yy} = E\left[n\left(\sin^2\theta + 1\right) - \frac{1}{2} \right] \tag{D-35}$$

where E is total wave energy, θ is angle between the direction of wave propagation and the x axis (representing onshore direction), and n is the ratio of group velocity to wave celerity.

The radiation stress term representing the flux of the longshore component in the onshore direction is:

$$S_{xy} = \frac{E}{2} n \sin 2\theta \tag{D-36}$$

Vertically-varying radiation stress formulations have been developed (Mellor, 2008) and is being considered to be included into the SSMS, however, additional effort is required to implement and test the method.

Wave-Enhanced Turbulent Mixing

For the vertical eddy viscosity, the equilibrium turbulence closure scheme developed by Sheng and Villaret (1989) was modified to take into account wave effects. To take into account the wave effects, an additional term was added to the vertical eddy viscosity:

$$A_z = A_{zc} + Mh(D_b / \rho)^{1/3} \tag{D-37}$$

where A_{zc} is the eddy viscosity due to the mean currents as computed by Sheng and Villaret's equilibrium closure model, D_b is the wave energy dissipation resulted from wave breaking and bottom friction, h is the water depth and M is a constant. The second term on the right hand side of equation (D-37) represents the contribution to turbulence by waves following Battjes (1975) and De Vriend and Stive (1987).

LIST OF REFERENCES

AHPS, 2009. National Weather Service Advanced Hydrologic Prediction Service. US Department of Commerce, National Oceanic and Atmospheric Administration, National Weather Service, Office of Hydrologic Development. [updated July 30, 2009, cited September 1, 2009]. Available from: http://www.nws.noaa.gov/oh/ahps.

Alymov V., 2005. Integrated modeling of storm surges during hurricanes Isabel, Charley, and Frances. Dissertation, University of Florida, 2005.

Baptista, A.M., Zhang, Y.-L., Chawla, A., Zulauf, M.A., Seaton, C., Myers, E.P., Kindle, J., Wilkin, M., Burla, M., Turner, P.J., 2005. A cross-scale model for 3D baroclinic circulation in estuary-plume-shelf systems: II. Application to the Columbia River. Continental Shelf Research, 25, 935-972.

Barron, C.N., Kara, A.B., Martin, P.J, Rhodes, R.C., Smedstad, L.F., 2005. Formulation, implementation and examination of vertical coordinate choices in the Global Navy Coastal Ocean Model (NCOM). Ocean Modeling 11, 2006, pp. 347-375.

Battjes, J.A., 1975. A note on modeling of turbulence in the surf-zone. Proc. Symp. on Modeling Techniques, San Francisco, CA, pp. 1050-1061.

Black, T.L., 1994: The new NMC mesoscale eta model: Description and forecast examples. Wea. Forecasting, 9, 265-278.

Bleck, R., 2002. An oceanic general circulation model framed in hybrid isopycnic- Cartesian coordinates. Ocean Modeling, 4, 55-88.

Bleck, R., Benjamin, S., 1993. Regional weather prediction with a model combining terrain-following and isentropic coordinates. Part I: Model description. Mon. Wea. Rev., 121, 1770-1785.

Blumberg, A. F., Mellor,G.L., 1987. A description of a three-dimensional coastal ocean circulation model, In Three-Dimensional Coastal Ocean Models, N. S. Heaps (Ed.), 1-16, American Geophysical Union, Washington, DC, 1987.

Booij, N., Ris, R.C., Holthuijsen, L.H., 1999: A third-generation wave model for coastal regions: 1. Model description and validation. Journal of Geophysical Research 104, 7649-7666.

Bright, R.J., Alsheimer, F., Lindner, B.L., Miller, G., Timmons, D., Johnson, J., 2008. An interactive website designed to enhance public understanding of storm surge threats. [cited January 18, 2009]. Available from: http://ams.confex.com/ams/pdfpapers/137579.pdf.

Burchard, H., Baumert, H., 1995. On the performance of a mixed-layer model based on the *k -e* turbulence closure. J. Geophys. Res., 100 (C5), 8523-8540.

Byrne, M., 2006: Monitoring Hurricane Wilma's Storm Surge. Sound Waves, Monthly Newsletter (USGS). February, 2006.

Chen, C., Cowles, G., Beardsley, R.C., 2006. An unstructured grid, finite volume coastal ocean model: FVCOM User Manual, Second Edition. SMAST/UMASSD Technical Report-06-0602, pp. 315.

Chen, C. P. Xue, P., Ding, P., Beardsley, R. C., Xu, Q., Mao, X., Gao, G., Qi, J., Li, C., Lin, H., Cowles, G., Shi, M., 2008. Physical mechanisms for the offshore detachment of the Chanjiang diluted water in the East China Sea, Journal of Geophysical Research, 113.

Cressman, G.P. 1959. An operational objective analysis system. Monthly Weather Review. 87:367-374.

Crossett, K.; Culliton, T.J.; Wiley, P., Goodspeed, T.R., 2004. Population Trends along the Coastal United States, 1980–2008. Silver Spring, Maryland: National Oceanic and Atmospheric Administration, 47p.

Davis, J.R., Paramygin, V. A., Sheng, Y.P., Ganguly, A., Figueiredo, R.J., 2006. Simulation of storm surge using Grid computing. Journal of Estuarine and Coastal Modeling, 2006, vol.9, pp. 357-374.

Davis, J.R., Paramygin, V.A., Sheng, Y.P., 2007. On the use of probabilistic wind fields for forecasting storm surge and inundation. Proc. 10th Conf. Estuarine and Coastal Modeling, 2007, pp. 447-466.

De Vriend, H.J., Stive, M.J.F., 1987. Quasi-3D modelling of nearshore currents, Coastal Engineering 11, 1987, pp. 565-601.

Donelan, M. A., Dobson, F. W., Smith, S. D., Anderson, R. J., 1993. On the dependence of sea-surface roughness on wave development. Journal of Physical Oceanography, 23, pp. 2143-2149.

Eaton, B., Gregory, J., Drach, B., Taylor, K., Hankin, S., 2009. NetCDF Climate and Forecast (CF) Metadata Conventions. Version 1.4, 27 February, 2009.

Emanuel, K. A., 2005. Increasing destructiveness of tropical cyclones over the past 30 years. Nature, 436, 686-688.

FCMP, 2008. Florida Coastal Monitoring Program. University of Florida Civil and Coastal Engineering. [updated September 5, 2008, cited May 12, 2009]. Available from: http://fcmp.ce.ufl.edu.

Florida Coastal and Ocean Coalition, 2008. Preparing for a Sea Change in Florida. A Strategy to Cope with the Impacts of Global Warming on the State's Coastal and Marine Systems. Report, 2008. [cited May 18, 2009]. Available from: http://www.flcoastalandocean.org/PreparingforaSeaChange.

Florida Department of Environmental Protection, 2006. Economics of Beach Tourism in Florida. [cited May 18, 2009] Available from: http://www.dep.state.fl.us/beaches/publications/pdf/phase2.pdf.

Masters, F. J., 2004: Measurement, Modeling and Simulation of Ground Level Tropical Cyclone Winds. PhD Dissertation, 2004, University of Florida.

Garratt, J. R., 1977. Review of drag coefficients over oceans and continents. Monthly Weather Review, 105, pp. 915-929.

GEODAS, 2009. NGDC/WDC MGG, Boulder-Geophysical Data System (GEODAS). [updated July 30, 2009, cited September 1, 2009]. Available from: http://www.ngdc.noaa.gov/mgg/geodas).

Graber, H. C., Donelan, M. A., Brown, M. G., 2009. Real-Time Forecasting System of Winds, Waves and Surge in Tropical Cyclones. [cited May 17, 2008]. Available from: http://hurricanewaves.org.

Grant, W. D., Madsen, O. S., 1979. Combined wave and current interaction with a rough bottom. Journal of Geophysical Research, 84, pp. 1797-1808.

Granthem, K. N., 1953. Wave run-up on sloping structures. Transactions of the American Geophysical Union 34 (5): 720–724.

Grid Appliance Team, 2009. Grid appliance user interface. [cited May 20, 2009]. Available from: http://www.grid-appliance.org.

Haas, K.A., Svendsen, I.A., 2000. Three-dimensional modeling of rip current systems. Rep. No. CACR-00-06, 250 pp.

Halliwell, Jr., G. R., Bleck, R., Chassignet, E., 1998. Atlantic Ocean simulations performed using a new hybrid-coordinate ocean model (HYCOM). EOS, Trans. AGU, Fall 1998 AGU Meeting.

Halliwell, Jr., G.R., Bleck, R., Chassignet, E. P., Smith, L.T., 2000. Mixed layer model validation in Atlantic Ocean simulations using the Hybrid Ocean Model (HYCOM). EOS, 80, OS304.

Hasselmann, K., Barnett, T. P., Bouws, E., Carlson, H., Cartwright, D. E., Enke, K., Ewing, J. A., Gienapp, D.E., Hasselmann, P., Kruseman, A., Meerburg, A., Muller, A., Olbers, D.J., Richter, K., Sell, W., Walden, H., 1973. Measurements of wind-wave growth and swell decay during the Joint North Sea Wave Project (JONSWAP). Dtsch Hydrogr. Z., A 8(12).

Holland, G.J., 1980. An Analytic Model of the Wind and Pressure Profiles in Hurricanes. Monthly Weather Review, Vol. 108, 1980.

HRD, 2006. Hurricane Research Division FAQ page. [updated April 21, 2006, cited May 20, 2009]. Available from: http://www.aoml.noaa.gov/hrd/tcfaq/D4.html.

IPET, 2008. IPET (Interagency Performance Evaluation Taskforce) final report. [cited Februay 20, 2008] Available from: https://ipet.wes.army.mil.

Janjic, Z.I., 1994: The step-mountain eta coordinate model: Further developments of the convection, viscous sublayer, and turbulence closure schemes. Mon. Wea. Rev., 122, 927-945.

Janjic, Z., Black, T., Pyle, M., Chuang, H., Rogers, E., DiMego, G., 2004. An Evolutionary Approach to Nonhydrostatic Modeling. NCEP, Camp Springs, Maryland, 50 Years of NWP, June 14-17, 2004.

Jelesnianski, C. P., J. Chen, and W. A. Shaffer, 1992. SLOSH: Sea, lake, and overland surges from hurricanes. NOAA Tech. Rep. NWS 48, 71 pp. [Available from NOAA/AOML Library, 4301 Rickenbacker Causeway, Miami, FL 33149.]

Kalnay, M., Kanamitsu, Baker, W.E., 1990. Global numerical weather prediction at the National Meteorological Center. Bull. Amer. Meteor. Soc., 71, 1410-1428.

Kanamitsu, M., 1989. Description of the NMC global data assimilation and forecast system. Wea. and Forecasting, 4, 335-342.

Kanamitsu, M., Alpert, J.C., Campana, K.A., Caplan, P.M., Deaven, D.G., Iredell, M., Katz, B., Pan, H.L., Sela, J., White, G.H., 1991. Recent changes implemented into the global forecast system at NMC. Wea. and Forecasting, 6, 425-435.

Kaplan, J., DeMaria, M., 1995. A simple empirical model for predicting the decay of tropical cyclone winds after landfall. Journal of Applied Meteorology, vol. 34, 1995.

Kaplan, J., DeMaria, M., 2000. On the decay of tropical cyclone winds after landfall in the New England area. Journal of Applied Meteorology, vol. 40, 2000.

Knabb, R. D, Rhome, J. R., Brown, D. P., 2005. Tropical cyclone report: Hurricane Katrina: 23-30 August, 2005. National Hurricane Center. [updated August 10, 2006, cited February 10, 2008]. Available from: http://www.nhc.noaa.gov/pdf/TCR-AL122005_Katrina.pdf.

Komen, G. J., Cavaleri, L., Donelan, M., Hasselmann, K., Hasselmann, S. and Janssen, P. A. E. M., 1994. Dynamics and Modeling of Ocean Waves. Cambridge University Press, 532 pp.

Kurihara, Y., Bender, M.A., Tuleya, R.E., Ross, R.J., 1995. Improvements in the GFDL Hurricane Prediction System. Monthly Weather Review, 123, 2791-2801.

Kurihara, Y., Tuleya, R.E., Bender, M.A., 1998. The GFDL Hurricane Prediction System and its performance in the 1995 hurricane season. Monthly Weather Review, 126(5), 1306-1322.

LAPACK, 2009. Linear Algebra PACKage, version 3.2.1. [cited August 30, 2009]. Available from: http://www.netlib.org/lapack.

Longuet-Higgins, M. S., Stewart, R. W., 1964. Radiation stresses in water waves; a physical discussion, with applications. Deep-Sea Research, 11:529-562.

Luettich, R., Westerink, J. J., Scheffner, N. W. 1992. ADCIRC: an advanced three-dimensional circulation model for shelves coasts and estuaries, report 1: theory and methodology of ADCIRC-2DDI and ADCIRC-3DL. Dredging Research Program Technical Report DRP-92-6, U.S. Army Engineers Waterways Experiment Station, Vicksburg, MS, page 137.

Luettich, R., Westerlink, J., 2004. Formulation and numerical implementation of the 2D/3D ADCIRC finite element model version 44.XX. 12/08/2004.

Lynett, P. and Liu, P. L.-F., 2004a. Linear analysis of the multi-layer model. Coastal Engineering, v. 51(6), p. 439-454.

Lynett, P. and Liu, P. L.-F., 2004b. A two-layer approach to water wave modeling. Proc. Royal Society of London A. v. 460, p. 2637-2669. 2004.

The MapServer Team, 2009. The MapServer Documentation, Release 5.4.0. [cited June 11, 2009]. Available from: http://mapserver.org.

Mattocks, C., Forbes, C., 2008. A real-time, event-triggered storm surge forecasting system for the state of North Carolina.

Mellor, G. L., 2003. Users guide for a three-dimensional, primitive equation, numerical ocean model (June 2003 version), 53 pp., Prog. in Atmos. and Ocean. Sci, Princeton University, 2003.

Mellor, G., 2008. The depth-dependent current and wave interaction equations: a revision. Journal of Physical Oceanography, 38: 2587-2596.

Mellor, G. L. and Yamada, T., 1982. Development of a turbulence closure model for geophysical fluid problems. Rev. Geophys. Space Phys., 20, 851-875.

Mukai, A.Y., Westerlink, J.J., Luettich, R.A, Jr., Mark, D., 2002. Eastcoast 2001, A Tidal Constituent Database for Western North Atlantic, Gulf of Mexico, and Carribean Sea. USACE Tech. Report, ERDC/CHL TR-02-24.

National Oceanic and Atmospheric Administration, 2004. Population Trends Along the Coastal United States: 1980-2008, Population Growth of Counties – Florida. [cited June 30, 2009]. Available from: http://www.epodunk.com/top10/countyPop/coPop10.html.

NHC SLOSH, 2009. Official SLOSH page on the National Hurricane Center website. [cited on February 18, 2009] Available from: http://www.nhc.noaa.gov/HAW2/english/surge/slosh.shtml.

NOAA Tides and Currents, 2009. NOAA Tides and Current Website. [cited March 8, 2009]. Available from: http://tidesandcurrents.noaa.gov.

NOGAPS, 2009. NOGAPS model home page. [cited March 19, 2009]. Available from: http://meted.ucar.edu/nwp/pcu/nogaps/index.htm.

NOAA-NOS, 1999. NOS Procedures for Developing and Implementing Operational Nowcast and Forecast Systems for PORTS. NOAA Technical Report NOS CO-OPS 0020.

NOAA-NOS, 2003. NOS Procedures for Developing and Implementing Operational Nowcast and Forecast Systems for PORTS. NOAA Technical Report NOS CO-OPS 39.

NOAA NWS Weather Service Operational Manual. WSOM Chapter C-41, Tropical Cyclone Program. Effective date: June 1, 2001.

NRL, 2008. GODAE: Global Data Assimilation Experiment. Naval Research Laboratory Marine Meteorology Division Monterey, CA. [updated December 1, 2008, cited January 15, 2009]. Available from: http://www.usgodae.org.

NSTC Joint Subcommittee on Ocean Science and Technology, 2007. Charting the course for ocean science in the United States for the next decade. PDF. [cited June 7, 2009]. Available from: http://ocean.ceq.gov/about/docs/orppfinal.pdf.

Oey, Ezer, Wang, Fan and Yin, 2006. Loop Current warming by Hurricane Wilma, Geophysical Research Letters, 33, L08613.

Oey, Ezer, Hu & Muller-Karger, 2007. Baroclinic tidal flows and inundation processes in Cook Inlet, Alaska. Ocean Dyn, 57: 205-221.

OpenLayers, 2009. OpenLayers Documentation. Release 2.7, 2009. [cited June 20, 2009]. Available from: http://openlayers.org.

Pasch, R.J., Blake, E.S., Cobb III, H.D., Roberts, D.P., 2006. Tropical Cyclone Report, Hurricane Wilma, 15-25 October 2006. NOAA/NWS/Tropical Prediction Center/National Hurricane Center, Miami, FL. [cited October 20, 2008]. Available from: http://www.nhc.noaa.gov/pdf/TCR-AL252005_Wilma.pdf.

Powell, M.D., Houston, S.H., Amat, L.R., Morisseau-Leroy, N., 1998. The HRD real-time hurricane wind analysis system. Wind Engineering and Industrial Aerodynamics. 77-78, 53-64.

Powell, M.D., Houston, S.H., Reinhold, T.A., 1996. Hurricane Andrew's landfall in South Florida. Part I: Standardizing measurements for documentation of surface wind fields. Weather forecast, 11, pp. 304-328.

Preisendorfer, R.W., 1988. Principal component analysis in meteorology and oceanography. Elsevier, 1988.

Resio, D.T., 1987. Shallow-water waves. I. Theory. J. Wtrway., Port, Coast. and Oc. Engrg., ASCE, 113(3), pp. 264-281.

Resio, D.T., 1988a. Shallow-water waves. II. Data comparisons. Journal of Waterways, Ports, Coastal and Oceanographic Engineering., ASCE, 114(1), pp. 50-65.

Resio, D.T., 1988b. A steady-state wave model for coastal applications. Proc. 21st Coastal Engineering Conference, ASCE, pp. 929-940.

Ris, R.C., Booij, N., Holthuijsen, L.H., 1999. A third-generation wave model for coastal regions, Part II, Verification, Journal of Geophysical Research C4, 104, 7667-7681.

Rogers, W. E., Kaihatu, J. M., Hsu, L., Jensen, R. E., Dykes, J. D., Holland, K. T., 2006. Forecasting and hindcasting waves with the SWAN model in the Southern California Bight. Coastal Engineering 54, 1-15.

RTOFS, 2009. Real-Time Ocean Forecast System (Atlantic). National Weather Service, Environmental Modeling Center. [updated February 6, 2009, cited September 2, 2009]. Available from: http://polar.ncep.noaa.gov/ofs.

Sheng, Y. P., 1983. Mathematical modeling of three-dimensional coastal currents and sediment dispersion: Model development and application. Technical Report CERC-83-2, Aeronautical Research Associates of Princeton, Princeton, New Jersey.

Sheng, Y. P., 1986. A three-dimensional numerical model of coastal and estuarine circulation and transport in generalized curvilinear grids. Technical Report No. 587.

Sheng, Y.P., 1987: On modeling three-dimensional estuarine and marine hydrodynamics. Three-dimensional models of marine and estuarine dynamics, pp. 35-54.

Sheng, Y. P., 1990. Evolution of a three-dimensional curvilinear-grid hydrodynamic model for estuaries, lakes and coastal waters: Estuarine and Coastal Modeling I, ASCE, pp. 40-49.

Sheng, Y.P., Alymov, V., Paramygin, V., Davis, J.R., 2006. An integrated modeling system for forecasting of storm, surge and coastal inundation, in Estuarine and Coastal Modeling, IX, ASCE., 2006.

Sheng, Y.P., Alymov, V., Paramygin, V.A., 2009. Simulation of storm surge, wave, currents, and inundation in the Outer Banks and Chesapeake Bay during Hurricane Isabel (2003):The importance of waves. Submitted.

Sheng, Y.P., Davis, J.R., Paramygin, V., Park., K., Kim, T., Alymov, V., 2003. Integrated-process and integrated-scale modeling of large coastal and estuarine areas, in Estuarine and Coastal Modeling, VIII, ASCE., 2003.

Sheng, Y. P., Paramygin V. A., Alymov V., Davis J. R., 2006: A Real-Time Forecasting System for Hurricane Induced Storm Surge and Coastal Flooding. Estuarine and Coastal Modeling, 2006, pp. 585-602.

Sheng, Y. P., Paramygin V. A., Zhang, Y., Davis, J. R., 2007. Recent enhancements and applications of an integrated storm surge modeling system. Proc. Estuarine and Coastal Modeling, X, ASCE, 2007.

Sheng, Y. P., Paramygin, V. A., Zhang, Y. and Davis, J. R., 2008: Recent enhancements and application of an integrated storm surge modeling system: CH3D-SSMS. Estuarine and Coastal Modeling, Proc. of the Tenth International Conference, ASCE, pp. 879-892.

Sheng, Y.P., Kim, T., 2009. Skill assessment of an integrated modeling system for shallow coastal and estuarine ecosystems. Journal of Marine Systems, 76(1-2), pp. 212-243.

Sheng, Y. P. and Villaret, C., 1989. Modeling the effect of suspended sediment stratification on bottom exchange process. Journal of Geophysical Research., pages 14229-14444.

Signell, R. P., Beardsley, R. C., Graber, H. C., Capotondi, A., 1990. Effect of wave-current interaction on steady wind-driven circulation in narrow, shallow embayments. Journal of Geophysical Research, 95, pp. 9671-9678.

Skamarock, W. C., Klemp, J. B., Dudhia, J., Gill, D. O., Barker, D. M., Wang, W. and Powers, J. G., 2005. A Description of the Advanced Research WRF Version 2.

Spindler, T., Rivin, I., Burroughs, L., Lorano, C., 2006. NOAA Real-Time Ocean Forecasting System (RTOFS) – (Atlantic). Technical Procedure Bulletin, MMAB 2006-02.

SSMS Team, 2009. CH3D-SSMS Storm Surge Modeling System. [updated September 4, 2009, cited: September 4, 2009]. Available from: http://ch3d-ssms.coastal.ufl.edu.

Stewart, S.R., Beven II, J.L., 2009. Tropical Cyclone Report, Tropical Storm Fay, 15-26 August 2008. NOAA/NWS/Tropical Prediction Center/National Hurricane Center. [cited June 20, 2009]. Available from: http://www.nhc.noaa.gov/pdf/TCR-AL062008_Fay.pdf.

Sun, D., Sheng, Y.P., 2008. Three dimensional numerical modeling of wave-induced circulation, unpublished manuscript.

The SWAN team, 2009. Scientific and technical documentation SWAN Cycle III version 40.72AB. [cited June 18, 2009]. Available from: http://vlm089.citg.tudelft.nl/swan/online_doc/swantech/swantech.html.

Thompson, J.F., Warsi, Z.U.A. and Mastin, C.W., 1985. Numerical grid generation - foundations and applications. North-Holland, New York, 1985.

Tolman, H. L, 1999. User manual and system documentation of WAVEWATCH-III version 1.18. NOAA / NWS / NCEP / OMB Technical Note 166, 110 pp.

Tolman, H.L., 2002. User manual and system documentation of WAVEWATCH-III version 2.22. NOAA / NWS / NCEP / MMAB Technical Note 222, 133 pp.

Tolman, H. L., Chalikov, D., 1996. Source terms in a third-generation wind-wave model. J. Phys. Oceanogr, 26, 2497-2518.

USGS, 2001. National Land Cover Dataset, 2001. [cited April 20, 2009]. Available from: http://landcover.usgs.gov.

USGS NED, 2009. National Elevation Dataset. [updated August 26, 2009, cited August 30, 2009]. Available from: http://seamless.usgs.gov.

WAMDIG, 1988. The WAM model - A third generation ocean wave prediction model. Journal of Physical Oceanography, 18, 1775-1810.

WikiMedia Commons, 2009. WikiMedia Commons. [cited June 5, 2009]. Available from: http://wikipedia.org.

Wilson, B. W., 1960: Note on Surface Wind Stress over Water at Low and High Wind Speeds. Journal of Geophysical Research, 65(10), 3377–3382.

Xie, L., Bao, S., Pietrafesa, L. J., Foley, K., Fuentes, M., 2006. A Real-Time Hurricane Surface Wind Forecasting Model: Formulation and Verification. Monthly Weather Review, May 2006.

Zhang, Y.F., 2007. Storm surge simulation of hurricane Ivan and Hurricane Dennis. Dissertation, University of Florida, 2007.

Zhang, Y.L., Baptista, A.M. and Myers, E.P., 2004. A cross-scale model for 3D baroclinic circulation in estuary-plume-shelf systems: I. Formulation and skill assessment. Cont. Shelf Res. 24: 2187-2214.

BIOGRAPHICAL SKETCH

Vladimir A. Paramygin was born on June 30th, 1979 in Barnaul, Russia. He graduated from a High School #69 in Barnaul and Darby High School in Darby, Montana (as an exchange student) in 1996. Vladimir received a B.S. degree in Applied Mathematics from Altai State University (Barnaul, Russia) in 2000 and joined the Coastal Engineering and Oceanographic program at the University of Florida where he earned his M.S. degree in 2002 and continued to pursue a Ph.D. in coastal engineering.